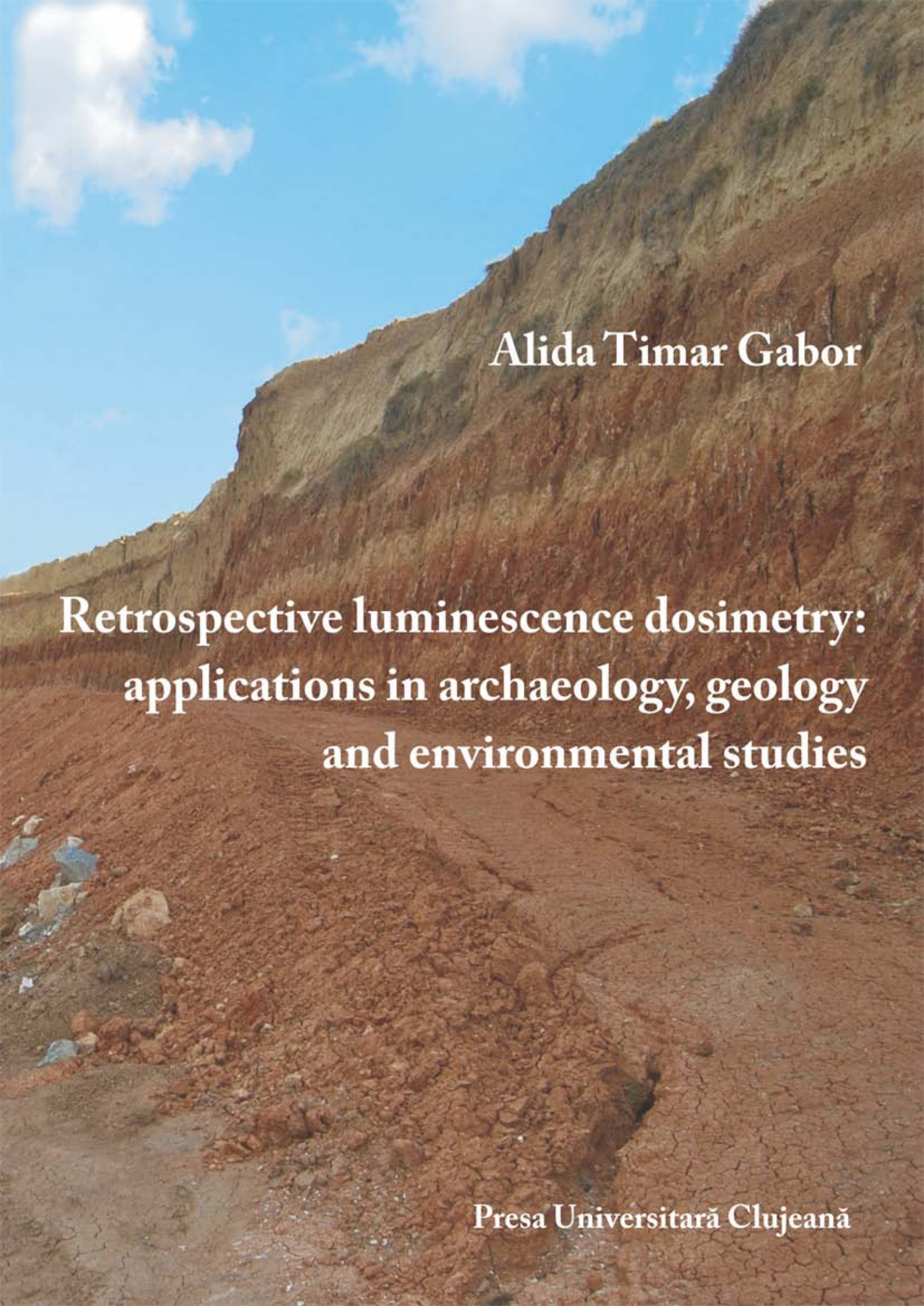

Alida Timar Gabor

Retrospective luminescence dosimetry: applications in archaeology, geology and environmental studies

Presa Universitară Clujeană

ALIDA IULIA TIMAR GABOR

RETROSPECTIVE LUMINESCENCE DOSIMETRY: APPLICATIONS IN ARCHAEOLOGY, GEOLOGY AND ENVIRONMENTAL STUDIES

(TEZĂ DE DOCTORAT – UNIVERSITATEA BABEŞ-BOLYAI, 2010, FACULTATEA DE ŞTIINŢA ŞI INGINERIA MEDIULUI)

Referenţi ştiinţifici:

Prof. dr. Călin Baciu
Prof. dr. Constantin Cosma
Prof. dr. Bogdan Petroniu Onac
Conf. dr. Cristian George Panaiotu
Dr. Dimitri Vandenberghe

ISBN 978-973-595-668-4

Universitatea Babeş-Bolyai
Presa Universitară Clujeană
Director: Codruţa Săcelean
Str. Hasdeu nr. 51
400371 Cluj-Napoca, România
Tel./fax: (+40)-264-597.401
E-mail: editura@editura.ubbcluj.ro
http://www.editura.ubbcluj.ro/

ALIDA IULIA TIMAR GABOR

RETROSPECTIVE LUMINESCENCE DOSIMETRY: APPLICATIONS IN ARCHAEOLOGY, GEOLOGY AND ENVIRONMENTAL STUDIES

PRESA UNIVERSITARĂ CLUJEANĂ

2014

CUVÂNT ÎNAINTE

Doamna Alida Iulia Timar-Gabor s-a născut în orașul Beclean și a absolvit Liceul Liviu Rebreanu din Bistrita în 2001. Ca elevă a participat și s-a evidențiat la fazele locale și naționale ale Olimpiadelor de fizică. A urmat și absolvit cu rezultate foarte bune cursurile Facultății de Fizică în perioada 2001-2005 și apoi secția de masterat „Metode atomice și nucleare în studiul mediului" absolvită în 2006 în cadrul Facultății de Știința și Ingineria Mediului. Teza de licentă cu titlul "Aplicații ale dozimetriei termoluminescente în măsurarea fondului radioactiv natural" a fost primul contact cu viitoarele preocupări care aveau să-i marcheze evoluția științifică ulterioară. A fost admisă la doctorat cu frecvența în octombrie 2006 iar din 2008 ocupă prin concurs un post de asistent în cadrul Departamentului de Analiza și Ingineria Mediului în carul Facultății de Știința și Ingineria Mediului, unde susține seminarii și lucrări de laborator foarte apreciate de studenți la disciplinele de Fizica mediului, Radioactivitatea mediului, Geocronologie nucleară și Radioecologie.

În perioada studiilor de masterat D-na Alida Gabor Timar a efectuat un stagiu de cercetare de 8 luni în Laboratorul de datare al Universității din Gent unde a intrat în contact direct cu problemele specifice ale metodelor de datare luminescenta, teza de masterat cu titlul: "Comparing Quartz OSL and Polymineral IRSL Ages for Chinese Loess: A case study" fiind primul contact serios cu aspectele dificile ale datării luminescente. A urmat apoi Școala Doctorală din facultate "Evoluția sistemelor terestre și mediul ambiant", perioadă în care, pe lânga o abordare foarte laborioasa și extinsă, atât a cercetarilor de pionerat cat și a celor mai noi publicații în domeniu, a avut o contribuție esențială la implementarea în România a primului laborator de datare luminescentă care este funcțional și în care doctoranda a obținut o buna parte a rezultatelor din prezenta teză. În perioada doctoratului d-na Alida Timar Gabor a menținut constant legatura cu Laboratorul de datare din Gent (dr. D. Vandenberghe) efectuând înca doua stagii mai scurte la invitatia acestui laborator (prof. P. Van de Haute) precum și o vizita și un scurt stagiu la Risø National Laboratory (centrul mondial al datării luminescente), ocazie cu care i s-a propus de către prof. Murray (somitatea nr.1 în domeniu) abordarea unei teze de doctorat în acel insitut. Am avut șansa ca Alida să renunțe la aceasta foarte onorantă propunere și în acest fel în foarte scurt timp Romania să se poată etala cu un astfel de laborator.

Alida Timar Gabor a participat cu comunicări, majoritatea orale, la conferințe internaționale de ținuta în domeniul datărilor în Austria, Germania, China, Serbia, Polonia și România. La a 12-a Conferință internațională de datare prin luminescenta și rezonanță electronică de spin, Septembrie 2008 din Pekin a obținut un prestigios premiu acordat pentru cele mai bune prezentări studențești. Aș mai remarca de asemenea foarte buna și eficienta colaborare pe care a d-na Gabor a stabilit-o cu grupul profesorului Panaiotu (Universitatea din București), grup consacrat internațional pe probleme de datare a loess-lui din România, colaborare care deschide în prezent abordarea unor probleme interesante de paleoclimatologie.

În momentul de față doamna Gabor a publicat un număr de 25 de lucrări științifice în reviste ISI cu factor de impact, fiind autor principal la aproape jumătate (10). Are de asemenea citari în literatura de specialitate.

Prezenta teză de doctorat a fost susținută public în luna iunie 2010. Este redactată foarte ingrijit în limba engleză fiind structurată în introducere, cinci capitole și concluzii.

Primul capitol este unul introductiv bazat pe referințe și cunostințe de bază atent selectate și cuprinde noțiuni teoretice despre fenomenul de luminescență, despre proprietățile fizice și optice ale materialelor utilizate, precum și descrierea fenomenelor fizice implicate în datarea prin termoluminescență și luminescență stimulată, punând accentul pe analiza semnalului eliberat prin încălzire și prin stimulare optică continuă și în pulsuri. De asemenea sunt prezentate noțiunile esențiale în întelegerea și aplicarea în practică a datării, precum forma semnalului emis, spectrul semnalului și fadingul anormal. Prezentarea acestor fenomene este facută în prin exemple proprii. Întelegerea perfectă a acestor principii fizice pe care se bazeaza datarea luminiscenta au fost de mare ajutor în implementarea și dezvoltarea rapidă a laboratorului de datare din cadrul Universității Babeș-Bolyai.

Al doilea capitol abordează bazele experimentale ale măsurătorilor dozei echivalente descriind și exemplificând prin măsurători proprii tehnicile folosite în măsurarea semnalului luminescent. Sunt prezentate principalele etape ce trebuie parcurse pentru a ne asigura că informația primită de la proba analizată este cuantificabilă și reproductibilă. Sunt evidențiate principalele avantaje ale protocolului SAR legate de precizia, rapiditatea și posibilitatea corecțiilor de sensibilitate. A doua problemă foarte importantă în măsurarea dozei echivalente este prepararea probelor supuse datării. Procedeele fizico-chimice de extracție, separare și pregătire a microcristalelor de cuarț în vederea obținerii semnalului luminos sunt o suită de operațiuni complexe și care au fost parcurse cu succes așa cum au demonstrat testele ulterioare asupra cuarțului extras. În ultima parte a capitolului este prezentată pe scurt instalatia folosită și sunt efectuate testele de calibrare a sursei de Sr-90 precum și testele de stabilitate termică și cele legate de funcționarea fotomultiplicatorului.

Capitolul 3 tratează și prezintă principalele aspecte și respectiv rezultate obținute de către doctorandă legate de determinarea dozei anuale. Deoarece o buna parte din erorile metodei de datare luminescentă provin din corectitudinea cu care se masoară acest parametru lucrarea a acordat o atenție deosebită acestor determinări. Dupa prezentarea elementelor radiaoctive implicate, a modului cum radiațiile emise de către acestea interacționează cu granulele minerale de diferite dimensiuni precum și a factorilor care influențează acumularea semnalului arheologic sau geologic util, incluzând efectele de umiditate, atenuare și etching, sunt prezentate rezultatele experimentale obținute de doctorandă pe probele selectate pentru datare. Deoarece radiu și uraniu se pot găsi în probe nu totdeauna în echilibru radioactiv, o atenție deoasebită a fost acordată determinărilor de radiu direct din picul acestuia care este puternic interferat cu picul uraniului 235 la energia de 186 keV. Determinarea Ra din energiile descendentilor acestuia ridică întotdeauna probleme legate de scăpările de radon incontrolabile care intervin în multe cazuri în materialul de datat. Această problemă a fost rezolvată cu eleganță prin analiza complexă a spectrului gama și a principalelor energii implicate emise de matricea analizată. Pentru verificarea analizelor din laborator asupra conținutului de U și Th (principalele contribuții la doza anuală) rezultatele au fost verificate prin comparație cu masurători similare în laboratorul din Gent și Veszprem și de asemenea prin măsurători prin spectrometrie alfa și cu rezultate obținute prin activare cu neutroni efectuate la Sucursala pentru Cercetări Nucleare de la Mioveni, Pitești. Așa cum au arătat rezultatele acestor intercomparări, există o bună concordanță între dozele anuale determinate prin metode diferite.

În Capitolul 4 sunt prezentate rezultatele asupra determinărilor de vârstă pentru probe neolitice provenite din situl arheologic Lumea Nouă. Rezultatul obținut plasează originea acestor ceramici la tranziția dintre cultura Foeni și cultura Petrești. Metodele luminescente au fost aplicate pe 4 fragmente de ceramică. Protocolul unialicota SAR a fost aplicat atât pentru emisia în UV a cuarțului grosier (90-125 μm) prin stimulare în albastru (OSL) cât și prin emisia în albastru a granulelor fine (4-11 μm) poliminerale extrase și stimulate în infraroșu. Pentru comparare a fost utilizată și tehnica obisnuită a dozelor aditive pe mai multe alicote și stimulare termică. Vârstele obținute prin aceste trei metode diferite sunt bună concordanță, dar s-a concluzionat că tehnica SAR OSL este mai robustă și obține aceleași rezultate ca și analiza pe granule poliminerale corectată de fading, în timp ce determinările multialicotă și cele pe granule mici necorectate de fading obțin rezultate deplasate spre vârste mai tinere. Rezultatele au fost comunicate și publicate in reviste de specialitate atragând atenția asupra alegerii metodei potrivite pentru aplicarea acestei metode în arheologie.

În prima parte a Capitolului 5, după o abordare foarte bine documentată a importanței în paleoclimatologie a studiilor pe loess și prezentarea ariei studiate sunt descrise pe larg rezultatele obținute pe secțiunea Mircea Vodă de unde doctoranda a

recoltat 13 probe, 11 din primul strat de loess (L1) si celelalte doua din stratele L2 şi L3. Măsurătorile de doză echivalentă şi doză anuală s-au facut foarte îngrijit şi au fost repetate de multe ori în asa fel ca să se obţina o bună statistică a masurătorilor. De asemenea, la măsurarea dozei echivalente s-au administrat toate testele necesare în aşa fel încât rezultatele să aibă cea mai mică eroare posibilă. Vârstele obţinute confirmă faptul că primul paleosol s-a format în perioada ultimului stagiu interglaciar şi indică faptul că depunerile eoliene din ultimul stadiu glaciar-interglaciar au avut loc continuu. De asemenea studiul remarcă apariţia unei discontinuitaţi în viteza de depunere în urmă cu 50-60 mii de ani când aceasta prezintă valori mult mai mari, aproape duble şi semnalează o schimbare climatică clară. Aceleaşi observaţii s-au facut şi pe loess-ul chinezesc în 2008. Analize recente efectuate de doctorandă (primele semnalate în literatura de specialitate) scot în evidenţă faptul că determinările de vârstă pe granule de cuarţ mari şi mici arată sistematic o diferenţă deşi toate testele impuse de metodologia acestor două tehnici sunt trecute cu succes. Au fost avansate mai multe ipoteze de lucru, dar până în prezent problema nu a fost soluţionată şi rămâne deschisă. Explicarea acestei diferenţe îi poate aduce autoarei o binevenită poziţie în rândul specialiştilor de clasă în domeniul metodelor luminescente. **În partea doua a Capitolului 5** este abordată în premieră datarea unor paleosoluri utilizând tehnica luminescentă bazată pe analiza granulelor mari şi metoda SAR. Doza anuală a fost determinată prin spectrometrie gama iar rezultatele plasează cele doua probe analizate (sol albic si cernoziom) corespunzător tranziţiei de la un climat uscat (Subboreal) la unul mai umed (Subatlantic). Vârstele determinate de 4 Ka şi 9.2 Ka corespund tranziţiei menţionate.

Toate cele mentinate mai sus recomandă din plin teza şi activitatea doctorandei Alida Timar-Gabor ca o realizare personală de excepţie. Recunoaşterea calităţii cercetării desfaşurate în cadrul prezentei teze o constituie şi faptul că a fost inclusă de către CNCSIS, alături de alti 6 participanţi în Ediţia 2010 a Poveştii Doctoratului Meu, apariţie editorială ce doreste să mediatizeze cele mai bune rezultate obţinute de tineri cercetători din România.

Consider că prezenta teză de doctorat poate deservi ca model pentru alţi tineri doctoranzi în domenii precum fizică sau ştiinţele pământului. De asemenea, prezenta teză este o lucrare de referinţă pentru cei interesaţi în implementarea unui laborator de datare şi dozimetrie prin luminiscenţă. Nu in ultimul rând, lucrare poate deservi ca valoroasă sursă de informare pentru toti cei interesaţi în principiile şi potenţialele aplicaţii ale datării prin luminescenţă.

Cluj Napoca,
21 Februarie 2012
Prof. Dr. Constantin Cosma

The research discussed in the present thesis has been mainly carried out at the Environmental Radioactivity and Nuclear Dating Centre, Institute for Interdisciplinary Experimental Research, Babeş-Bolyai University Cluj-Napoca, Romania. Alida Timar performed several research stages in Gent Luminescence Dating Laboratory and was enrolled (in total for about eight months) as a visitor junior researcher in Gent University, Belgium under the scientific supervision of Dr. Dimitri Vandenberghe and Professor Dr. P. Van den haute. Part of the work presented was carried out during the frame of these visits. The transfer of knowledge and logistic support provided by Gent Luminescence Dating Laboratory is highly acknowledged as well as the financial support of CEEX-749/2006 and CNCSIS TD-395 research grants.

Scopul acestei teze a constat în implementarea metodelor moderne de datare prin luminescență în cadrul Universității Babeş-Bolyai şi aplicarea acestor tehnici pentru obținerea de vârste absolute pentru materiale relevante studiilor arheologice, geologice şi de mediu. Primele trei capitole ale tezei prezintă metodele luminescente şi testele procedurale şi de rigoare intrinsecă aplicate. În capitolul IV este prezentată aplicarea metodelor luminescente pentru datarea de ceramnică Neolitică. Aceast studiu reprezintă în momentul de față una dintre puținele aplicații la nivel internațional care utilizează tehnicile SAR-OSL şi IRSL pentru datarea ceramicilor şi demonstrează potențialul folosirii lor pentru caracterizarea evoluției cronologice a siturilor arheologice. Ultimul capitol al tezei prezintă datarea secventelor de loess-paleosol din Romania. Cercetări de natură aplicativă dar şi fundamentală sunt prezentate, rezultatele obținute fiind de relevanță atât pentru specialişti în Ştiințele Pământului cât şi pentru comunitatea ştiințifică de datare prin luminescență.

INTRODUCTION

1. RETROSPECTIVE LUMINESCENCE DOSIMETRY: DEFINITION OF TERMS

The term retrospective dosimetry refers to techniques used for evaluation of past radiation exposure in media of interest.

Luminescence phenomena encompass a very wide range of processes. Generically, based on the decay times associated with the luminescence emission, these processes are divided into fluorescence (decay times ranging from 10^{-9} to 10^{-3} seconds (Ropp, 2004)) and phosphorescence (delayed emission, with a decay time of more than 10^{-3} seconds).

For the purpose of retrospective dosimetry only optically stimulated luminescence (OSL) and thermoluminescence (TL) processes are of interest (Bøtter-Jensen et al., 2003a). OSL and TL is the luminescence emitted from an irradiated insulator or semiconductor during exposure to light or heat, respectively. According to the classification based on the decay times, OSL and TL can be regarded as a fluorescencent process. However, it should be emphasized that OSL and TL are stimulated processes, and they are usually accompanied by photoconductivity phenomena. The luminescence signal emitted is dependent on the irradiation history of the sample. In the case of OSL the wavelength of the emitted signal is shorter than the wavelength of the stimulation. Thus, materials used in retrospective luminescence dosimetry are anti-Stokes phosphors.

Based on luminescence methods, retrospective dosimetry has two main applications: dating and accident dosimetry. Luminescence dating is based on the property of certain minerals to store the energy of nuclear radiation. A weak flux of ionizing radiation is omnipresent in nature being derived from the radioactive decay of elements (mainly the Uranium and Thorium series and Potassium-40) and from cosmic rays. By stimulation with heat or light, these minerals can release part of this energy by emitting a small amount of light, which is called luminescence. As previously mentioned, the intensity of this luminescence signal is related to the total accumulated radiation dose. The dose rate in the environment can be determined from the concentration of radionuclides in the media and is assumed to be constant throughout time. Thus, the aim of luminescence dating is to determine the total radiation dose absorbed in minerals throughout time from which an age can be derived. In accident dosimetry the goal is to reconstruct the doses absorbed by

available materials as a consequence of radiation accidents. These doses are superimposed on the doses determined in dating applications (Bailiff, 1999; Bailiff et al., 2000; Göksu et al., 2002; Bailiff et al., 2004). The techniques used in accident dosimetry and dating applications are identical (Banerjee, 1999; McKeever, 2001; Bøtter-Jensen et al., 2003a; Thomsen, 2004).

2. AIM OF OUR WORK

Luminescence methods are important analytical techniques for dating worldwide (reference can be made to review works of Aitken, 1985, 1998, 1999; Roberts, 1997; Stokes, 1999; Duller, 2004; Lian et al., 2006; Wintle, 2008a, b, respectively Cosma et al., 2008b,d and Timar, 2008b, 2009c-in Romanian). Despite this, the method was not thoroughly applied in Romania up to now. It should be mentioned that some attempts in using thermoluminescence for dating were made in the past by Professor V.V. Moraiu in Cluj in the 1980s and by a group in Bucharest in 1990s (Labău et al., 1996) but the research was abruptly ceased for reasons we are not aware of. The interest of the group of Professor Cosma in luminescence dating dates for more than one decade ago (Văsaru and Cosma, 1999), and our first applications have been carried out using a Harashaw 2000 dosimetric system (Cosma et al., 2006; Cosma et al., 2008a,c). In 2006, the material means necessary to develop a modern luminescence laboratory affiliated to the Faculty of Environmental Sciences of Babeş-Bolyai University Cluj were finally obtained through a research grant. The work presented in this thesis started in the same year and its structure is undoubtedly linked to the development of the first state of the art luminescence dating laboratory in Romania.

The first aim of our work was to ensure that the methodology applied in the Luminescence Dating Laboratory in Cluj, both in the case of gamma spectrometric measurements (for radionuclide specific activity determination in environmental samples) as well as for sample preparation and luminescence measurements are robust in order to be able to obtain accurate values for both anual dose and equivalent doses of investigated samples. In order to do that, both internal checks and intercomparison tests with other laboratories have been performed. The second but more important aim of this thesis was to apply state of the art luminescence methodology in dating archaeological and geological materials of interest.

For archaeological applications, the Lumea Nouă, a well known site of Neolithic painted pottery was chosen, as this location is considered to be of major importance for reconstructing the Neolithic and Aeneolithic periods in Romania.

Most efforts were conducted into appling luminescence for dating geological materials, in particular the famous loess/ palaeosol sequences from Mircea Vodă outcrop. We have chosen this application because it is widely recognized that Romanian loess

sequences preserve a significant terrestrial record of Quaternary climate change but in comparison to similar sequences elsewhere in Central and Eastern Europe, the deposits in Romania have been less extensively studied (Frechen et al., 2003). Obtaining an absolute chronostratigraphical framework for the Romanian loess deposits is essential to determine (i) the timing of climatic events archived in the loess, (ii) the rate of processes such as sedimentation and pedogenesis and (iii) the correlation between the loess sequences that are spread all over Europe. Moreover having an absolute chronology on Romanian loess sequences is of uttermost importance as these sequences are thought to be amongst the thickest and most complete in Europe, and that they form the link between the glacial loess deposits of Western and Central Europe and the non-glacial loess deposits that extend all the way to China. We point out as well that by reconstructing past climates and the climatic variation throughout time the data obtained can be used to test the accuracy of computer models that simulate climatic change. Simulations of the radiative impacts of dust under present climate conditions have been performed and already incorporate the effects of anthropogenically derived dust (Tegen et al., 1996). However, the impact of the changes in the productivity of natural dust sources over geological time and the incorporation of dust deflation, transport and deposition processes is just beginning (Harrison et al., 2001). Spatially extensive data sets documenting the observed changes in dust accumulation rates during the last interglacial-glacial cycle are required in order to test model simulation of dust cycles Thus, investigation of sediment deposition in relation to palaeoclimatic changes is a major focus in modern earth modeling systems. Having an accurate knowledge of the aeolian sedimentation rates during the Quaternary may help in creating extended models of dust cycles and thus of climate change, with eventually making predictions on future trends possible (Sun et al., 2000). Thus dating sedimentary deposits is important for environmental sciences not only as a matter of reconstructing the past trends but also for predicting future ones.

3. OUTLINE OF THE THESIS

The thesis is structured in five chapters.

Chapter I presents the basic principles of luminescence processes and how these phenomena can be used for dating, including a discussion on signal growth and lifetime. The general one trap model is presented as well as the more complex model developed by Bailey (2001) for optical stimulated luminescence of quartz, and the model proposed by Hütt et al. (1988) for IRSL emission of feldspars. Excitation and emission spectra of quartz and feldspars are presented as well as a comparison of their decay curves with more emphasize on quartz signal components under the two stimulation modes used routinely in this work (continuous wave optically stimulated luminescence CW-OSL, respectively

linearly modulated luminescence LM-OSL). A presentation of anomalous fading of feldspars is also included along with the method used in this work (Huntley and Lamothe, 2001) for correcting for this malign phenomenon. Although this chapter is based on the study of literature it also contains own research in order to illustrate the properties described.

Chapter II briefly presents the techniques and methodologies available for equivalent dose estimation. Emphasize is placed on the SAR protocol as this technique was used throughout the present work. The underlying assumptions of the protocol are presented and their fulfillment is exemplified by showing the behavior of samples investigated in this work. This chapter contains also the description of the sample preparation techniques used throughout this work in order to extract coarse (90-125μm, 63-90μm, 35-50 μm) quartz, polymineral fine grains and respectively fine quartz (4-11μm), along with a short presentation of luminescence measurement facilities used, including the checks routinely performed in order to verify their suitable functioning. The calibration procedure of the radioactive sources used in our study is described to a somehow grater detail.

Chapter III is structured in two parts. The first part presents specific aspects associated with the evaluation of the annual dose. In the following part gamma spectrometric methodologies used for natural radionuclides specific activities measurement implied in our laboratory are presented. These are based our previous experience with environmental radioactivity evaluation (Begy et al., 2007, 2009a,b; Cosma et al., 2007, 2009a, b, c; Timar et al., 2007, 2008a). An intercomparison exercise for determining the radionuclides concentration in soil samples performed between our laboratory and two other laboratories using independent methods (-alpha spectrometry carried out in the Laboratory of Radiochemistry Veszprem, Hungary respectively instrumental neutron activation analysis carried out at the Institute for Nuclear Research, Pitesti, Romania) in order to validate our methods is presented.

Chapter IV presents the actual application of luminescence dating in archaeology, work being carried out on four pottery fragments excavated at Lumea Nouă (Alba Iulia, Romania). The application of single-aliquot regenerative-dose (SAR) protocol to both blue (OSL) and infrared stimulated luminescence (IRSL) signals from coarse (90-125 μm) quartz and polymineral fine (4-11 μm) grains, respectively is described in detail, along with a more conventional approach, which used a multiple-aliquot additive-dose (MAAD) protocol and thermoluminescence (TL) signals from polymineral fine grains. Quartz OSL ages obtained are compared to the conventional TL ages and to the fading corrected IRSL ages and the reliability of the investigated protocols is discussed. Data presented are based on a former collaboration of colleagues in Babeş-Bolyai University of Cluj, Appulum University of Alba Iulia and Gent Luminescence Dating Laboratory (Benea et al., 2007) and serve as an example on how luminescence dating, especially by the use of the state-of-

the-art techniques can contribute to establishing a complete chronological framework for the ancient cultural development in Neolithic sites.

Chapter V presents the application of optical methods on geological samples. The main part of the chapter (V.I) presents the detailed description of the application of optical dating using quartz as a dosimeter for the purpose of establishing an accurate chronology of deposition for Mircea Vodă section in South Eastern Romania (Cosma and Timar 2008e; Timar et al. 2008c; Timar et al., 2009 a, b; Timar et al., 2010a,b,c). The behavior of both fine (9-11 μm) quartz grains and silt sandy (63-90 μm) quartz grains in the SAR protocol is presented in great detail, along with a comparison of equivalent doses obtained from fine grains in our laboratory and Gent Luminescence Dating Laboratory. A thorough study on the luminescence optical properties (thermal stability tests, LM-OSL analysis, growth curve characteristics, equivalent dose distribution analysis etc.) of the two grain fractions is also presented. The potential and the limitations of applying SAR OSL dating on quartz for dating Romanian loess is discussed in detail. In Section V.2 luminescence techniques are applied for dating soil covers from the forest steppe zone in Transylvanian Basin.

The studies presented serve to illustrate the contribution that luminescence dating methods can make to archaeological and paleoclimatic research in Romania and **conclusions** are subsequently summarised.

CHAPTER I
GENERAL PRINCIPLES OF LUMINESCENCE DATING

I.1. INTRODUCTION

Luminescence dating is based on the property of certain minerals to store the energy of nuclear radiation. A low level of nuclear radiation is omnipresent in nature, and the longer the minerals are exposed, the more energy they store. By stimulation with heat or light, the minerals can release part of this energy by emitting a small amount of light, which is called luminescence. The intensity of this luminescence signal is proportional to the total accumulated radiation dose, and hence also to the total acquisition time.

There are two variants of luminescence dating, namely thermoluminescence (TL) and optically stimulated luminescence (OSL) dating, depending on whether the luminescence is stimulated by heat or light, respectively. OSL dating is also simply referred to as optical dating. More specific terms can be used depending on the wavelength of the stimulating light, such as infra-red stimulated luminescence (IRSL), green light stimulated luminescence (GLSL or GSL) or blue light stimulated luminescence (BLSL or BSL).
In all of the cases the latent dating information is carried in the form of trapped electrons. These electrons are produced by the interaction of the nuclear radiations with the atoms of the mineral and then may get trapped in certain defects of the crystalline structure. The number of trapped electrons is a measure for the total dose (the total amount of energy absorbed from the ionizing radiation) the mineral has received over a certain period of time. If also the rate is determined by which the mineral has been absorbing the dose, this period of time (i.e. an age), can be determined.

The moment that is dated with luminescence techniques is a zeroing event during which all the effects on the mineral of its exposure to radiation are removed. In the case of pottery, the zeroing is caused by the firing, the final part of the manufacturing process. For sediments, the zeroing event is the exposure of the sediment grains to sunlight during transportation, prior to deposition. Once the zeroing agent is removed, for instance when sedimentary minerals are deposited and shielded from sunlight by other grains falling on top of them, the luminescence signal starts to build up again. The signal can also be removed in the laboratory by exposing the mineral grains to the same zeroing agents (heat

or light). This time, the luminescence signal is measured and used to determine the time that has elapsed since it was last set to zero. This is illustrated in **Figure I.1**, for the specific case of the luminescence dating of sediments.

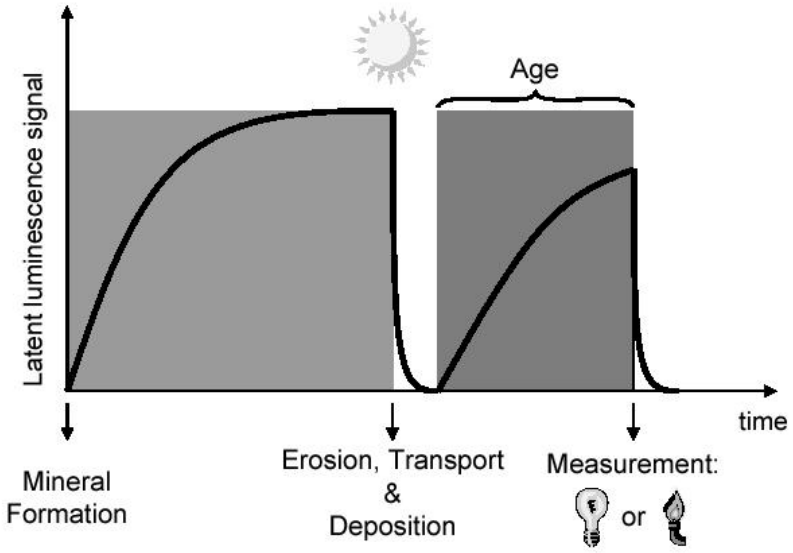

Figure I.1: *Schematic representation of the event that is dated in luminescence dating of sediments.*

I.2. DATING OF ARCHAEOLOGICAL AND GEOLOGICAL MATERIALS BY MEANS OF RETROSPECTIVE LUMINESCENCE DOSIMETRY-SHORT HISTORICAL PERSPECTIVE

The occurrence of luminescence processes has been known for hundreds of years, TL experiments being described for the first time in a work of Sir Robert Boyle (Boyle, 1664). However, understanding and making use of these phenomena started only in the late 1940s -1950s with the advent of development of sensitive photomultipliers.

Following the landmark publication of Daniels et al. (1953) on the potential geological and archaeological applications of TL, progress in dating pottery and other heated materials of archaeological interest started to take place (see for example Kennedy and Knopff, 1960; Grogler et al., 1960; Aitken et al., 1964, 1968; Fleming, 1966, 1970; Zimmerman, 1966, 1971; Mejdahl 1969). At the present TL methods are firmly established for testing the authenticity of art ceramics and for comprehensive reviews on applications of luminescence methods in dating archaeological materials reference is made to the work Aitken (1985, 1999) and Roberts (1997) just to name a few. Regarding the applications in geology, luminescence dating is a method of major importance for the study of the quaternary, as its applicability time range (a few 10s of years to several hundred of

thousand years) makes it one of the very few dating methods that can temporally bridge radiocarbon to methods applicable to older ages such as potassium-argon of fission track dating methods. Wintle and Huntley (1979, 1980) and Wintle (1981) were the first to present a valid application of TL methods in dating sediments. Their first work concerned dating of deep sea core sediments but the technique was subsequently extended to a wide variety of sediments (see for example the reviews of Wintle, 1990; Prescott and Robertson, 1997; Wintle 2008 b). In 1985 Huntley et al discovered that a luminescence signal that comes from traps that are stable over geological times can be stimulated in quartz using light from a green argon-ion laser (514.4nm) instead of heat. The next significant advance was made by Hütt et al (1988) who showed that IR stimulation can result in luminescence from feldspars and that this signal is useful for dating. It was suggested, and later confirmed, that optical dating is a better method for dating sediments than TL, as it is based on analyzing the exact signal that has been reset in nature by the bleaching process.
Technological advances lead to the development of instrumentation in luminescence dating. Early luminescence readers consisted of devices for which only aliquot could be measured at a time and irradiations and thermal treatments had to be performed in separately (Aitken 1985). Probably the biggest advance in instrumentation was the introduction of high-power light emitting diodes for stimulation that replaced expensive lasers thus making the equipment affordable for more laboratories (see review by Bøtter-Jensen, 1997). The first automated luminescence readers produced by Risø became available in 1983 (Bøtter-Jensen, 1997). Nowadays more than 200 laboratories in this world are equipped with this kind of machines and detailed description of the instrumentation can be found in Markey et al., 1997; Bøtter-Jensen et al., 1997, 1999, 2000, 2002, 2003a, b and Thomsen et al., 2006.

Due to the advances in methodology (Hütt et al., 2001) and in particular the development of single aliquot protocols (Murray and Wintle, 2000, 2003; Wintle and Murray, 2006) increased precision is available for determining equivalent doses, optical dating being at the moment the mainstream in luminescence dating research (Stokes, 1999; Duller, 2004; Koster, 2005; Lian et al., 2006; Wintle, 2008a; Roberts 2008).
Because of the variability in the luminescence properties of natural minerals (Choi, 2003; Huot, 2003; Kiyak et al., 2007; Li et al., 2006; Roberts, 2006; Steffen et al., 2009) it is continuously required that workers in this field to give a detailed account of the methodology used also to discuss of the reliability of the ages presented. This led to advances in the past decades that are rarely matched by other methods and to a degree of quality control seldom seen with other dating techniques. (Lian et al., 2006)

I.3. MINERALS USED FOR DATING

The choice of mineral and grain size used for dating usually depends on the availability within the sample. In sediments, quartz and feldspars are ubiquitous minerals.

The use of a mineral fraction instead of a mixture of minerals is advantageous because it gives a much better insight of the luminescent phenomenon. Quartz is SiO_2. The most common form of quartz that exists in nature is trigonal alpha quartz which is composed exclusively of $[SiO_4]^{4-}$ tetrahedra with all oxygens joined together in a three-dimensional network. Defect centers (point defects, as they are important in luminescence) in quartz can be divided can be divided in two main types: defects caused by foreign ions (foreign ions centers and interstitial defects) and centers associated with empty oxygen and silicon positions **(Table I.1)**; however the inter-relationship between these two types of defects is very strong.

Table I.1: ***Known defect centres in quartz adopted from Preusser et al., (2009)***

Defect	Annealing temperature	Magnetic properties
Intrinsic defects		
$[O_3Si{:}SiO_3]$	Thermodynamic equilibrium	Diamagnetic
$[O_3SiOOSiO_3]$	Thermodynamic equilibrium	Diamagnetic
E′- centers	400 °C	Paramagnetic
E′′-centers	60-100 °C	Paramagnetic
NBOHC	500 °C	Paramagnetic
$[O_3SiOO^-]$	300-350 °C	Paramagnetic
Impurity related defects		
$[H_4O_4]^0$	Stable	Diamagnetic
$[H_3O_4]^0$	90-150 °C	Paramagnetic
$[AlO_4/H^+]^0$	Stable	Diamagnetic
$[AlO_4/M^+]^0$	Stable	Diamagnetic
$[AlO_4]^0$	260 °C	Paramagnetic
$[AlO_4/H^+]^+$	< -123 °C	Paramagnetic
$[FeO_4/H^+]^0$	300-450 °C	Paramagnetic
$[FeO_4/M^+]^0$	300-450 °C	Paramagnetic
$[TiO_4]^0$	Stable, formed at high temp.	Diamagnetic
$[TiO_4/M^+]^0$	200-300 °C	Paramagnetic
$[TiO_4/H^+]^0$		
$[TiO_4/H^+]^+$		Paramagnetic
$[TiO_4]^-$		
$[GeO_4]^0$	Stable	Diamagnetic
$[GeO_4/Li^+]^0$	300 °C	Paramagnetic
$[GeO_4/Na^+]^0$	< -20 °C	Paramagnetic
$[GeO_4]^-$	20 °C	Paramagnetic
$[SiO_4^-/M^+]^0$	-93 °C	Paramagnetic
$[SiO_4/Li^0]^0$	< -83 °C	
$[O_3POAlO_3]$	Stable	Diamagnetic
$[O_3POAlO_3]^+$	300 °C	Paramagnetic

In the last years quartz seems to have become the mineral of choice in luminescence dating. This is caused by the development of single-aliquot procedures, more specifically the single-aliquot regenerative-dose protocol (Murray and Roberts, 1997; Murray and

Wintle, 2000, 2003) that has proven to be very reliable, and to give reproducible and accurate results (see, e.g., Stokes et al., 2000; Murray and Olley, 2002; Duller, 2004; Vandenberghe, 2004). Furthermore, there has been a lot of progress in understanding the mechanism of luminescence from quartz. Kinetic models have been developed (Bailey, 2001), while the linear modulation technique allows the identification and characterization of the different components of the OSL signal (Bulur et al., 2001; Singarayer 2002; Singarayer and Bailey, 2003; Jain et al., 2003; Choi et al., 2006; Kiyak et al., 2007).

Quartz is a usually an abundant mineral in sediments, and it has certain advantages with respect to (micro) dosimetry and anomalous fading. Anomalous fading is a malign phenomenon that may cause a severe underestimation of the age. Minerals such as zircon and feldspars suffer from anomalous fading, while it has been generally accepted that quartz is not affected by this phenomenon.

Apart from fading, however, feldspars do present a wide range of advantages. First of all, feldspars saturate at much higher doses than quartz. Therefore, they might prove to be advantageous for dating older deposits and. A second advantage is that feldspars are brighter than quartz (Aitken, 1998). As quartz is relatively dim, this may limit the use of this mineral for dating very young samples. Using a brighter mineral could improve the signal to noise ratio. Last but not least, feldspars can be stimulated and measured in the presence of quartz, but not the other way around, because as it will be further discussed in the following chapter, IR wavelengths can be used for stimulating feldspars, but not for quartz. At the very moment, the studies for use of feldspars in dating seems to be rejuvenating (Thomsen et al., 2008; Buylaert et al., 2009; Murray et al., 2009).

I.4. THE MECHANISM OF LUMINESCENCE

I.4.1. General one trap model

The mechanism of luminescence production is highly complicated and not yet fully understood. Even in the case of luminescent dosimetry where artificially created and doped phosphors such as the ones based on LiF are used there is still not a consensus about the complete causes for the different phenomenon that are observed. Natural crystals such as quartz or feldspars that are used for dating are even far more complicated systems. However, the following simplified representation does allow understanding how luminescence is produced in minerals, and how this phenomenon can be exploited for dating.

Luminescence is related only to materials that have more or less order in their structure. Hence, it is a property of crystals and some vitreous materials. The existence of order or at least local order makes us think in terms of delocalized energetic states or

bands. Another feature of the materials that display luminescence is that they are either semiconductors or insulators. This implies that the main delocalized energy bands are separated by an energy gap. In the case of a perfect crystal, there are no energy levels possible inside this gap. Naturally formed crystals, however, contain defects, such as impurities and missing atoms or ions, which give rise to localized states or intermediary energy levels inside the energy gap.

Three fundamental steps can be distinguished in the luminescence process (**Figure I.2**):

Irradiation: during the interaction of ionizing radiation with a crystal electrons from the valence band get a surplus of energy and can leave this band ascending to the conduction band. For every electron that is raised into the conduction band a hole (that can be seen as a positive charge) is left behind in the valence band. An important feature now is that electrons can not be accumulated in the conduction band. So the concentration of electrons in the conduction band has to be quasistationary. So for these electrons there are two possibilities: to return to the valence band or to get trapped at a defect. The same thing can happen to the holes.

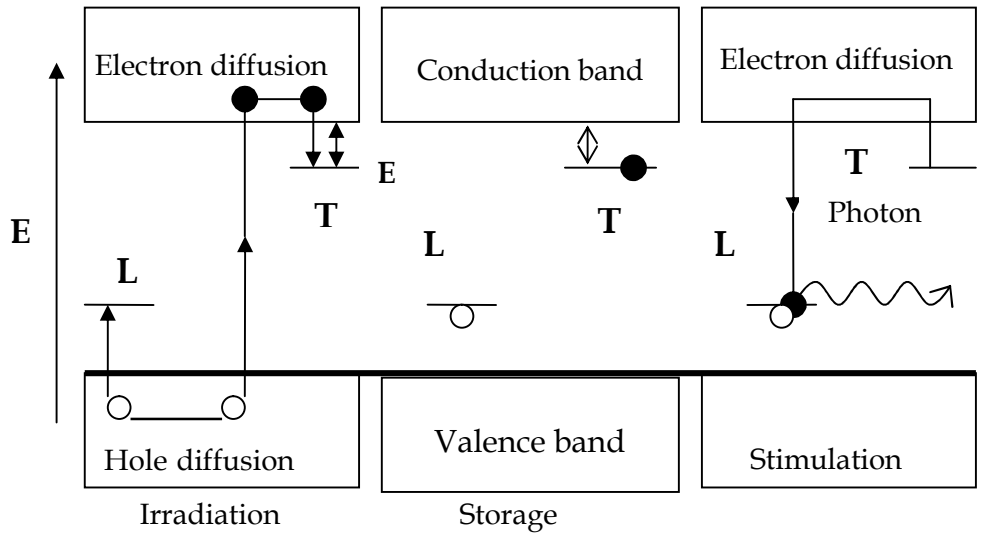

Figure I.2: *Schematic representation of luminescence process (Adopted from Aitken, 1998) T represent electron traps while L represent luminescence centers.*

Storage: Part of the energy of the nuclear radiation is now stored in the crystal lattice in the form of trapped electrons. Due to Pauli's exclusion principle, one trap can accommodate a maximum number of two electrons. The effectiveness of a given type of trap for storing electrons is determined by the energy E, the energetic difference between the bottom of the conduction band and the localized level. E is usually referred to as the trap depth. For

dating we are interested in traps that are deep enough for the lifetime of the electrons in these traps to be at least several million years.

Eviction: if we expose the crystal to heat or light the electrons may absorb enough energy to jump into the conduction band again. The electrons can subsequently be trapped again, or they can recombine with the holes in the so-called recombination centers. These recombinations can be accompanied either by a phonon emission (that is absorbed by the lattice) or by the emission of a photon. The latter emission is called luminescence and the center where it occurs a luminescence center. The wavelength of the emitted photon is a characteristic of the type of center. The luminescence emitted is proportional to the accumulated dose.

It is worth mentioning that OSL and TL signals are often accompanied by photoconductivity phenomena, and OSL is not to be confused with the related phenomenon of photoluminescence (PL) that can be stimulated from similar materials but which is generally not dependent upon irradiation of the sample. PL is the excitation, via the absorption of light, of an electron in a crystal defect within the material, resulting in excitation of the electron from the defect's ground state to the excited state. Relaxation back to the ground state results in the emission of luminescence, the intensity of which is proportional to the concentration of excited defects. Ionization of the electron from the defect (i.e. a transition from a localized to a de-localized state) does not generally occur, however, and there is no associated photoconductivity. As a consequence of the above mechanism, the wavelength of the emitted luminescence is longer than that of the excitation light (Stokes` shift), while in the case of OSL things are the other way around. (Bøtter-Jensen et al, 2003a)

The model presented in the above is referred to as the general one trap (GOT) model. It is an oversimplification as in reality there are more than one type of traps and recombination centers competing for charge. Exposure to radiation can also produce more defects, but this is generally not the case for the low radiation doses encountered in natural environment.

1.4.2. Modeling processes giving rise to OSL in quartz

Models of varying complexity have been developed over time to explain the mechanism of luminescence (see e.g. McKeever and Chen, 1997). The simplest of these are based on first order kinetics, which is the assumption that after eviction from a trap the probability of retrapping is negligible compared to the probability of recombination. Still, even the simplest models involve sets of coupled, non-linear, first order differential equations which cannot be solved analytically.

The large volume of experimental data published on quartz OSL led Bailey (2001) to formulate a model specifically for this material. To encompass the width information on

TL and OSL Bailey (2001) proposed that there should be five electron trapping centres and four recombination centres, The electron traps correspond to the 110 ^{o}C respectively 230 ^{o}C TL peaks, the fast respectively the medium components of the OSL (see section 1.3.5) an additional deep thermally disconnected trap. Electrons trapped in the deep trap and the 230 ^{o}C TL peak trap can not be optically stimulated. Of the recombination centres two are thermally unstable and non- radiative (R1 and R2). The third centre (L) is thermally stable and radiative. This is the centre where recombination of the electrons gives rise to the OSL signal. The last recombination centre (K) is thermally stable but non-radiative.

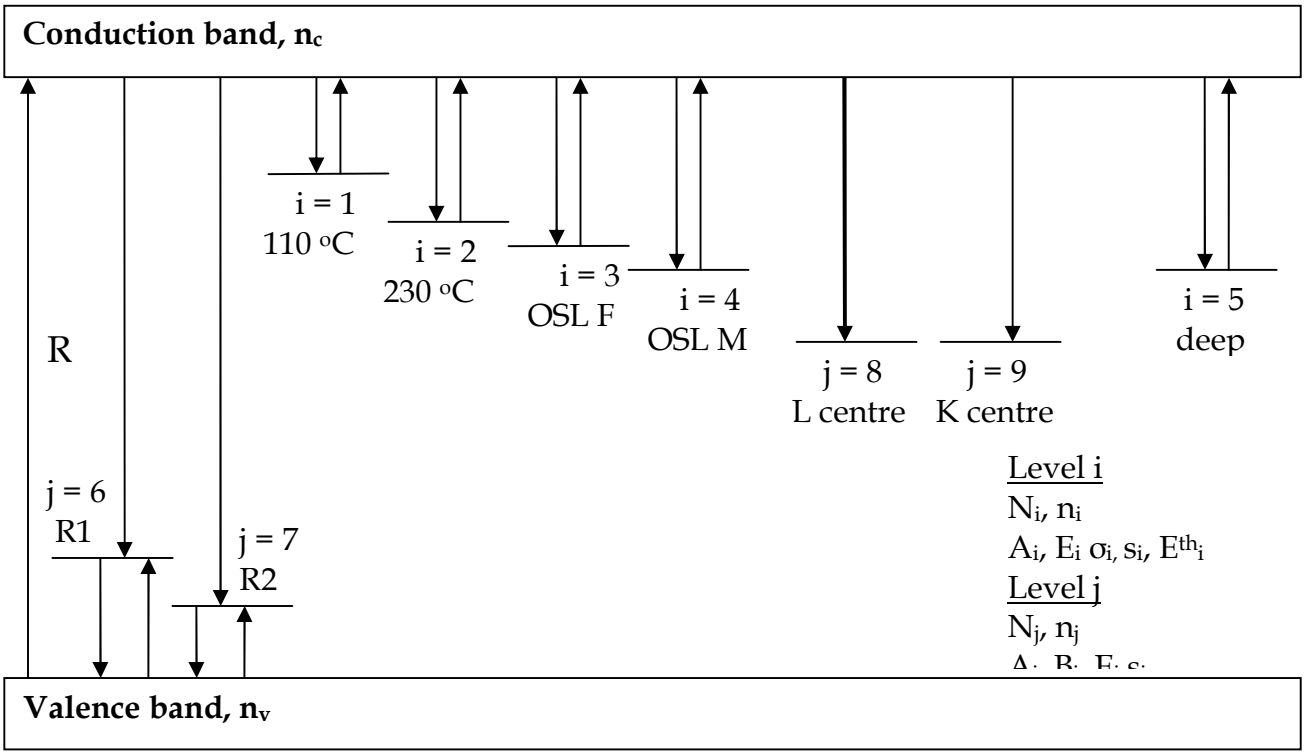

Figure I.3: *Band diagram of quartz as modeled in Bailey (2001) and Bailey (2004). Electron trapping centres are denoted by suffix i and hole trapping centres by j. The vertical position of each centre indicates the energy. Following Huntley et al (1996) the band gap is 7.4 eV. Allowed charge transitions are indicated by arrows. The OSL signal used for dating is a consequence of the transitions depicted in color.*

Figure 1.3. represents the model simulated by Bailey (2001). Where:
- n_c represents the concentration of electrons in conduction band (cm $^{-3}$)
- N_i represents the concentration of electron traps (cm $^{-3}$)
- n_i represents the concentration of trapped electrons (cm $^{-3}$)
- Ai represents the conduction band to electron trap transition probability (s^{-1})
- E_i represents the electron trap depth below the conduction band (eV)
- σ_i represents the photo-ionization cross section (cm ^{2})
- s_i represents the frequency factor (s^{-1})

- E^{th}_i represents the thermal energy required to raise electrons from the ground state of the trap to excited levels within the trap (eV)
- N_j represents the concentration of hole traps (cm^{-3})
- n_j represents the concentration of trapped holes (cm^{-3})
- Aj represents the valence band to hole trapping probability (s^{-1})
- Bj represents the conduction band to hole trapping probability (s^{-1})
- E_j represents the hole trap depth above the conduction band (eV)

The model was shown to reproduce empirical data for measurements of dose response, thermal activation, temperature and power dependency of the OSL signal, among others. Later, simulations of the dose absorption in quartz over geological timescale and their implications for the precision and accuracy of optical dating were presented based on this model (Bailey 2004). This will be further discussed in Chapter V.

I.4.3. Stimulation and emission spectra of quartz and feldspars

Stimulation spectra give information related to the trap depths, while emission spectra give information about the recombination centers. The first information is very important for selecting a certain signal while the latter helps selecting the most appropriate detection window for dating as different emissions might have different characteristics. Interpretation of stimulation and emission spectra of natural crystals is not straightforward due to the large variety of possible defects. As a consequence the energetic band in which natural crystals can be stimulated is wide and also a wide range of different luminescence emission bands occur. Nevertheless, it has been observed that certain emissions are dominant or specific to certain minerals. For detailed accounts on spectral information from minerals relevant for luminescence dating, reference is made to the reviews of Duller (1997) and Krbetschek et al. (1997).

Bøtter-Jensen et al. (1994) investigated the stimulation spectrum of quartz. They found an increase in the signal intensity with decreasing stimulation wavelength (increasing energy). Wavelengths in IR-region are inefficient in stimulating luminescence from quartz at room temperature. However, increasing the temperature helps the eviction and at higher temperatures even low energy photons may be effective. This phenomenon is called thermal assistance.

Over time, a variety of light sources have been used for stimulating quartz. Nowadays, most laboratories use the powerful blue (470nm) LED`s developed by Bøtter-Jensen.

Using the 514nm line from an argon ion laser, Huntley et al. (1985) showed that not only quartz, but also feldspars, can be stimulated using visible wavelengths. The first stimulation spectrum from feldspars was published by Hutt et al. (1988). They observed a

large stimulation peak in the near infrared (1.4eV) and demonstrated that the charge thereby evicted comes from traps which are stable enough to permit dating. The mechanism they proposed to explain their observations is represented in **Figure I.4.**

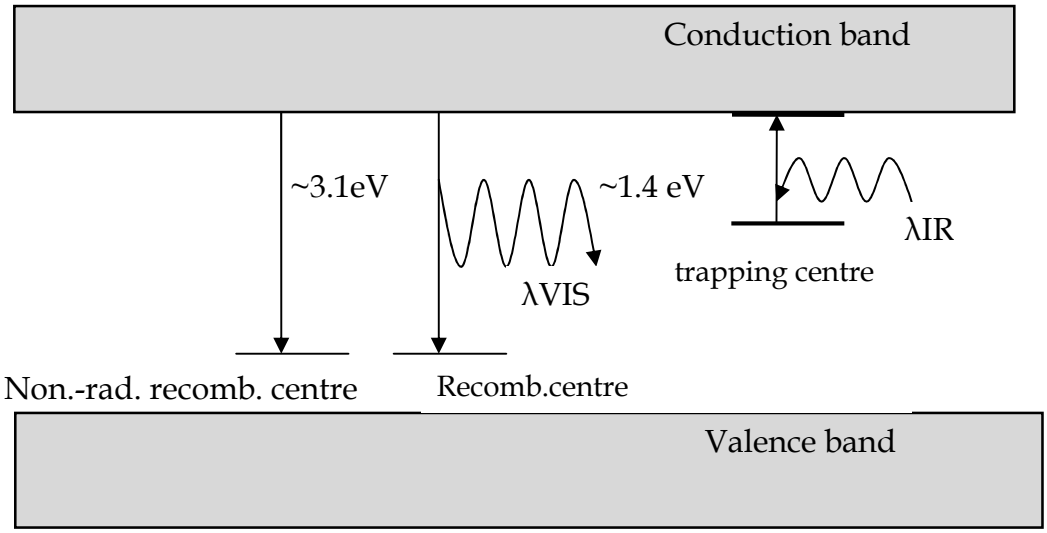

Figure I.4: *Two stage detrapping process (photon-phonon) of IRSL production in feldspars as suggested by Hutt et al. (1988). The figure is redrawn from L. Bøtter-Jensen, S.W.S. McKeever and A.G. Wintle (2003).*

The model involves a two stage detrapping process. In the first stage, photons of infrared raise electrons from the ground state into an excited state. In the second stage, some electrons are raised from the excited state into the conduction band thermally, i.e. by lattice vibrations, and then by diffusion some reach luminescent centers. This is a resonant process, as supported by the fact that the peak in the stimulation spectrum was observed to have a Gaussian shape. The model allows for stimulation in the visible region as well, in which case the transition is a direct one into the conduction band.Other explanations of the phenomenon have been given throughout time. The donor-acceptor theory of Poolton (Poolton, 2002a) proposes that a small thermal energy is required to hop the electron from an excited state of the trap directly to an excited state of the recombination center. The existence of band tail states arising from random fluctuations in bond length and angles in disordered crystals was also proposed (Poolton, 2002b). For further details reference is made to Bøtter-Jensen et al (Bøtter-Jensen et al, 2003a, section 2.4.5 and the literature cited therein).The explanation of Hutt et al. (1988) and depicted in the figure still remains widely accepted. Concerning the TL of quartz though three main emission bands have been observed around 360-440, 460-500 and 600-650nm (Krbetschek et al., 1997). In any one sample the observed emissions in these regions may be composite bands (Bøtter-Jensen et al., 2003a).

There is little information related to spectral emission of quartz under optical stimulation. Huntley et al. (1991) reported a single emission band centered at 365 nm

under stimulation with 647 and 541nm laser light. While Stoneham and Stokes (1991) reported this emission at about 380nm. Studies infer that OSL signals and the 110 ^{o}C and 325 ^{o}C TL peaks share a common recombination centre and this emission is assigned to electron recombination at Al centres with a trapped hole $[AlO_4]^o$ (Martini et al., 2009).
More information is available concerning feldspars. Blue emission is believed to be characteristic for all feldspars and it was observed by Hutt et al. (1988) under stimulation peaks of 2.23 eV (550nm), 1.43eV (865nm), 1.33 eV (930) and 1.29eV (960nm). Bailiff and Poolton (1991) and Huntley et al. (1991) reported emissions at about 320-340nm, 400nm and 560-570nm. Krbetschek and Rieser (1995) also showed IR-OSL at about 280nm and also in the red /IR range.

I.4.4. Thermal stimulation -TL glow curves

As it was previously mentioned the trapped electrons can be released by heating (TL) or by the action of light (OSL or IRSL).

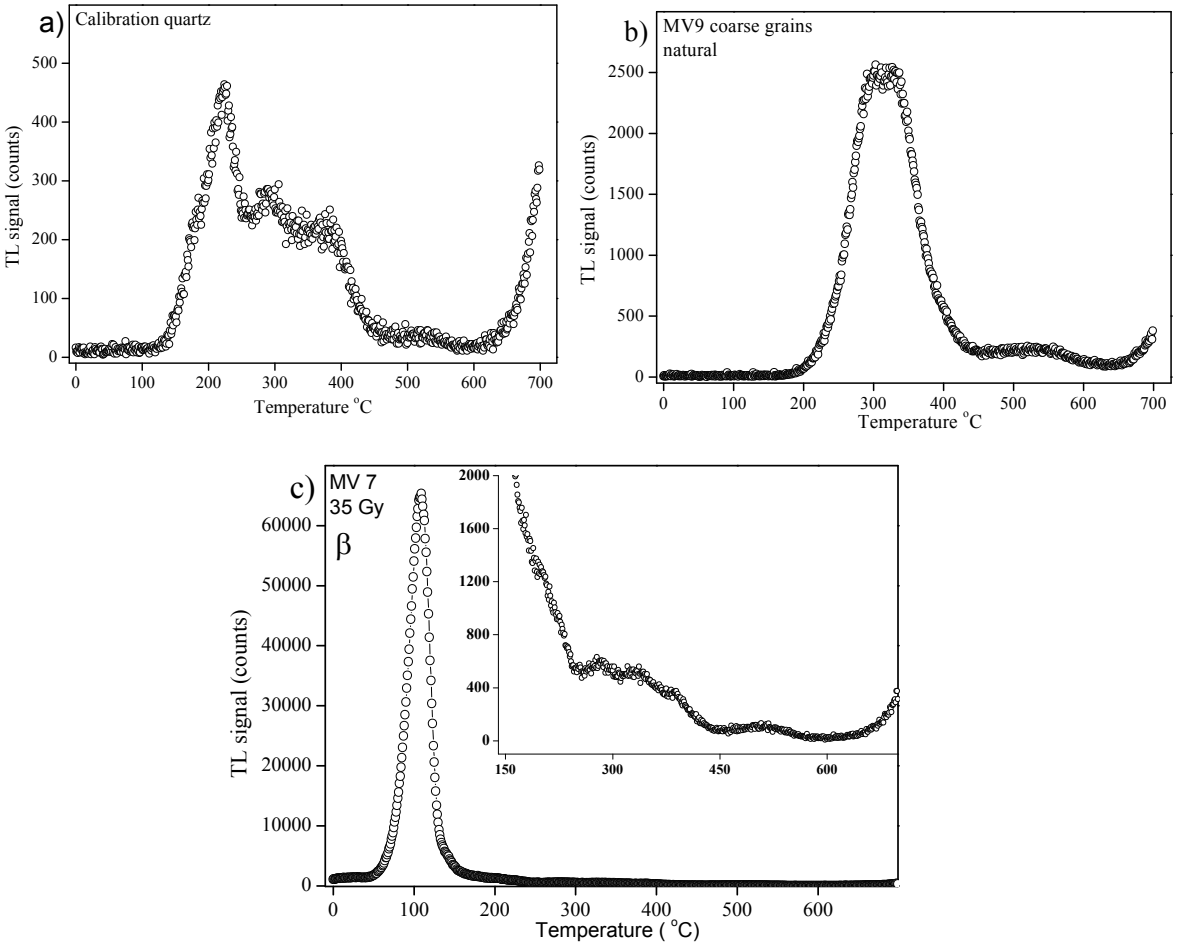

Figure I.5: *TL glow curves(heating rate of 5 ^{o}C/s) of a) calibration quartz, b) natural signal from coarse grains of quartz extracted from loess, c) artificially induced signal in coarse grains of quartz extracted from loess measured immediately after irradiation.*

In the case of thermoluminescence, the sample is gradually and rapidly heated and the information obtained has the shape of a glow curve. The peaks indicate the thermal depth of the traps that are emptied. Glow curves of sedimentary quartz grains analyzed in this work are presented in the previous figure.

Calibration quartz is quartz that has been gamma dosed approximately one year ago. In the glow curve (**Figure I.5.a)**) the TL peaks at 190 ^{o}C (with a thermal lifetime of $0.7*10^{3}$ years (Aitken 1985, Appendix E)), 230 ^{o}C (with a thermal lifetime of $130*10^{3}$ years (Aitken 1985, Appendix E)), 325 ^{o}C (with a thermal lifetime of $100*10^{6}$ years (Aitken 1985, Appendix E)) and 375 ^{o}C (with a thermal lifetime of $>10^{6}$ years (Aitken 1985, Appendix E)) are appear. In the natural signal, accumulated over geological time is dominated by the long lived signals (**Fig 1.5.b**) while in the case of measurements performed immediately after irradiation (**Fig 1.5.c**) the brightest peak is the one at 110 ^{o}C (with a thermal lifetime of $1*10^{-3}$ years (Aitken 1985, Appendix E)). Note that the long lived peaks exist though (see inset).

1.4.5. Continuous wave optically stimulated luminescence CW-OSL- shine down curves

In the case of continuous wave optically stimulated luminescence (CW-OSL and CW-IRSL), however, the luminescent signal is recorded as function of stimulation time (at constant power and wavelength range). The resulting plot is called a shine down curve.
For age determination of aeolian sediments optical stimulation has great advantages over TL. This is because preferential measurements are performed on the part of the luminescence signal that is most sensitive to light and so the OSL signal is reset to zero (bleached) by exposure to light more rapidly and completely than the TL signal.

In OSL the electrons are evicted from traps by absorption of photons. The rate of eviction depends on the intensity of the stimulation light and the sensitivity of that certain trap to light. Also it is important to realize that the thermal depth of a trap is not the same as the optical depth of a trap. The energy necessary to optically empty a certain trap type is usually greater than the thermal energy that is needed. The cause of this seems to be that the process of photo eviction is more rapid than the relaxation time of the lattice whereas the process of thermal eviction is not (Aitken, 1998).
Obviously, for a photon to be effective it has to have energy at least equal to the thermal depth of the trap but this is not the only parameter that characterizes the light sensitivity of the trap (Aitken, 1998). Still it is normal to have a general tendency that the shorter the wavelength the more effective stimulation.

The OSL/ IRSL signal is usually recorded at constant stimulation power as function of stimulation time. The resulting plot is called a shine-down curve.

After a prolonged stimulation all the light-sensitive traps are emptied. The area beneath the shine-down curve (the light sum) is proportional to the number of electrons that were trapped, and hence the accumulated dose. In practice, only the first part of the shine-down is used because this signal comes from the most light sensitive traps. The latter part of the shine down is used for background estimation.

Theoretically one would expect that the shine-down exhibits a singe-exponential decay. Indeed, assuming that the loss of trapped electrons per unit of time (expressed as a percent of those remaining trapped) remains constant throughout the shine-down, the number remaining is expected to decrease exponentially.

The OSL emitted per unit of time is proportional to the rate at which the electrons are evicted from their traps. Hence, one would expect the decay of OSL with stimulation time to follow an exponentially decaying law of the form:

$$I_{OSL} = I_0 \exp(-t / \tau_d) \quad (1.1)$$

Where I_0 is the initial OSL intensity, t represents the stimulation time and τ_d is a decay constant.

More explicitly it can be wrote that:

$$I_{OSL} = n_0 p \exp(-t \cdot p) \quad (1.2)$$

Where n_0 is the concentation of electrons in the trap of interest at the start of stimulation, and p is the rate of stimulation (in units of s^{-1}) of electrons from the trap and is related to the incident photon flux Φ and the optical photoionization cross-section σ for a given wavelength:

$$p = \Phi \cdot \sigma \quad (1.3)$$

It should be noted that the popular OSL systems like the Risø machines used in this work use a band of stimulation wavelengths. Since both Φ and σ vary with wavelength, a range of values for p will result. However, a single exponential decay is still expected, with the decay constant now given by $\tau_d^{-1} = \int \sigma(\lambda)\, \Phi(\lambda)$ and the evaluated effective decay constant is the mean of the distribution of decay constants caused by the broad band stimulation. (Bøtter-Jensen et al., 2003a). However, a slower than exponential behavior is typically noticed in the case of quartz. This is illustrated in **figure I.6**. A number of possible causes have been suggested to explain the slower-than exponential decay, including the possibility of multiple traps contributing to the OSL signal, retrapping, and changes in luminescence intensity. (Aitken, 1998). Smith and Rhodes (1994) demonstrated that the OSL signal could be broken down into three components which they called "fast", "medium" and "slow" according to their decay throughout the stimulation **(Figure I.6).** Possible experimental effects due to the use of broad band stimulation or laser stimulation

were later on tested and found to be negligible. Thus, using the superposition principle, it can be written that:

$$I_{OSL} = \sum n_{i0} \cdot \Phi \cdot \sigma_i \exp(-t \cdot \Phi \cdot \sigma_i) \qquad (1.4)$$

In the case of IRSL from polymineral fine grains, it is no longer to be expected for the shine-down to exhibit an exponential decay. The signal originates from different traps characteristic to the different feldspar types present in the sample. A hyperbolic function ($L=L_0 (1+Bt)^{-P}$) has been reported as a good fit for IRSL shine-down curves of a number of feldspars. (Duller, 1997; Aitken, 1998). B is a factor depending on the initial population of trapped electrons, while p is a constant, generally having a numerical value between 1 and 2. **(figure I.7)**.

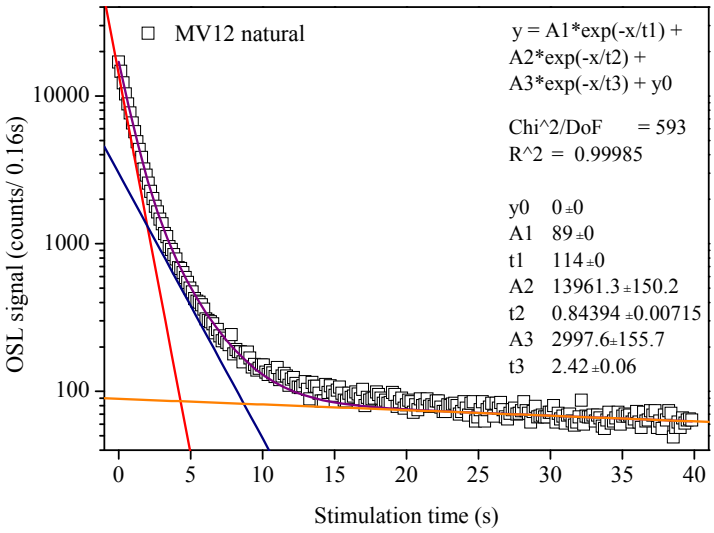

Figure I.6: *Shine down curve of natural signal for quartz fine grains of sample MV12 showing the contributions of the "fast", "medium" and "slow" components. Please note the logarithmic y axis. The slow component was derived from the last part of the decay curve and fixed during the fitting procedure.*

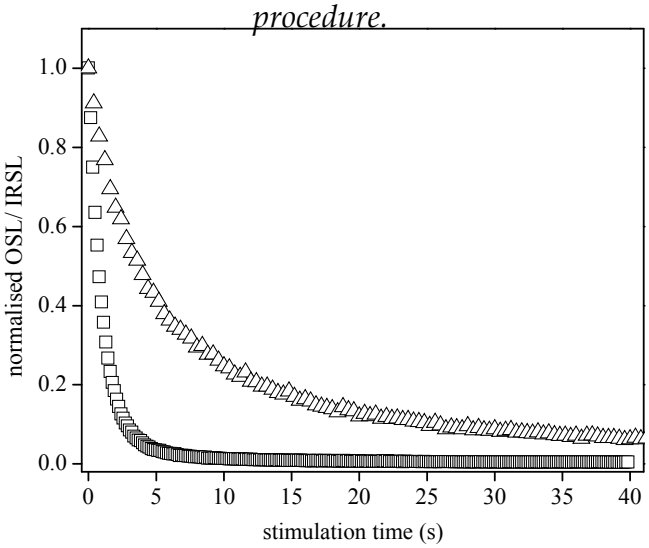

Figure I.7: *A comparison between the shine down curves of quartz (squares) and feldspar grains (triangles) extracted from loess- (Timar, 2006).*

Both the OSL and IRSL signals are influenced by the temperature during stimulation. The higher the power of stimulation, the higher the light output. At low temperatures (room temperature) the eviction rate increases about 1% per ^{o}C (Aitken, 1998). This is due to thermal assistance. On the other hand, there exists also a competing process, called thermal quenching, which causes the efficiency of luminescence centers to decrease with increasing temperature.

The reason of implying such a relatively high temperature for quartz (i.e. 125 ^{o}C) stimulation is that it was reported by many authors that charge transfer can occur both in and out of the shallower traps (like the one related to the 110 ^{o}C TL peak) during optical stimulation. Therefore Murray and Wintle (1998) suggested performing the measurements near this elevated temperature to eliminate these second order effects.

Both the OSL and IRSL signals are influenced by the power of the stimulation source and temperature during stimulation. The higher the power of stimulation, the higher the light output (see eq 1.10, **Figure I.8**).

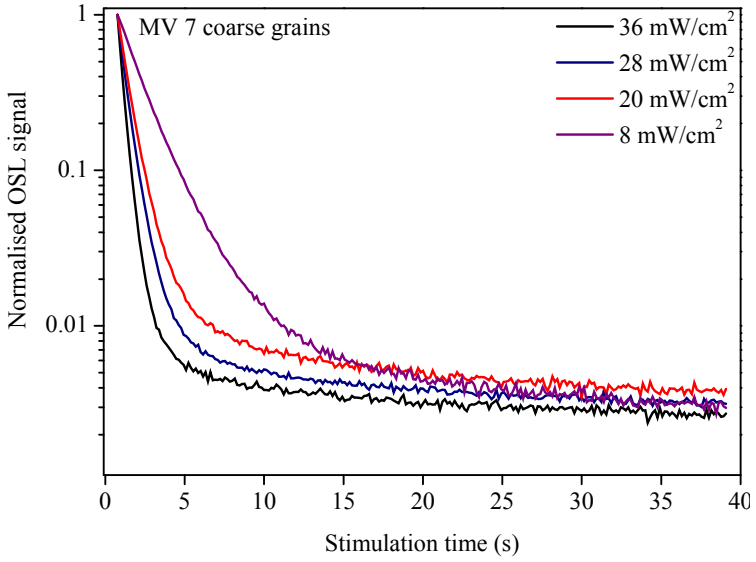

Figure I.8.: *A comparison between the shine down curves of coarse quartz from sample MV7 analyzed in this work as function of diode (λ = 470 nm) stimulation power.*

However using different stimulation powers should have no effect on the doses measured in retrospective luminescence dosimetry as there is a linear dependence between the OSL response and the stimulation power (Spooner, 1994a; Bulur, 2001). **Figure 1.9** present a comparison between the equivalent doses measured for a sample of quartz investigated in this work as function of stimulation power. For more details about equivalent dose determination reference is made to Chapter II.

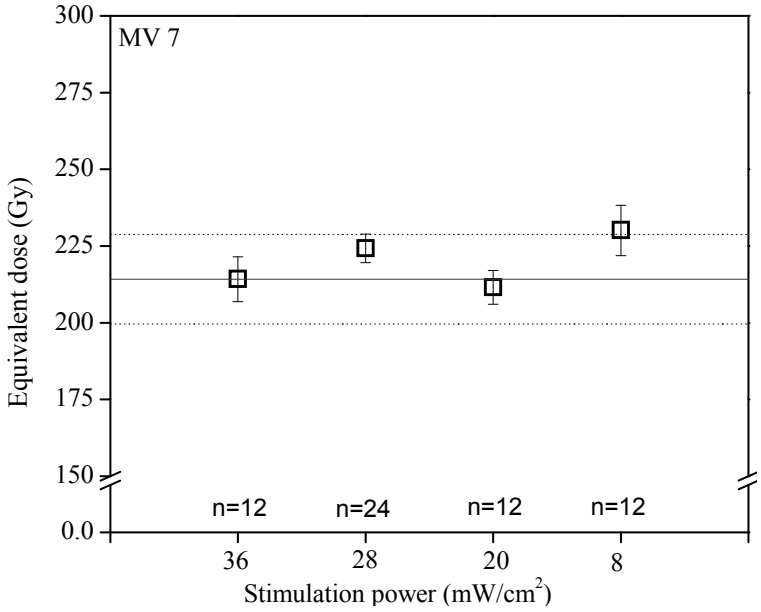

Figure I.9: *Comparison of equivalent doses obtained on coarse quartz from a sample analyzed in this work as function of diode stimulation power. n represents the number of aliquots annualized for each stimulation power. The solid red line (eye guide) represents the average of all aliquots analyzed. The dotted lines (eye guides) represent 1 standard error of mean deviation from the average.*

I.4.6. Linearly modulated optical stimulated luminescence -LM-OSL

The linear relationship between the detrapping probability and stimulation power is evidence for electron un-trapping as a result of a single-photon process and led Bulur (2001) to introduce an alternative technique for measuring OSL, called linear modulation (LM), in which the stimulation power is linearly increased **Figure I.10).** A plot of LM-OSL as function of time shows peaks similar to those observed in a thermoluminescence glow-curve, enabling a much easier separation of the different OSL components.
If the intensity is linearly ramped from a zero to a maximum value Φ_m according to:

$$\Phi(t) = \gamma \cdot t \tag{1.5}$$

Than according to equations 1.9.and 1.10

$$I_{LM-OSL} = n_0 \cdot \sigma \cdot \gamma \cdot t \cdot \exp\left(-\left(\frac{\sigma \cdot \gamma}{2} \cdot t^2\right)\right) \tag{1.6}$$

And applying the superposition principle, following Wintle and McKeever (2001) we can write:

$$I_{LM-OSL} = \gamma \cdot t \sum_{i=1}^{k} n_{oi} \sigma_i \exp\left(-\left(\frac{\sigma_i \cdot \gamma}{2} \cdot t^2\right)\right) \quad (1.7)$$

An experimental LM-OSL curve from a sample in which several traps are emptied simultaneously, but at different rates, can thus be described as a simple sum of first-order LM-OSL curves. It should be noted that each peak starts at from t=0, no matter what the values of σ and γ are. The shape of a LM-OSL curve of a single trap is that of a linearly increasing function (in proportion to the linear increase of stimulation power) followed by a Gaussian decrease in the OSL intensity as traps deplete. The time at which the maximum is achieved is given by:

$$t_{\max} = \sqrt{\frac{1}{\sigma \cdot \gamma}} \quad (1.8)$$

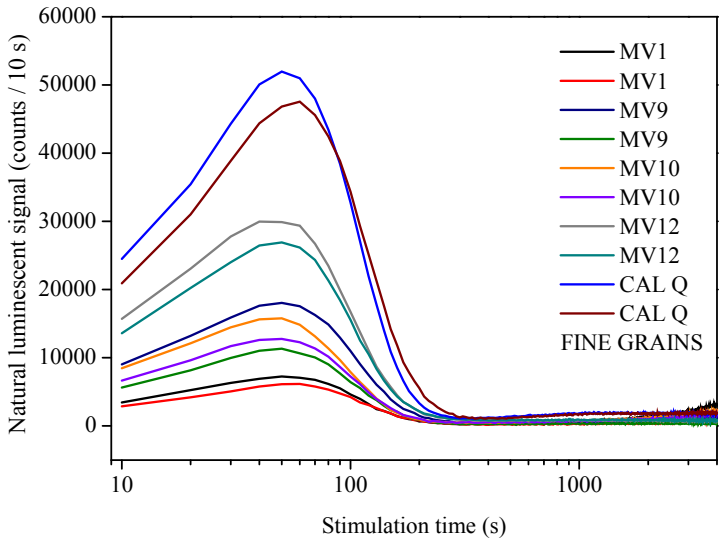

Figure I.10: *LM-OSL curves of natural signal for quartz fine grains of different samples analyzed.*

And the maximum LM-intensity is:

$$I_{\max}^{LM-OSL} = \frac{n_0}{t_{\max}} \exp(-\frac{1}{2}) \quad (1.9)$$

We can observe though that the position of the maximum is dependent on σ and the modulation ramp rate γ, thus LM measurement can serve as an empirical tool by visual comparison of signal derived from different samples.

I.4.7. Pulsed optically stimulated luminesecence (POSL)

The third major stimulation mode POSL the stimulation light is pulsed and the OSL is only measured in between the pulses There are several reasons why it may be advantageous to measure the POSL signal.

- pulsing enables reduction of the filtering required to separate the stimulation light from the emitted luminescence. More overlap between the stimulation and detection wavelengths can be tolerated for a given background.
- pulsing provides insight into the luminescence recombination process. The POSL signal after the stimulation pulse decays according to the lifetime of the luminescence centres being stimulated.

For quartz, time resolved spectra are registered after stimulation pulses of a few microseconds and allow the determination of luminescence centres lifetimes. Bailiff (2000) reported values of 40±0.6μs for synthetic quartz and an average of 33±0.3μs for granular quartz, luminescence being detected in 280-380nm region for stimulation wavelengths from 600-450nm. Chitambo and Galloway, 2000a,b, measured a lifetime of about 35μs for daylight bleached quartz for stimulation at 525nm, while Chitambo and Galloway, 2001 and Chitambo, 2003 reported s value of 40±1 μs for quartz OSL luminescence lifetimes measured below 100^{o}C in the fast, medium and slow component regions.

In a recent study Ankjaergaard et al (2009) analyzed TR spectra of 14 feldspar samples both under green and blue light stimulation. For green light stimulation, two components with average lifetimes of 41±0.1ns and 810±9 ns described the decay adequately, while in the case of blue light stimulation three components with average lifetimes of 1.37±0.02 μs, 6.9±0.1, respectively 43±1 μs were needed

- different luminescence centres have different relaxation lifetimes, which means that POSL provides an instrumental way of separating the luminescence emitted from different phosphors (further discussed in chapter II, section 5).

I.4.8. Signal growth and lifetime

The intensity of the luminescent signal is proportional to the number of trapped electrons: as more electrons become trapped, the luminescence intensity increases accordingly. However, the maximum amount of charge that can be stored is limited by the number of traps that is available. The longer the crystal lattice is exposed to radiation, the more traps are being filled until ultimately a situation of saturation is reached. On the other hand, the possibility also exists that, even at ambient temperature, electrons are

spontaneously evicted from their traps. Taking these effects into account, we can describe the amount of signal dL built up in a period dt of irradiation as:

$$dL = D^* \cdot S \cdot dt - \lambda_S \cdot L \cdot dt - \lambda_T \cdot L \cdot dt \tag{1.10}$$

Where

D^* is the dose rate of the irradiation

S is the sensitivity of the sample (the luminescent response per unit of dose)

λ_S and λ_T are decay constants associated with the aforementioned processes of saturation and thermal detrapping, respectively.

If we associate lifetimes τ_S and τ_T to the decay constants, equation 1.10 becomes:

$$dL = D^* \cdot S \cdot dt - \frac{1}{\tau_S} \cdot L \cdot dt - \frac{1}{\tau_T} \cdot L \cdot dt \tag{1.11}$$

Assuming at t=0, L=0 and integrating we get:

$$L(t) = S \cdot D^* \cdot \frac{\tau_s \cdot \tau_T}{\tau_s + \tau_T} \cdot (1 - \exp(-t/(\frac{\tau_s \cdot \tau_T}{\tau_s + \tau_T}))) \tag{1.12}$$

Equation 1.12 can be simplified to:

$$L(t) = L_{\max} \cdot (1 - \exp(-t/(\tau)) \tag{1.13}$$

Equation 1.13 shows that, theoretically, the increase in luminescence with time takes the form of a saturating exponential. The initial build up of luminescence through time ($t << \tau$) is approximately linear. In terms of doses, we can write (Wintle, 1997)

$$I = I_{\max}(1 - \exp(-D/D_c) \tag{1.14}$$

Where I is the intensity of luminescence corresponding to a dose D, I_{max} is the maximum signal attainable, and D_c is a parameter which characterizes the curve and the onset of saturation. A single saturating exponential is generally used for fitting the dose-response curves. As also pointed out by Wintle (1990), it is remarkable that the luminescence signal from a very large number of grains with different properties shows this exponential behavior. A linear term can be added to the exponential function for certain samples. This will be further discussed in Chapter V.

Going back to the thermal lifetime of a certain trap now, so the thermal lifetime of an energetic level placed in the energy gap at the distance E from the bottom of the valence band, and considering first order kinetics, so a very slight probability of recapturing after detrapping , it can be written that:

$$\tau_T = s^{-1} \exp(E/k_B T) \tag{1.15}$$

Where:

s is the frequency or pre-exponential factor (interpreted as the number of interactions per second with the lattice, multiplied by a transition probability, multiplied by a factor that takes into account the change in entropy associated with the transition from the trap to the delocalized band (McKeever and Chen, 1997)

T is the absolute temperature at which the sample is held (in K)

k_B is Boltzmann`s constant

E is the trap depth

So it can be assumed that due to thermal effects at a constant temperature the number of trapped electrons from a certain trap decays following a law of the form:

$$n = n_0 \cdot \exp(-t / \tau_T) \qquad (1.16)$$

Where n_0 is the number of trapped electrons at t=0 and n is the number of remaining electrons at time t.

When calculating the number of electrons that escape due to thermal effects during the time interval that is to be dated, it should be taken into account that there are no electrons in the traps at the beginning (t=0) and that they become trapped at an uniform rate thereafter. For such a situation, it can be shown (Aitken, 1985) that the fractional loss of luminescence due to escape during the sample's age span, t, is given by ½ (t/ τ_T) as long as t does not exceed one third of τ_T. This means that to avoid an age underestimation of, say, 5%, the thermal lifetime of the trap used needs to be at least 10 times the age.

Predicting lifetimes is important it helps to establish the likely time range over which a signal is useful for dating. Lifetimes can be predicted by determining s and E and techniques can be found in McKeever and Chen (1997). Some reported values of E and s for quartz have been summarized by Vandenberghe (2004), for values for activation energies for feldspars reference is made to the recent publication of Meisl and Huntley (2005). The corresponding lifetimes suggest that the OSL and IRSL signals usually employed for dating are sufficiently stable to permit dating over the entire time range of the Quaternary.

In the case of quartz Murray and Wintle used single aliquots to determine the decay curves of the initial OSL signal. A trap depth of 1.59 ± 0.05 eV was obtained, giving a calculated lifetime of 21×10^6 years at room temperature.

An approach of obtaining and displaying data on thermal stability of the OSL signal is to plot the OSL signal remaining after a fixed time at various thermal treatments. This procedure is termed pulse annealing and will be further described in Chapter V of this work.

I.4.9. Bleaching response spectrum

The first spectral information concerning the initial fast component of the OSL signal came from detailed studies of the bleaching of the OSL signal (Spooner, 1994a) concerning the initial fast component of the OSL signal came from detailed studies of the bleaching of the OSL signal (Spooner, 1994a). The OSL signal was measured using short exposures to the 514.5 nm argon-ion laser line and observed at room temperature with 2mm of Schoott BG-39 and 5.1 mm of Corning 7-51 filter glass in front of the photomultiplier tube. Bleaching was achieved with narrow band (10nm FWHM) interference filters in front of an 800W halogen lamp. The resulting decay curves for wavelengths from 400nm to 900nm were registered and it was observed that there is negligible bleaching for wavelengths greater than 690nm. Thus, no signal would be expected when quartz is stimulated using infra-red LEDs. Based on these findings, the lack of infra-red stimulated luminescence (IRSL) at room temperature is regularly used as a test of purity of quartz extracted from sediments. For wavelengths around 400nm, the stimulation is 10 times faster than at 514.5 nm, thus it can be inferred than it would be advantageous to use shorter stimulation wavelengths. As a result Bøtter-Jensen et al., (1999) selected blue LEDs with peak emission at 470nm.

To avoid measuring the stimulation light, it is very important that the stimulation and the emission wavelengths are well separated from each other. Also, the stimulation wavelength must be longer than the one from the desired luminescence, to avoid the use of signals originating from traps that are not relevant to dating (Aitken, 1998). At the same time, the stimulation light must be sufficiently energetic for the stimulation to be efficient. As an observation it is worth being said that in most dating studies the emission window was biased towards the blue region of the spectrum due to the fact that these short wavelengths are easier to be separated from the thermal background emission. During the last years, the red emission was given further attention due to the fact that it is believed that in the case of feldspars this emission is not affected by anomalous fading (Fattahi et al.; 2004; Stokes et al.; 2003; Lai et al., 2003). Still the UV-blue emission luminescence was proven to be very reliable as an integrating dosimeter for quartz, and there should be no obvious reason for the blue emission of feldspars not to perform well as long as monitoring for anomalous fading is performed.

A significant advantage a bleaching spectrum for the OSL spectrum of quartz is that it can be compared directly withy the bleaching of the TL peaks in quartz. Spooner (1994a) concluded the bleaching of the 325 ^{o}C TL peak and the prompt emission of OSL are both related to single-photon-absorption photo-ionization direct to the conduction band. Wintle and Murray (1997) observed 325 ^{o}C TL peak and the OSL during exposure to blue-green light from a filtered halogen lamp. Both signals decayed proportionally and were

effectively erased by an exposure of 10s, corresponding to 130 mJ/cm^2. Thus the correlation of the two signals was confirmed.

I.4.10. Sensitivity changes

The sensitivity of a sample is defined as the luminescence produced per unit of dose. It is well-known that sensitivity changes do occur during measurement cycles and mainly during preheating. This means that the signal emitted by a sample after a certain irradiation will differ from the signal obtained from the same dosing upon reusing.

There has been a lot of investigation on the sensitivity changes of quartz (Wintle and Murray, 1999, 2000, 2006; Murray and Wintle, 2000; Bailey, 2001). It seems that the sensitivity of quartz is an intrinsic property and changes in a complex manner during irradiation, heating and illumination. Actually, much of the research on sensitivity changes lead to the development of the SAR protocol for quartz (see following sections) which is based on the idea that sensitivity changes can be monitored and corrected for.
Less progress has been made in the understanding of sensitivity changes with respect to IRSL dating of feldspars. Nevertheless, it is well documented in literature that, here, sensitivity changes do occur as well. Roberts and Wintle (2003), e.g., investigated the sensitivity changes for polymineral fine grains of loess from Northern part of the Chinese loess plateau during IRSL. They observed an increase in the IRSL sensitivity with measurement cycle, with also a slight dependence on the preceding dose. Whatever the mineral used, sensitivity changes have to be taken into account.

I.5. THE AGE EQUATION

The target event to be dated by luminescence techniques is the time of sediment deposition. The underlying assumption is that at that moment the signal had been completely removed by sunlight exposure. If the signal was not totally removed, the sample is said to be incompletely or partially bleached. In such a case, the OSL age will overestimate the true age (as an example reference can be made to Olley et al 1998).
A comprehensive review on the setting-to-zero of IRSL and OSL signals from feldspars and quartz, respectively, is presented in Aitken (1998, Chapter 6).
The basic equation used to determine the age is:

$$Age = \frac{Palaeodose}{Annual \quad Dose} \tag{1.17}$$

The annual dose (Gy a^{-1}) refers to the radiation energy that is annually absorbed per unit of mass. It is usually derived from the measurement of the radiation emitted by the naturally occurring isotopes or from a determination of their concentrations

The palaeodose (Gy) is the dose absorbed by the minerals grains since they were last exposed to daylight. As this is a combined dose, resulting from exposure to α, β and γ radiation, it cannot be measured directly. Therefore, it is determined as an equivalent dose, i.e. the amount of artificial dose delivered by irradiation in the laboratory that induces a luminescence signal identical to the natural one in the sample. Thus:

$$Age = \frac{Equivalent \quad Dose}{Annual \quad Dose} \tag{1.18}$$

The equivalent dose is the natural luminescence signal divided by the luminescence sensitivity, and the luminescence sensitivity is the measure for the amount of luminescence resulting from the absorption of a given dose. Thus we can rewrite equation 1.27 as:

$$Age = \frac{OSLsignal}{OSLsensitivity \times AnnualDose} \tag{1.19}$$

I.6. ANOMALOUS FADING

The term fading is used to denote a parasitical loss of luminescent signal. This loss can be due to many causes. It can, for instance, be thermally or optically induced. For some minerals, however, fading is observed even after storage in the dark and at low temperatures. This phenomenon is termed anomalous fading, as the signal loss exceeds that predicted from the lifetime of the traps.

Lunar samples from the Apollo 11 and 12 missions have been amongst the first materials for which an anomalous loss of TL was reported. Wintle (1973) was the first to note the effect for terrestrial minerals. Subsequently, the phenomenon has been observed and investigated in a number of studies, such as those by Wintle (1977) and Spooner (1992; 1994b), to name a few. More recently, Huntley and Lamothe (2001) showed that anomalous fading is ubiquitous for sedimentary feldspars in North America. In the context of dating, the result of anomalous fading is an age underestimation. This has been reported in several dating studies using either TL or IRSL signals from feldspars or polymineral fine grains. For this reason, it is necessary to test for the presence of anomalous fading whenever the dating involves the use of feldspars. It can be pointed out here that samples showing age shortfall do not always show loss during laboratory tests. As a result, a number of authors associate the term anomalous fading with samples showing such loss and class as “long term fading” whatever effects are responsible for shortfall in samples which do not show laboratory loss (Aitken, 1998, Appendix D).

Tunneling has been the favored explanation since the first observations of anomalous fading **Figure I.11** shows the possible escape routes of an electron from a trap. Routes 1

and 2 represent thermal eviction, the probability of detrapping being a function of temperature of Arhenius type (see equation 1.7). Routes 3 and 4 represent escape by tunneling. The difference between 3 and 4 is that in the case of 4 the electron tunnels the barrier from its bottom, while in the case of 3 the particle hops first into an excited level by receiving thermal energy and then tunneling occurs. Tunneling is a quantum mechanical effect which cannot be explained din classical terms. It basically represents the fact that there is a finite probability for the particle to escape the potential barrier even if it does not have the necessary kinetic energy.

In the case of trapped electrons and recombination centers in a crystal the probability of recombination via quantum mechanical tunneling is given by the overlapping of the two wavefunctions of the pair trap-centre.

For a trap and a recombination center separated by a distance R the tunneling rate (meaning the probability per unit of time for the transition to occur) can be written as:

$$P(R) = s \cdot \exp(-R/a) \tag{1.20}$$

Where s is the frequency factor and a is a constant, roughly half the Bohr radius of the electron in the trap. So the probability of decay is an exponential function of the barrier thickness, temperature not being involved in the dependence anymore. That is why fading by tunneling is generically called athermal fading.

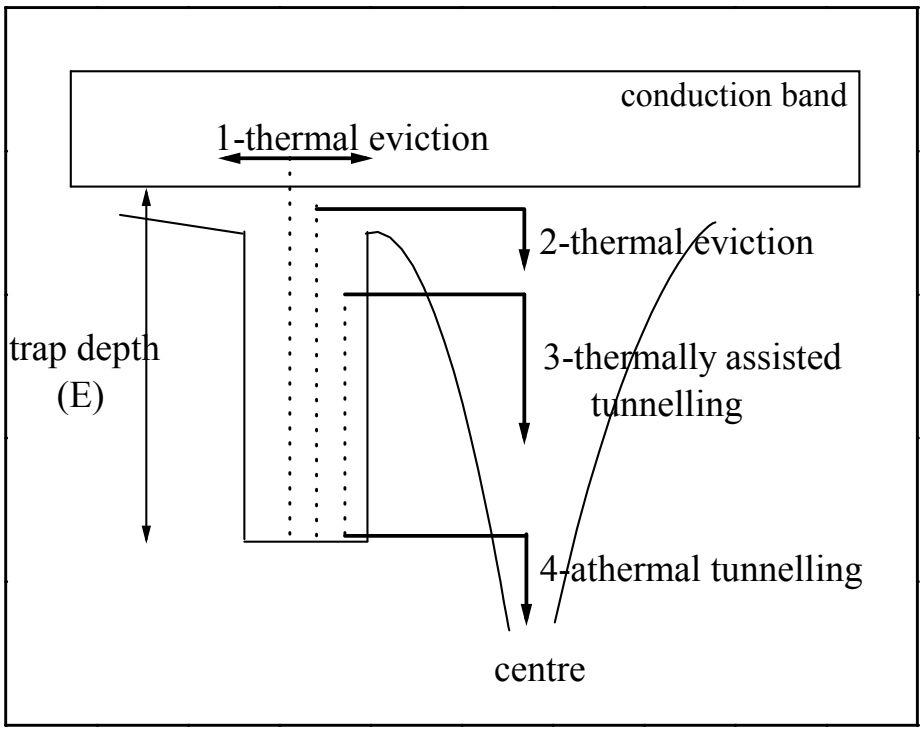

Figure I.11: *Escape routes from a trap. Redrawn from Aitken 1985.*

There is a very important implication of this formula: the critical dependence on the separation distance of the traps and recombination centers. This means that even for electrons with the same trap depth the probability of recombination via quantum mechanical tunneling can vary dramatically. The closest pairs will recombine first, and as time passes it will be more and more difficult for recombination to occur. This leads to a slow decrease in the detrapping rate, with roughly hyperbolical time dependence (1/t) as it was observed experimentally.

The dependency on the proximity of centers implies that if they are randomly distributed then high concentrations are required. This leads to the idea that bright minerals are more likely to be affected (and this is easily observed, feldspars being brighter than quartz); Then the state of crystallization seems also to be a factor (Aitken 1985). It is expected that crystals with more structural defects like the ones that come from volcanic rocks to suffer more from fading than the ones nicely crystallized such the case of plutonic rocks. Still, as a note it must be added that a very recent study of Huntley and Lian (2006) concluded by analyzing 77 K-feldspar extracts that the fading rates of K-feldspars from sediments derived largely from volcanic bedrock are not higher than those from non-volcanic bedrock.

The dependency on the trap/centre distance leads to the prediction that the rate of detrapping is proportional to t^{-1}, t being the time elapsed since irradiation. The number of electrons lost through tunneling is then proportional to log t. It can be shown (Aitken, 1985; Appendix F) that the number of electrons detrapped and, therefore, the luminescence L_i lost in the time between t_1 and t_2 owing to tunneling is given by

$$\frac{L_2 - L_1}{L_1} \approx \ln^2(st_1)\ln(t_2/t_1) \qquad (1.21)$$

as long as the number of electrons detrapped is small compared to the number trapped at time t_1. A logarithmic signal decay has been observed experimentally, and these observations lend strong support to an explanation of fading in terms of tunneling.

Besides tunneling, other mechanisms have been put forward to explain fading. For more details on these, and other suggested causes of age shortfall, reference is made to Aitken (1985; Appendix F; 1998, Appendix F) and Bøtter-Jensen et al. (2003a)

For the sake of completeness the most important ones will be outlined below:

- Localized transitions model (Templer 1986)
- Erroneous trap parameters
- Enhanced trapping efficiency for laboratory irradiation due to high dose rate.
- Absorption of UV within large grains of K-feldspar (Duller 1997; Wallinga and Duller 2000)

These mechanisms can be operable to a certain extent in certain synthetic or natural crystals and can lead to age shortfall but in the case of feldspars quantum mechanical

tunneling explanation is highly sustained by the correlation with low temperature phosphorescence or tunneling afterglow.

Strong support for quantum mechanical tunneling as an explanation for anomalous fading is provided in measurements of phosphorescence when recently irradiated samples are taken down to liquid nitrogen temperature. This phosphorescence was called "tunneling afterglow" by Visocekas (1985). It can be observed in the wavelength region of 590-890nm, but not in the region from 305-590nm.

A typical afterglow observed for feldspar is represented in **figure I.12.** The sample was irradiated at room temperature and the luminescence was measured. At first the signal results from recombination due to thermal eviction at room temperature. As the temperature is lowered, the signal decreases as the traps can no longer be thermally emptied. However the signal does not reach zero, indicating another source of luminescence. This is the tunneling afterglow, a phenomenon which cannot be explained in terms of other auxiliary effects such as retrapping or competition. On storage at LNT, the luminescence emission decays with time. Finally, the sample is heated. The luminescence observed first decreases owing to thermal quenching, and then takes the shape of a TL glow curve.

Visocekas et al. (1994) observed the tunnel emission from 23 feldspar samples and compared the presence or absence of afterglow with the measured fading behavior. They found a close correlation between the samples that showed tunneling afterglow and those for which anomalous fading was detected. Spooner (1994b) also concluded that the dominant mechanism governing anomalous fading is tunneling.

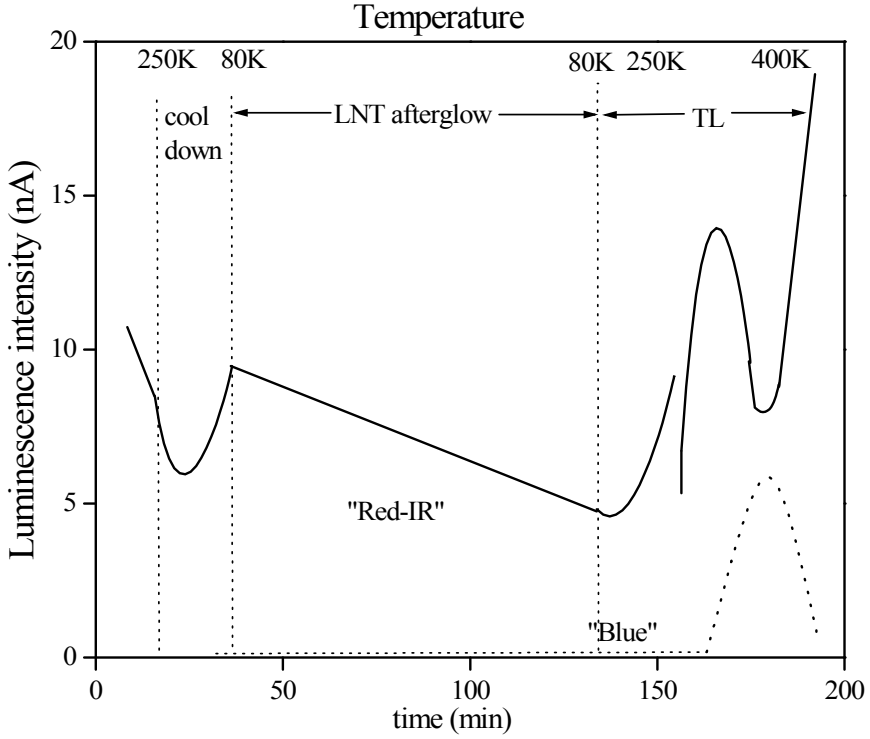

Figure I.12: *Typical afterglow for feldspars. Redrawn from Visocekas et al (1994)*

As tunneling-type fading is largely immune to thermal effects, and hence cannot be circumvented by any existing laboratory procedure, monitoring for anomalous fading is essential. A second consequence of this mechanism is that the data obtained from the monitoring should be plotted using a logarithmic time scale. The use of a linear representation of remanent luminescence versus storage time is misleading, as it gives the impression that the fading reaches a stable level.

In essence the clear conclusion is that in the case of feldspars anomalous fading cannot be circumvented by any existing laboratory procedure such as preheating, because it is a quantum mechanical tunneling process and largely immune to thermal effects (Prescott and Robertson 1997).

This means that testing for it is the ultimate solution. Rejection of certain samples or correction for the effects is the final step. Detection can be made either by monitoring the afterglow i.e. observing the luminescence emitted by recombination via tunneling either by conducting storage test in which the luminescent signal is measured at different time intervals i.e. quantifying the loss in the signal which occurred due to recombination by tunneling.

If the loss of luminescence is proportional to log (t), then the loss between 1 hr and 10 h is the same as the loss between 10h and 100h and between 100h and 1000h and so on. The fading (the percentage of signal loss) occurring between two times differing by a factor of ten is denoted by the symbol *g* (Aitken, 1985). **Figure I.13** shows the signal loss as a function of storage time for several theoretical fading rates (Visocekas, 1985). It can be seen that if a sample has g = 5% per decade, this would lead to an age underestimation between 40 and 60% for samples in the range from 1ka to 1Ma. Samples showing a fading rate of ~20% cannot be dated.

Several methods to deal with anomalous fading in dating studies have been proposed. According to Huntley and Lamothe (2001), they can be classified into three categories: circumvention, variability and correction.

Circumvention involves the use of a signal that does not exhibit fading. Combinations of heating, storage and/or exposure to low energy photons have been tried with the purpose of eliminating the fading signal component(s). Other approaches involve the use of deeper traps or of a luminescence emission that exhibits a long-term stability (such as the far-red TL emission). (Li, 1991).

Variability methods are based on the observation that different grains from a deposit have different fading rates. Grain to grain variability in fading behavior has been demonstrated by Lamothe and Auclair (1997) and Huot and Lamothe (2003). A plot of the equivalent doses as function of the fading rates for individual grains, when extrapolated to zero fading rate, should yield the correct equivalent dose. This is the “Fadia “method developed by Lamothe and Auclair ((1999, 2000), Lamothe et al 2003) and they showed

that extrapolation can result in the correct age. A proposal using the same principle, but for multiple-grain aliquots, was made by Huntley (1997), but has not yet been tested.

The correction approach is based on the idea that if one can measure the fading rate in the laboratory, one might be able to make a correction for the age. This approach was tested by Huntley and Lamothe (2001) and they obtained very promising results. The model put forward by Huntley and Lamothe (2001) for correcting optical ages for anomalous fading was also tested in this work (Chapter IV), and it can be summarized as follows.

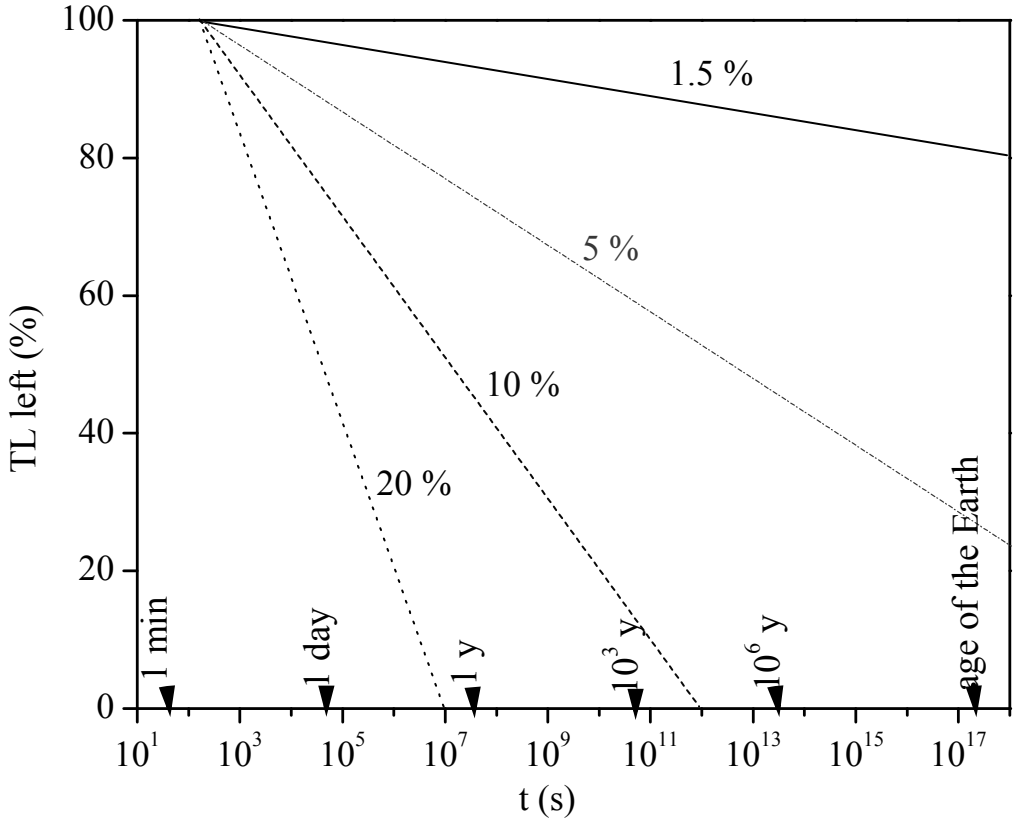

Figure I.13: *Percentage TL left after anomalous fading as a function of storage time in semi-logarithmic coordinates theoretical fading rates. Redrawn from Visocekas 1985.*

Following from the tunneling model, the luminescence intensity I measured at a time t after a short radiation dose can be described by:

$$I = I_c(1 - \kappa \ln(\frac{t}{t_c})) = I_c(1 - \frac{g}{100}\log(\frac{t}{t_c}))$$

(1.22)

Where I_c corresponds to the intensity at an arbitrary time t_c, and κ and g are constants representing fading rates. The relation between g and κ is:

$$g = 100\kappa \ln(10) \tag{1.23}$$

The actual value of κ and *g* depends on the choice of t_c as it can be seen from equation 1.19. It is then assumed that the effect of any particular radiation is independent of that of any other radiation dose. This assumption is expected to hold in the low-dose linear-response region. The luminescence intensity is built-up by a continuous exposure to radiation over a time T. To find this luminescence intensity, Eq. 1.22 must be written in differential form and integrated. Choosing a time scale such that t′ =0 at the beginning of the irradiation and t′=T at the end of irradiation, the luminescence intensity contributing at measurement due to the irradiation during a time interval δt′ can be written:

$$\delta I_f = (I_0 / T)\delta t' \left[1 - \kappa \ln(\frac{T + T_L - t`}{t_c}) \right] \tag{1.24}$$

Where I_0 is the intensity owing to irradiation in time T if there was no fading, and T_L is a time interval during which there was no irradiation. T_L can be understood as the time between sample collection and measurement. Integrating Eq. 1.24 from t′ = 0 to t′ = T, and assuming that T_L << T yields:

$$I_F = I_0 \left\{ 1 - \kappa \left[\ln(\frac{T}{t_c}) - 1 \right] \right\} \tag{1.25}$$

We now choose t_c to be the time between laboratory irradiation and luminescence measurement for the equivalent dose determination. However, the laboratory irradiation is continuous, starting at t_2 and finishing at t_1, with both t_1 and t_2 being time before measurement. To take this into account, it can be shown (Aitken, 1985) that t_c is given by

$$t_c = \frac{1}{2.7} \frac{t_2^{\,t_2/(t_2 - t_1)}}{t_1^{\,t_1/(t_2 - t_1)}} \tag{1.26}$$

Subsequently, we evaluate κ (or *g*) appropriate for this t_c (using Eq. 1.22). As intensity, equivalent dose, and age are all proportional, the formula for correcting an optical age affected by anomalous fading is obtained from 1.25 as:

$$\frac{T_F}{T} = \frac{D_f}{D_e} = \frac{I_f}{I} = 1 - \kappa \left[\ln(\frac{T}{t_c}) - 1 \right] \tag{1.27}$$

Where T is the true age, and D_e and I are the equivalent dose and luminescence intensity, respectively, that would be obtained in the absence of fading. The subscript f indicates a value affected by fading. To obtain the true age T, Eq. 1.27 must be rewritten as:

$$0 = T\left\{1 - \kappa\left[\ln(\frac{T}{t_c}) - 1\right]\right\} - T_F \tag{1.28}$$

from which T is obtained using an iterative procedure.

CHAPTER II
THE EQUIVALENT DOSE

II.1. INTRODUCTION

The assumptions on which the determination of the equivalent dose is based are:
a) the signal selected for dating comes from traps stable in geological time (the signal has to be carefully selected and the unwanted components have to be removed);
b) trap filling is the same during laboratory and natural irradiation (this assumption is difficult to be tested);
c) the luminescence per unit of trapped charge is the same during all measurements.

Different techniques are available for determining the equivalent dose. In essence, they can be divided into two categories, namely additive and regeneration techniques. Reviews have been presented by Aitken (1998), Wintle (1997), Bøtter-Jensen et al. (2003a), Vandenberghe (2004) and Wintle and Murray (2006) just to name a few.

II.2. MULTIPLE-ALIQUOT TECHNIQUES

Multiple-aliquot techniques in OSL dating are conceptually the same as the techniques used in TL dating (Aitken 1998). For multiple aliquot TL applications dating reference can be made to Forman (1991), Van den haute et al (1998) and Van den haute et al (2003) just to name a few.

In the multiple-aliquot additive-dose technique (MAAD) a large number of aliquots are prepared and divided into groups. From one group the natural signal is evaluated, while the other groups are given different radiation doses on top of their natural dose in the laboratory. All the aliquots are subsequently preheated and measured. The plot of luminescence intensity as function of added dose yields the growth curve. The equivalent dose is determined by extrapolation. This has the disadvantage that the obtained value is highly influenced by the mathematical function used for fitting. This drawback is circumvented using regeneration techniques. However, this procedure has the disadvantage that sensitivity changes can occur owing to the processes of heating, bleaching and dosing. If, for instance, the bleached aliquots become more sensitive than the ones used for the measurement of the natural signal, the growth curve becomes

steeper and the equivalent dose will be underestimated. If there is a decrease in sensitivity, the equivalent dose will be overestimated.

To overcome the disadvantages of both the additive and the regenerative technique, Prescott et al (Prescott et al 1993) developed the so called Australian slide technique. In this technique, the equivalent dose is determined as the amount of displacement along the dose axis that is necessary to bring the regenerative and the additive dose growth curves into coincidence.

Multiple-aliquot techniques have several important disadvantages. They require many aliquots (many tens for obtaining just one equivalent dose) and are relatively time-consuming. Usually, some form of normalization is required to allow for aliquot-to-aliquot differences in luminescence sensitivity. Furthermore, multiple-aliquot techniques are based on the assumption that each aliquot has the same luminescence characteristics and equivalent dose. This was shown to be an oversimplification (Murray and Olley, 2002). Multiple-aliquot techniques yield an average equivalent dose for the particular aliquots that are measured. In the case of partial bleaching, this will result in an inaccurate estimation of the equivalent dose.

To overcome most, if not all, of these disadvantages, single-aliquot procedures were subsequently developed. These are analytical procedures, in which all the measurements necessary to obtain an equivalent dose are performed on one aliquot.

II.3. SINGLE ALIQUOT TECHNIQUES

The first single-aliquot protocol was developed by Duller (1991) for K-feldspar and using IRSL signals. Murray et al. (1997) were the first to present a single-aliquot protocol for sedimentary quartz. This protocol was generically named the SAAD (single-aliquot additive-dose) protocol. The application of SAR to polymineral fine grains was first suggested by Banerjee et al. (2001). They tested the suitability of the protocol for measuring equivalent doses using the blue stimulated luminescence from both quartz and feldspars, the infrared stimulated luminescence from feldspars only, and the blue stimulated luminescence following infrared stimulation (the post-IR blue OSL), which originates from both quartz and, to a lesser degree, also from feldspars. The approach is also known as the double SAR approach. Concerning SAR and double SAR on polymineral fine grains reference can be also made to Roberts and Wintle 2001, Balescu et al 2003, Wang et al 2006, Buylaert et al 2007).

Further investigations on the problem of sensitivity changes occurring in quartz ultimately led to the development of the single-aliquot regenerative-dose (SAR) protocol as described by Murray and Wintle (2000, 2003). The SAR protocol truly revolutionized optical dating, and it is nowadays considered as the technique of choice for determining

the dose accrued in quartz (Stokes et al., 2000; Murray and Olley, 2002; Duller, 2004; Vandenberghe, 2004, Wintle and Murray, 2006).

The previously mentioned three assumptions for determining the equivalent dose were tested for the SAR protocol in the following way:

a) The signal selected for dating comes from traps stable in geological time (the signal has to be carefully selected and the unwanted components have to be removed);

Wintle and Murray (1997) showed that the initial OSL signal is directly proportional to the integral OSL signal. Isothermal decay experiments (Murray and Wintle 1999) showed that the initial (first 0.4 s of stimulation) natural OSL is dominated 99% by a signal with a lifetime of 10^{8} years at 20 ^{o}C. However, the regenerated signals contained a significant additional unstable component with a lifetime of 400 y at room temperature. This unwanted component comes from the trap giving rise to the 110 ^{o}C TL peak and can be removed by a applying a preheat before measuring the OSL.

b) Any competition for charge during trap filling is the same during laboratory irradiation as during natural irradiation (i.e. trap filling is the same during laboratory and natural irradiation)

As previously mentioned this assumption is difficult to be tested in the laboratory and was empirically showed to be fulfilled by comparing ages luminescence ages obtained by applying the SAR protocol with ages obtained on the same samples by applying other independent methods.

It must be pointed out that the SAR protocol was developed and validated for samples having OSL signal dominated by a fast component.

c) The luminescence per unit of trapped charge is the same during all measurements.

As discussed in a) applying a thermal treatment before measuring regenerated quartz OSL signals is mandatory in order to isolate the stable (in archaeological / geological time) component. A further reason would be the need to redistribute trapped charge in order to prevent thermal transfer to the dosimetric trap during measurement. However, this treatment may also redistribute holes and thus can cause sensitivity changes. For further details, reference is made to Wintle and Murray (1999), Murray and Wintle (2000; 2003), and Vandenberge (2004).

The main assumption underlying the SAR protocol is that sensitivity changes occurring throughout a measurement cycle can be corrected for by using the luminescence responses to a constant test dose. The regenerated OSL signals can than be corrected for sensitivity changes by normalizing them to the corresponding test dose responses.

This means that by repeating paired measurements of a constant regeneration dose and a constant test dose the relationship between the OSL test dose signal and the regenerated OSL must be linear and the intercept of this relationship must be small compared to the measured OSL signals **Figure II.1** shows the OSL response to a regenerative dose as function of the OSL response to a test dose for coarse and fine grains of quartz that was analyzed in this work.

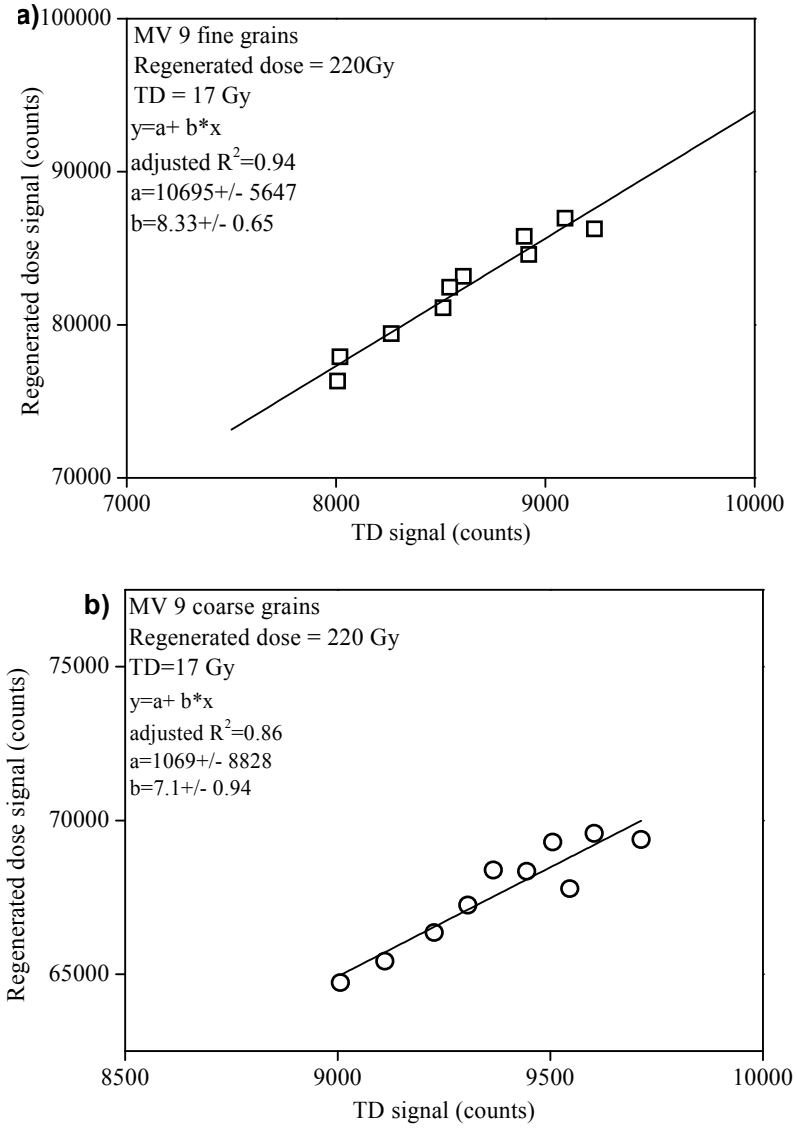

Figure II.1: *OSL signal (counts) resulted from a regenerative dose as function of the OSL signal from the immediately subsequent test dose obtained for fine quartz grains (a) and coarse grains (b) of sedimentary quarts extracted from sample (MV9 Chapter V) subjected to repeated (10) SAR cycles. Note that the regenerative dose was kept constant (220 Gy) as well as the test dose (17 Gy). It can be noticed that the relationship is linear. The fitted line was not forced through the origin and a small intercept compared to the dose response was obtained. The values of the slope (8.3, respectively 7.1 are smaller than the ratio of the given doses as a result of the choice of a large dose causing the response to be well up the dose response curve (details in Chapter V).*

It should be pointed out that it is not essential to minimize any sensitivity change between the measurement of the regenerated dose and the test dose; it is only important that the size of any change in the test dose response relative to that in the preceding regenerated signal to be constant for a given dose and so independent of measurement cycle. Thus the OSL sensitivity measured using the test dose should be directly proportional to the sensitivity of the preceding regeneration dose. If this condition is fulfilled there is no impediment in repeating paired measurements of regenerated OSL signals / test dose signals keeping the test dose constant and using different irradiation doses for the regenerated OSL signals. By doing this a sensitivity corrected growth curve is obtained onto which the natural signal can be interpolated in order to derive the equivalent dose. **Figure II.2** shows a typical growth curve for sedimentary quartz constructed in a SAR protocol.

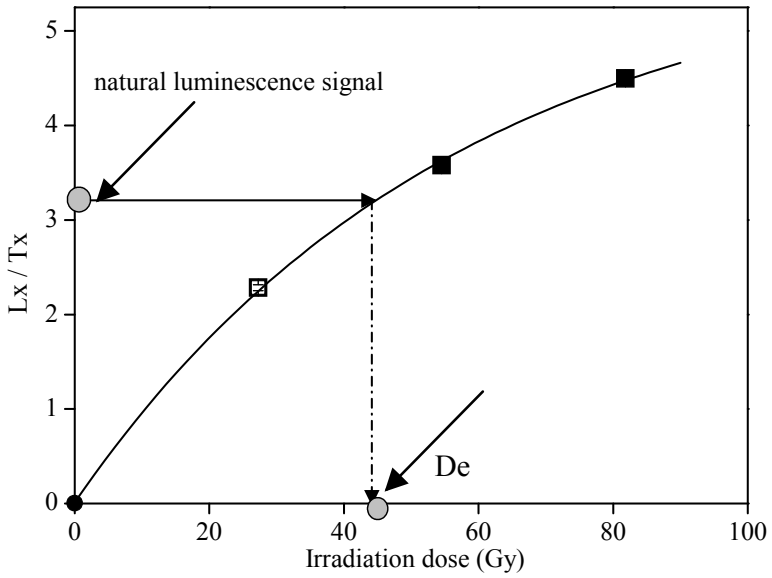

Figure II.2: *Typical growth curve for sedimentary quartz constructed in a SAR protocol. The recycling point is represented as an open square while the zero-dose response is shown as solid circle. (Timar A, 2006)*

A typical SAR measurement sequence for quartz as proposed by Wintle and Murray is presented in **Table II.1.** The measurement procedure starts with the measurement of the natural OSL signal after the aliquot has been preheated ($D_{i=1}$=0 Gy). A test dose is then given, followed by another preheat and the measurement of the OSL response to the test dose. The test-dose preheat (cutheat) is meant to empty the shallow traps. This measurement cycle is then repeated after a regenerative dose is given, and this as many times as desired. Various regenerative doses can be used throughout the experiment but the test dose is kept constant. By dividing the regenerated OSL signals by the

corresponding test dose signals, a growth curve is obtained, which is corrected for sensitivity changes.

Table II.1: ***Generalized SAR measurement sequence for quartz***

Step	Treatment	Observe
1.	Give dose Di	-
2.	Preheat (at a temp between160 and 300^{o}C for 10s)	-
3.	Optically stimulate for 40s at 125 ^{o}C	**Li**
4.	Give test dose Dt	-
5.	Heat to T < preheat in step 2 (cutheat)	-
6.	Optically stimulate for 40 s at 125 ^{o}C	**Ti**
7.	Optically stimulate for 40 s at T> preheat in step 2 (280 ^{o}C) (ETOSL)	-

In the SAR protocol, it can be checked for if the sensitivity correction is working properly. This is done by repeating a measurement of the response to a dose that had been previously administrated. If the responses are indistinguishable, this means that sensitivity correction is working properly. The ratio of these two corrected OSL or IRSL signals is called the "recycling ratio" and should ideally be equal to 1. The deviation of the recycling ratio from unity can be a criterion for acceptance or rejection of aliquots. A good recycling value can be also considered as evidence that the growth curve patter obtained is real and not a sensitivity artifact (Wintle and Murray 2006).

A second important test is to check whether the dose-response curve starts indeed at the origin. This is accomplished by measuring the response to a zero regenerative dose. Although one would expect this to give a zero signal, in practice a small signal is observed. The "recuperation" of the signal arises from thermal transfer of charge inserted by the test dose into thermally shallow but light insensitive traps which are not emptied by the cutheat. These traps are emptied by the preheat and some of this charge can be trapped into the light sensitive traps. In most cases it has been shown that this transfer is mainly not into the main OSL trap (fast component) but into other OSL traps (medium component) (Jain 2003). Step 7 at the end of each cycle was later introduced into the SAR protocol in order to reduce recuperation. For more details, reference is made to Vandenberghe (2004) and the original works of Murray and Wintle. For a sample that behaves well in the SAR protocol, recuperation should be negligible. The amount of recuperation that is observed can be used as a criterion for acceptance or rejection of an aliquot.

The ultimate test for checking the performance of the SAR protocol is the "dose recovery test". This test was first suggested for feldspars by Wallinga et al. (2000) and was subsequently recommended by Wintle and Murray (2003) for quartz as well. The dose recovery test consists of optically zeroing a sample (**Figure II.3**); irradiating it with a

known dose and then measuring this given dose using the SAR protocol as if it was an unknown dose.

If De measurement and dose recovery tests are performed for different preheat temperatures and a preheat plateau is obtained this is evidence that:

- any unwanted thermal transfer is not relevant.
- sensitivity changes are properly corrected for (as different thermal treatments may lead to a different degree of sensitivity change)
- the dosimetric signal investigated comes from traps that are thermally stable.
-

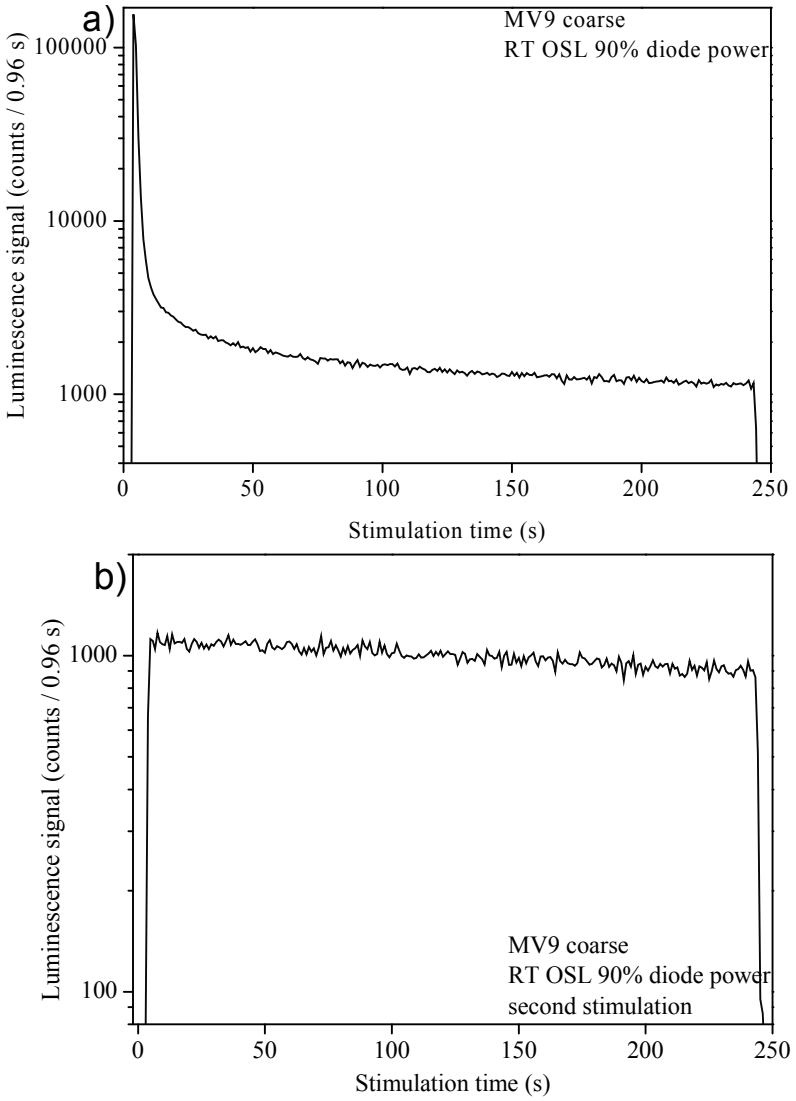

Figure II.3: *Decay curves of coarse quartz obtained for a disk with coarse quartz grains obtained in the bleaching protocol used in dose recovery tests throughout this work for quartz (two optical stimulation at room temperature with blue diodes 90 % diode power(36 mW/cm^2) with a 10000s pause in between). The second bleach reduces the signal to a constant background composed only from the counts of the blanc disk and the slow components of quartz grains.*

The measurement protocol is proven to be useful if the given dose can be measured accurately. However, as pointed out by Murray and Wintle (2003), an accurate recovery of the known dose does not necessarily imply an accurate determination of the naturally acquired dose as well. Nevertheless, the dose recovery test does serve to increase confidence in the measurement procedure. Murray and Wintle (2003) also showed that the dose recovery test is a more diagnostic than the recycling ratio for evaluating the applicability of the SAR procedure to a given sample.

To conclude, the advantages of the SAR protocol can be summarized as follows:

- There is no need for normalization between aliquots;
- Equivalent doses can be determined with higher precision;
- Multiple estimations of the equivalent dose can be performed for one sample enabling the detection of partial bleaching or variations in microdosimetry;
- Less sample is needed (important for situations in which quartz is scarce, as was the case for the samples investigated in this work);
- Equivalent dose estimation is rapid and can be fully automated;
- The influence of different measuring parameters can be efficiently investigated;
- Sensitivity changes occurring throughout the measurement cycle are corrected for.

II.4. SAMPLE AND ALIQUOT PREPARATION

Conventional procedures (Zimmerman, 1971; Lang et al., 1996; Frechen et al., 1996) were used to extract coarse sized quartz, fine quartz grains and polymineral fine (4-11µm) grains from the samples. All sample preparation was carried out under subdued red and orange light (Encapsulite R-10, Ilford 902 safelights).

Samples were treated overnight with diluted HCl (10%) to remove carbonates, and then repeatedly washed with distilled water. To remove organic materials, 10% H_2O_2 was added and the mixture was again left overnight. The following day more concentrated 30% H_2O_2 was added. The mixture was left for 24h to assure a complete removal of organic materials, and was subsequently washed several times with distilled water. Following this pretreatment, wet sieving was performed.

After sieving, this fraction consists of an undifferentiated mixture of minerals, including quartz, feldspars and heavy minerals. These minerals have slightly different densities and can be separated in suspension using heavy liquids. The heavy liquids used were solutions of sodium metatungstate $Na_6[H_2W_{12}O_{40}]$ xH2O (a heavy inorganic salt) with distilled water. The principle is outlined in **Figure II.4**

First the polymineral sample is suspended in a solution with a density of 2.62 g/cm^3. This enables the separation of quartz and plagioclase grains from the lighter minerals such as clay, potassium and sodium feldspars. Subsequently, the mineral grains are suspended

in a solution with a density of 2.75 g/cm^3. In this case, quartz and plagioclase feldspars will float while heavy minerals such as zircons and apatite will sink. The floating fraction was kept, washed and dried.

Quartz can no longer be separated from plagioclase by means of difference in density. Therefore, a treatment with 40% hydrofluoric acid (40 min) was performed for coarse grains, respectively, 35 % hidrofluorosilicic acid ($H_2 Si F_6$) (5 days) for quartz fine grains. The feldspars are less chemically resistant and are dissolved. The etching also removes the outer surface of the quartz grains, which reduces the external alpha particle contribution to these grains to a negligible level. A 60 min wash with warm (50^{o}C) dilute HCl was applied after etching to remove any precipitated fluorides. This was followed by repeated washing with distilled water and drying. Finally the product was sieved again sieve.

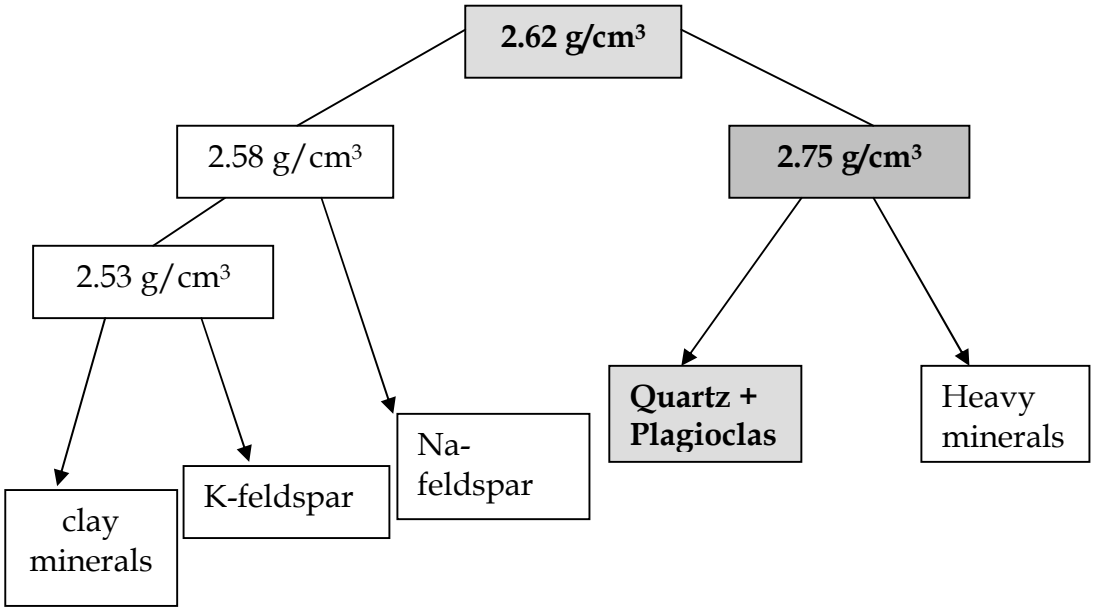

Figure II.4: *Flow chart of density separation (after Mejdahl 1985); the left branch indicates the floating fraction, the right the one that sinks.*

To extract polymineral fine grains, the fraction < 36µm was first put in beaker and (NH_4OH) was added for deflocculating. The fraction less than 11µm were then isolated by settling in Atterberg cylinders according to Stokes' law. The removal of the grains < 4 µm was carried out in a centrifuge using the method described by Frechen et al. (1996).
For measurement, the quartz grains were sparingly poured through a sieve on stainless steel disks. Silicon oil was used as adhesive. The silicon oil used was tested and it was concluded that it does not give any parasitic signal.

For polymineral fine grains and quartz fine grains aluminum disks were used. Aluminum is advantageous because it has the same scattering characteristics as quartz

and feldspars. For measurement, aliquots were made by pipetting a 1 ml suspension of the fine grains (2mg of grains /1 ml acetone) onto each aluminum disc. Prior to pipetting, the solution was homogenized in an ultrasonic bath. The acetone was then allowed to evaporate either at room temperature, or in an oven at ~50°C.
A flow chart of sample preparation for loess samples from Mircea Voda (Chapter V) is presented in the following.

Table II.2: *Preliminary treatment*

SAMPLE CODE	MASS OF BULK SAMPLE TO BE PREPARED (g)	MASS of X1 (g)	MASS of X2 (g)
MV1	240.8	33.9	173
MV2	267.2	38.8	85.3
MV3	357.9	47.9	43.4
MV4	277.0	45.1	42.4
MV5	335.9	50.7	42.4
MV6	321.0	30.6	69.9
MV7	319.2	41.9	46.7
MV8	300.6	44.1	56.7
MV9	292.1	49.4	125.2
MV10	293.4	40.0	55.4
MV12	288.4	35.0	57.6
MV13	128.3	17.6	43.0

- 10% HCl to dissolve carbonates, wash
- 10% H_20_2 , 30% H_20_2 to remove organic matter , wash
- wet sieving on 63 μm sieve
- dry sieve the > 63 μm fraction on 90 and 125 μm sieves.

Table II.3: Sieving, after preliminary treatment

SAMPLE CODE	> 125 μm (g)	90-125 μm (g)	63-90 μm (g)	< 63 μm (g)
MV1	0.27	0.44	4.03	147.80
MV2	0.32	0.69	5.03	154.77
MV3	0.59	1.02	8.84	201.09
MV4	2.22	1.92	8.44	158.56
MV5	3.01	1.91	11.20	208.05
MV6	2.66	2.72	10.43	206.89
MV7	3.16	2.80	9.02	193.12
MV8	1.21	1.93	8.59	216.98
MV9	0.98	1.58	8.06	205.73
MV10	0.39	1.45	8.04	173.13
MV12	0.73	1.11	4.98	188.23
MV13	0.81	1.04	4.41	175.12

A) Extraction of 63-90 μm quartz grains

- heavy liquids density separation
- use two densities 2.62 g/cm^3 and 2.75 g/ cm^3 + etch with HF

Table II.4: *Heavy liquid separation*

SAMPLE CODE	63-90 μm after heavy liquids	63-90 μm after heavy liquids and etching
MV1	0.28	0.12
MV2	0.11	0.05
MV3	0.45	0.16
MV4	0.29	0.13
MV5	1.16	0.54
MV6	1.30	0.60
MV7	1.59	0.68
MV8	0.94	0.43
MV9	1.26	0.53
MV10	0.92	0.47
MV12	0.28	0.12
MV13	0.10	0.04

B) Extraction of quartz fine grains and polymineral fine grains

The procedure is based on Stokes law. PFG (4-11μm) from 20 g of material with a grain size smaller than 63 μm were extracted. QFG (4-11μm) were extracted from the same amount of material based on the same procedure and a five days etching with hidrofluorosilic acid.

Table II.5: *Fine grain extraction*

SAMPLE CODE	4-11 μm PFG (g)	4-11 μm QFG (g)
MV1	1.71	0.45
MV2	2.04	0.56
MV3	0.92	0.32
MV4	2.24	0.28
MV5	2.21	0.66
MV6	1.95	0.46
MV7	2.37	0.54
MV8	2.77	0.34
MV9	2.26	0.32
MV10	1.28	0.41
MV12	2.02	0.52
MV13	2.94	0.91

D) Extraction of silt quartz grains

a. et sieving of 11-36μm fraction left after the extraction of fine grains, starting from 40 g of <63μm material:

b. Etching with fluorosilicic acid.

Table II.5: *Silt grain extraction*

SAMPLE CODE	11-36 μm (g)	36-50 μm (g)	36-50 μm ETCHED (g)	50-63 μm (g)
MV1	25.95	2.38	1.13	2.80
MV2	25.83	3.40	1.41	1.45
MV3	27.34	5.70	2.87	1.02
MV4	26.42	4.66	2.58	2.38
MV5	24.41	4.53	2.54	1.65
MV6	24.45	5.33	2.72	3.13
MV7	25.99	4.26	2.11	2.74
MV8	25.36	5.02	2.54	1.99
MV9	28.04	3.96	2.07	1.68
MV10	27.37	5.93	2.69	1.79
MV12	27.34	4.12	1.63	1.42
MV13	25.74	3.40	1.08	1.08

II.5. TESTING THE PURYTY OF QUARTZ EXTRACTS

Theoretically, complete feldspar removal from samples is desirable. In practice however, it is important to have a negligible contribution from feldspars in the signal analyzed for equivalent dose estimation. Several tests have been used to check the purity of quartz extracts in this work.

In most studies, a signal above background in response to IR stimulation is attributed to feldspars, as at room temperature the fast component of quartz OSL is not stimulated by IR (Aitken, 1998), whereas a large variety of feldspars respond to IR excitation by emitting in the UV (Krbetschek and Rieser 1995, Krbetschek 1997). All samples have been analyzed based on this criterion and yielded negligible IR signal compared to signal collected under blue stimulation (**Figure II.5**).

The "IR depletion ratio" test (Duller, 2003), uses the ratio of the sensitivity corrected [post-IR]-OSL, ($L_{x\ post\text{-}IR}$ / $T_{x\ OSL}$) to the sensitivity corrected OSL (L_x / $T_{x\ OSL}$). This test is based on the assumption that the UV recombination centers in feldspars responsible for IRSL and OSL share the same source traps, as indicated by Jain and Singhvi (2001). This test has been applied to every aliquot analyzed throughout this work by making an additional measurement at the end of each SAR run. It was extremely rare that aliquots

were rejected based on this criterion. Average values obtained for this test for samples analyzed are quoted in Chapter IV and Chapter V.

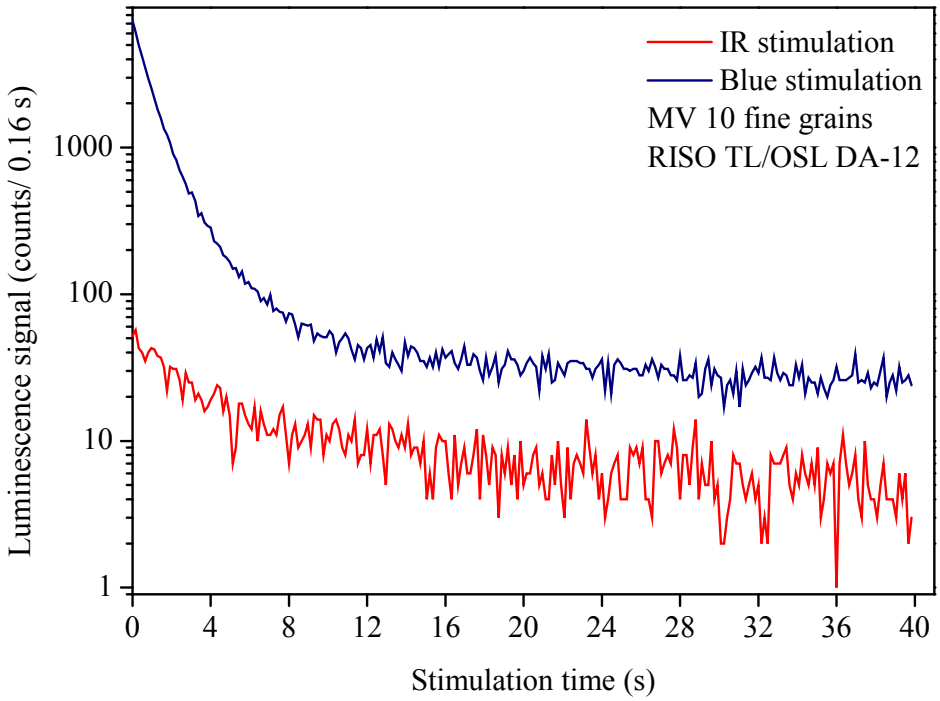

Figure II.5: *UV signals stimulated in blue light (at 125 °C), respectively IR (at 60 °C for sample MV10 fine grains (natural).*

A general observation that has been made is that during measurement the OSL signal from quartz tends to decrease rapidly, and to a low residual level (Smith and Rhodes, 1994, Bailey et al 1997), while for feldspars the initial decrease is slower and a significant tail is observed even after prolonged stimulation (Bailiff and Poolton, 1991). This different behavior potentially provides a mean of differentiation (Duller, 2003).

It is known as well that pulsed optically stimulated luminescence characteristics of quartz and feldspars are very different, and the use of differences in luminescence lifetimes to discriminate between quartz and feldspar signals under pulsed stimulation has been suggested (Denby et al, 2006).

As luminescence lifetimes associated to the fast component of quartz OSL are around 30 μs (see section I.4.7 for more details), using a pulse timing of this magnitude leads to virtually recording only the quartz signal during the off time as feldspar signals are dominated by a fast lifetime component which rises and falls with the on-period of the stimulation LEDs.

Figure II.6 presents a comparison of decay curves obtained on calibration quartz and fine and coarse grains of quartz extracted from loess analyzed in this work under continous wave stimulation, respectively pulsed stimulation on time: 50 μs, off time 50μs.

It can be observed that the decay rates are indistinguishable proving that any feldspar contamination is negligible.

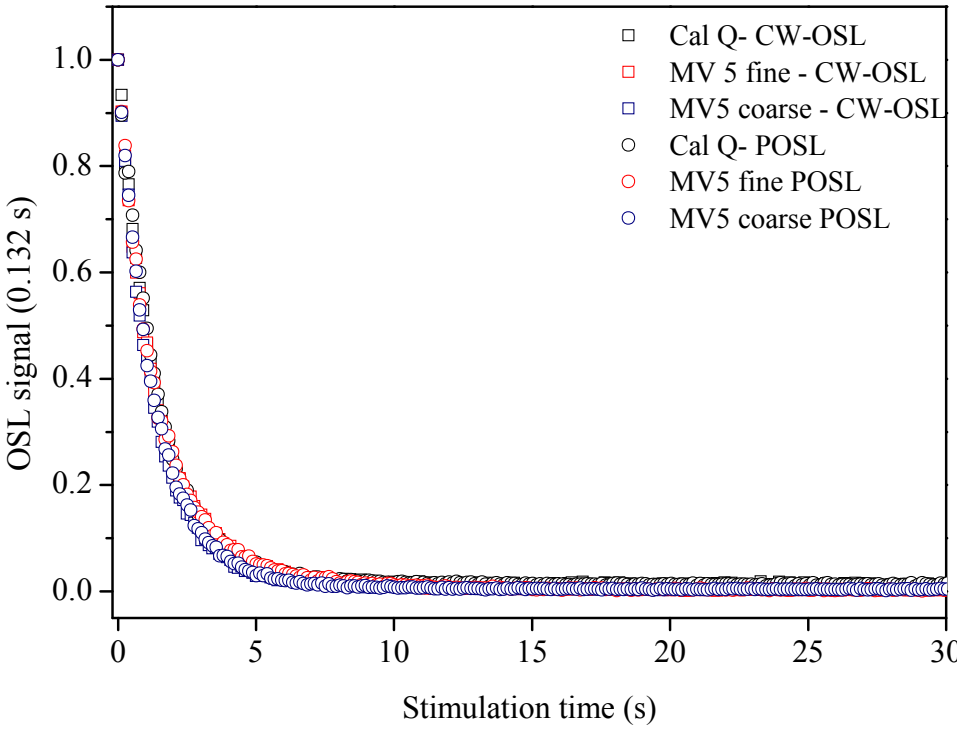

Figure II.6: *Comparison of decay curves of calibration quartz and MV5 fine (4-11 µm), respectively coarse (60-90 µm) grains under continous wave stimulation, respectively pulsed (on time: 50 µs, off time 50µs). Signals have been recorded after a preheat of 10 s at 220 °C. Signal are normalized to initial intensities.*

II.6. MEASUREMENTS AND IRRADIATION FACILITIES

II.6.1. Short description of Risø TL/OSL-DA luminescence readers

Measurements on quartz were performed using a Risø TL/OSL-DA-12, TL/OSL-DA-15 (in Ghent) readers respectively a Risø TL/OSL-DA-20 device in Cluj. These systems allow fully automated sequences to be run.

The reader consists of a light tight chamber and holds a turntable in which the aliquots can be placed. The turntable places the aliquots above a lift mechanism that raises the samples into the measurement positions. On the top of the lift mechanism, a heater element is mounted which allows a reproducible heating of the aliquots (for preheating, measuring OSL and IRSL at elevated temperatures, or recording thermo luminescence. On each reader, an irradiation unit containing a $^{90}Sr/^{90}Y$ beta source is mounted. For optical stimulation of the quartz, the TL/OSL–DA-12 is equipped with an array of 42 blue LEDs (light emitting diodes) having a peak emission at 470nm. The OSL signals passed through

a 7.5mm thick Hoya U-340 filter and were detected using an EMI 9235QA bialkali photomultiplier.

For measuring the IRSL from polymineral fine grains, the TL/OSL-DA-15 reader is equipped with a stimulation unit consisting of 21 powerful IR LEDs, emitting at 875nm.The IRSL signals passed through a combination of a BG39, CN 7/59 and GG 400 filter(410nm) and were detected using an EMI 9235 QB bialkali photomultiplier.

Before each measurement a dark count measurement was performed to check the stability of the photomultiplier tubes. All stimulations were performed at 90% of the maximum attainable power, as a compromise between maximizing the light output and avoiding overrunning of the diodes. A more detailed description of the equipment as installed in the Ghent Luminescence Laboratory can be found in Vandenberghe (2004).

The Risø TL/OSL–DA-20 (ICEI CLUJ NAPOCA) automatic measurement system enables measurement of both thermoluminescence and optically stimulated luminescence. The system allows up to 48 samples to be:

1) Individually heated to any temperature between room temperature and 700°C. Heating is provided by a non-switching continuous full sine wave generator operating at 20 kHz. The heating system is able to heat samples at linear heating rates from 0.1 to 30 K/s.

2) Optically stimulated using various light sources.

Infrared (IR) LEDs emitting at 875 nm arranged in three clusters each containing seven individual LEDs. The maximum power from the 21 IR LEDs is approximately 135 mW/cm^{2}at the sample position.

Blue LEDs emitting at 470 nm (FWHM = 20 nm) arranged in four clusters each containing seven individual LEDs. The total power from these 28 LEDS is approximately 40mW/cm^2 at the sample position. Light emitting diodes (LEDs), are compact, fast and enables electronic control of the illumination power density linear modulation luminescence measurements being achievable. The emitted luminescence is measured by a light detection system comprising a bialkali EMI 9235QA photomultiplier tube and filters (**Figure II. 7**).

3) Individually irradiated by radioactive beta (^{90}Sr/^{90}Y) 1.48 GBq (40 mCi) source delivering approximately 0.15 Gy/s in quartz, respectively LiF at irradiating position.

Further relevant references on instrumentation include Markey et al 1997, Bøtter-Jensen et al 1997, 1999, 2000, 2002, 2003a, b and Thomsen et al 2006.

II.6.2. Calibration of the radioactive sources

The dose rate that a sample receives from a beta source is strongly influenced by effects as build-up, backscattering and attenuation (Aitken, 1985). Consequently, a whole variety of parameters (such as the distance from the source, the grain size, the density of

the material, the grain size, and the substrate on which the grains are deposited) determine the effective calibration.

Calibration of the beta source is performed by comparing the luminescence induced in a sample by a known dose (usually administrated by a calibrated gamma source) with the luminescence induced in the same sample by a given duration of irradiation by the beta source of unknown strength.

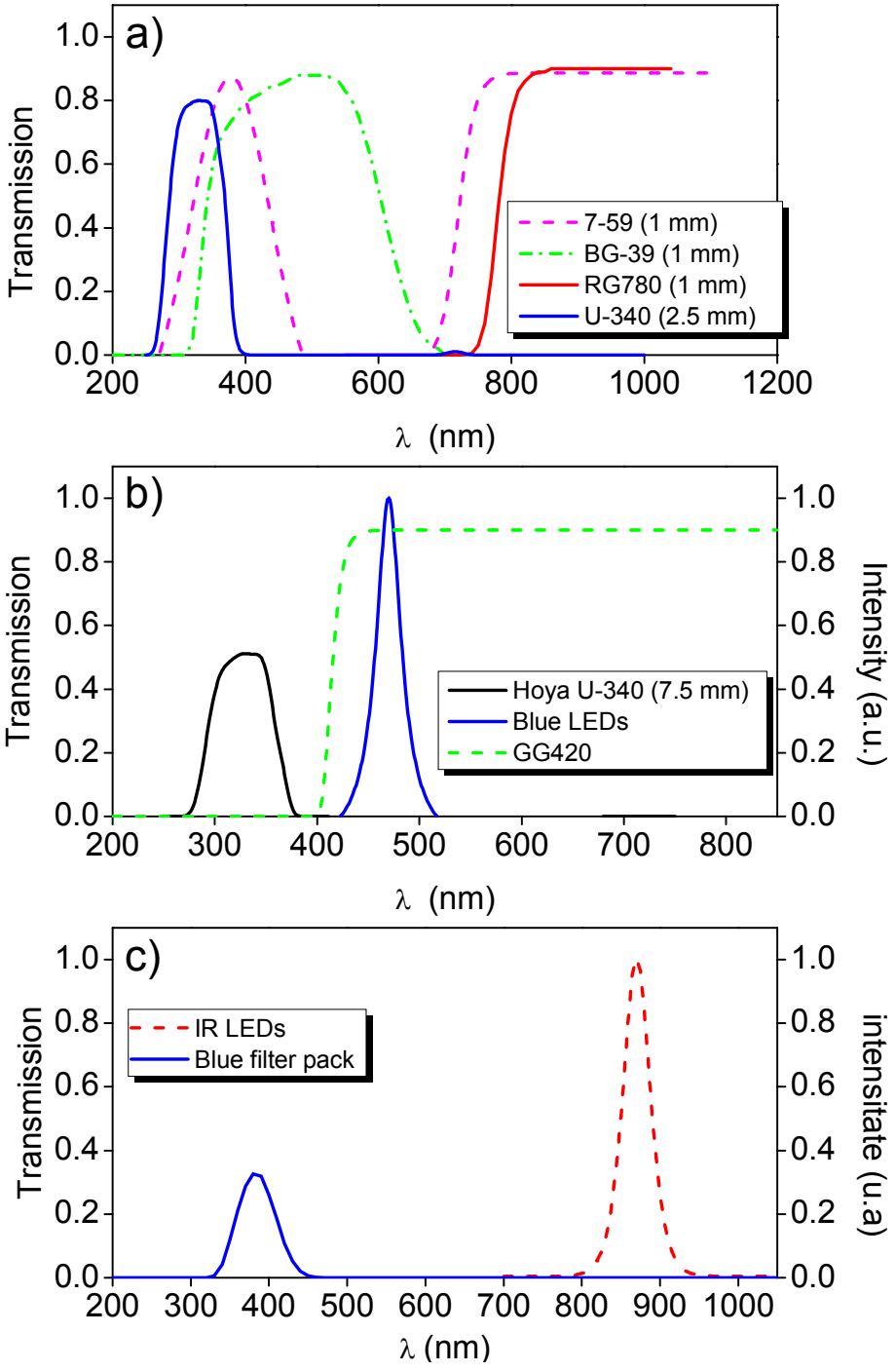

Figure II. 7: *transmission characteristics of the filters used throughout this work (a- all filters, b)UV filter pack used for quartz compared to the blue LEDs emission region, c) blue filter pack used for feldspars comparer to the IR diodes emission).*

Because of the aforementioned effects of build-up, backscattering and attenuation, the calibration applies only to the precise conditions of the beta irradiation. New calibrations must be carried out for other grain sizes, substrates, etc. (Armitage and Bailey 2005, Chen S. et al 2009) For calibrating the beta sources, use was made of the calibration quartz produced by Risø National Laboratory.

This calibration quartz is quartz that had been annealed to a high temperature and subsequently received a known gamma dose. Calibration quartz of different grain sizes is available. The calibration was performed using the SAR protocol. This yields a value in seconds from which the source strength is easily derived. This is illustrated in **Figure II.8 a and b**. The dose rate for the Da-12 reader (Ghent) for fine grains was 0.057 Gy/s (reference date March 2008), while for the DA-20 machine (Cluj Napoca), values of 0.175 Gy/s for the coarse grains on stainless steel disks, respectively 0.135 Gy/s for the fine grains on aluminium disks (June 2008). For all the irradiations that were carried out after the calibration, allowance was made for the decrease in the strength of the sources owing to the radioactive decay of ^{90}Sr ($T_{½}$ = 28.74 y).

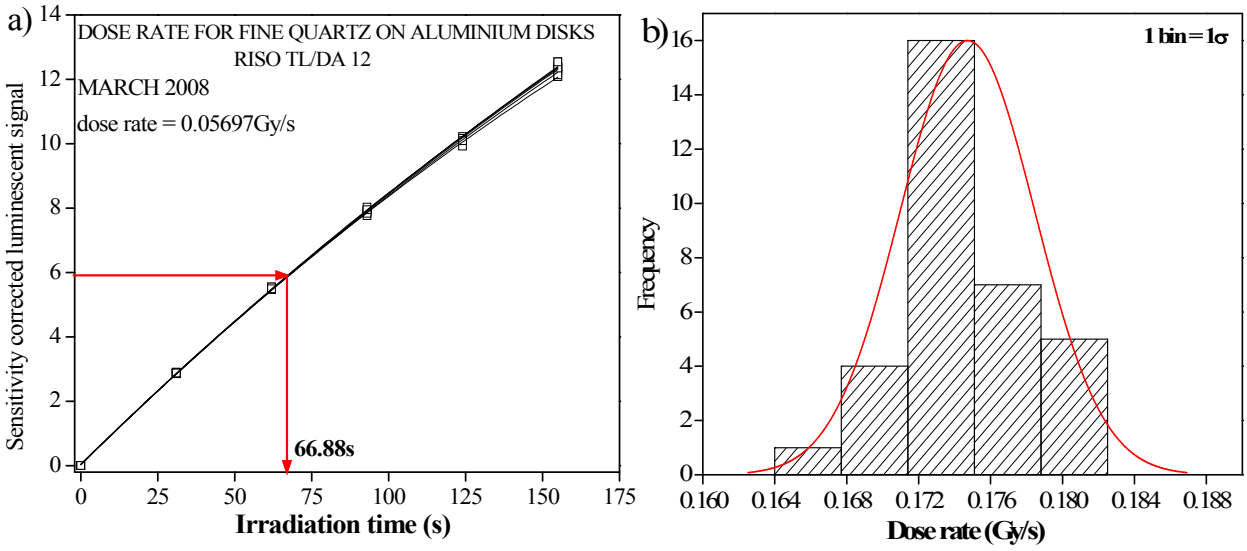

Figure II.8. *a) Calibration of the $^{90}Sr/^{90}Y$ beta source on TL/OSL–DA-12 reader using 9-11μm calibration quartz (3.81 Gy) in a SAR protocol. Histogram of equivalent dose obtained in Calibration of the $^{90}Sr/^{90}Y$ beta source on TL/OSL–DA-20 reader using coarse calibration quartz (4.00 Gy) in a SAR protocol. A tight normal distribution can be observed with a relative standard deviation of 2.6%)*

II.6.3. Testing for thermal stability of the heating plate

The thermal stability and the constancy of the heating rate (5 °C/s) for the kanthal heater element was constantly monitored making use of the 110 °C TL peak of quartz, as it is known from the kinetics of the luminescence phenomena that TL peaks will shift to

higher temperatures as the heating rate increases. **Figure II.9** shows 110 ºC TL peaks recorded during different measurements during 2 months measurement time on the Risø DA-12 machine.

II.6.4. Testing for stability of the photomultiplier tube

Before each measuremet was performed photomultiplier dark counts were registered for 10s. Risø systems also include a blue calibration LED. Measuring the counts using this LED assures that there is no breakthrough of the blue stimulation light into the photomultiplier through the thick Hoya UV filter when performing OSL measurements on quartz. The photomultiplier dark counts registered for 120s on the DA-20 machine are shown in **figure II.10.**

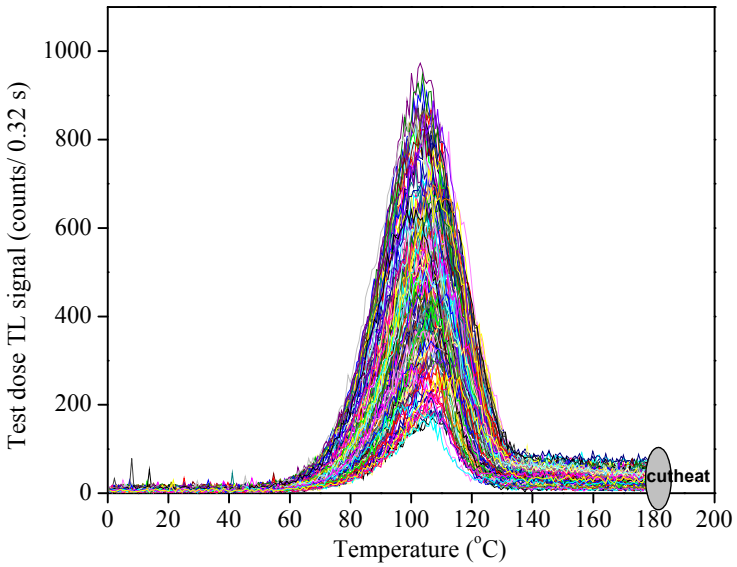

Figure II.9: *Quartz 110 ºC TL recorded during cutheat thermal treatments for different measurements on fine quartz samples analyzed on the Risø DA-12 (February-March 2008).*

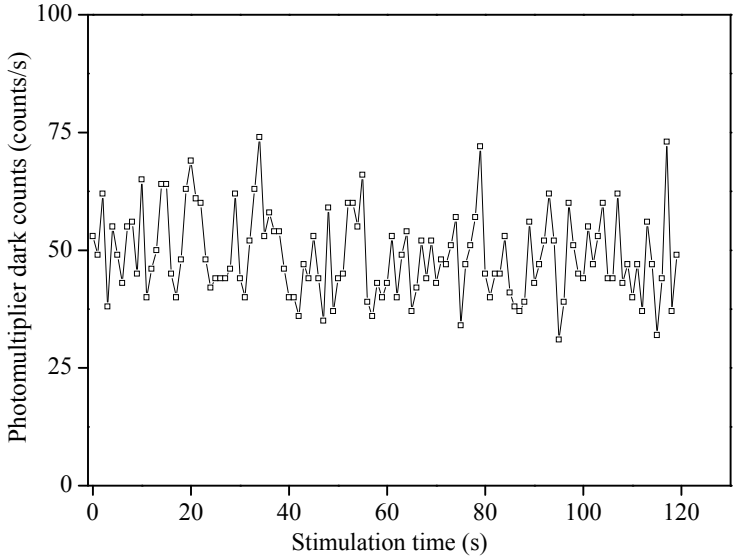

Figure II.10: *PM dark counts registered for 120 s on the Riso DA-20 machine (June 2009)*

II.7. Data collection and processing

The windows based program Sequence Editor (Risø National Laboratory) was used to steer both readers through the so called GENI-SYS (TL/OSL–DA-12), MINI-SYS (TL/OSL-DA-15), CONTROLLER (TL/OSL–DA-12) computer. In the sequence editor any measurement sequence can be created and subsequently directly run through Windows. The reader carrying the measurements automatically. Data were processed using the software "Analyst" (authored by G.A.T. Duller), Microsoft Excel 2003 and Microcal Origin version 8.0.

CHAPTER III
THE ANNUAL DOSE

III.1. INTRODUCTION

The annual dose refers to the rate at which mineral grains absorb energy from the flux of nuclear radiation that exists in every natural environment. The radiation (α, β, and γ) is emitted by the naturally occurring long-lived radionuclides ^{232}Th, ^{238}U, ^{235}U and their daughters, ^{40}K and ^{87}Rb. In addition, there is also a contribution from cosmic radiation. The decay schemes of the naturally occurring radionuclides are represented in **figures III.1- III.4**.

Regarding the cosmic radiation, the main component of interest is the secondary hard component, which is composed mainly of muons. The soft electronic component is absorbed by the upper half meter of sediment. The cosmic dose rate is usually not measured directly. Expressions are available in the literature for calculating cosmic dose rates at any depth, altitude and geomagnetic latitude (Prescott and Hutton, 1994).

Dose rate calculation relies on the infinite matrix assumption. This means that within a volume having dimensions greater than the ranges of the radiations, the overall rate of energy absorption is equal to the rate of energy emission. If assume that the matrix is uniform both in radioactivity and absorption coefficient, it follows that the absorption per unit of mass is equal to the emission per unit of mass. The latter is available from nuclear data tables. Consequently, using these nuclear data, the dose rate corresponding to a given concentration of radionuclides in the sediment can be calculated

Several techniques are available to determine the dose rate. Indirect techniques encompass instrumental neutron activation analysis, alpha counting, beta counting, atomic absorption spectrometry, NaI (Tl) gamma-ray spectrometry both in field and in low background laboratory conditions, and extended energy range Ge gamma-ray spectrometry in low background laboratory conditions.

These techniques yield concentrations or a count-rate from which the annual dose can be derived using conversion factors. As an example we present the alfa, beta and gamma contributions to the dose rate assuming a sample containing 1ppm natural uranium, 1ppm natural thorium, and 1% natural K, respectively Rb.

Table III.1: *Contribution to the dose rate of 1ppm U, 1ppm Th, 1% natural K and 1% Rb (Aitken 1985)*

	ALPHA (mGy/ka)	BETA (mGy/ka)	GAMMA (mGy/ka)
K	**-**	**830**	**244**
Rb	**-**	**23**	**-**
Th-series	**738**	**28.6**	**51.4**
Th- pre thoron	**308**	**10.3**	**20.8**
U- series	**2779**	**146.1**	**114.9**
U- pre radon	**1260**	**61.0**	**5.6**

The most recent factors to convert concentrations to dose-rates are those tabulated by Adamiec and Aitken (1998). Direct determination of the dose rate is accomplished through the use of highly sensitive TL or OSL phosphors such as $CaSO_4$, CaF_2:Dy or Al_2O_3:C. Detailed accounts on these radio-analytical techniques can be found in Aitken (1985, 1998), Knoll (2000), Hossain (2003), and references therein.

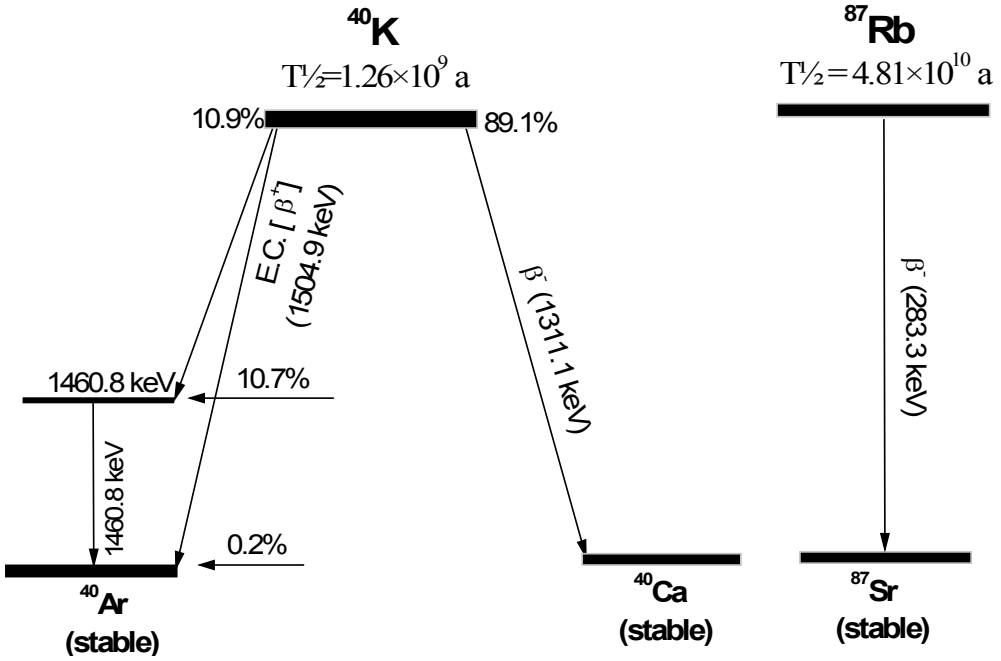

Figure III.1. *Decay schemes of ^{40}K and ^{87}Rb-87.*

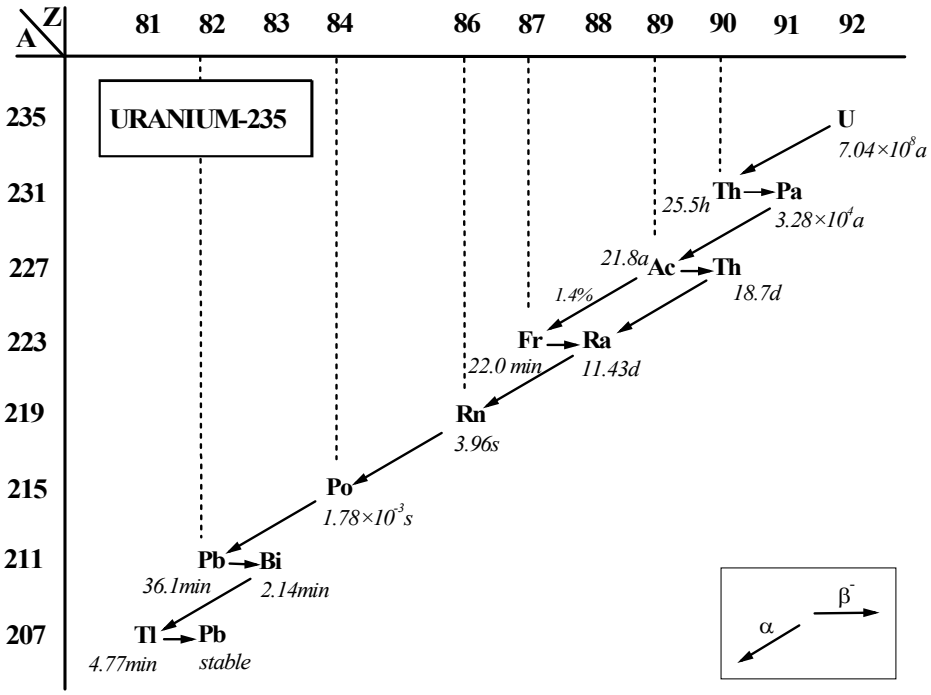

Figure III.2. *Decay scheme for the ^{235}U series.*

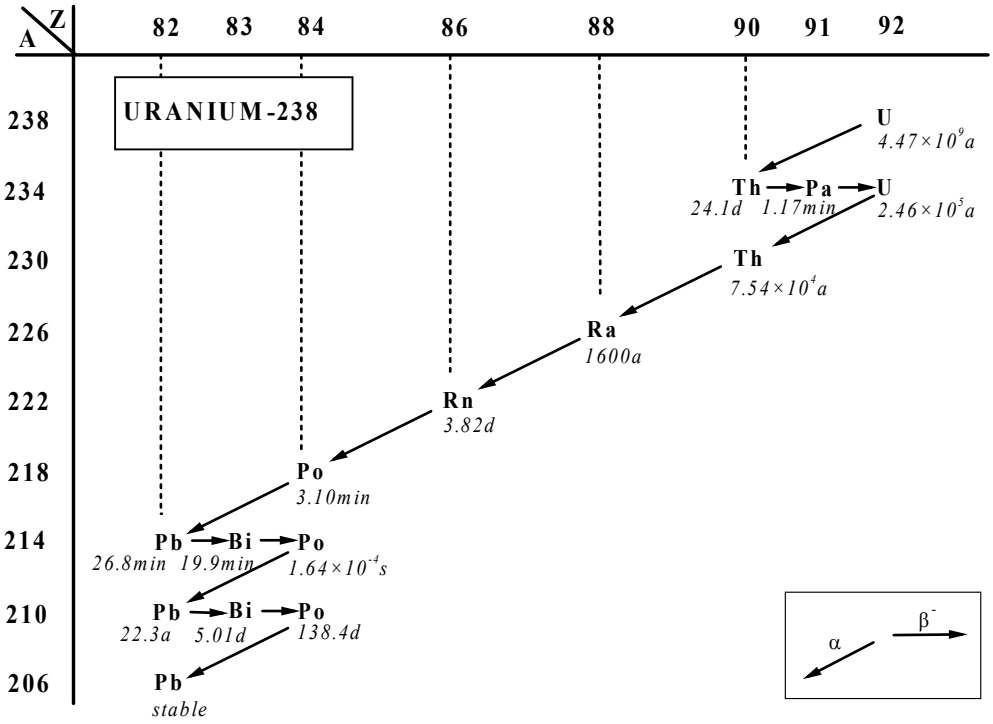

Figure III.3. *Decay schemes for the ^{238}U series.*

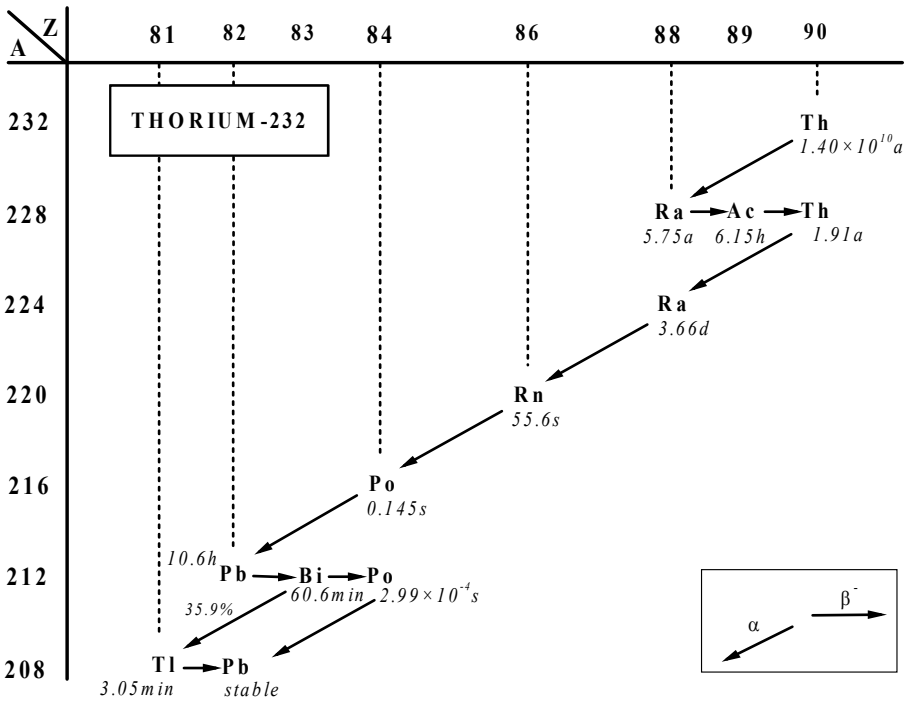

Figure III.4. *Decay scheme for the ^{232}Th series.*

III.1.1. Penetrating powers of the nuclear radiations

The range of alpha particles and beta and gamma radiation are very different in any medium. In silicate minerals, the travel distance of alpha particles is about 25μm, beta radiation has a range of about 2 mm, while γ-rays can penetrate up to about 50cm (**Figure III. 5**). The different penetration powers can be exploited to facilitate the dose-rate calculations, namely by selecting only a certain grain size fraction for the luminescence measurements.

Fine-grain techniques use minerals with a grain size in the range of 4 to 11μm. These grains are small enough to ensure complete penetration by all three types of radiation. Coarse-grain techniques use grains which are large enough (of the order of 100μm) to enable removal of the outer surface layer that was affected by alpha radiation. This leaves only the contribution from gamma rays and a partially attenuated contribution from beta radiation.

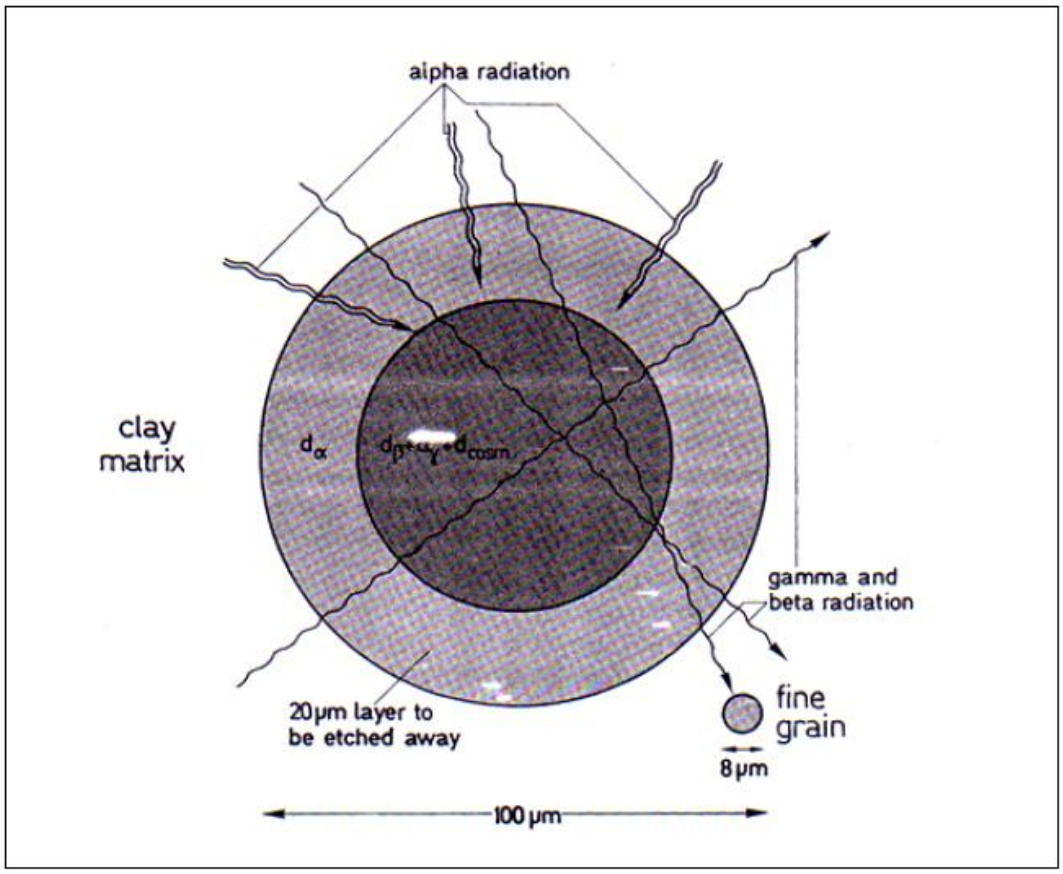

Figure III.5. *Penetrating powers of natural nuclear radiations in silicate materials.*

As far as internal radioactivity is concerned, quartz is generally assumed not to contain radioactivity. Potassium feldspars, on the other hand, commonly have contents in the range of 10-14% potassium and 0.02-0.05% rubidium (Aitken, 1998). The proportion of beta energy deposited within a grain increases with the grain size). For fine-grains the internal beta contribution can be considered negligible.

III.1.2. Efficiency in inducing luminescence of the nuclear radiations

Beta and gamma radiation have the same efficiency in inducing luminescence, meaning that if equal doses of gamma or beta radiation will result in the same luminescent response.

Unlike beta and gamma radiation the luminescence induced by alfa radiation is not proportional to the energy deposited in the sample but approximately proportional to the total track length and thus to the travel range of the alpha particle.

Due to their highly ionizing nature, alpha particles are different; their efficiency being one order of magnitude lower than the efficiency of beta and gamma radiation. When alpha particles travel through a material, they produce such a great amount of electrons that the traps lying on the central track will get saturated. A higher proportion of the deposited energy hereby goes to waste than is the case for the more lightly ionizing beta and gamma radiations. As a result, the amount of luminescence produced per unit of gray is lower for alpha irradiation.

Because the equivalent dose is determined using beta irradiation), allowance must be made for the lower contribution from alpha particles. This can be accomplished by separately evaluating this contribution and subsequently, by multiplying this by an experimentally determined efficiency factor that relates the luminescence response to alpha radiation to that arising from beta or gamma irradiation. The efficiency factor is usually expressed as the a-value (see Aitken, 1985, Appendix K).

In the case of coarse grains, the external alpha contribution is removed by etching. For fine grains, there is full penetration by alpha particles, and the effective alpha contribution must be evaluated. This is a rather time consuming task, and often, a relative efficiency is assumed of about 0.1 (Aitken, 1985). Rees and Jones (1995) reported a values of 0.032- 0.043 for 4 samples using additive alpha and beta dose response curves, while Singhvi (2001) gives values ranging from 0.05 to 0.2In a more recent study Mauz et al (2006) obtained a value of 0.3 for samples exhibiting a linear beta dose response. Another important conclusion of their study is also the fact that for samples exhibiting exponential saturating beta dose response the a values are higher, confirming the dose dependence of alpha effectiveness in quartz.

The conclusion emerging from the things previously presented is that in the case when the efficiency in inducing luminescence of alpha radiations is not determined for each sample analyzed but assumed, this leads to uncertainties in the ages obtained; this will be further discussed in Chapter V.

III.1.3. Attenuation and the effect of etching

In fine grain technique, grains are small enough to ensure a full penetration by alpha and beta particles. Consequently the effect of attenuation of these radiations can be neglected. In the quartz coarse or relatively coarse grain techniques on the other hand the effect of attenuation is significant and has to be taken into consideration. This basically means that the dose rate to the quartz grains is less than the dose rate that is derived from the radioactivity of the surroundings. Etching also causes a further reduction. For alpha radiation it is assumed that etching removes all the contribution while for the dose rate of beta radiation have to be corrected when using coarse grains. For detailed information

regarding attenuation within grains reference is made to Aitken (Aitken, 1985, Appendix C) and Mejdahl (Mejdahl, 1979).

III.1.4. The influence of moisture content

Water in the sediment pores absorbs part of the radiation that would otherwise reach the mineral grains. It has been calculated that, compared to silicates, the absorption coefficient of water is 50% higher for alpha radiation, 25 % higher for beta radiation and 14% higher for gamma radiation (Zimmerman, 1971; Aitken and Xie, 1990). This means that the effect of moisture content on the annual dose is strong and if the values obtained on dry sediment are applied, one will underestimate the real age. If the dose rates are obtained on dry material the wet doses can be calculated by introducing the appropriate attenuation factors as follows:

$$D_{\alpha} = \frac{D_{\alpha,dry}}{1+1.5 \cdot W \cdot F} \tag{3.1}$$

$$D_{\alpha} = \frac{D_{\alpha,dry}}{1+1.25 \cdot W \cdot F} \tag{3.2}$$

$$D_{\gamma} = \frac{D_{\gamma,dry}}{1+1.14 \cdot W \cdot F} \tag{3.3}$$

In the formulas above, W is the saturation level. It is calculated as the ratio of the mass of water the sample takes up at full saturation to the mass of the dry sample. F denotes the fraction of saturation corresponding to the assumed average water content over the entire burial period. Uncertainty on how the water content may have varied throughout the entire burial period of the sample is a fundamental limitation in the accuracy attainable with the luminescence dating method.

III.1.5. Radioactive equilibrium and disequilibrium

An important assumption in luminescence dating is that the dose rate has remained constant throughout the period that is to be dated. It is well known that in a closed system the naturally occurring decay series attain a condition of radioactive equilibrium. This means that the activity of all the nuclides in the chain is the same. However, if the system is open, and one or more of the daughters can be removed or added, a situation of

radioactive disequilibrium can occur. Typical causes of radioactive disequilibrium are escape of the gaseous daughter ^{222}Rn, and the escape or enrichment of the soluble daughter ^{226}Ra.

Disequilibria are unlikely to occur in the ^{232}Th series due to the relatively short half-lives of the daughters involved. In the ^{238}U series, however, the half-lives of the nuclides that have a tendency for being mobile are long enough (^{222}Rn: $T_{1/2}$=3.8d; ^{226}Ra: $T_{1/2}$=1600a) for being transported in and/or out of a sediment sample.

High resolution Ge gamma-ray spectrometry in low-background conditions can be used for checking whether or not disequilibria are present. Using this technique, the concentration of certain key isotopes at different positions in the decay series is measured. In this way, the depletion or enrichment of one or more daughter-isotopes can be identified and quantified and assumptions about the conditions in geological time can be made. For more details, reference is made to Hossain et al., 2002; Hossain, 2003; Vandenberghe, 2004 and De Corte et al., 2005.

III.1.6. Annual dose equation

Taking into consideration the previous sections the equation for the annual dose in luminescence dating can be written as:

$$Annual\ dose = a \cdot \frac{D_{\alpha(U,Th)}}{1+1.5WF} + \frac{D_{\beta(U,Th,K,Rb)}}{1+1.25WF} + \frac{D_{\gamma(U,Th,K)}}{1+1.14W_1F} + D_{\cos} \qquad (3.4)$$

Where:

a – is the alpha efficiency factor

W - is the water saturation level -W=W_1 in the case of sediment dating

-W refers to the water saturation level of the ceramic shred in the case of pottery dating

-W refers to the water saturation level of the surrounding soil in the case of pottery dating

F- fraction of saturation

Dα, Dβ, Dγ- are the α, β,γ dose rate contribution derived from radioactive elemental concentration or specific activities using conversion factors. And Dcos is the cosmic dose rate.

III.2. ESTIMATION OF ENVIRONMENTAL RADIONUCLIDE CONCENTRATION IN SOILS, A COMPARISON OF METHODS FOR THE ANNUAL DOSE DETERMINATION IN LUMINESCENCE DATING IN ARCHAEOLOGY- A CASE STUDY

III.2.1. Introduction

The assessment of the annual radiation dose is an important step in the dating process since it influences directly the final result and its uncertainty is linearly transferred to the age.

However, in the determination of the dose rate for luminescent dating it is important to distinguish between the dose absorbed by the soil matrix and by the grain showing luminescence. For example, quartz grains separated from the soil are almost free of internal radioactivity, and the outer layer of large grains can be etched, reducing thus the contribution of alpha radiation to zero. On the contrary, the fine grain technique is concerned only with grains that have received the total matrix dose. In particular, humidity is also an important factor, influencing mostly the alpha dose received by grains (Aitken, 1985). Therefore the annual dose rate of radiation has to be divided at least into three contributions to the varied absorption of alpha, beta and gamma radiation.

Thus, the determination of the dose rate in luminescent dating implies two steps. Firstly, the activities of the above mentioned isotopes have to measured and then the relevant activities have to be converted to the energy released per disintegration. This energy has to be related to the alpha, beta and gamma contribution. As usual, Auger and internal conversion electrons are included in the beta part, X-ray and bremsstrahlung radiation in the gamma contribution. Conversion is performed using factors calculated from nuclear data tables, the most recent system being the one proposed by Adamiec and Aitken (Adamiec and Aitken, 1998).

In this work three of the most important methods available for natural radioactive isotope concentration measurement are compared, namely: instrumental neutron activation for measuring ^{238}U, ^{232}Th and ^{40}K, high resolution gamma spectrometry for determine the activities of ^{234}Th, ^{226}Ra, ^{214}Pb, ^{214}Bi, ^{210}Pb, ^{228}Ac, ^{208}Tl, as well as ^{40}K, and, moreover, concentrations of ^{210}Po, ^{226} Ra and ^{238} U were also determined through alpha spectrometry.

It should be mentioned that no special efforts were made to measure the Rb-annual dose rate, which can be derived with sufficient accuracy from an assumed average K: Rb concentration ratio of 200:1 (Aitken 1985). Also, our measurement do not yield information on ^{235}U. This is however of minor importance in view of its small contribution to the total U activity (~4.4%). Nevertheless, its contribution can be taken into account via ^{238}U, assuming a natural isotopic ratio of ^{235}U to ^{238}U. Finally, the contribution from cosmic

radiation amounts to a few percent and can be calculated using the formula developed by Prescott and Hutton (Prescott and Hutton, 1994).The case study chosen was the Neolithic archaeological site of Lumea Nouă, Romania. The analysis was carried out on five soil samples collected from the depths of: 0.8-1 m (sample 1), 0.4-0.5 m (sample 2), 1.5-1.7 m (sample 3), 1-1.2 m (sample 4), and 0.8-1 m (sample 5).

III.2.2. Methodologies and experimental set-ups

III.2.2.1. High resolution gamma spectrometry

High resolution gamma ray spectrometry analysis was carried out on an ORTEC hiperpure germanium detector having the following characteristics: active volume of 181 cm^3, 0.878 keV FWHM at 5.9KeV, 1.92 keV FWHM and 34.2 % relative efficiency at 1332.5 keV. The system was calibrated in energy using a standard Eu source.

The detector is mounted in a lead castle and has a 0.5mm beryllium window which makes it suited for measuring several U and Th decay products, down to ^{210}Pb with a gamma ray energy of 46.5keV. This is important, because it is an indicator for possible radon escape in archaeological or geological times. In addition to this nuclide, other lines that were investigated are ^{234}Th (63.3keV), ^{226}Ra (186.2keV), ^{214} Pb (295.2 and 351keV), ^{214}Bi (609keV). The line at 609 keV of ^{214}Bi was later on excluded from calculation as it was concluded that suffers consistent sum out effects. This is in agreement with other studies as well (for example Garcia-Talavera et al 2001) The lines at 63.3keV and 186.2keV are moderately to heavily interfered by the 63.8 and 185.7keV lines of ^{232}Th and ^{235}U, respectively, thus requiring proper corrections (Hossain, 2002). In the ^{232}Th decay chain we measured ^{228}Ac (338.3 and 911keV) and ^{208}Tl (583.2keV) (**Figure III.6**).

Eventually, also the 1460.8keV gamma ray of ^{40}K can be measured. The activity of each nuclide in the sample is derived from the equation:

$$\Lambda = \frac{N}{t_m \cdot \varepsilon \cdot y} \tag{3.5}$$

Where N represents the net number of counts (intensity) under the peak of interest, t_m is the spectrum acquisition time, ε is the computed efficiency of the sample-detector and y represents the absolute intensity (emission probability) of the gamma line.
A typical soil spectrum is shown in **Figure III.7**.

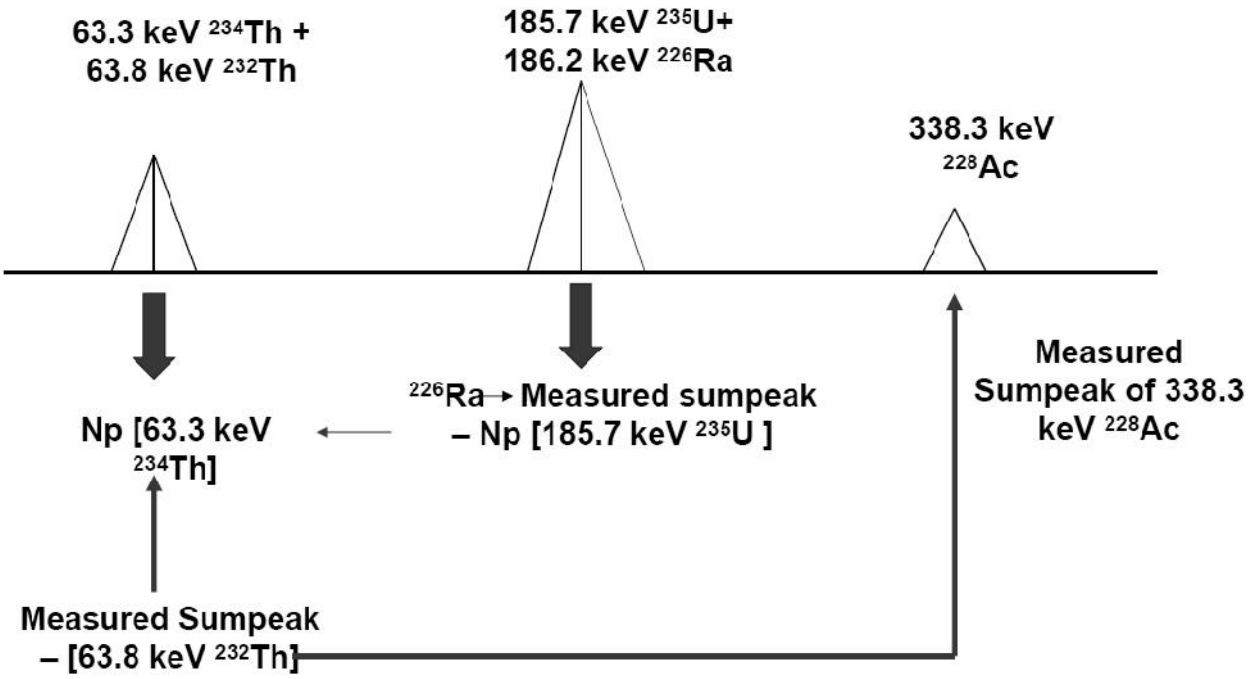

Figure III.6: *The principle for direct measurement of Ra-226 activity from the 185.7 keV gamma line.*

Detection efficiencies were computed for the energies of interest using a Monte Carlo Code (GES-Gamma Electron Efficiency Simulator version 2.7 (Fulea, 2009). Moreover, in order to validate the procedure used we also determined the detection efficiencies experimentally, using radiometric reference materials RGU-1 (400 ± 2 μg/g) and RGTh-1 (800 ± 16 μg/g), measured in the same geometry as the soil samples, issued by the IAEA (IAEA Report, 1987). In these standards the U and Th decay series are in equilibrium. A comparison of the values obtained by the two methods is represented in **Figure III.8**. The differences that can be observed are to be expected due to the differences of chemical composition and packing density thus there is reason to have confidence in the values obtained by simulation.

The influence of the measurement time on the minimum detectable activity was studied in order to determine the optimum measurement time for the samples. The dependence is shown in **Figure III. 9.** All the samples were measured for at least 150000 seconds the measurement geometry being a cylinder in all cases.

Before being measured the samples were homogenized and dried till constant weight. We also estimated the percentage radon loss due to this procedure. Radon loss due to sample preparation was estimated at 15%, thus we stress upon the need for storing the samples for three weeks before measurement in order to for the radioactive equilibrium to be reached again.

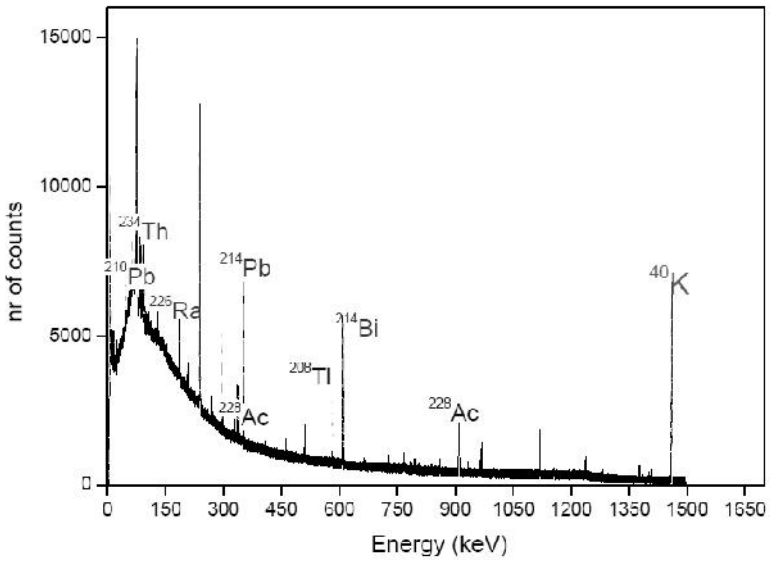

Figure III.7: *Typical high resolution gamma spectrum of a soil sample (soil sample number 5). The measurement time was 500000 seconds.*

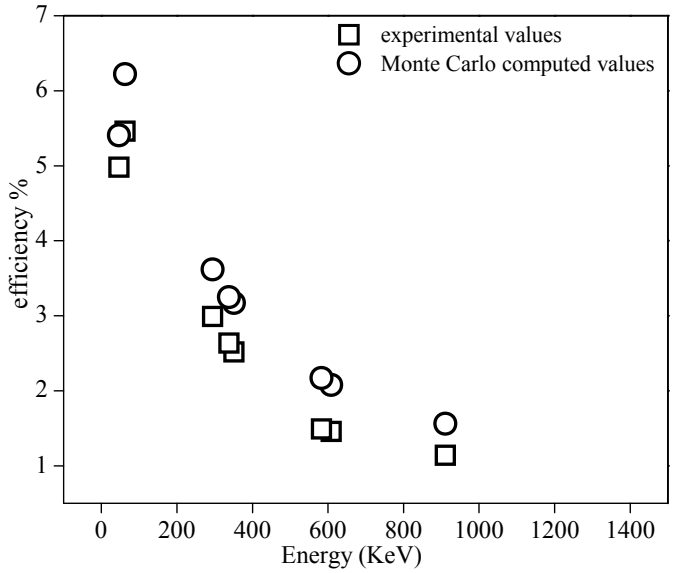

Figure III.8: *Comparison between efficiency values determined experimentally using IAEA RGU-1 and RGTh-1ores and Monte Carlo computed values for soil.*

As previously mentioned, ^{226}Ra 186.2keV is heavily interfered by the ^{235}U 185.7keV line and a correction for this interference is needed to obtain unambiguous results, directly obtained values for ^{226}Ra being of major importance as usually in soils equilibrium cannot be assumed between ^{238}U and ^{226}Ra the latter being soluble and thus being subjected to transportation by percolating groundwater.

Correction for the interference was made following a suggestion of De Corte et al (2005). This is based on the calculation of ^{235}U 185.7 peak area from the rather intense ^{234}Th peak at 63.3keV. Two assumptions have to be made in this case: that ^{238}U and ^{235}U are present in their isotopic natural ratio and that ^{238}U and its immediate daughter ^{234}Th are in

equilibrium. Moreover 63.3 keV ^{234}Th peak is also spectrally interfered by a ^{232}Th peak at 63.8 keV. The correction for this interference is made using ^{228}Ac peak at 338.1keV, obviously assuming equilibrium between ^{232}Th and ^{228}Ac.

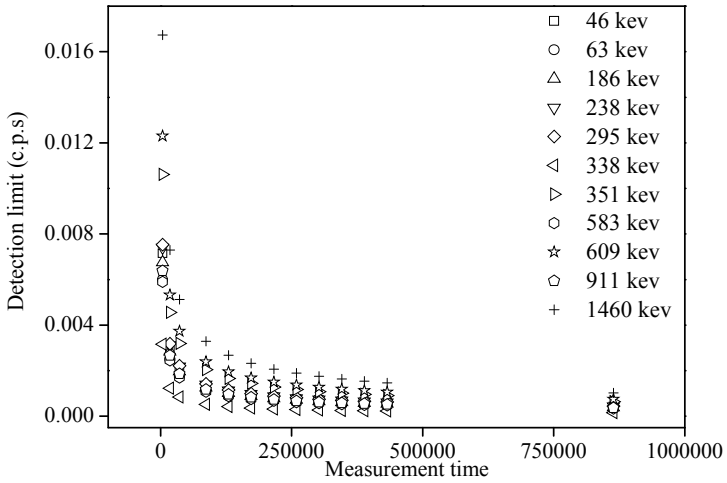

Figure III.9: *Minimum detectable count rate for different peaks as function of measurement time. The values represent the minimum count rate necessary in order to elliminate both false negative and false positive results above background count rate.*

The procedure was validated by measuring IAEA-312 radionuclides in soil standard. Values obtained experimentally and values given by IAEA are plotted in **Figure III.10**. It can be seen that a very good agreement within error limits was obtained. Thus the procedure was applied for all measured samples.

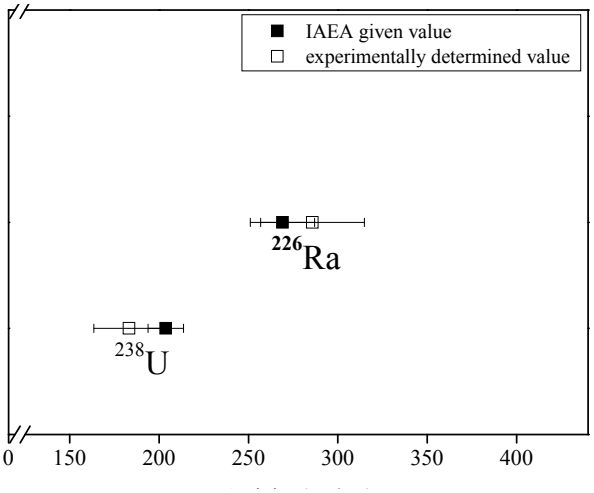

Figure III. 10: *comparison between the experimentally calculated values and the values given by IAEA for the specific activities for uranium, radium and thorium for standard material "IAEA-312 radionuclides in soil".*

III.2.2.2. Instrumental neutron activation

For elemental concentration determination of ^{238}U, ^{232}Th and ^{40}K the Zirconium standardisation method was used (De Corte 1987). Two of the five stable isotopes of zirconium (^{94}Zr and ^{96}Zr) generate the short live radioisotopes ^{95}Zr ($T_{1/2}$=64.02d) and respectively ^{97}Zr ($T_{1/2}$=16.9h) by neutron capture reactions. The zirconium monitor has a double utilization. The thermal to epithermal neutron flux ratio and the concentration of analysed element can be obtained from ^{95}Zr and ^{97}Zr. The elemental concentration is obtained according to:

$$\rho_i = \frac{A_{sp,i}}{S \cdot D \cdot C \cdot w} \cdot \frac{1}{k_{anal} \cdot A_{sp,c}} \tag{3.6}$$

Where ρ_i is elemental concentration; $A_{sp,i}$ are the photo peak count rates, representing the full-energy peak and counting time ratio; S is the saturation factor = 1-exp($\lambda_i \cdot t_i$) ; λ is the decay constant =(ln2)/$T_{1/2}$; D is the decay factor = exp (- $\lambda_i \cdot t_d$) , t_d is the cooling time; C is a "measurement" factor = (1-exp(-$\lambda_i \cdot t_c$)/ ($\lambda_i \cdot t_c$); w = mass of irradiated element and k_{anal} is a nuclear constant.

Due to the decay scheme of both radioisotopes and the induced reaction rate, ^{95}Zr, ^{97}Nb is advisable to perform measurement time range of 3 – 6 day from end of irradiation. Handy manipulation, small neutron self-shielding factor and a good accuracy for thermal neutron flux greater than 10^{10}n/cm^2*sec are the main advantages of Zr foil utilization in the neutron activation analysis technique.

Before irradiation the samples were de-hydrated, weighed and then packed into Teflon cartridges. The samples were irradiated in a pneumatic rabbit in the D11 dry channel of the TRIGA-ACPR reactor. During irradiation time the ACPR reactor was operated in stationary mode (100 KW).The samples were irradiated together with Zr monitor, in order to determine the thermal neutron flux (E<0,5eV) to epithermal neutron flux ratio; the irradiation time was of 2 hours. The samples were measured after 48 hours to allow ^{24}Na decay ($T_{1/2}$ = 15 h) which is formed by neutron capture in significant quantities in all the samples. Both the Zr monitor as well as samples induced activities were measured with a high-resolution gamma spectrometer with a 128cm^3 HpGe detector type GEM-20180 and 20% relative efficiency. The system was calibrated for efficiency for certain source-to-detector distances with some sets of standard sources (^{241}Am, ^{133}Ba, ^{137}Cs, ^{60}Co and ^{152}Eu). The thermal to epithermal neutron flux ratio determined from the reaction rates induced in the two Zr nuclides is f=10.56. The gamma spectra were processed using GENIE2000 software analysis package. The element concentrations were calculated using a home developed software (Barbos and Paunoiu, 2004).

III.2.2.3. Alpha spectrometry

Measurements were performed using a Canberra 7410 alpha spectrometer with a PIPS detector having a resolution of 19keV. The peaks of interest were 5.305MeV for ^{210}Po, 4.784 for ^{226}Ra and 4.196MeV for ^{238}U.

The first step in the chemical separation procedure implied was dissolving the soil samples. For this use was made of a Microwave Milestone ETHOS labstation, equipped with a EasyWave EasyControl Software. For each 0.5g of samples 8ml of 65%NO_3, 5 ml of 37% HCl and 1.5ml of 40%HF were added. Then a three step heating treatment was performed up to 210^{o}C.

In the case of ^{210}Po, samples with a thickness of 1-2 microns were prepared on 18.5 mm CrNi disks by spontaneous electrodeposition. As it is quite difficult to control the pH in the solutions before depositions and thus sometimes a low recovery is spotted (Lee, 2000). ^{209}Po was added as a tracer, its peak at 4.866 MeV being also analyzed in order to be able to make the necessary corrections. Ra samples were prepared using the Cathion exchange column method. This is a very effective method and the only correction that had to be implied was related to the filtering efficiency; for this the coprecipitation of $BaSO_4$ was implied.

In the case of uranium, the disks were prepared by electrodeposition. The efficiency of the ion exchange column and the chemical processes was checked analyzing the peak at 5.320MeV of ^{232}U which was added as a tracer.

III.2.3. Results and discussions

Natural radionuclide concentrations were determined using three different methods in five soil samples that surrounded Eneolitical ceramics with the purpose of determining the annual gamma dose absorbed by coarse quartz grains inside the ceramic shreds. Specific activities of the nuclides of interest measured in the uranium series are presented (see **Table III.2**). They are clearly divided taking into consideration the possible cases of disequilibria (radium enrichment or depletion and radon loss).

Values obtained for ^{238}U by instrumental neutron activation are consistent within error limits with the values obtained for ^{234}Th through high resolution gamma spectrometry. As equilibrium between the above mentioned nuclides can be regarded as a fair assumption in the case of soils, we can conclude that the emission at 63 keV of ^{234}Th can be used with satisfying accuracy for gamma spectrometric measurement of ^{238}U. The assumption that radium disequilibrium is not unusual in soils was supported by the results obtained both through gamma spectrometry in the cases of sample 2 and sample 3, where a certain degree of radium enrichment can be noticed. Even though, the degree of disequilibrium is not sufficiently severe to have an important influence on the final age of

ceramics taking into consideration the overall precision of the luminescence method (see **figure III.11**). Nevertheless, taking into consideration the fact that gamma spectrometric data are supported by alpha spectrometric results for ^{226}Ra we do stress upon considering the detailed investigation on the concentration of this nuclide as a worthwhile procedure when performing gamma spectroscopic measurements.

Table III.2: *Specific activities of the nuclides in the uranium series measured by high resolution gamma spectrometry (^{234}Th, ^{226}Ra, ^{214}Pb and ^{210}Pb), neutron activation analysis (^{238}U) and alpha spectrometry (^{226}Ra and ^{210}Po). Errors quoted represent 2s uncertainty and were obtained according to the classical laws of error propagation.*

Sample	Uranium specific activity (Bq/kg)						
	Pre- Ra		Ra		Post-Rn	^{210}Pb and ^{210}Po	
	Gamma Spect. ^{234}Th	Neutron activation ^{238}U	Gamma Spectr. ^{226}Ra	Alpha Spectr. ^{226}Ra	Gamma Spectr. ^{214}Bi	Gamma Spectr. ^{210}Pb	Alpha Spectr. ^{210}Po
1	**24.8±6.9**	**23.3±2.1**	**18.1±2.0**	**-**	**23.8±1.9**	**31.1±10.1**	**20.4±3.6**
2	**23.1±7.7**	**22.7±1.9**	**40.3±10.6**	**36.0±6.0**	**26.0±2.1**	**14.6±7.0**	**23.1±4.1**
3	**16.8±9.5**	**19.8±1.7**	**35.0±15.7**	**30.0±6.0**	**24.3±2.2**	**24.5±8.1**	**26.7±4.5**
4	**31.9±8.2**	**24.1±1.5**	**21.1±11.2**	**17.0±5.0**	**23.0±2.2**	**31.9±7.3**	**27.7±4.1**
5	**22.1±7.4**	**21.6±2.0**	**33.5±8.8**	**-**	**22.6±8.1**	**21.2±8.7**	**29.2±8.8**

Deriving the activity ^{210}Pb is also of major importance as this nuclide can serve as an indicator of radon loss throughout geological or archaeological time. Due to the low energy emission of this nuclide (46.5 keV) gamma spectrometric measurements are difficult to be performed with sufficient precision unless special detectors in ultra low background conditions are being used. Thus we consider data on ^{210}Po derived through alpha spectrometry to yield more reliable results.

Table III.3: *Specific activities of ^{232}Th and ^{40}K measured in the investigated soil samples by high resolution gamma spectrometry (using ^{228}Ac and ^{208}Tl in the case of thorium series and ^{40}K for potassium) and instrumental neutron activation analysis. Errors quoted represent 2s uncertainty and were obtained according to the classical laws of error propagation.*

Sample	Thorium specific activity (Bq/kg)		^{40}K specific activity (Bq/kg)	
	Gamma Spectr. ^{228}Ac and ^{208}Tl	Neutron activation ^{232}Th	Gamma Spect. ^{40}K	Neutron activation ^{40}K
1	**32.5±3.8**	**41.2±3.5**	**465±25**	**-**
2	**36.2±4.4**	**32.2±2.7**	**585±26**	**487±42**
3	**28.6±3.4**	**30.1±2.5**	**491±51**	**486±42**
4	**29.0±4.0**	**34.8±2.9**	**489±30**	**510±43**
5	**33.2±4.2**	**36.2±3.0**	**598±97**	**537±44**

In the case of thorium series equilibrium can be assumed and the specific activities measured are presented (see **Table III.3**) together with the measured concentrations for ^{40}K.

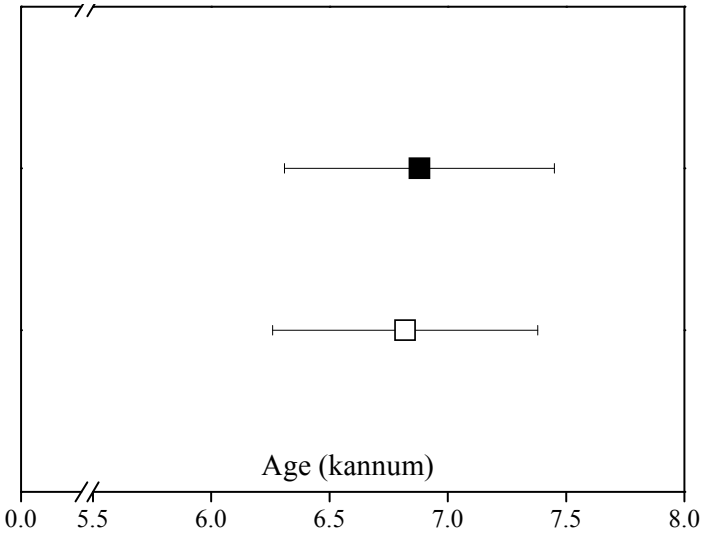

Figure III.11: *Calculated ages for an Eneolitic shred collected from Lumea Nouă archaeological site taking into consideration the dosimetric information for soil sample 2 provided by gamma ray spectrometry (□) (taking into consideration radium enrichment) and by neutron activation analysis (■) (method that does not take into consideration the possible cases of disequilibrium in uranium series).Internal dose rate was taken from Cosma et al. (2006).*

A relatively good agreement between the two methods (gamma spectrometry and instrumental neutron activation) can be seen thus both methods can be accurately used for dosimetric purposes. Nevertheless, it can concluded that despite the better precision of instrumental neutron activation the method of choice for obtaining routine dosimetric information regarding natural nuclides in soils in luminescence dating can be considered to be gamma spectrometry due to the less efforts involved in the experimental procedure and the advantages it offers on the possibility of checking for radioactive disequilibrium in uranium series. For the sake of clarity all specific activities measured in the three laboratories are presented in **Figure III.12**.

Gamma dose rates from the contribution of surrounding soil were quatified using the conversion factors of Adamiec and Aitken (1998) and are presented in **figure III.13**.

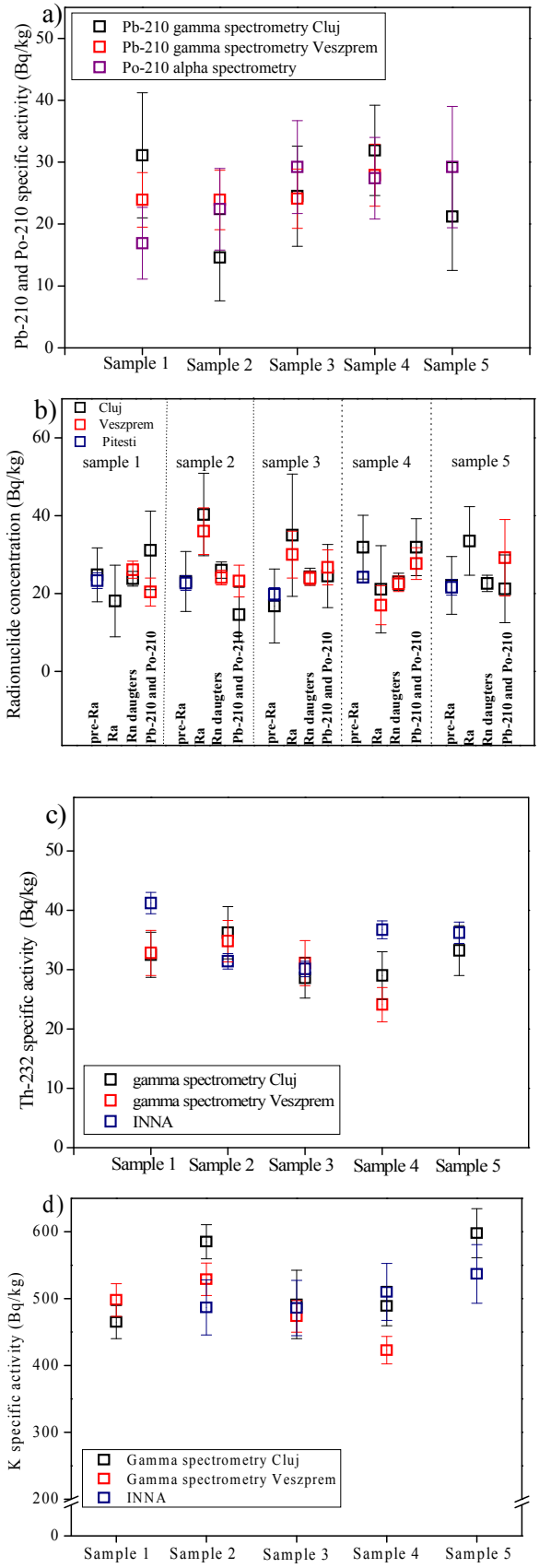

Figure III.12: *Comparison between specific activities of radionuclides of interest obtained in the three different laboratories.*

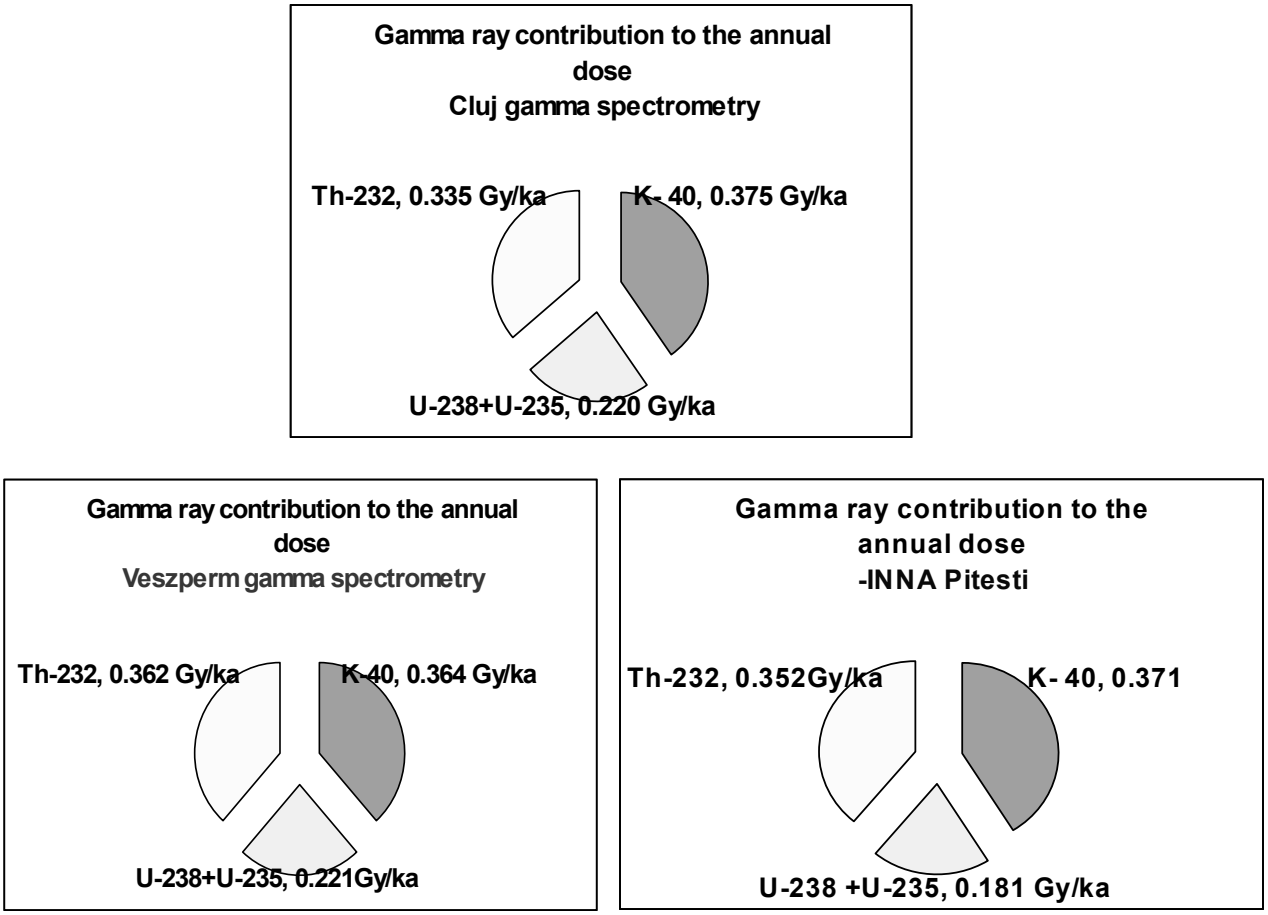

Figure III.13: *External gamma dose rate computed from the specific activities determined in the three different laboratories.*

Considering an equivalent dose of 19.97 ± 0.810 and an average of the internal dose rates presented in Benea et al 2007, the luminescence ages calculated taking in to consideration the external dose rates determined by elemental radionuclide concentration with the above described methods yield the following ages: CLUJ GAMMA SPECTROMETRY- Age = 6.82 ± 0.57 ka,VESZPREM -Age = 6.79 ± 0.56 Ka, INNA PITESTI- Age = 6.88 ± 0.57 Ka, leading us to conclude that annual dose rates necessary in order to calculate luminescence ages can be determined with sufficient confidence using gamma spectrometry measurements in our laboratory.

CHAPTER IV
APPLICATIONS OF LUMINESCENCE DATING IN ARCHAEOLOGY

IV.1. INTRODUCTION

Pottery is often the most abundant material found on archaeological sites and is the basis of many chronological frameworks for the Neolithic, especially in Southeast Europe. Pottery sherds can be dated by four methods: stylistic features, archaeomagnetic intensity, ^{14}C assay of carbon on or within the shred and luminescence analysis of the constituent mineral grains. The most important limitation of stylistic dating is that it can provide only a relative chronology, and it must therefore rely on associations in order for ages to be obtained. Archaeomagnetic intensity analysis is a promising method (McIntosh et al., 2006), but at the moment is not widely applied. Dating through this method can be performed only when a reference curve is established for the region concerned. Very detailed reference curves have been constructed for Bulgaria and Serbia (Kovacheva, 1997), but no such record is available for Romania. Radiocarbon dating is a well-known and established method, and generally allows dating at high levels of precision. Luminescence dating, on the other hand, has the two major advantages. It is an absolute technique giving the age in calendar years and a technique that dates the ceramic object directly.

The possibility of dating ceramic objects by the use of their thermoluminescent properties was first proposed by Grogler et al. (1960) and Kennedy and Knopff (1960). Since then, the method has been extensively studied and applied (see e.g. the reviews by Aitken, 1985 and Roberts, 1997). In the last few years, there have been major developments in both luminescence dating instrumentation and measurement methodology. The introduction of optically stimulated luminescence (OSL) signals in combination with single-aliquot measurement protocols has led to a significant increase in precision, while less sample material is required; this makes luminescence dating a potentially much more useful chronometric tool in archaeology. Nevertheless, the application of luminescence to burnt pottery appears to have benefited only little from these advances in dating technology. Only a few studies are available in the literature and some relevant reports include those by Hong et al. (2001), Takano et al. (2003) and Lamothe (2004). The latter

author applied state-of-the-art luminescence dating procedures (i.e. using the single-aliquot regenerative-dose (SAR) protocol, and both infrared and blue stimulated luminescence signals) to heated artefacts from archaeological sites in Quebec (Canada), and demonstrated that these procedures are able to provide a reliable chronological framework.

In this study, luminescence dating was applied to four pottery fragments excavated at Lumea Nouă (Alba Iulia, Romania). Although the Lumea Nouă settlement has been investigated for over 6 decades now, there is still no accurate and precise chronology available for the excavated Neo-Aeneolithic habitation levels. Therefore, the aim of this study was to apply new approaches in optical dating to improve the chronological framework for the site. To this purpose, the single-aliquot regenerative-dose (SAR) protocol was applied to both blue (OSL) and infrared stimulated luminescence (IRSL) signals from coarse (90-125 μm) quartz and polymineral fine (4-11 μm) grains, respectively. For the sake of comparison, a more conventional approach, which uses a multiple-aliquot additive-dose (MAAD) protocol and thermoluminescence (TL) signals from polymineral fine grains, was applied as well.

IV.2. ARCHAEOLOGICAL CONTEXT AND SAMPLES

The prehistoric settlement at Lumea Nouă (Alba Iulia, Romania) was accidentally discovered in 1942 as a result of public utility works. The first archaeological campaigns were carried out between 1944 and 1947, and systematic excavations have been carried out since then. Although the site is considered to be of major importance for reconstructing the Neolithic and Aeneolithic periods in Romania, a solid and absolute chronological framework has not yet been established for the different cultural levels discovered at the settlement.

The site is located in the north-eastern part of the city of Alba Iulia (Alba County; **Fig. IV.1**), and has acquired an important place on the archaeological map of Romania, especially due to the identification of the painted pottery type that was later named after the settlement – Lumea Nouă.

At present, following the intensification of archaeological excavations and the setting out of research units at different points of the site, we know that the surface of the Neolithic settlement at Alba Iulia – Lumea Nouă exceeds 40 ha. The Neolithic habitations of the Lumea Nouă settlement belong – in chronological order – to Vinča, Lumea Nouă, Foeni, and Petreşti cultures (Paul 1992). Recent investigations have led to the discovery of a habitation level that was attributed to the Foeni group, on the basis of the rich and representative archaeological material found there. Foeni-type pottery at Lumea Nouă depicts a developing community. It is thought that the site contains a wealth of

information which could significantly improve our understanding of the genesis of the Petreşti culture (Gligor, 2006).

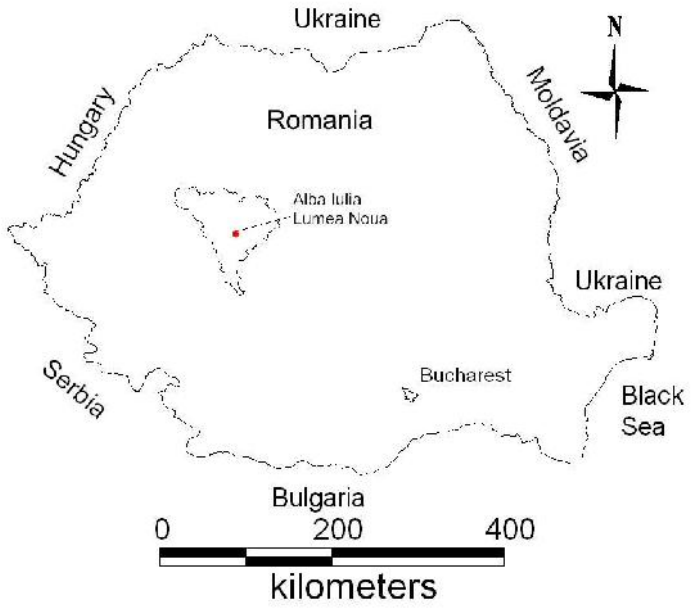

Figure IV.1: *Location of the archaeological site Lumea Nouă (Alba Iulia, Alba County, Central Romania).*

The stratigraphy of the sampling site is the following (**Figure IV.2**):

0 – 0.5 (0.7) m: a blackish layer containing isolated materials in a secondary position. It is considered to be a filling layer, and is possibly a contemporary anthropogenic deposit;

0.5 (0.7) – 0.8 (0.9) m: a black pigmented and granulated layer belonging to the Petreşti culture;

0.8 (0.9) m – 1.0 (1.1) m: a grey pigmented layer containing Foeni and Petreşti materials;

1.0 (1.1) m – 1.7 m: a brownish and clayey layer containing Vinča materials (phase B) and Lumea Nouă painted pottery;

1.7 m – 1.8 m: a yellow pigmented layer. It is a clayey, sometimes sandy unit containing calcareous concretions and no artifacts.

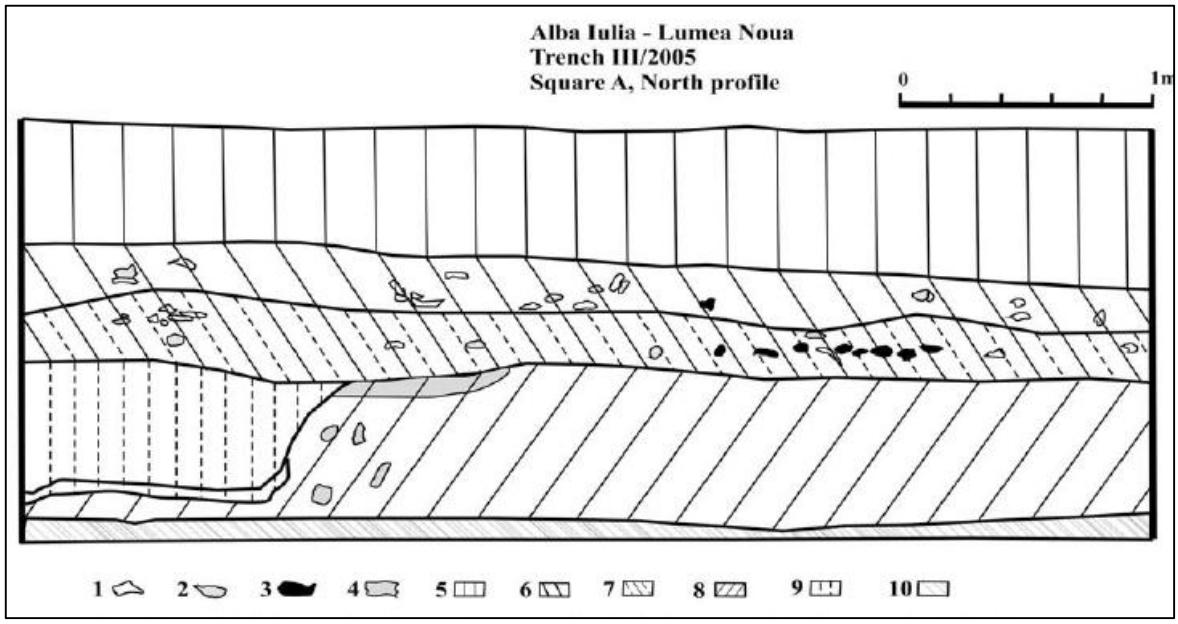

Figure IV.2: *Stratigraphy of the sampling site. 1: pottery; 2: bone; 3:stone; 4: calcareous formation; 5: black layer of filling material; 6: black granular layer belonging to the Petreşti culture; 7: grey figmented layer containing Foeni and Petreşti materials; 8: brownish and clayey layer containing Vinča (phase B) materials; 9: black and clayey layer containing Vinča (phase B) materials; 10: archaeological sterile unit.*

The pottery sherds were collected from the cultural layer, at a depth of 0.8 - 0.9 m, thus from the layer indicating the transition from Foeni to Petreşti culture. The fragments were manufactured using medium sand as a degreasing agent, and thus the resulting pottery belongs to the medium-fine category. From a typological and stylistic point of view, the sherds lack diagnostic characteristics that would allow a precise cultural framing. The lack of ornamental elements is a minus in this respect.

IV.3. LUMINESCENCE ANALYSIS

IV.3.1. Sample preparation

All sample preparation was carried out under dim red or orange light conditions. The outer 2 mm of each pottery fragment was removed, and the inner part was gently crushed using an agate pestle and mortar. The material was then treated with H_2O_2 and HCl to remove organic material and carbonates, respectively, and was sieved using a 63 μm sieve. Polymineral fine (4 - 11 μm) grains were isolated from the fraction < 63 μm using standard procedures (Zimmerman, 1971; Frechen et al., 1996). Aliquots of

polymineral fine grains were prepared by deposition on aluminum discs. Coarse (90 - 125 μm) grains were isolated through dry sieving. Quartz grains were extracted by density separation using sodium polytungstate solutions of 2.62 and 2.75 g cm^{-3}, followed by etching for 40 min with 40% HF. A 60 min wash with warm (ca. 50°C) dilute HCl was applied after etching to remove any precipitated fluorides. Finally, the extracts were dried and sieved again. For measurement, the quartz grains were fixed on stainless steel discs using silicon spray.

IV.3.2. Experimental facilities

All luminescence measurements were carried out using automated Risø TL/OSL readers. The TL signals from polymineral fine grains were measured up to 500°C at a heating-rate of 5°C/s in a pure nitrogen atmosphere. Emission light was detected through a heat absorbing HA-3 and a blue transmitting CN7-59 filter combination. Coarse quartz grains were stimulated using blue (470±30 nm) light-emitting diodes, and the OSL signals were detected through a 7.5 mm tick Hoya U-340 filter. Polymineral fine grains were stimulated with infrared (875 nm) light-emitting diodes. The IRSL signals were detected through a combination of a BG-39, CN-59 and GG-400 filters (410 nm). Details on the measurement apparatus can be found in Bøtter-Jensen et al. (2003).

IV.3.3. TL measurements using polymineral fine grains

The equivalent dose (D_e) was determined using a standard TL multiple-aliquot additive-dose procedure. For each sample, 48 aliquots were used. All samples were stored for 4 weeks at room temperature between irradiation and measurement. A first set of 24 aliquots was used for the measurement of the natural TL signal. To build up the dose-response curve, a second set of 24 aliquots was used, divided in groups of six aliquots. The supralinearity correction was evaluated from the second-glow growth characteristic of the set of aliquots that provided the natural TL data. The equivalent dose was determined using the signals integrated over the plateau region in a plot of the apparent accumulated dose versus temperature (Aitken, 1985). A single saturating exponential was fitted to both the additive-dose and the second-glow growth data. The equivalent dose and the intercept, respectively, were then obtained by extrapolation. The TL glow curves obtained for sample A1 are illustrated in **Figure IV.3 a)** along with the plateau test (**Figure IV.3b)**), and growth curve and second-glow growth characteristic for evaluation of the supralinearity correction (**Figure IV.3 c)**). The results of the equivalent dose determination using TL signals from polymineral fine grains are summarised in **Table IV. 3**.

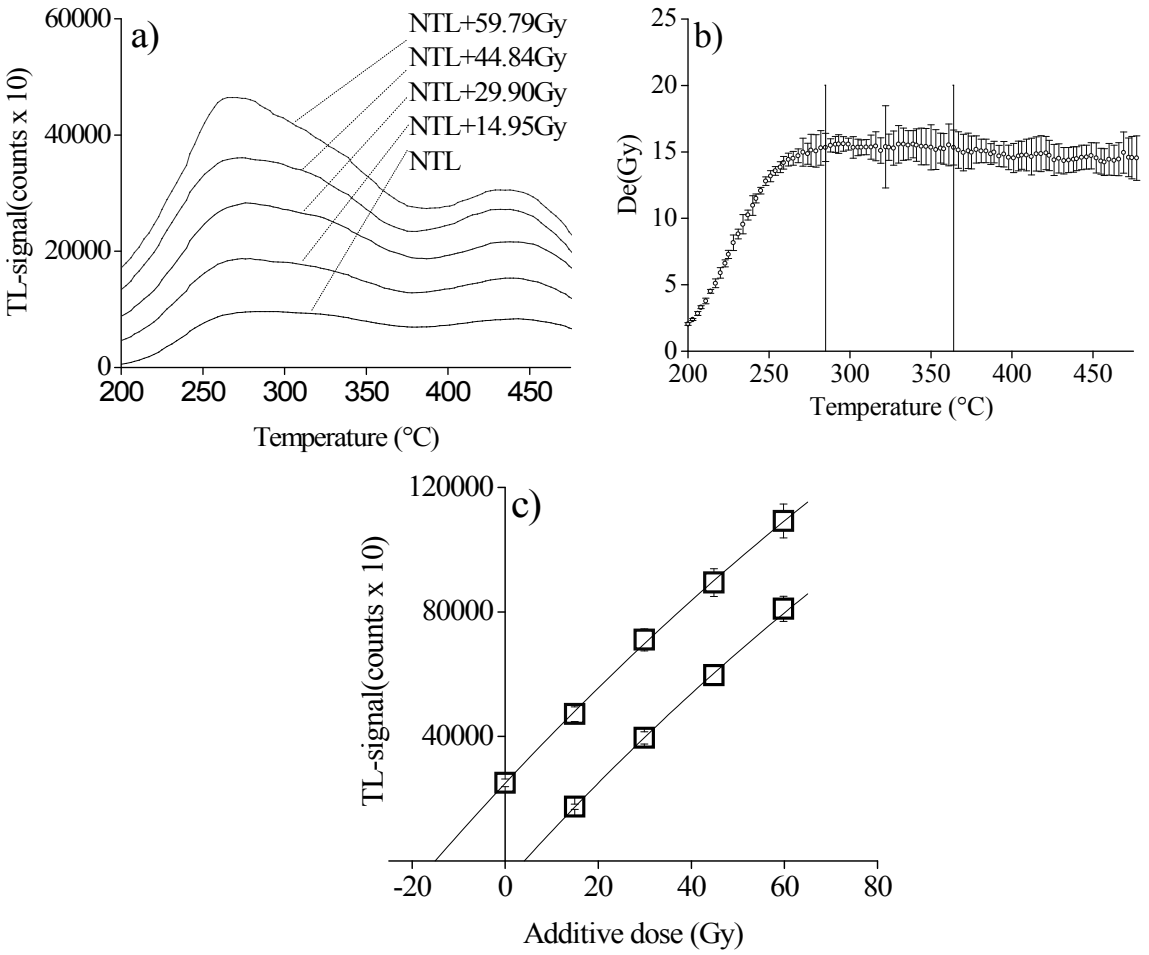

Figure IV. 3: *TL data for sample A1; (a) TL additive glow curves, (b) plateau range, and (c) additive growth-curve (solid squares) and second-glow growth characteristic (solid circles).*

IV.3.4. OSL measurements using coarse quartz grains

Coarse quartz grains were stimulated with the blue diodes for 40s at 125°C and a single-aliquot regenerative-dose (SAR) protocol (Murray and Wintle, 2000; 2003) was used for equivalent dose determination.

The characteristics of the OSL signals were first investigated in terms of behavior in the SAR protocol, dose response and dose recovery. All samples behaved well in the SAR-OSL protocol, with recycling ratios close to unity and recuperation of less than a few % of the corrected natural OSL signal. The growth of the OSL signals with dose could be well-approximated by a single-saturating exponential function. **Figure IV.4** represents a growth curve for sample V1. For sample V3 the dependence of the measured dose on the preheat temperature was investigated through dose recovery tests (Murray and Wintle, 2003).

Aliquots were first bleached twice using the blue diodes for 250s at room temperature, separated by a 10 ks pause. They were then given a dose close to the

expected natural dose, and measured using the SAR protocol. The results are shown in **Figure IV. 5**.

It can be seen that the measured dose underestimates the given dose for preheats in the range of 180-225°C. For a preheat of 10s at 240°C, a measured to given dose ratio of 1.10 ± 0.08 was obtained, which is quite acceptable.

In a following series of experiments, dose recovery tests were carried out for samples A1, V1 and V2 as well. Owing to the limited amount of sample available, these tests were carried out for a preheat of 10s at 240°C only. The complete set of results obtained for this preheat are summarized in **Figure IV 6 a)** and **Figure IV 6b)**. For all samples, the given doses can be recovered to within 10% and the overall average measured to given dose ratio is 1.03±0.04. From these findings, a preheat of 10s at 240°C was selected for determining the equivalent dose using OSL signals from quartz and the SAR protocol. It can be added that a cutheat to 160°C was used in all experiments. The results of the D_e determination are summarized in **Table IV. 3**.

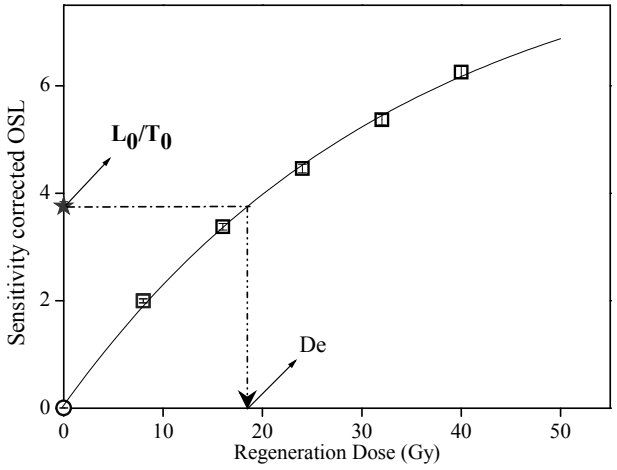

Figure IV. 4: *Sensitivity corrected OSL growth curve for sample V1. Data points were fitted using a saturating exponential. Zero dose and recycling points are represented as a solid circle and solid square, respectively.*

IV.3.5. IRSL measurements using polymineral fine grains

Polymineral fine grains aliquots were stimulated using the IR diodes for 100s at 40°C, and the measurements were performed following a SAR sequence as developed for quartz. The same preheat was applied to both the regenerative and test doses as this enhances the reproducibility of the luminescence measurements (Blair et al., 2005). All samples behaved well in the SAR-IRSL protocol, with recycling ratios close to unity and recuperation values not exceeding a few % of the corrected natural IRSL signal.

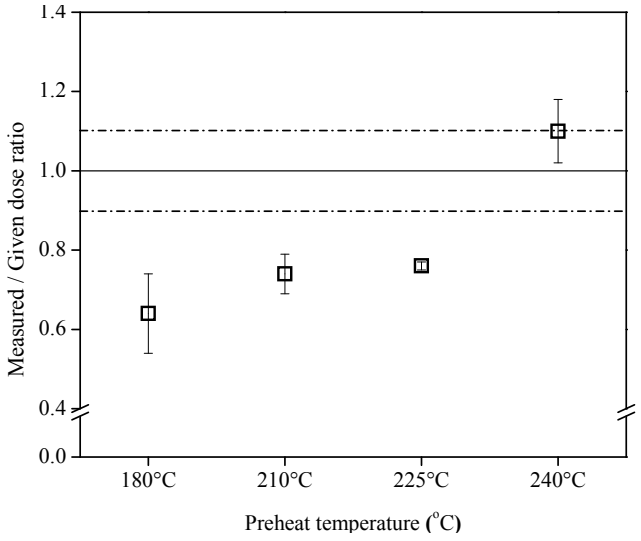

Figure IV.5: *Quartz SAR-OSL dose recovery data for sample V3 as measured to given dose ratios as a function of preheat treatment. The solid and dashed lines (eye guides) represent a measured to given dose ratio equal to unity and a 10% deviation of this ratio from unity, respectively.*

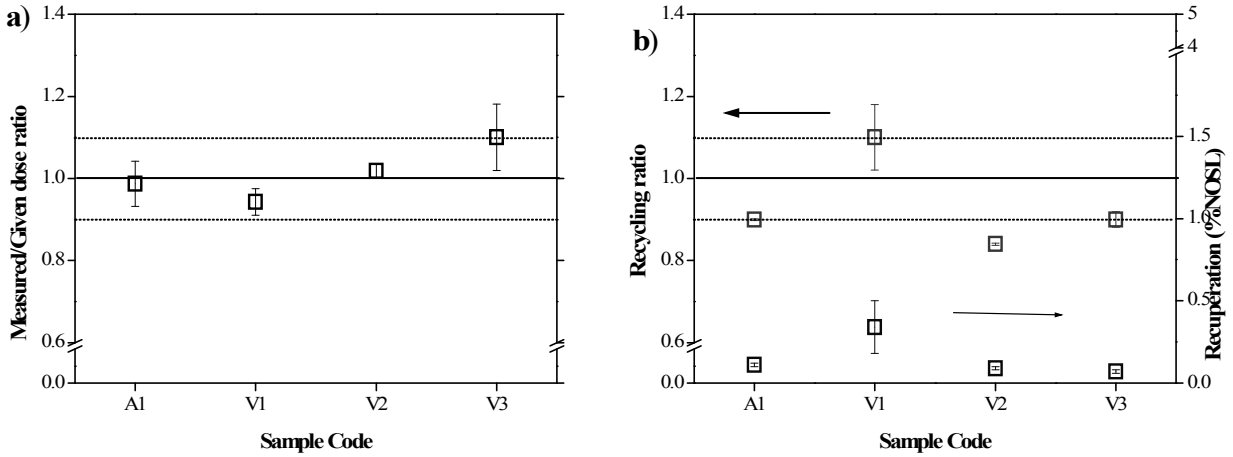

Figure IV. 6: *a) Summary of quartz SAR-OSL dose recovery data obtained for all for samples using a preheat of 10s at 240°C and a cut heat to 160°C. The solid and dashed lines (eye guides) represent a measured to given dose ratio equal to unity and a 10% deviation of this ratio from unity, respectively* ***b)*** *recycling ratios and recuperation . The solid and dashed lines (eye guides) represent a recycling ratio equal to unity and a 10% deviation from unity, respectively. Error bars represent 1 standard error.*

The growth of the sensitivity corrected IRSL signal with dose could be well represented by a single saturating exponential function. A typical average growth curve for sample A1 is illustrated in **Figure IV. 7**. A first series of experiments consisted of an investigation of dependency of the recovered dose on the stringency of the preheat. These experiments were carried out for sample A1. Groups of aliquots were first bleached for 1 hour in a Hönle SOL 2 solar simulator, and were subsequently given a dose close to the

expected natural dose. The aliquots were then measured using the SAR protocol, with each group being preheated for a different length of time at 220°C (10s, 30s and 60s). The results are shown in **Figure IV. 8**. The measured dose shows no dependence on preheat regime and approximates the given dose rather well. For the remaining three samples, dose recovery tests were carried out for a preheat of 10s at 220°C only. The dose recovery results for all samples at this preheat are summarized in **Figure IV. 9a)**. Within analytical uncertainty, the measured to given dose ratios are all consistent with unity. The overall average measured to given dose ratio obtained with the SAR-IRSL protocol is 1.01±0.02. **Figure IV. 9b)** shows the corresponding recycling ratios and recuperation values; the overall averages for recycling ratio and recuperation are 1.06±0.02 and 1.9±0.6%, respectively.

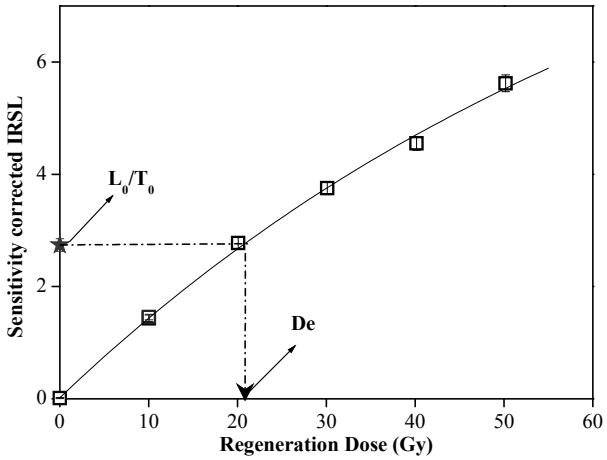

Figure IV.7: *Sensitivity corrected IRSL growth curve for sample A1. Data points were fitted using a saturating exponential. Zero dose and recycling points are represented as a solid circle and solid square, respectively.*

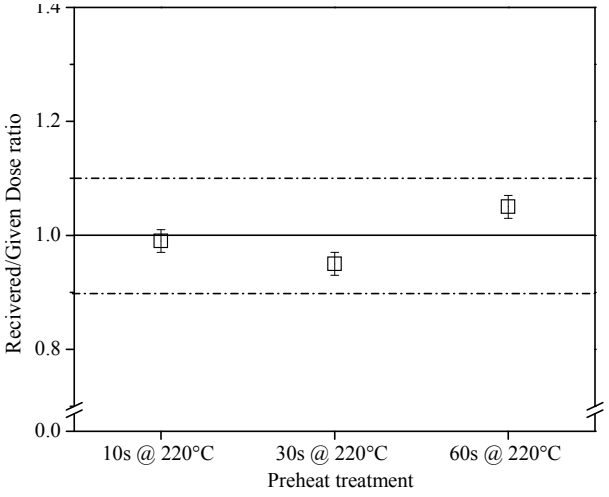

Figure IV. 8: *SAR-IRSL dose recovery data for polymineral fine grains extracted from sample A1 as function of preheat treatment*

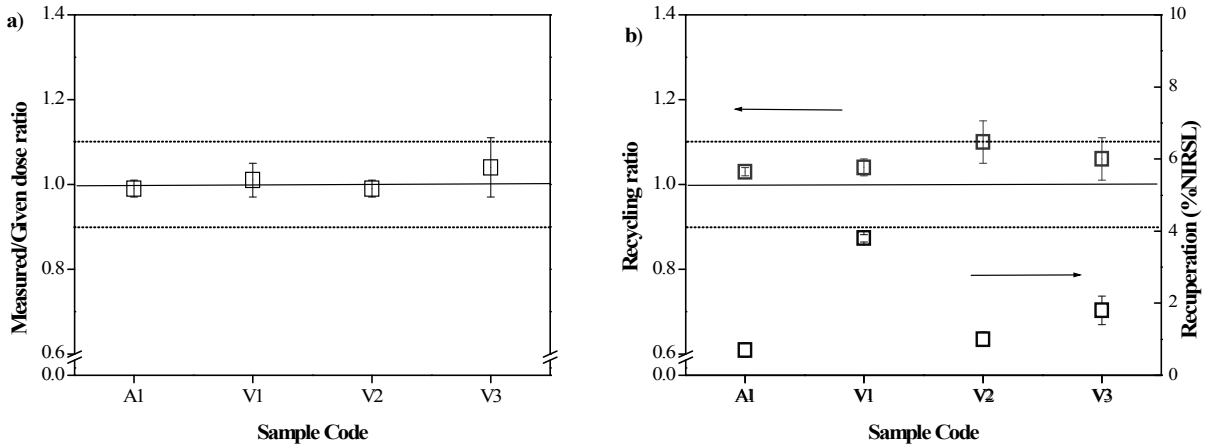

Figure IV. 9: *SAR-IRSL dose recovery data for all investigated samples using polymineral fine grains. The thermal treatments consisted of 10s preheat at 220°C and cut heat to 220°C.* ***a)*** *measured to given dose ratios;* ***b)*** *recycling ratio and recuperation. Error bars represent 1 standard error.*

IV.3.6. Anomalous fading tests

For each sample, anomalous fading measurements of the blue TL emission (detected through a HA-3 and CN7-59 filter combination) and of the 410 nm IRSL emission (detected through a BG39, CN7-59 and GG400 filter combination) by polymineral fine-grains were carried out.

In the case of TL measurements, for each sample a group of six natural aliquots was irradiated with the highest beta dose that had been administrated to construct the additive dose growth curve. Signals measured immediately after irradiation were compared to the signals measured after storage (first glow test-Aitken 1985, p. 58). The time elapsed between the prompt and the delayed measurement was one month.

For IRSL signals, the anomalous fading tests were carried out in a SAR protocol following the procedure proposed by Auclair et al. (2003). For each sample, three aliquots were bleached for one hour in the Hönle SOL2 solar simulator after these had been used for D_e determination. These aliquots were then put through repeated cycles of measuring the response to a regenerative dose (L_i) and a test dose (T_i). Prompt measurements were made, for which the L_i/T_i ratio was measured immediately after irradiation, as well as delayed measurements, for which the L_i/T_i ratio was measured after the aliquots had been stored at room temperature for different lengths of time after irradiation and preheating. Each delayed measurement was followed by a prompt measurement, in order to enable distinguishing the true signal loss caused by fading from experimental variability in the measurements. The L_i and T_i measurement conditions were the same as for the equivalent dose determinations. For each aliquot, the fading rate was then obtained from a plot of the L_i/T_i ratios versus the logarithm of the time elapsed between irradiation and measurement. All fading rates were quantified as g_{2days}-values (the percentage decrease of

intensity per decade of time, normalised to a measurement time of 2 days after irradiation; Aitken, 1985; Huntley and Lamothe, 2001). Anomalous fading was observed in every aliquot examined. **Figure IV. 10** shows representative anomalous fading data for an aliquot of sample A1. Mean values of g_{2days} are summarised in **Table IV. 1** together with the percentage signal loss for thermoluminescence measurements. The amount of fading observed in IRSL signal is similar in all the samples investigated. In the case of TL, percentage loss is comaparable in the case of the first three samples. No fading was observed in the last sample but due to the high scatter in data we assume that this is due to lack of measurement precision or sensitivity changes that were not properly quantified.

Table.IV.1: *Results from anomalous fading tests. In the case of TL measurements, the fading is expressed as the percentage of signal loss observed after a storage time of one month. In the case of IRSL measurements, fading rates were quantified as g_{2days}-values (the percentage decrease of intensity per decade of time, normalised to a measurement time of 2 days after irradiation; Aitken, 1985; Huntley and Lamothe, 2001).*

Sample	signal loss (%) TL	g_{2days} (% per decade) IRSL
A1	9.4 ± 3.3	4.2 ± 0.2
V1	11.8 ± 2.7	2.98 ± 0.4
V2	16.0 ± 3.6	3.63 ± 1.06
V3	-1.08 ± 7.6	3.33±1.03

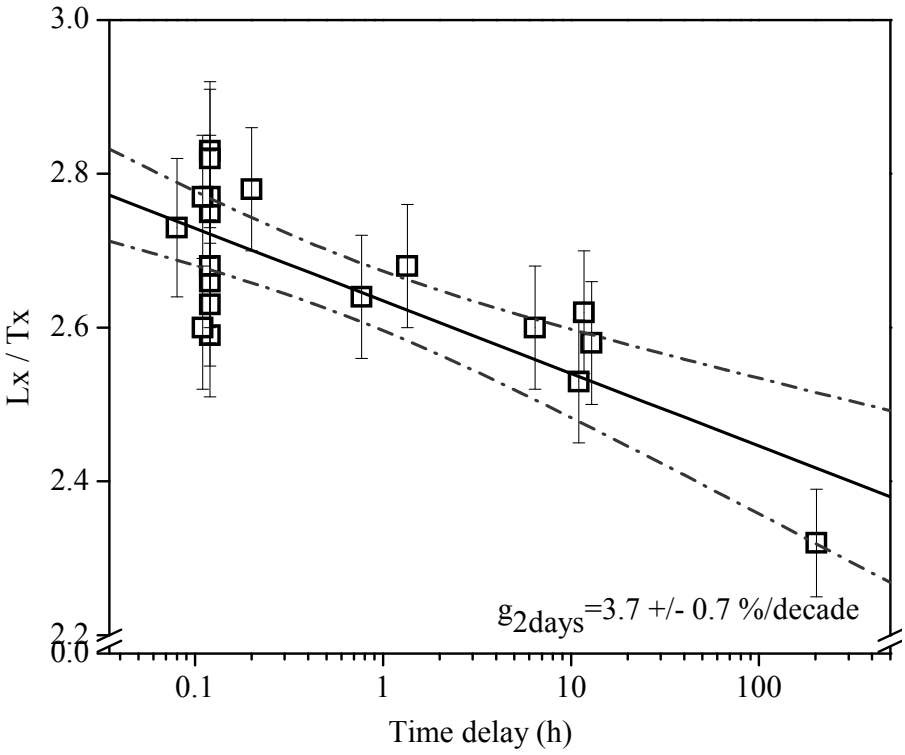

Figure IV.10. *Anomalous fading data for a representative aliquot of sample A1. Plotted are the measured L_i/T_i ratios versus the logarithm of the time elapsed since the end of the irradiation.*

IV.4. ANNUAL DOSE ESTIMATION

The concentration of uranium and thorium in the ceramics was obtained through instrumental neutron activation analysis using the zirconium standardisation method (De Corte, 1987), while the K content was determined using atomic absorption spectrometry. Low-background high-resolution gamma-ray spectrometry provided the dosimetric information for the surrounding soil (Hossain et al., 2002; Vandenberghe, 2004).

Concentrations were converted into annual doses using the conversion factors given by Adamiec and Aitken (1998). The contribution of cosmic rays to the dose rate was calculated following Prescott and Hutton (1994). For the polymineral fine grains, an a-value of 0.10±0.05 was used to allow for the lower efficiency of alpha radiation in inducing luminescence. For the calculation of the beta dose rate to 90-125 µm quartz grains, a beta attenuation factor of 0.92±0.05 was adopted, based on the calculations by Mejdahl (1979). The saturation content (W-value; Aitken, 1985) of all pottery sherds was determined in the laboratory; the sherds were assumed to have been in saturation for 80% of the time. **Table IV.2** summarises all the dosimetric information.

Table IV.2: *Elemental concentrations of natural radioactive nuclides in the ceramic sherds and surrounding soil, and estimates of past water content.*

Sample		^{238}U (mg kg^{-1})		^{232}Th (mg kg^{-1})	^{40}K (%)	Water content (%)
A1		2.47±0.06		10.45±0.26	2.25±0.01	11±3
V1		2.45±0.05		11.44±1.32	2.27±0.03	15±4
V2		1.89±0.05		10.15±0.25	1.87±0.03	9±2
V3		2.53±0.06		11.75±0.29	1.68±0.02	17±5
SOIL	^{234}Th (mg kg^{-1})	^{226}Ra (mg kg^{-1})	^{210}Pb (mg kg^{-1})			
	1.37±0.21	3.10±0.22	1.95±0.18	10.73±0.15	1.87±0.02	

IV.5. LUMINESCENCE AGES AND DISCUSSIONS

The presence of anomalous fading in the 410 nm IRSL emission as well as blue TL emission indicates that our IRSL and TL ages would underestimate the true ages. To correct the SAR-IRSL results for fading, we applied correction procedure proposed by Huntley and Lamothe (2001). No correction was applied to the TL results, as it not valid to correct the bulk signal originating from an undifferentiated fine-grained mineral mixture using the fading observed from only part of this mixture.

The TL, SAR-OSL and SAR-IRSL ages (both corrected and uncorrected) are presented in **Table IV. 3**; for the sake of visualisation, they are also plotted in **Figure IV. 11**. In general, the uncorrected TL-ages are consistent with the uncorrected SAR-IRSL ages, and both are lower than the quartz SAR-OSL ages. The uncorrected TL age for sample V2 is higher than the uncorrected SAR-IRSL age, but this might be due to a lack in measurement precision. The fading corrected ages. Compared to the TL method, the IRSL and OSL approaches are based on a more robust dating methodology. Therefore, they are expected to yield the most reliable age information. As SAR-OSL dating of quartz yields the most precise age estimates, this is considered to be the technique of choice.

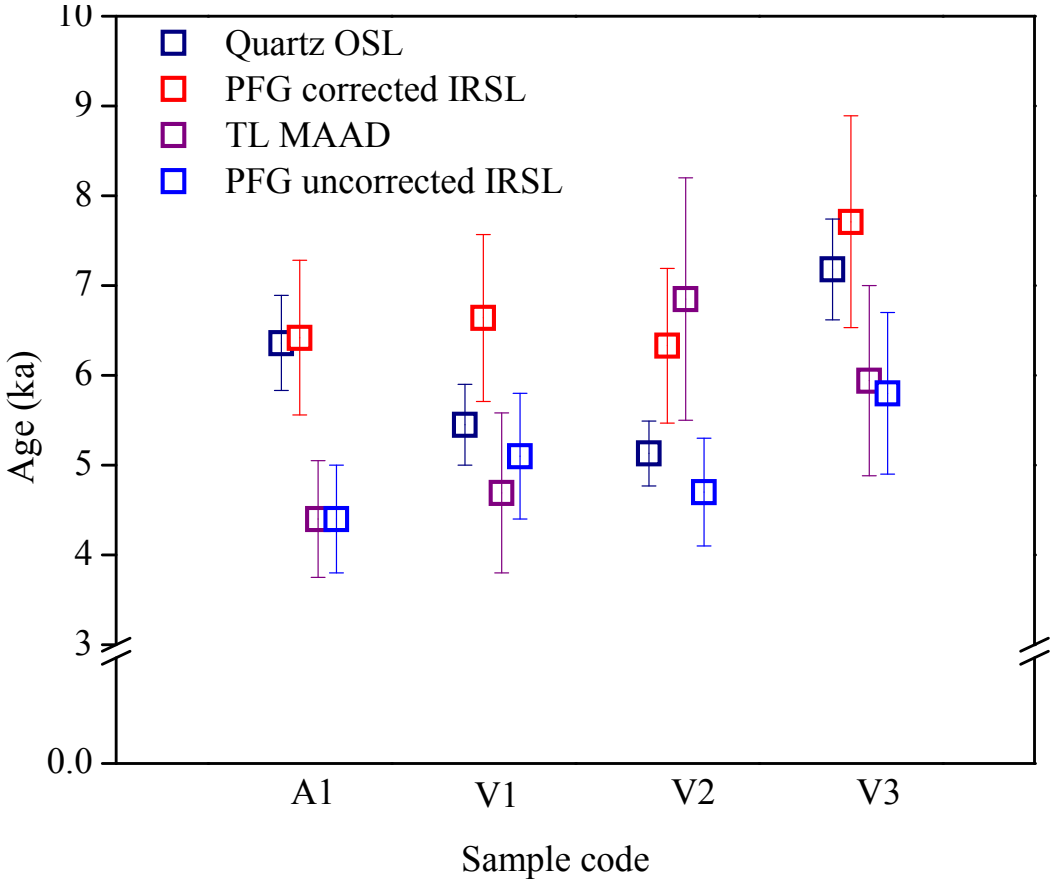

Figure III. 11: *Illustrative comparison of the ages obtained through the methods used.*

Table IV. 3: *Summary of equivalent doses (D_e), calculated dose rates and ages. Uncertainties mentioned with the D_e's and dose rates are random and represent 1 sigma. The uncertainties on the ages were calculated following the error assessment system proposed by Aitken and Alldred (1972) and Aitken (1976).*

Sample	Method	Mineral fraction	D_e (Gy)	Dose rate to 90-125 µm Q (Gy ka^{-1})	Dose rate to 4-11 µm PFG (Gy ka^{-1})	Uncorrected age (ka)	Random uncertainty (%)	Systematic uncertainty (%)	Total uncertainty %	Total uncertainty ka	Corrected age (ka)
A1	TL MAAD	4 - 11µm PFG	19.2 ± 1.2			4.4	6.4	13.3	14.8	0.7	
	OSL SAR	90 - 125 µm Q	20.0 ± 0.8	3.14±0.02	4.36±0.02	6.4	4.1	7.2	8.3	0.5	
	IRSL SAR	4 - 11µm PFG	19.0 ± 0.2			4.4	1.0	13.3	13.3	0.6	6.4 ± 0.9
V1	TL MAAD	4 - 11µm PFG	20.1 ± 2.6			4.7	13.0	13.9	19.0	0.9	
	OSL SAR	90 - 125 µm Q	16.8 ± 0.5	3.09±0.03	4.29±0.02	5. 5	2.9	7.8	8.3	0.5	
	IRSL SAR	4 - 11µm PFG	21.8 ± 0.4			5.1	2.0	13.4	13.5	0.7	6.6 ±0.9
V2	TL MAAD	4 - 11µm PFG	27.1 ± 4.0			6.9	14.8	13.1	19.8	1.4	
	OSL SAR	90 - 125 µm Q	14.7 ± 0.2	2.87±0.03	3.95±0.02	5.1	1.9	6.9	7.2	0.4	
	IRSL SAR	4 - 11µm PFG	18.4 ± 0.7			4.7	3.6	13.1	13.6	0.6	6.3 ±0.9
V3	TL MAAD	4 - 11µm PFG	24.1 ± 2.5			5.9	10.3	14.6	17.9	1.1	
	OSL SAR	90 - 125 µm Q	20.2 ± 0.6	2.81±0.02	4.06±0.02	7.2	3.2	7.2	7.9	0.6	
	IRSL SAR	4 - 11µm PFG	23.6 ± 0.8			5.8	3.2	14.9	15.2	0.9	7.7 ±1.2

As mentioned before, there is no age control for Lumea Nouă site. The only possibility to evaluate the accuracy of our dates is by comparing them to age information that is available from other archaeological sites in Romania. Based on radiocarbon dating, Draşovean (2005) places the Foeni culture between 4798 ± 122 and 4520 ± 60 cal BC. For the beginning of the Petreşti culture (phase A), the ^{14}C data obtained for the settlement at Daia Română – Părăuț give us the interval 3855 ± 95 cal BC (Paul, 1992). The average of the four quartz SAR-OSL ages presented above would place the transition from Foeni to Petreşti culture at Lumea Nouă site around 6.2±0.5 ka; taking into consideration the archaeological information, this age seems extremely plausible. Further investigations are needed for establishing a complete chronological framework for the ancient cultural development at Lumea Nouă. Nevertheless the present study clearly illustrates how luminescence dating, especially by the use of state-of-the-art techniques can contribute to this purpose.

CHAPTER V
APPLICATIONS OF LUMINESCENCE DATING IN GEOLOGY AND ENVIRONMENTAL STUDIES

V.1. OPTICAL DATING OF ROMANIAN LOESS

V.1.1. The importance of having accurate and absolute age information on loess sections

Loess originates from silty material blown out of sparsely vegetated areas during dry and cold periods of the Pleistocene. During interglacials and most interstadials soil formation prevailed. Thus, the alternation of cold and warm periods throughout the Quaternary led to the formation of loess- palaeosol sequences (LPSS). Loess deposits cover significant areas in Europe, extending from NW-France and Belgium through to Central Europe, the Ukraine and Western Russia. These deposits preserve a potentially important and detailed archive of Pleistocene climate change; however, their significance can only be fully understood if their absolute chronology is precisely known (Frechen et al., 2003, Roberts, 2008). For the European loess deposits, such a chronological framework is largely lacking. Indeed, age information for European loess is mainly based on relative methods (such as pedostratigraphy and magnetic susceptibility) and correlation of sequences with comparable features. The major difficulty with these approaches is that they assume that the sedimentary record is complete (i.e. no erosive hiatuses or disconformities are present) and/or that loess deposition has occurred at a constant rate. Application of newly developed absolute dating methods (notably luminescence dating), however, yields convincing evidence for both varying accumulation rates and erosive hiatuses. This contests some fundamental ideas regarding the nature, formation and significance of loess records, and questions the stratigraphic position of several palaeosols and the way in which they should be correlated. Consequently, absolute dates are essential to determine (i) the timing of climatic events that are registered in the loess, (ii) the rate of processes such as sedimentation and pedogenesis and (iii) the correlation between the loess sequences that are spread all over Europe.

The Romanian loess-palaeosol sequences **(Figure V.1)** preserve a significant terrestrial record of Quaternary climate change. In comparison to similar sequences elsewhere in Central and Eastern Europe, the deposits in Romania have been less extensively studied (Frechen et al., 2003). A chronostratigraphical framework for the Romanian loess deposits has previously been established through geomorphological, lithological and pedostratigraphical analysis (Conea, 1969). Recent studies of the magnetic properties of the loess /palaeosol sequences have demonstrated the potential of magnetic susceptibility as a climatic proxy (see e.g. Panaiotu et al., 2001; Buggle et al., 2008 a); the variations in magnetic susceptibility are then matched to orbitally tuned $\delta^{18}O$ records to derive a depositional chronology for the sequences. However, this approach assumes that the deposits are complete (i.e. no erosive hiatuses are present), and it can only provide indirect age information for entire units. Absolute dates are essential to confirm the stratigraphic position of the palaeosols (and the way in which they should be correlated), and to determine the precise rate of processes as sedimentation and pedogenesis.

An important interference that emerges from detailed studies is the fact that loess record is seldom continuous and even during the last interglacial-glacial cycle large amplitude changes in sedimentation rates occurred. This is very important as it makes possible the understanding of changes in climatic gradients during transitional phases from cooler to warmer conditions and vice-versa. Thus, out of the terrestrial archives, loess sections can provide the most detailed records of mass accumulation rates during the last interglacial-glacial cycle that can be used as input data for dust circulation in Earth modeling systems, eventually helping in predicting future climate change trends as changes in the atmospheric dust burden could have a significant effect on future climates.

Simulations of the radiative impacts of dust under present climate conditions have been performed and already incorporate the effects of anthropogenically derived dust (Tegen et al., 1996). However, the impact of the changes in the productivity of natural dust sources over geological time and the incorporation of dust deflation, transport and deposition processes is just beginning as spatially extensive data sets documenting the observed changes in dust accumulation rates during the last interglacial-glacial cycle are required in order to test model simulation of dust cycles (Harrison et al., 2001).

Luminescence techniques are increasingly providing a basis for the age assessment of these sedimentary deposits, being without any doubt the most proper independent method for dating aeolian sediments. The greatest advantage of the method is the fact that it relies upon the use of the sediment grains themselves and not upon related material. Actually, there is no other independent method that presents this advantage. Nowadays, one of the biggest concerns of the luminescence community is pushing the age limit further back in time. The maximum attainable age is limited by the process of saturation of the electron traps of the crystals used as natural dosimeters. Every mineral saturates at a different absorbed dose characteristic to its defect structure. On the other hand the maximum age that can be dated can be seen as the time required to saturate the natural

dosimeter which is in turn dependent upon the dose rate. So, the maximum attainable age depends upon two factors: the type of mineral used for dating and the dose rate. Loess dose rates do not vary more than a factor of three, no matter on which continent they are found, but are usually quite high compare to other sediments (Wintle, 1990). Up to now, due to this limitation, luminescence dating can reliably be applied to sediments from the last glacial-interglacial cycle down to Oxygen Isotope Stage 5, around 110- 130ka, so it is basically bridging from radiocarbon to radioactive isotope methods.

Luminescence dating allows the direct determination of depositional ages for sediments from a wide variety of depositional environments (Murray and Olley, 2002). However, it has seen very little application to Romanian loess. We are only aware of the exploratory study by Balescu et al. (2003). In this study, four IRLS ages were obtained for a section near Tuzla (Dobrogea, SE Romania). Despite the limited dataset, they could demonstrate that the uppermost palaeosol in the section was formed during MIS5 and that the first three loess layers accumulated during the last three glacial periods (OIS 4, OIS 6, respectively OIS 8).

This work reports on luminescence investigations of the loess-sequence near Mircea Vodă (Dobrogea, SE Romania). It is an exploratory study that aims at establishing the potential of optical dating of quartz for determining the rate of loess sedimentation in Romania. The choice of using quartz is based on our previous work (Timar, 2006) where it was concluded that the correction of Huntley and Lamothe for anomalous fading of feldspars was concluded that the correction was valid for young samples (less than 20ka) but does not give satisfactory results for higher ages. In principle this is to be expected as this correction is applicable for the linear low dose region of the response curve. A method for correcting beyond this range was not available at the moment of caring out present study.

V.1.2. Study area

The study site is located near the village of Mircea Vodă, which is situated in the Dobrogea-plateau (SE Romania) at about 15 km from the River Danube **(Figure V.1).**

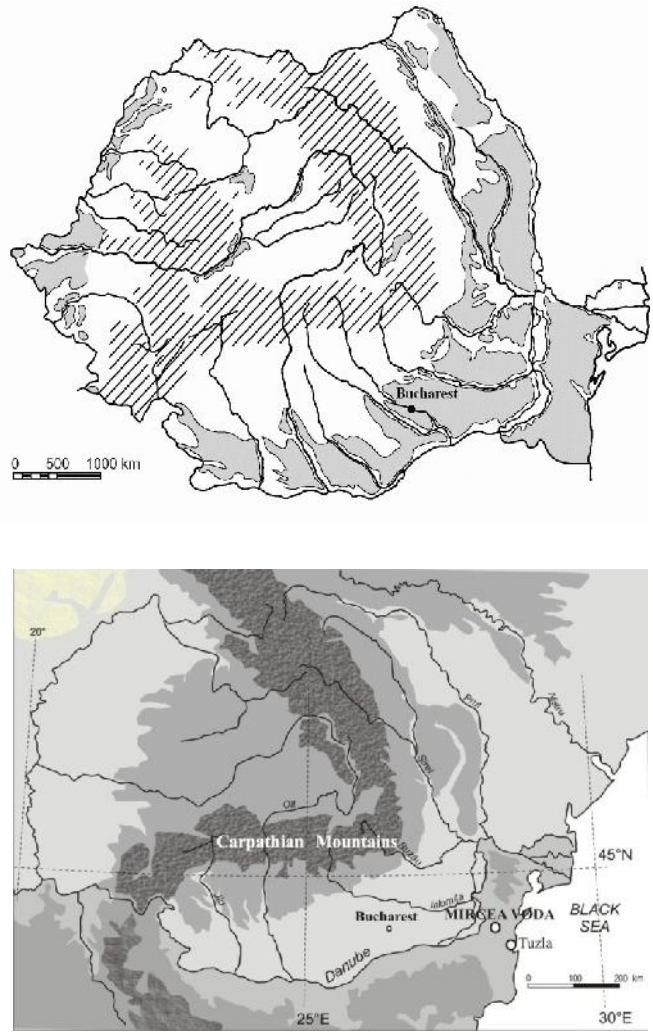

Figure V.1: *Map showing the distribution of loess-and loess-like deposits in Romania and the location of the sampling site (Mircea Vodă) in SE Romania. The location of the section studied by Balescu et al. (2003; Tuzla) is indicated as well.*

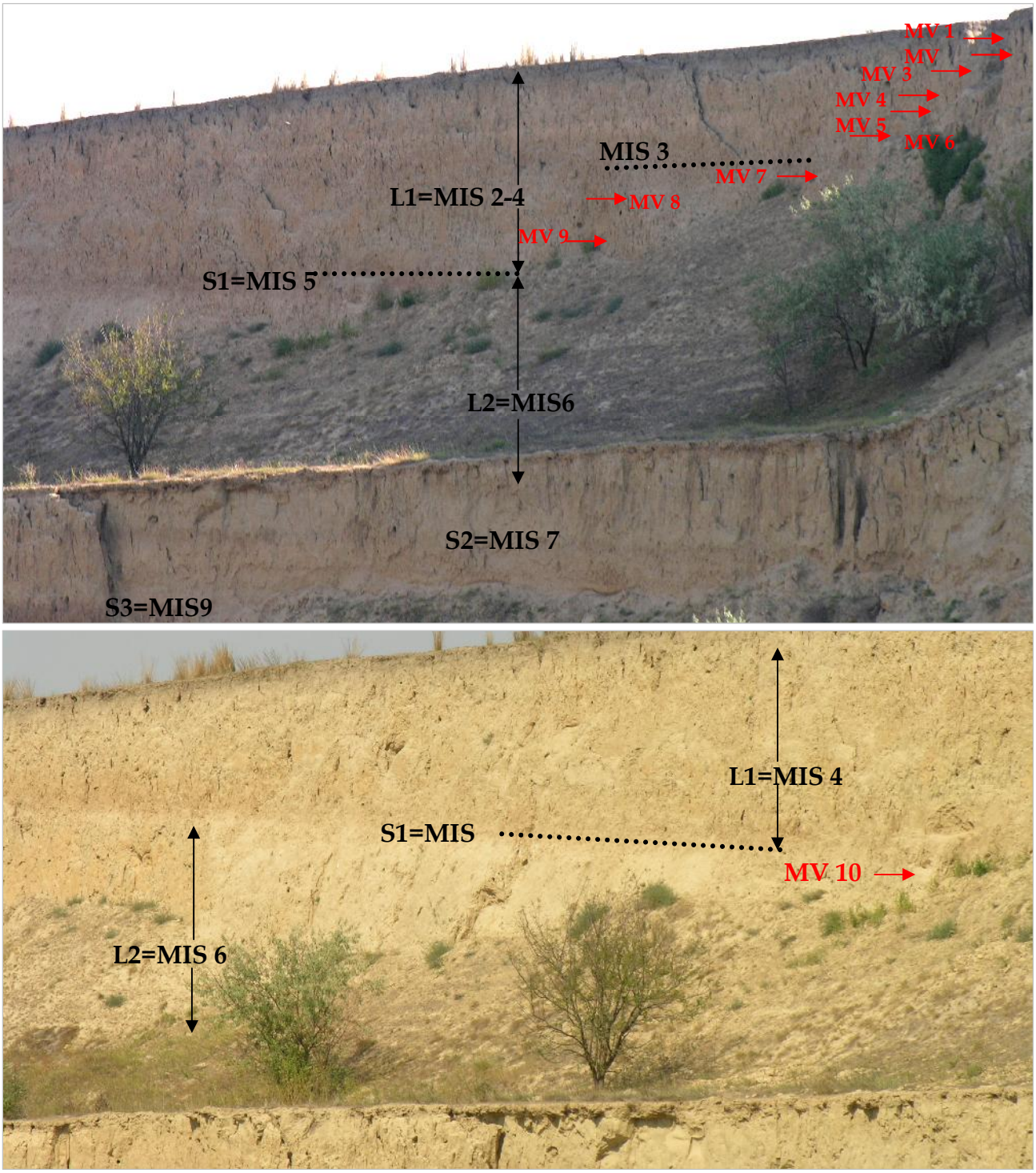

Figure V.2: *Mircea Vodă loess- palaeosol sequence. The sampling points are indicated*

V.1.3. Magnetic susceptibility and grain size analysis

Recent investigations by Buggle et al. (2008 b) indicate that the loess from the Dobrogea plateau is predominantly derived from Danube alluvium, with a minor but geochemical significant contribution from one or several additional aeolian source areas (Ukrainian glaciofluvial deposits / local sand dune fields). The section is ~26 m thick; it comprises six well developed palaeosols and intercalated loess layers, with no apparent evidence for remarkable hiatuses **(Figure V. 2).**

The loess-palaeosol sequence near Mircea Vodă had previously been sampled (at 10 cm intervals) for logging the magnetic susceptibility. These data are presented in **Figure V. 3.**

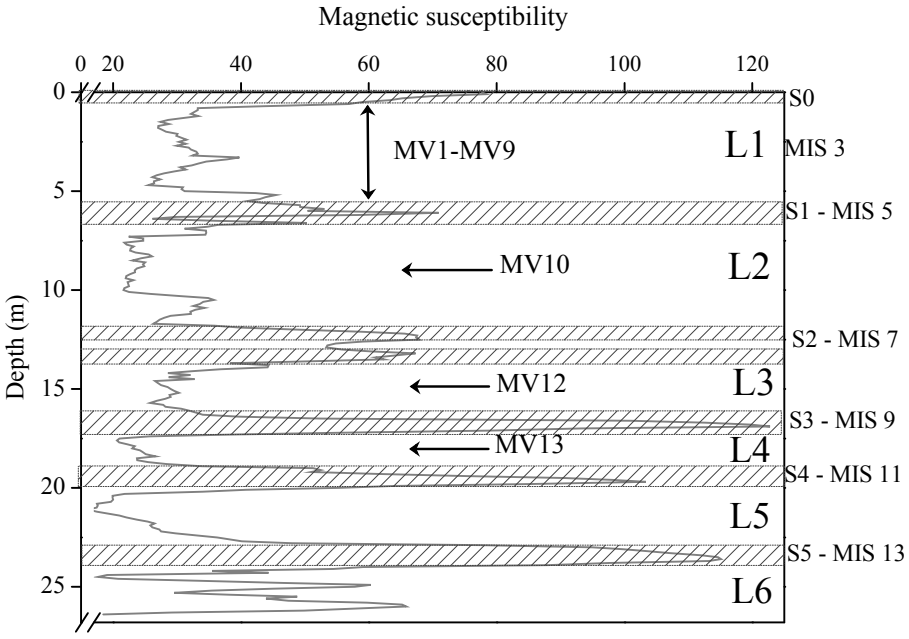

Figure V.3: *Schematic representation of the sampled section showing the loess (L) and palaeosol units (S), the magnetic susceptibility values and OSL sampling points.*

The susceptibility variations in the profile are similar to those recently observed in Serbian loess (Marković et al., 2006; Marković et al., 2008). Panaiotu et al. have used these magnetic susceptibility data to create an independent time-depth model (**Figure V.4**). To this purpose, a new approach was applied, which utilizes dynamic programming to find the globally optimal alignment of two records (Lisiecki and Lisiecki, 2002). Several time series for magnetic susceptibility were generated using the Match-2.3 software (Lisiecki and Lisiecki, 2002) and the stack of 57 globally distributed benthic $\delta^{18}O$ records as the target curve (Lisiecki and Raymo, 2005). To avoid circular arguments, no tie points were created between the magnetic susceptibility curve and the target curve. The only constraint imposed was to force the program so that the begin and end points of the signal

match the begin and end points of the target; the begin points were the top of the S0 soil and time 0, and the end points were the base of the last palaeosol and an age of ~626 ka.

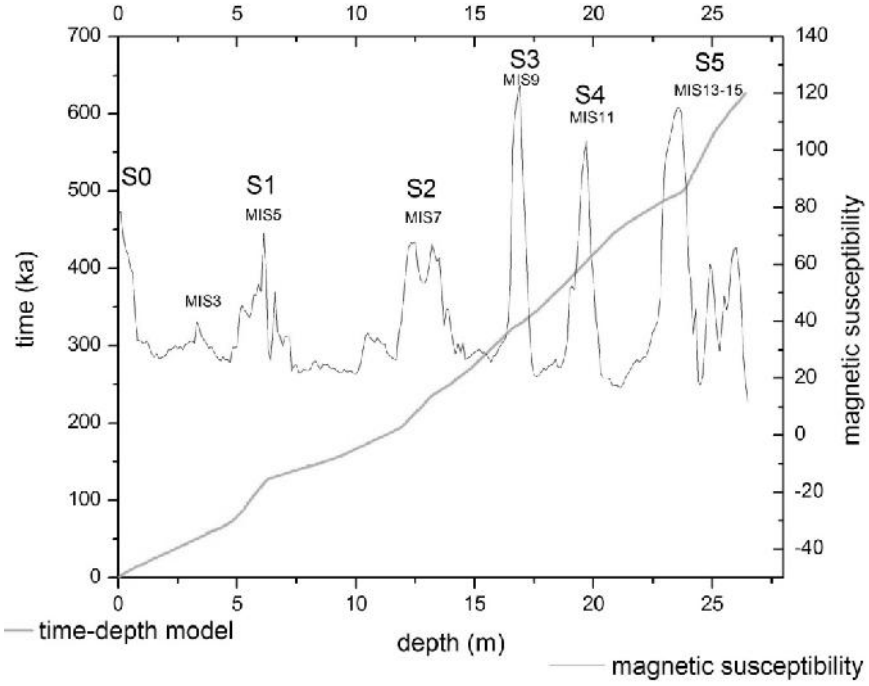

Figure V.4: *Time-depth model based on magnetic susceptibility profile for Mircea Vodă loess section (courtesy of C. Panaiotu).*

The results from the modeling show that the palaeosol and loess units correspond to interglacial and glacial periods, respectively. In particular, the magnetic time-depth model indicates that the first palaeosol (S1) was formed during MIS5; it also allocates a weakly developed soil in the middle of the L1 unit to the MIS3 interstadial.

Detailed grain size analysis has been carried out as well. The treated samples (with H_2O_2 for removal of organic matter; with HCl at pH 4 for removal of carbonates and dispersed with hexametaphosphate) were measured for grain size distributions with a Horiba laser instrument (LA950) at Sedimentology Laboratory from the University of Bucharest. As well as for magnetic susceptibility measurements, samples on which grain size analysis was carried out were collected at 10 cm interval from Mircea Vodă section.

The grain-size distribution is very consistent with the magnetic susceptibility variations – the pedogenic fraction (<5 μm) is concentrated in the layers exhibiting high magnetic susceptibility and the airborne fraction (>16 μm) is concentrated in the layers with lower susceptibility values (**Figure V.5**).

Throughout the entire section, the airborne dust (silt and fine sand above 16 μm) is present in large amount (generally over 50%). The pedogenic processes which involve hydrolysis of silicate minerals leading to formation of new clay-sized minerals (< 5 μm)

can also be seen throughout the entire section with values always above 10% in the loess layers and values above 20% in the paleosol layers, suggesting that even during loess deposition, weak pedogenesis was present. Larger amount of clay-sized material was observed in lower part of the section.

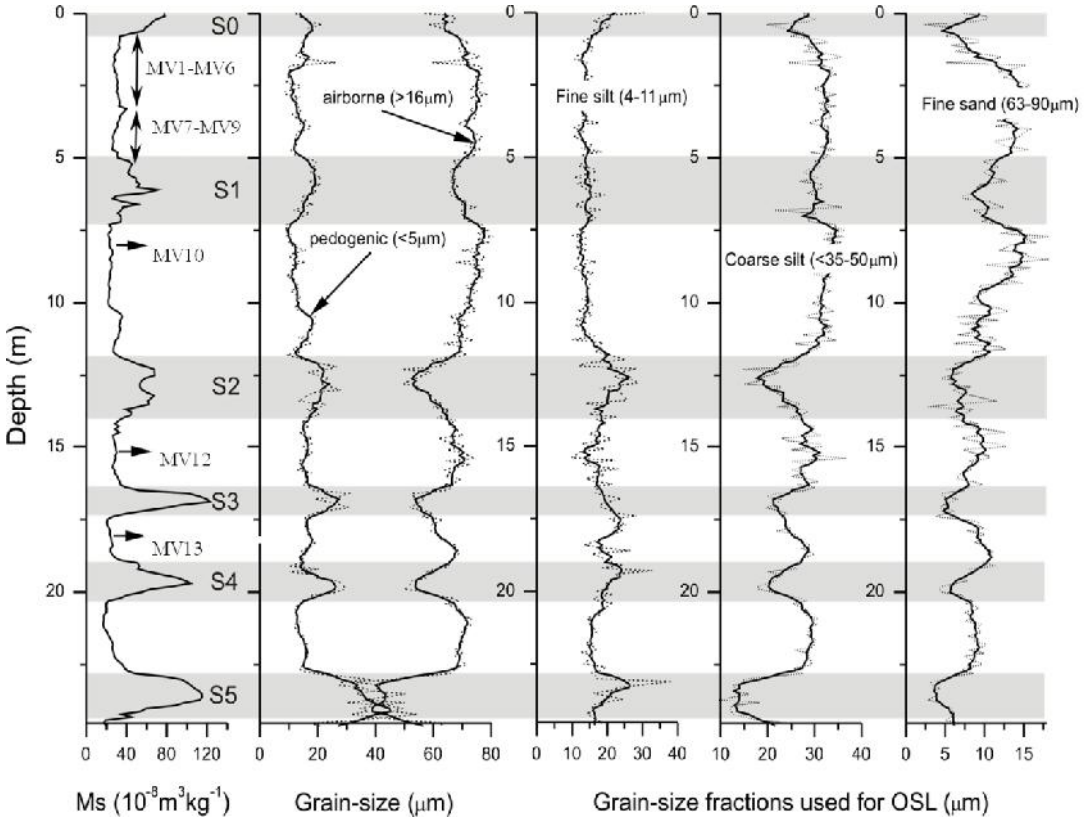

Figure V.5: *Schematic representation of the sampled section showing the loess and palaeosol units, the magnetic susceptibility values and OSL sampling points as well as different grain-size fractions abundance as function of depth: pedogenic clay fraction (<5 μm), airborne fraction (>16 μm); fine silt (4-11 μm), coarse silt (35-50 μm) and fine sand (63-90 μm)(courtesy of C. Panaiotu).*

The grain-size fractions usually selected for OSL dating: fine silt, coarse silt and fine sand material are present in substantial amount in the loess layers (above 10%, above 30% and above 10% respectively). This shows that the wind transportation competency was quite high at the time of loess deposition. Most of the grain-size distributions in the loess layers are bi-modal or even three-modal distribution, reflecting multiple sources of the clastic material (**Figure V.6**).

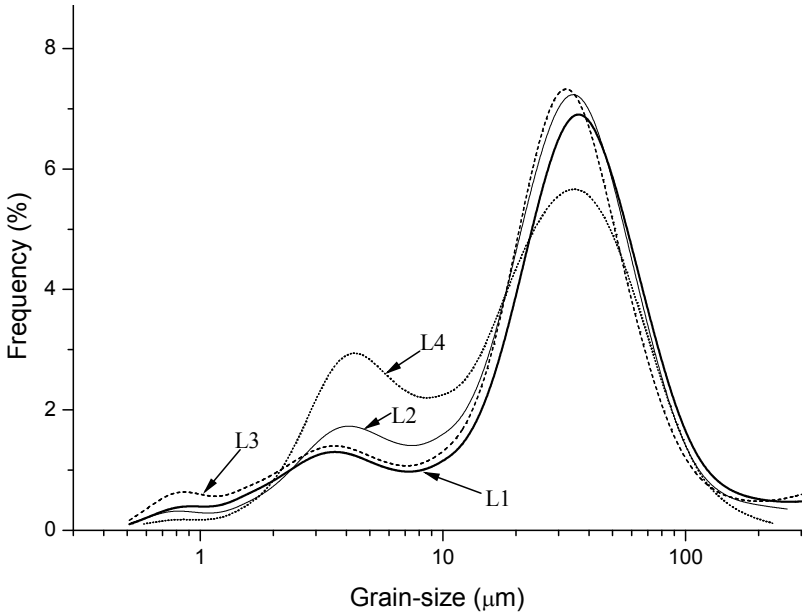

Figure V.6: *Grain-size distribution characteristic for different loess layers, showing the bi-modal aspect of the granulometric curve (courtesy of C. Panaiotu).*

The coarse silt and fine sand material could have proximal source (also indicated by their angular shape-**Figure V.7**), while the fine and medium silt could have a distant source. Such bimodal sources have been also suggested by recent geochemical investigations on the loess section from Mircea Vodă (Buggle et al, 2008b). They discussed about a local sedimentary source from the sand dunes fields along the lower Danube alluvium and a second source from the Ukrainian glaciofluvial deposits. We cannot confirm whether that the fine silt fraction originated from Ukrainian deposit, but certainly from a distal source wherefrom was transported by long term suspension.

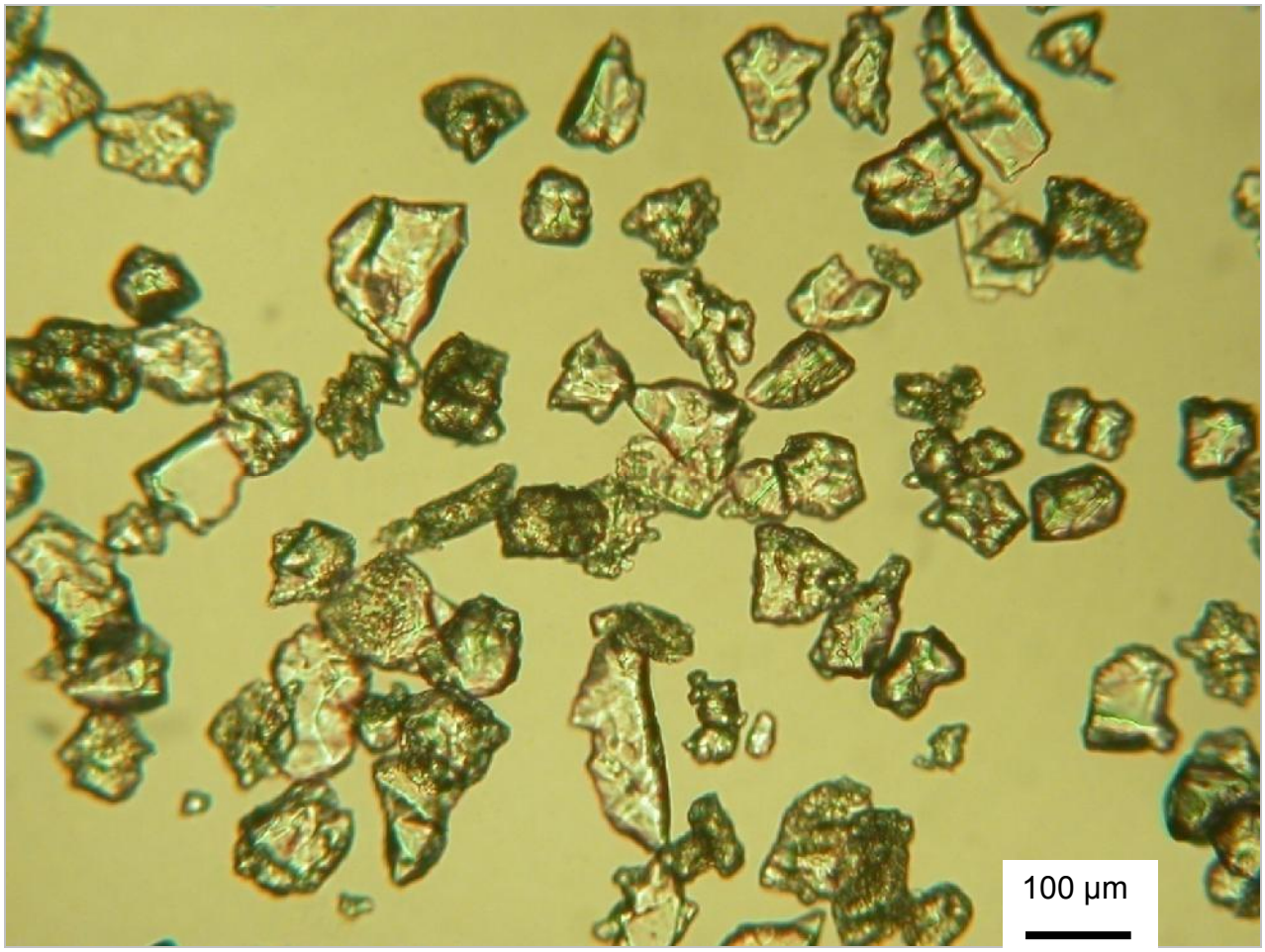

Figure V.7: *Microscopic image of 63-90 µm quartz grains- sample MV 6(courtesy of C.Panaiotu).*

V.1.4. Sampling and analytical facilities

Our luminescence study focuses on the loess from the last four glacial periods (**Figure V.3**). Nine samples (MV1 to MV9) were taken from the first loess layer (L1) between the recent soil (S0) and the first well developed chernozemic palaeosol (S1). Sample MV10 was taken from the second loess layer (L2), between S1 and a second chernozemic palaeosol (S2). The last two samples (MV12 and 13) were collected from the L3 and L4 loess units overlying the brown forest palaeosols S3 and S4, respectively.
For luminescence analysis, fine (4-11µm), silt (medium 35-50 µm), and silt sandy (coarse 63-90 µm) quartz grains were extracted from the inner material of the sampling tubes using conventional sample preparation techniques previously described in Chapter II, section 4. Luminescence measurements were performed using a Risø TL/OSL-DA-12 in Gent Luminescence Dating Laboratory respectively a Risø TL/OSL-DA-20 system in the Environmental Radioactivity and Nuclear Dating Laboratory of Babeş-Bolyai University in Cluj Napoca. The luminescence signals were detected through a 7.5 mm tick Hoya U-340 filter on both readers. The purity of the quartz extracts was confirmed by the absence of a significant infrared stimulated luminescence (IRSL) response at 60°C to a large

regenerative β-dose. The sensitivity to infrared stimulation was defined as significant if the resulting signal amounted to more than 10% of the corresponding OSL signal (Vandenberghe, 2004) or if the IR depletion ratio deviated more than 10% from unity (Duller, 2003).

V.1.5. Annual dose estimation

Annual dose were derived using conversion factors (Adamiec and Aitken, 1998) from radionuclide specific activities measured by high resolution gamma spectrometry both in Gent Luminescence Laboratory and in Environmental radioactivity and nuclear dating laboratory of Babes-Bolyai University in Cluj Napoca (**Table V.1**). Both laboratories use an absolute efficiency calibration and cylindrical sample geometry. Details on the method used in Cluj have been described in Chapter III. For the details concerning the methodology implied in Gent reference is made to De Corte et al. (2005) and Hossain et al. (2002). A good agreement was found between the data obtained in the two laboratories. Radioactive equilibrium was observed for uranium series in samples investigated **(Figure V.8.a)**. Concerning the total dose rate, samples investigated are radioactively homogeneous **(Figure V.8.d)**. Total dose rates for our samples range in between 2.78 ± 0.04 and 3.30 ± 0.05 Gy / ka for fine grained quartz, respectively in between 2.33 ± 0.03 and 2.76 ± 0.04 for silt sandy quartz (63-90 μm). The contribution of cosmic rays to the dose rate was calculated following Prescott and Hutton (1994), and values ranged between 0.2 Gy / ka for the uppermost sample (MV1- sampling depth = 0.85 m) and 0.05 Gy / ka for sample MV13 collected from a depth of about 18m. For alpha dose estimation in the case of fine grains an a value of 0.04 ± 0.02 was adopted, while for beta attenuation and etching factors we have used values of 0.94 ± 0.045 in the case of silt-sandy (63-90 μm), respectively 0.96 ± 0.045 in the case of silt grains (35-50) μm. The total moisture content (F*W) used was 0.2 ± 0.05 following Balescu et al. (2003).

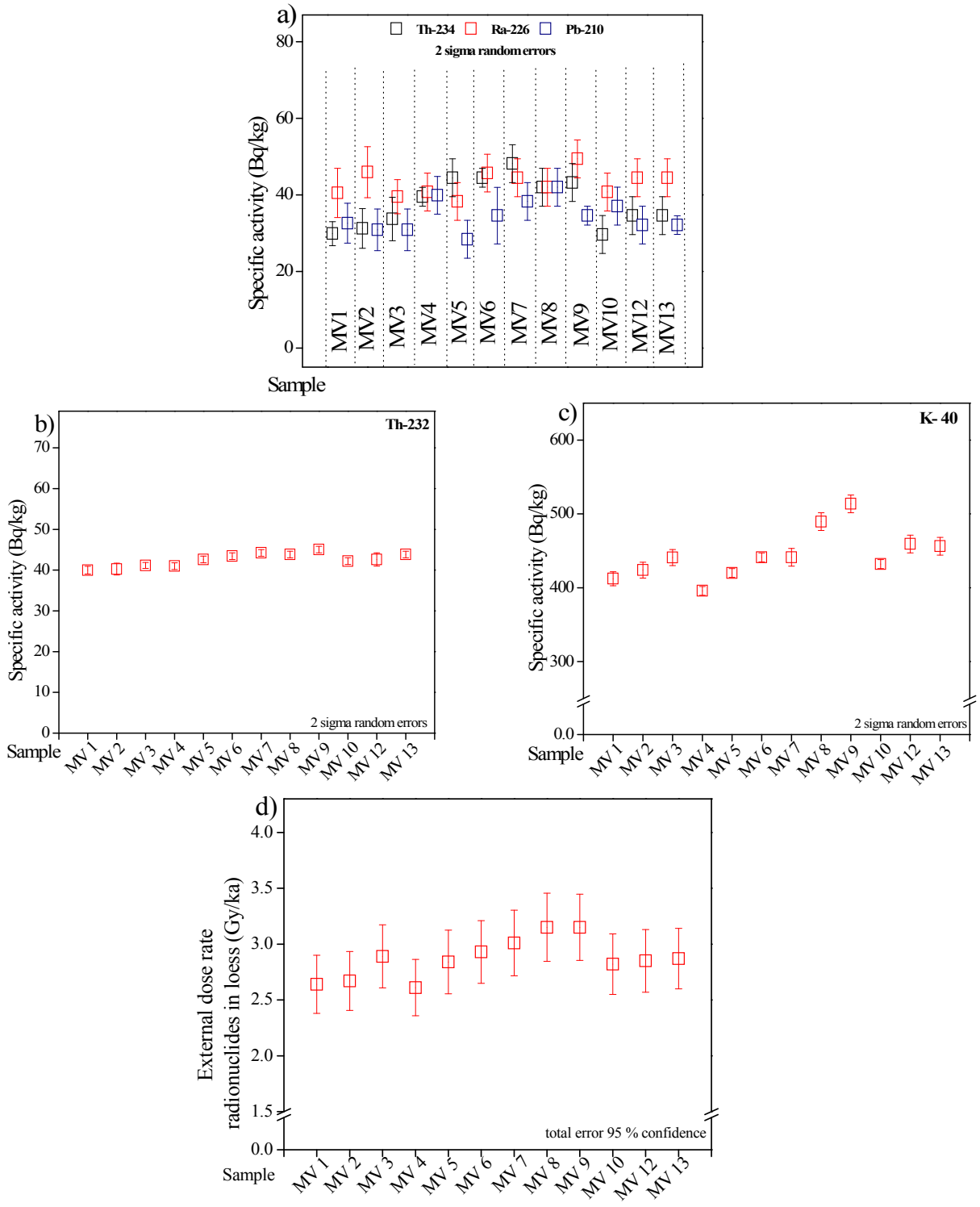

Figure V.8: *a), b), c) illustrates the relevant dosimetric information for dose rate calculation of samples investigated. In figure V.8.d. dose rates to fine grains (total alpha, beta and gamma contributions) due to radionuclides in sediment are presented, the assigned uncertainties including both random and systematic erro*

Table V.1: *Specific activities of radionuclides on interest determined by means of high resolution gamma spectrometry in Gent Luminescence Laboratory and in Environmental radioactivity and nuclear dating laboratory of Babes-Bolyai University in Cluj Napoca. Random errors are quoted and represent 1 sigma.*

Sample	Th-234 (Bq/kg)		Ra-226 (Bq/kg)		Pb-210 (Bq/kg)		Th-232 (Bq/kg)		K-40 (Bq/kg)	
	UBB	Gent	UBB	Gent	UBB	Gent	UBB	Gent	UBB	Gent
MV 1	27.9 ± 6.0	29.9 ± 1.6	40.2 ± 6.0	40.5 ± 3.2	27 ± 3.3	32.6 ± 2.6	35.7 ± 1.4	39.9 ± 0.5	401 ± 6	412 ± 5
MV 2	22.9 ± 5.5	31.2 ± 2.6	37.8 ± 5.5	45.9 ± 3.3	28.1 ± 2.9	30.9 ± 2.7	31.8 ± 1.5	40.3 ± 0.8	391 ± 9	423 ± 5
MV 3	36 ± 6.5	33.7 ± 2.8	20.7 ± 6.5	39.5 ± 2.2	19.2 ± 3.6	30.9 ± 2.7	28.8 ± 2.1	41.1 ± 0.4	424 ± 8	441 ± 5
MV 4	33.1 ± 5.4	39.5 ±1.2	30.9 ± 5.4	40.7 ± 2.5	11.6 ± 3.2	39.9 ± 2.5	35.6 ± 1.6	40.9 ± 0.4	363 ± 7	396 ± 3
MV 5	29.9 ± 5.6	44.5 ± 2.5	30.3 ± 5.6	38.3 ± 2.5	34 ± 3.3	28.4 ± 2.5	33.7 ± 1.6	42.6 ± 0.4	427 ± 6	420 ± 3
MV 6	47.1 ± 5.5	44.5 ± 1.2	49.4 ± 5.5	45.7 ± 2.5	34.4 ± 3.1	34.6 ± 3.7	33.6 ± 1.1	43.4 ± 0.4	436 ± 6	441 ± 3
MV 7	34.5 ± 6.1	48.2 ± 2.5	19.8 ± 6.1	44.5 ± 2.5	25.3 ± 3.4	38.3 ± 2.5	32.9 ± 1.3	44.2 ± 0.4	442 ± 7	441 ± 6
MV 8	41.6 ± 5.8	42.0 ± 2.5	41.2 ± 5.8	41.9 ± 2.5	31.8 ± 3.7	41.9 ± 2.5	38.7 ± 1.8	43.8 ± 0.4	485 ± 7	489 ± 6
MV 9	45.1 ± 6.4	43.2 ± 2.5	22.4 ± 6.4	49.4 ± 2.5	43.3 ± 4.6	34.6 ± 1.2	45.3 ± 2	45.0 ± 0.4	518 ± 8	514 ± 6
MV 10	40.9 ± 6.6	29.6 ± 2.5	28.9 ± 6.6	40.7 ± 2.5	31.6 ± 4.2	37.0 ± 2.5	29.2 ± 1.9	42.2 ± 0.4	425 ± 4	432 ± 3
MV 12	43.9 ± 7.9	34.6 ± 2.5	36.4 ± 7.9	44.5 ± 2.5	34.2 ± 4.8	32.1 ± 2.5	34.5 ± 1.9	42.6 ± 0.8	469± 9	459 ± 6
MV 13	29.6 ± 5.9	34.6 ± 2.5	44.0 ± 5.9	44.5 ± 2.5	25.5 ± 3.5	32.1 ± 1.2	36.4 ± 1.6	43.8 ± 0.4	449 ± 7	456 ± 6

V.1.6. Optical dating using fine (4-11 μm) grained quartz

V.1.6.1. Luminescence characteristics

The luminescence characteristics were studied using a single-aliquot regenerative-dose (SAR) procedure (Murray and Wintle, 2000). Unless otherwise indicated, a preheat of 220 °C and a cutheat to 180 °C cutheat were adopted. After the measurement of the response to a test dose (17.1 Gy), a high-temperature bleach for 40 s at 280 °C was performed (Murray and Wintle, 2003). The net signal was evaluated from the initial 0.32 s of the decay curve, less a background integrated between 1.60 and 2.24 s**.** Measurements were performed on a Risø TL/OSL DA-12 machine. **Figure V.9** shows an OSL decay curve and a typical SAR laboratory growth curve and is presented in **Figure V.10** for one of the older samples (MV10). Although the growth curve can be fitted acceptably to a single saturating exponential, the growth to high doses is represented best by the sum of a single saturating exponential and a linear component. It can be seen that, for this particular sample, the natural signal intersects with the linear region of the growth curve; this is at a dose level higher than $2D_0$* (with D_0* being defined as the saturation characteristic of the exponential term in this particular fitting function), but not higher than $2D_0$ (~ 85% of the saturation level for a monomolecular fit) limit suggested by Wintle and Murray (2006). **Figures V.9 - V.10** are representative examples of the luminescence characteristics exhibited by our samples and illustrates their generally good behavior the SAR protocol; recycling ratios are indistinguishable from unity and the growth curves pass very close to the origin.

Figure V.11 shows a comparison of the average dose response curves for six of our samples. A highly reproducible pattern of growth can be observed; with little variation in saturation characteristics with burial depth (see also **Table V.2**). It worth being mentioned that an apparent increase in the average characteristic dose (D_0) with burial depth was previously reported for coarse (63-90 μm) quartz grains extracted from Chinese loess (Buylaert et al., 2007). The similarity in luminescence characteristics could indicate that the source of the silt-sized quartz grains remained constant over four Interglacial/Glacial periods.

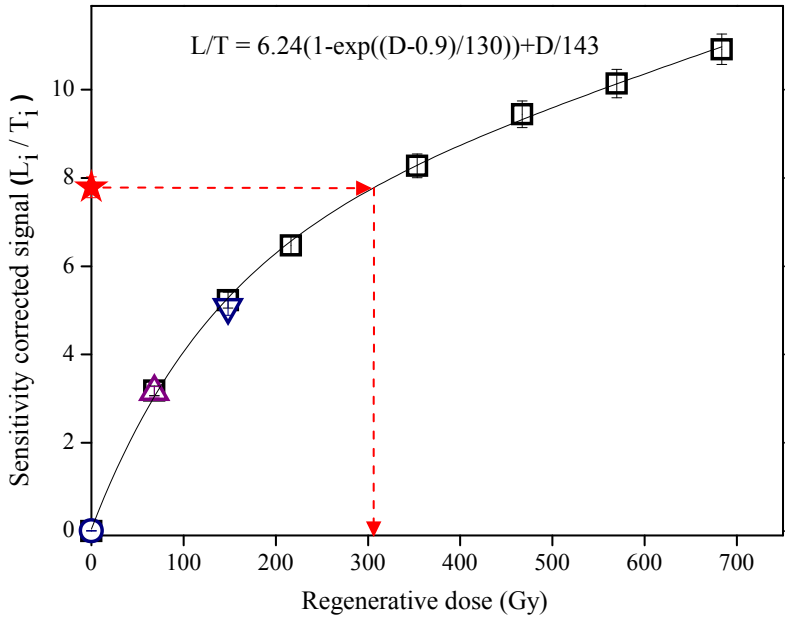

Figure V.9.: *Representative SAR growth curve for a single aliquot of fine-grained quartz extracted from sample MV 10. Recycling and recuperation points are shown as an open triangle and open circle.*

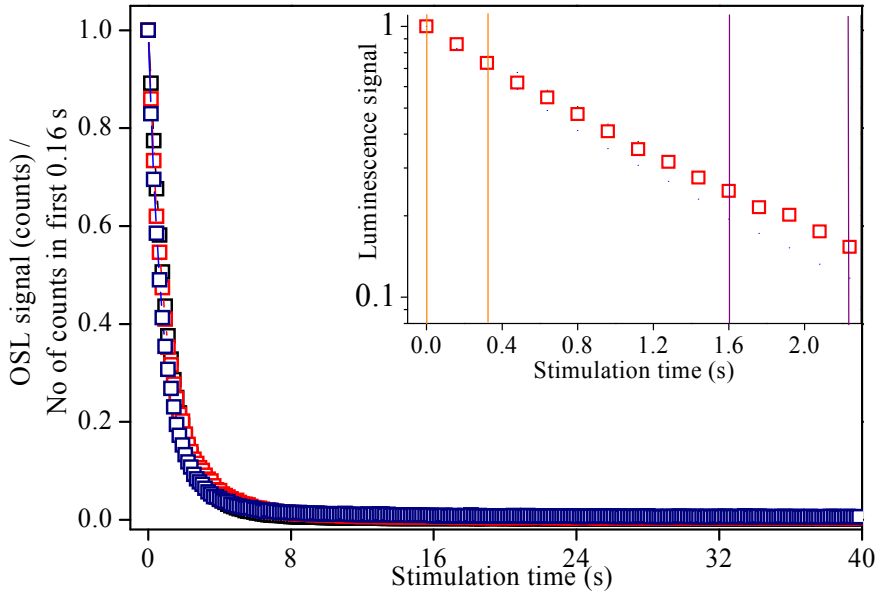

Figure V.10: *Typical decay curve of natural (red symbols) OSL signal of sample MV10 (fine quartz) compared to the regenerated signal (navy symbols) and the OSL decay of calibration quartz (black symbols).The measurement was performed on a Risø TL OSL DA-12 machine.*

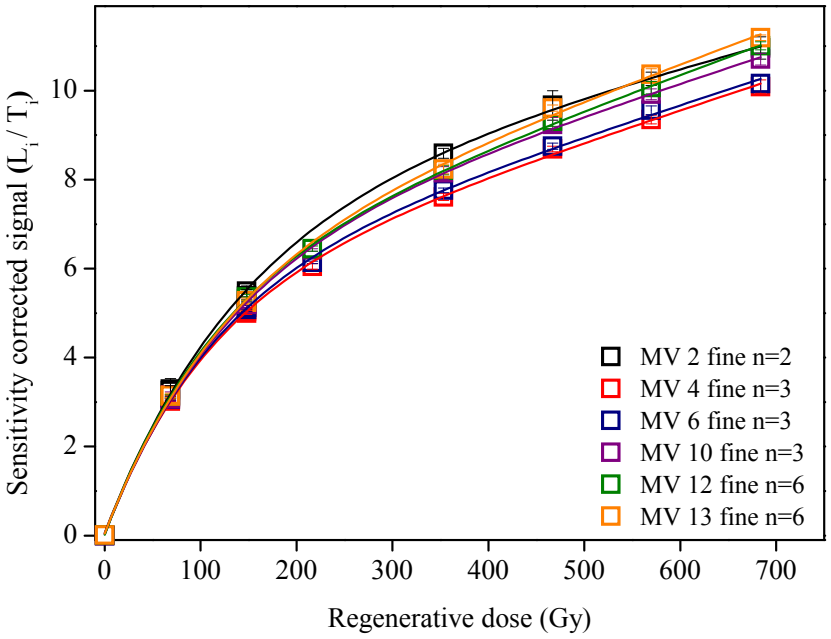

Figure V.11: *Comparison of average SAR-OSL growth curves for fine quartz from 6 samples of different ages.*

Table V.2: *Goodness of fit and values for the characteristic dose (D_0 and D_0*) for SAR growth curves for fine quartz from six samples of different ages. The dose-response curves were measured up to ~ 700 Gy using a constant test dose of 17.1 Gy. The functions used for fitting were a single saturating exponential $I=I_{max}(1-\exp(-(D+D_i)/D_0)$, and the sum of a single saturating exponential and a linear component $I=I_{max}^{*}(1-\exp(-(D+D_i^{*})/D_0^{*})+D\bullet a$. 85 % of saturation level in the case of a single saturation exponential fit is denoted as "practical limit".*

Sample code	$\chi 2$ / DOF (exponential fit)	D_0 (Gy)	D_0 error (Gy)	"Practical limit" (Gy)	$\chi 2$ / DOF (exponential + linear fit)	D_0* (Gy)	D_0* error (Gy)
MV2	0.085	225	25	426	0.011	126	12
MV4	0.092	235	27	446	0.014	108	13
MV6	0.091	238	27	452	0.010	110	11
MV10	0.101	241	28	457	0.010	112	10
MV12	0.096	255	29	448	0.017	113	9
MV13	0.134	255	38	484	0.027	116	18

Figure V.12.a shows a preheat plateau for sample MV10. Associated values for recycling and recuperation are shown in **Figure V.13.a.** There is no systematic variation in equivalent dose (D_e) with preheat temperature between 200 °C and 260 °C or cutheat temperature in the interval 160 °C and 220 °C (data not shown).

Over this temperature interval, the recycling ratios are consistent with unity and recuperation remains below ~0.2% of the corrected natural OSL signal. At higher preheat temperatures (> 260 °C), the signal is increasingly thermally eroded and the sensitivity correction not working as well.

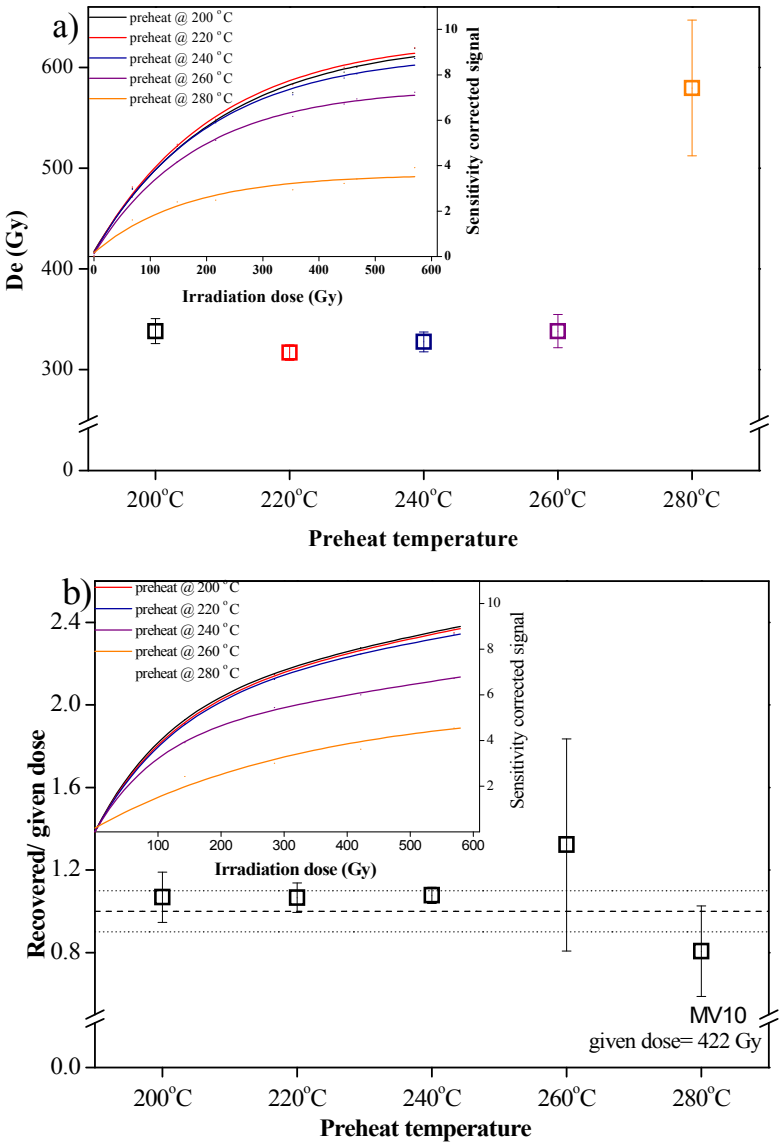

Figure V.12: *a) Dependence of D_e (a) and of the measured to given dose ratio; b) on preheat temperature for sample MV10. Each data point represents the average (± 1 standard error) of at least three replicate measurements. The dashed and dotted lines in (b) are meant as an eye guide and indicate a ratio of 1.0±0.1.*

The dependence of the measured dose on the preheat was further investigated using a dose recovery test for a laboratory dose of ~420 Gy. Three aliquots were measured at each of six preheat temperatures ranging between 200 °C and 280 °C. The dose recovery data are shown in **Figure V.12.b**. The corresponding recycling ratios and recuperation values can be found in **Figure V.13.b.** The measured dose appears insensitive to preheat temperature and matches the given dose reasonably well.

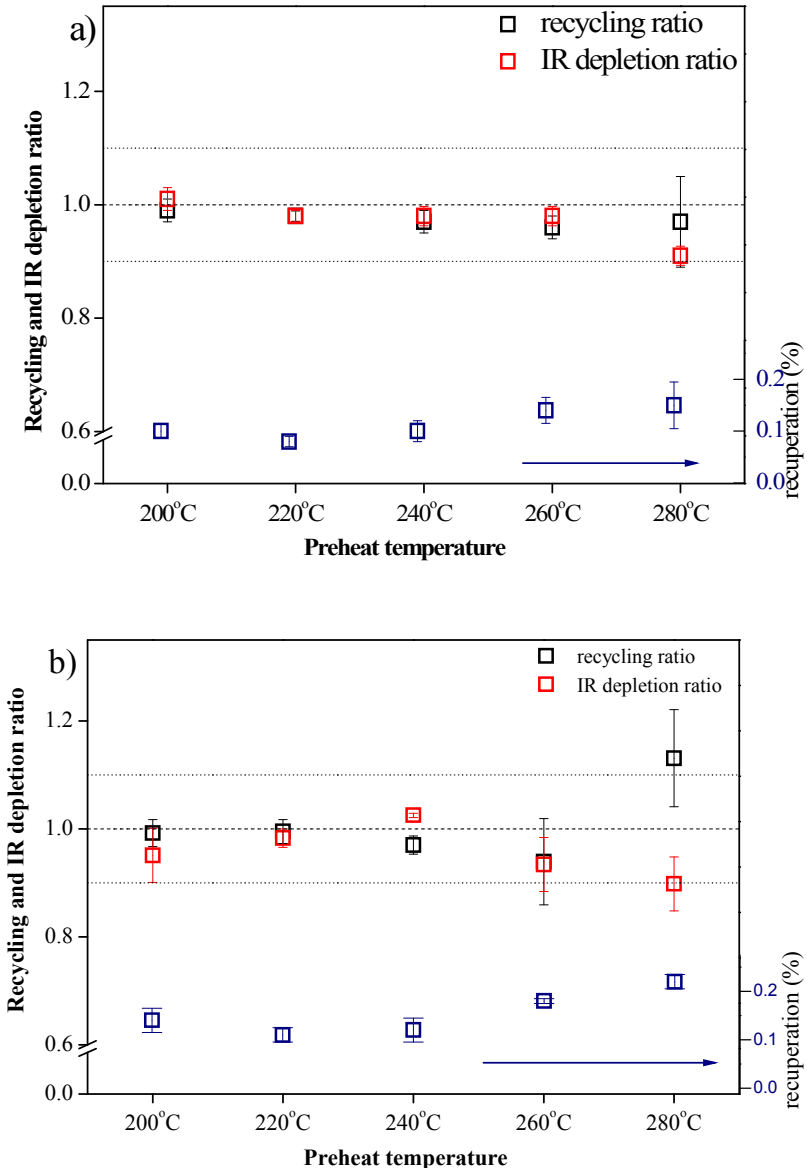

Figure V.13: *a) and b) presents the summary of recycling, IR depletion ratio and recuperation values for data presented in* ***Fig V.10*** *a) and b).*

The same observations were made for samples higher up in the sequence (i.e. with lower burial doses (MV2 – **Figure V.14.a, b and V.15.a, b**).

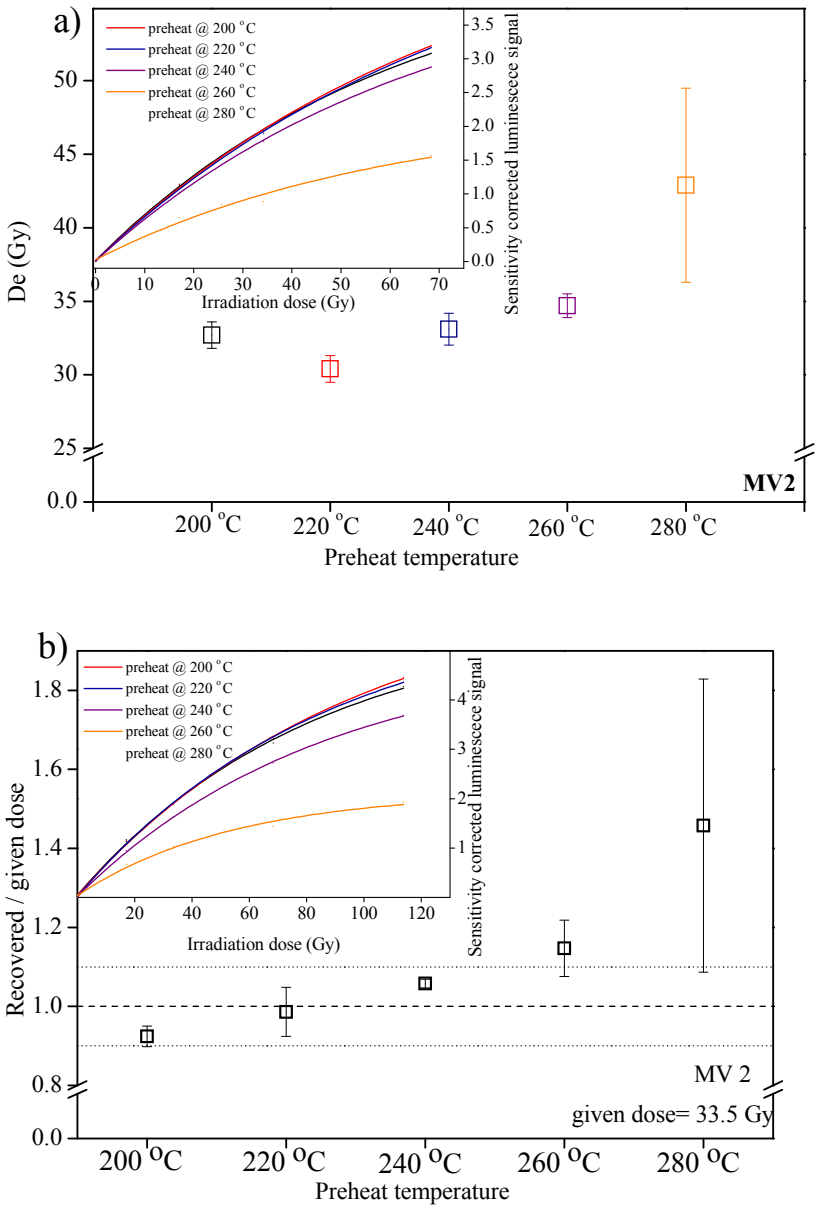

Figure V.14: *a) Dependence of D_e (a) and of the measured to given dose ratio; b) on preheat temperature for sample MV2.*

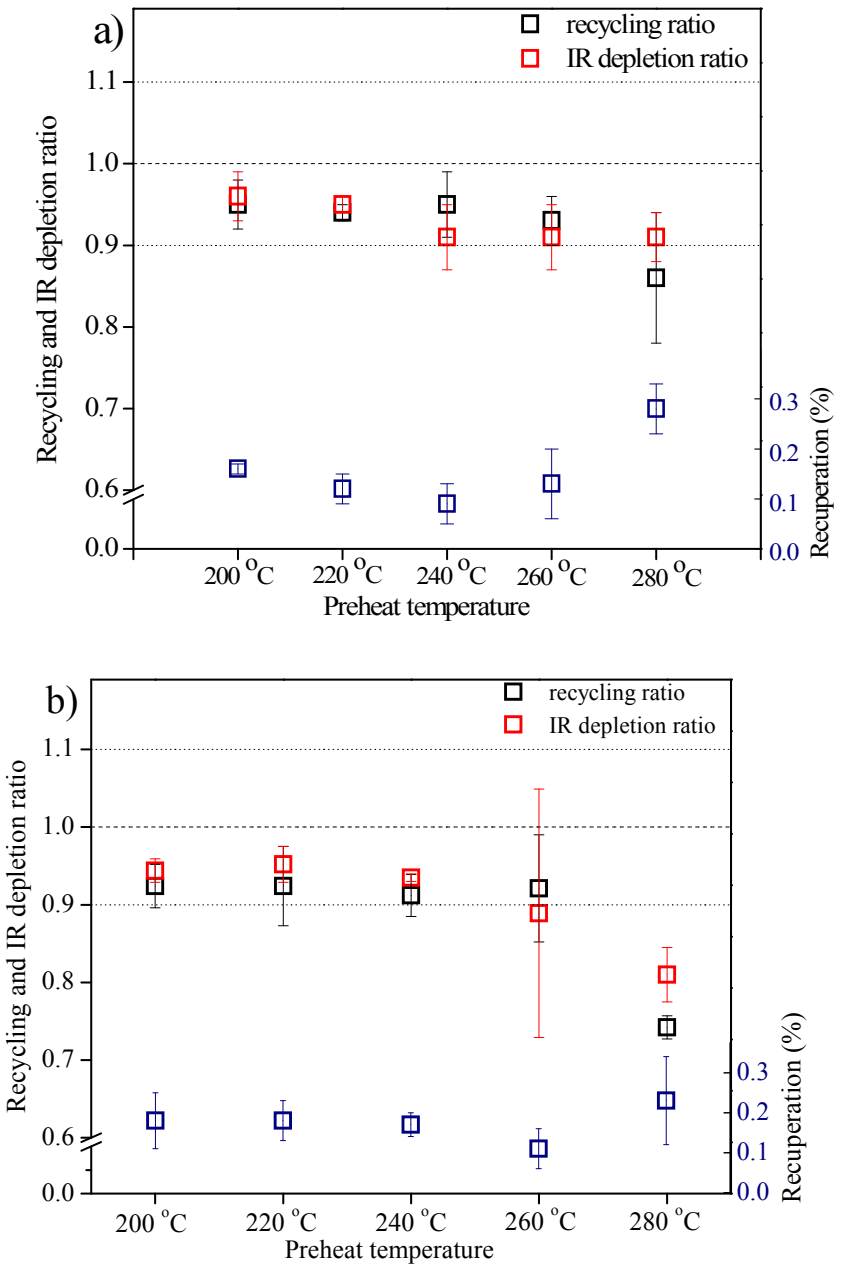

Figure V.15: *a and b presents the summary of recycling, IR depletion ratio and recuperation values for data presented in Fig. V.14 a) and b).*

A dose recovery test was then carried out on all samples, using a preheat of 10 s at 220 °C and a cutheat to 180 °C. This test was conducted as outlined in the above, with the given dose chosen to be equal to the estimated D_e in each sample. The measured doses are plotted versus the given doses in **Figure V.16**. It can be seen that the given dose can be recovered reasonably well over the entire dose range (i.e. from ~28 Gy to ~470 Gy). The overall (n=12) average measured to given dose ratio is 1.04 ± 0.04.

The dose recovery experiments indicate that our SAR protocol is able to accurately measure a laboratory dose given prior to any heat treatment. Note that good dose

recoveries were also obtained from the high dose linear region of the growth curve. Although the results give confidence in the reliability of the laboratory measurement procedure, they do not necessarily imply that natural doses can be measured accurately as well. For each sample, at least six replicate measurements of the D_e were made. The average values (± 1 standard error) are summarized in **Table V.4.**

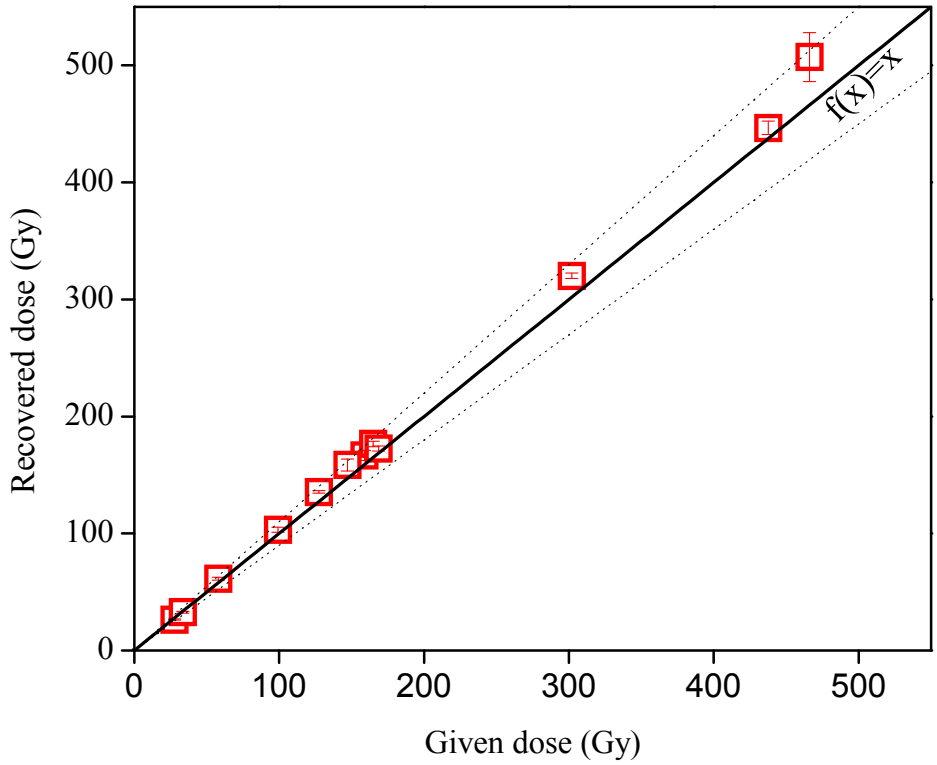

Figure V.16: *Summary of dose recovery data for all samples using a preheat of 10s at 220 °C). The given dose was chosen to approximate the equivalent dose; for sample MV10, the dose recovery test was carried out for given doses of ~300Gy and ~420Gy (data presented in Fig V.12). The solid line (eye guide) represents the 1:1 relation; the dotted lines (eye guide) bracket a 10% deviation from unity.*

V.1.6.2. A comparison between equivalent doses obtained in Ghent and Cluj Napoca Luminescence Laboratories

Aliquots of fine grains were re-measured in on the DA-20 reader in Cluj Luminescence Laboratory using the same protocol outlined above. Results obtained are resented in the following **Table V.3** and show a very good agreement between the data obtained in the two different laboratories.

Table V.3: *Comparison of equivalent doses obtained for different samples in Ghent and Cluj Luminescence Laboratories. N denotes the number of aliquots analyzed in Cluj the number of aliquots analyzed in Gent is indicated in Table V.4.*

SAMPLE	DE exp (Gy)	DE exp+lin (Gy)	Recycling	Recuperation (%)	IR depletion ratio	DE exp+lin UBB/ DE exp+lin Gent
MV1	**25.1 ± 0.3** (n=9)	**25.5 ± 0.4** (n=9)	0.98 ± 0.02	0.07 ± 0.03	0.97 ± 0.01	**1.02 ± 0.02**
MV3	**66.4± 0.6** (n=14)	**67.2 ± 0.7** (n=14)	1.00 ± 0.01	0.05 ± 0.01	1.00 ± 0.01	**1.04 ± 0.03**
MV7	**202 ± 2** (n=6)	**203 ± 2** (n=6)	1.00 ± 0.01	0.03 ± 0.01	0.99 ± 0.01	**1.03 ± 0.02**
MV9	**202 ± 2** (n=12)	**224 ± 2** (n=12)	0.98 ± 0.01	0.07 ± 0.01	0.99 ± 0.01	**1.01 ± 0.02**
MV10	**281 ± 4** (n=8)	**314 ± 4** (n=8)	1.00 ± 0.01	0.04 ± 0.01	1.00 ± 0.01	**1.01 ± 0.03**
MV12	**419 ± 17** (n=5)	**433 ± 18** (n=5)	1.00 ± 0.01	0.01 ± 0.01	0.99 ± 0.01	**1.01 ± 0.05**

V.1.6.3. Fine grained quartz optical ages

The optical ages are presented in **Table V.4**. It can be seen that the systematic uncertainty is dominant in the overall uncertainty on the ages, which amounts to ~14-15% (1σ). The large systematic uncertainty originates predominantly with our estimates of the uncertainties associated with the time-averaged water content and the a-value. As the sources of systematic uncertainty are largely correlated from sample to sample, only the random uncertainties (~2-3%) are considered to evaluate the internal consistency of the optical ages. Within this uncertainty, the dataset contains no outliers and the ages increase with depth (**Table V. 4**). Therefore, it is concluded that all sources of random uncertainty have been properly accounted for and that the observed variation in the age results is not larger than that expected from the individual uncertainties.

Optical ages ranging from 8.7±1.3 ka to 68±10 ka were obtained for the uppermost L1 unit, while the samples from the L2, L3 and L4 units yielded ages of 106±16 ka, 147±23 ka and 159±24 ka, respectively.

The optical ages indicate that this unit did not accumulate at a constant rate, with loess being deposited at a significantly lower rate during the past ~50 ka. This illustrates the limitations of proxy records (such as magnetic susceptibility) to interpret and derive a chronology for these deposits. The age results for the L1 unit contrast with the commonly held assumption that loess sedimentation in this region occurred at a constant rate. They are, however, in line with the ideas emerging from the study of Singhvi et al., 2001, and the recent insights gained from optical dating of Chinese loess, as at several localities in

the Chinese loess plateau, loess accumulation rates have been found to vary during the last glacial period (see e.g. Stevens et al., 2007; Buylaert et al., 2008). As such, our study further demonstrates the importance of absolute dates for interpreting these detailed archives of regional climate and environmental change.

The SAR-OSL ages obtained for the three samples taken below the S1 soil are interpreted as age underestimates, with the degree of age underestimation increasing with depth (optical ages of ~110 ka, ~150 ka and ~160 ka were obtained for samples taken from below the S_1, S_2 and S_3 Interestingly, the luminescence characteristics do not indicate such behavior: the signal continues to grow to high doses, the laboratory measurement procedure is accurate, and the ages increase with depth. These results are consistent with those reported for old (>70 ka) Chinese loess (Buylaert et al., 2007; 2008), but are in contrast to the findings by Murray et al. (2008) for quartz extracted from a deposit on the Seyda River in northern Russia. In the latter study, natural doses of ~350 Gy were obtained using the high dose linear region of the growth curve, which resulted in optical ages that were in excellent agreement with the independent age controls. At least for our samples, the results obtained from the high dose linear region of the growth curve do not appear to be accurate. The procedure underestimates the true burial age when applied to loess that was deposited before the last climatic cycle.

Table V.4. *Summary of equivalent doses (D_e), recycling ratios, recuperation values, IR depletion ratios, calculated dose rates, optical ages, and random (σ_r) and systematic (σ_s) uncertainties. The uncertainties mentioned with the luminescence and dosimetry data are random; the uncertainties mentioned with the optical ages are the overall uncertainty. All uncertainties represent 1σ. The number of replicate D_e measurements is given between brackets. The total dose rate includes the contribution from cosmic rays, and allowance was made for both the effect of moisture (assuming a water content of 20±5%) and the lower efficiency of alpha radiation in inducing luminescence (assuming an " a " value of 0.04 ± 0.02). Equivalent dose values determined interpolating on a single saturation exponential fit are compared to values obtained using a single saturation exponential plus a linear term. Ages are calculated upon the latter. Uncertainties on ages were calculated based on Aitken 1976 and Aitken and Alldred 1972.*

Laboratory code	Depth (cm)	D_e (exp fit) (Gy)	D_e (exp+ linear fit) (Gy)	Recycling ratio	Recuperation (%)	IR depletion ratio	External dose rate (Gy / ka)	Age (ka)	Relative random error (%)	Relative Systematic Error (%)
MV1	**85**	24.7 ± 0.3	**24.9 ± 0.4** (n=11)	0.95 ± 0.01	0.06 ± 0.02	0.94 ± 0.01	2.85 ± 0.05	**8.7 ± 1.3**	2.2	14.2
MV2	**105**	31.6 ± 0.8	**32.3 ± 0.9**(n=11)	0.94 ± 0.01	0.05 ± 0.02	0.95 ± 0.01	2.87 ± 0.05	**11.3 ± 1.6**	3.3	14.2
MV3	**130**	63 ± 1	**64 ± 2** (n=11)	0.96 ± 0.01	0.05 ± 0.02	0.96 ± 0.01	3.08 ± 0.05	**21 ± 3**	2.7	14.3
MV4	**185**	112 ± 1	**114 ± 2** (n=11)	0.99 ± 0.01	0.04 ± 0.01	1.00 ± 0.01	2.78 ± 0.04	**41 ± 6**	2.0	14.4
MV5	**225**	153 ± 2	**156 ± 3** (n=11)	1.00 ± 0.01	0.07 ± 0.03	0.98 ± 0.01	3.01 ± 0.06	**52 ± 8**	2.6	14.5
MV6	**280**	190 ± 3	**190 ± 3** (n=11)	0.98 ± 0.01	0.05 ± 0.02	0.99 ± 0.01	3.10 ± 0.04	**61 ± 9**	2.0	14.6
MV7	**375**	196 ± 3	**197 ± 3** (n=11)	1.01 ± 0.01	0.05 ± 0.01	1.01 ± 0.01	3.16 ± 0.05	**62 ± 9**	2.1	14.7
MV8	**400**	209 ± 4	**209 ± 3** (n=11)	1.00 ± 0.01	0.06 ± 0.01	0.97 ± 0.01	3.30 ± 0.05	**63 ± 9**	2.0	14.6
MV9	**500**	196 ± 4	**221 ± 5** (n=11)	0.97 ± 0.01	0.06 ± 0.01	0.91 ± 0.01	3.28 ± 0.03	**68 ± 10**	2.4	14.5
MV10	**800**	275 ± 7	**310 ± 9** (n=10)	0.98 ± 0.02	0.05 ± 0.01	1.00 ± 0.01	2.92 ± 0.04	**106 ± 16**	3.1	14.7
MV12	**1500**	385 ± 17	**430 ± 13** (n=6)	1.00 ± 0.01	0.07 ± 0.01	1.01± 0.02	2.91 ± 0.05	**147 ± 23**	3.3	14.8
MV13	**1800**	420 ± 15	**467 ± 11**(n=6)	1.01 ± 0.02	0.06 ± 0.02	1.01 ± 0.01	2.92 ± 0.03	**159 ± 24**	2.6	14.9

V.1.7. Optical dating using silt sandy (63-90 μm) quartz grains

V.1.7.1. Luminescence characteristics

We have continued our investigation by performing OSL measurements on the silt-sandy (63-90 μm) quartz fraction using the same measurement conditions as for the fine grains (preheat of 220 °C and cutheat to 180 °C cutheat, a test dose of 17.1 Gy, a high-temperature bleach for 40 s at 280 °C) in all experiments unless otherwise stated. Measurements were performed on a Risø TL/OSL DA-20 machine. **Figure V. 17** shows a typical OSL decay curve.

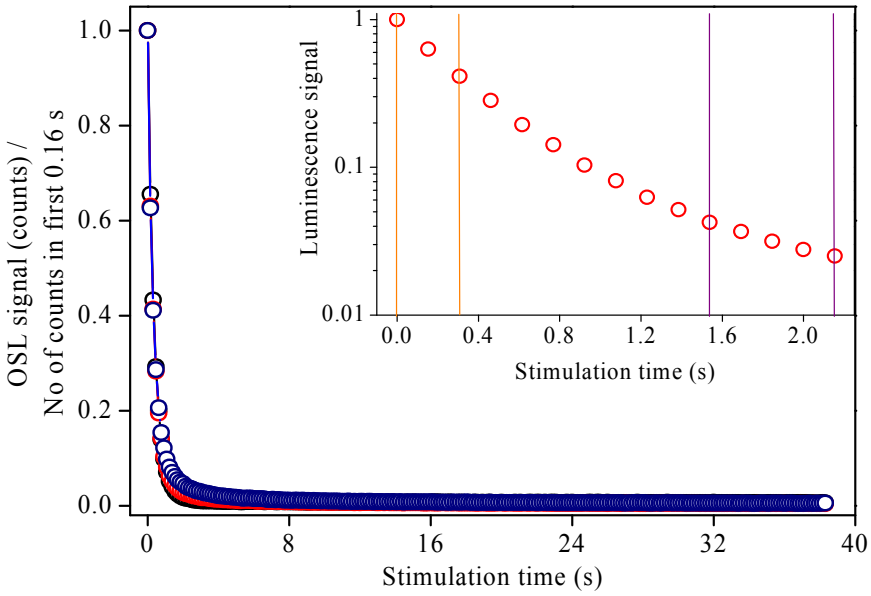

Figure V.17: *Typical decay curve of natural (red symbols) OSL signal of sample MV10 (silt-sandy quartz) compared to the regenerated signal (navy symbols) and the OSL decay of calibration quartz (black symbols). The measurement was performed on a Risø TL OSL DA-20 machine.*

All samples behave well in the SAR protocol with recycling ratios close to unity and growth curves passing through the origin. As well as for the fine grains the growth curves of the silt sandy quartz grains can be fitted acceptably to a single saturating exponential but the growth to high doses is represented best by the sum of a single saturating exponential and a linear component (**Figure V.18**). However the characteristics of the fitted curves differ from the ones obtained for fine quartz (**Table V.5**). This will be further discussed in the following section.

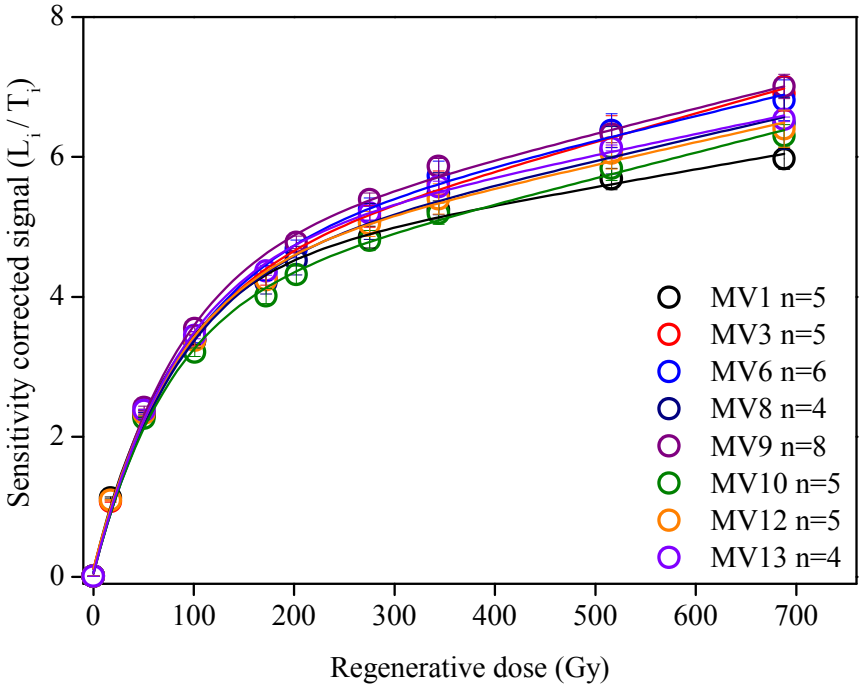

Figure V.18: *Comparison of average SAR-OSL growth curves for silt sandy quartz from 6 samples of different ages.*

Table V.5: *Goodness of fit and values for the characteristic dose (D_0 and D_0*) for SAR growth curves for silt-sandy quartz from six samples of different ages. The dose-response curves were measured up to ~ 700 Gy using a constant test dose of 17.1 Gy. The functions used for fitting were a single saturating exponential $I=I_{max}(1-\exp(-(D+D_i)/D_0)$, and the sum of a single saturating exponential and a linear component $I=I_{max}^{*}(1-\exp(-(D+D_i^{*})/D_0^{*})+D\bullet a$. 85 % of saturation level in the case of a single saturation exponential fit is denoted as "practical limit".*

Sample code	Nr. of aliq	Reduced χ^2 (exponential fit)	D_0 (Gy)	D_0 error (Gy)	"Practical limit" (Gy)	Reduced χ^2 (exponential + linear fit)	D_0* (Gy)	D_0* error (Gy)
MV 1	5	0.057	126	15	233	0.013	76	8
MV 3	5	0.084	177	23	325	0.016	81	10
MV 6	6	0.064	166	18	308	0.016	89	11
MV 8	4	0.068	157	18	291	0.016	82	10
MV 9	8	0.101	157	22	291	0.015	81	9
MV 10	5	0.084	164	22	302	0.013	74	8
MV 12	5	0.070	149	19	275	0.015	79	9
MV 13	4	0.072	143	17	266	0.012	83	8

Thorough dose recovery tests demonstrate that we can also successfully correct for sensitivity changes occurring during the first preheat. In **Figure V.19** we show that the given dose can be recovered reasonably well over the entire dose range (i.e. from ~28 Gy to ~495 Gy) using a preheat of 10s at 220°C and a cutheat to 180°C.

Furthermore, the measured to given dose ratio is independent of preheat temperature (**Figure V.20 a**). As well as the equivalent dose (**Figure V.20 b**). There is no systematic variation in equivalent dose (D_e) with preheat temperature between 200 °C and 260 °C. Over this temperature interval, the recycling ratios are consistent with unity and recuperation remains below ~0.2% of the corrected natural OSL signal. At higher preheat temperatures (> 260 °C), the signal is increasingly thermally eroded and the sensitivity correction not working as well. The lack of dependence of D_e on preheat temperature was observed for other samples as well (data not shown). As well no influence of varying the cutheat temperature on equivalent doses was observed (**Figure V.21**)

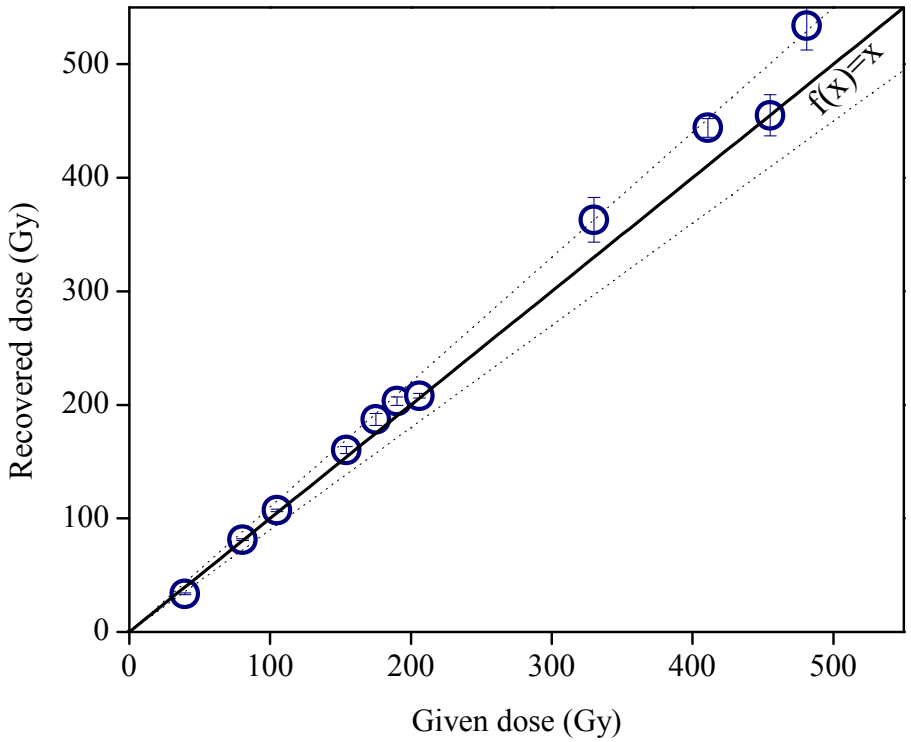

Figure V.19: *Summary of dose recovery data for all samples using a preheat of 10s at 220 °C). The given dose was chosen to approximate the equivalent dose. The solid line (eye guide) represents the 1:1 relation; the dotted lines (eye guide) bracket a 10% deviation from unity*

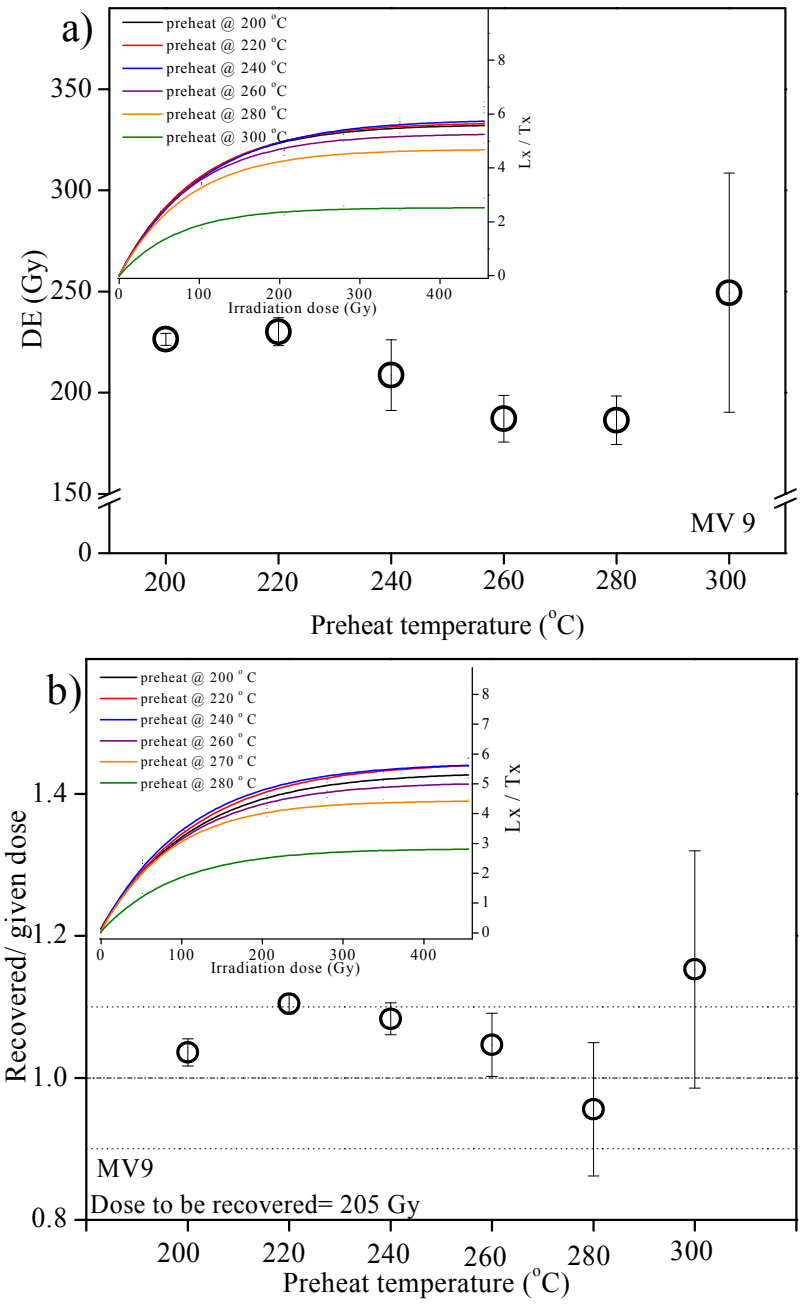

Figure V.20. *(a) Dependence of D_e (a) and of the measured to given dose ratio (b) on preheat temperature for sample MV9. Each data point represents the average (± 1 standard error) of at least three replicate measurements. The dashed and dotted lines in (b) are meant as an eye guide and indicate a ratio of 1.0±0.1.*

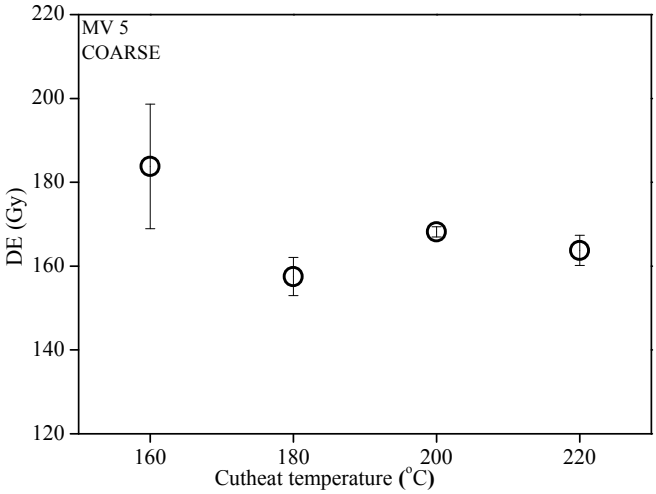

Figure V.21: *Dependence of equivalent dose on cutheat temperature using a preheat of 220° C. Data represents the average obtained on 4 aliquots.*

Equivalent doses obtained for silt sandy grains as well as the corresponding luminescence ages are presented in **Table V.6.**

V.1.7.2. Silt-sandy (63-90 μm) quartz optical ages

So far we have shown that both coarse and fine grains behave well in our measurement protocol. Unexpectedly, the De's in the sand-sized quartz are always higher than the De's in the silt-sized quartz, with the relative difference being more pronounced in the case of the younger samples.

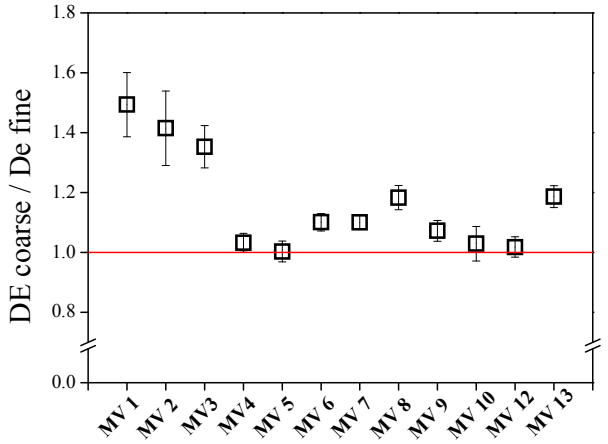

Figure V.22: *Comparison between the equivalent doses obtained on the two grain fractions analysed. The red line is meant as an eye guide.*

Table V.6. *Summary of equivalent doses (D_e), recycling ratios, recuperation values, IR depletion ratios, calculated dose rates, optical ages, and random and systematic uncertainties. The uncertainties mentioned with the luminescence and dosimetry data are random; the uncertainties mentioned with the optical ages are the overall uncertainty. All uncertainties represent1 sigma. The number of replicate D_e measurements is given between brackets. The total dose rate includes the contribution from cosmic rays, and allowance was made for both the effect of moisture (assuming water content of 20±5%) and the beta attenuation factor (assuming a value of 0.94 ± 0.045). Equivalent dose values determined interpolating on a single saturation exponential fit are compared to values obtained using a single saturation exponential plus a linear term fitting procedure. Calculated ages are based on the latter.*

Sample code	Depth (cm)	D_e (exp fit) (Gy)	D_e (exp+ linear fit) (Gy)	Recycling ratio	Recuperation (%)	IR depletion ratio	External dose rate (Gy / ka)	Age (ka)	Relative random error (%)	Rel. Syst. Error (%)
MV 1	**85**	37 ± 2	**37 ± 2** (n=11)	1.01 ± 0.01	0.27 ± 0.07	0.98 ± 0.01	2.40 ± 0.04	**16 ± 2**	7.1	12.4
MV2	**105**	46 ± 4	**46 ± 4** (n=8)	1.03 ± 0.01	0.06 ± 0.02	0.99 ± 0.01	2.42 ± 0.04	**20 ± 3**	8.5	12.5
MV 3	**130**	77 ± 3	**87 ± 4** (n=12)	1.00 ± 0.01	0.15 ± 0.03	1.00 ± 0.01	2.59 ± 0.04	**32 ± 4**	4.4	12.5
MV 4	**185**	105 ± 3	**118 ± 3** (n=10)	0.99 ± 0.01	0.09 ± 0.02	1.01 ± 0.01	2.33 ± 0.03	**51 ± 7**	2.8	12.6
MV 5	**225**	146 ± 6	**157 ± 5** (n=11)	1.02 ± 0.01	0.08 ± 0.01	1.01 ± 0.01	2.51 ± 0.05	**63 ± 8**	3.5	12.6
MV 6	**280**	206 ± 8	**210 ± 4** (n=40)	1.01 ± 0.01	0.08 ± 0.01	1.01 ± 0.01	2.59 ± 0.03	**82 ± 11**	2.5	12.6
MV 7	**375**	199 ± 4	**217 ± 3** (n=61)	1.01 ± 0.01	0.07 ± 0.01	1.01± 0.01	2.63 ± 0.04	**83 ± 11**	2.1	12.7
MV 8	**400**	228 ± 10	**247 ± 8** (n=20)	1.00 ± 0.01	0.09 ± 0.01	1.00 ± 0.01	2.77 ± 0.04	**89 ± 12**	3.4	12.8
MV 9	**500**	205 ± 7	**237 ± 6** (n=30)	0.99 ± 0.01	0.14 ± 0.01	1.00 ± 0.01	2.75 ± 0.02	**86 ± 11**	2.5	12.8
MV 10	**800**	253 ± 14	**319 ± 15** (n=12)	0.98 ± 0.01	0.12 ± 0.02	0.98 ± 0.01	2.44 ± 0.03	**132 ± 18**	4.9	12.9
MV 12	**1500**	----------	**438 ± 6** (n=5)	1.00 ± 0.01	0.17 ± 0.05	1.02 ± 0.01	2.43 ± 0.04	**200 ± 27**	2.1	13.6
MV 13	**1800**	----------	**554 ± 11** (n=4)	0.99 ± 0.01	0.11 ± 0.01	1.00 ± 0.01	2.43 ± 0.02	**230 ± 31**	2.3	13.2

Figure V.23 presents the optical ages obtained on both quartz fractions as function of depth compared to the magnetic time depth model. Given that no confidence limits can be defined for the time-depth model, we conclude that it is broadly consistent with the OSL age constraints for the L1 unit both in the case of fine and coarse grains. The inset in **Figure V.23** shows the optical ages obtained for the L1 unit as a function of depth to greater detail. At least two major phases in the history of loess accumulation can be distinguished. The ages for the samples taken at a depth of 500 cm to 280 cm, indicate a first phase that is characterized by a sedimentation rate of ~25 cm/ka. The uppermost 280 cm of loess was deposited at a much lower rate of ~ 3.5 cm/ka. The ages obtained on the 63-90µm fraction are consistent with the stratigraphic position of the samples. However they are consistently significantly older than the ages obtained on the silt-sized quartz. Samples taken from below the S_1, S_2 and S_3 palaeosols yield optical ages of ~110ka, ~150ka and ~160ka for fine grains; the corresponding optical ages obtained using the coarse grains are ~130ka, ~180ka and ~230ka. The optical ages obtained on coarse grains are in between ~20 to ~70 % higher than those obtained on the silt-sized fraction, with the difference being more pronounced in the case of the younger samples.

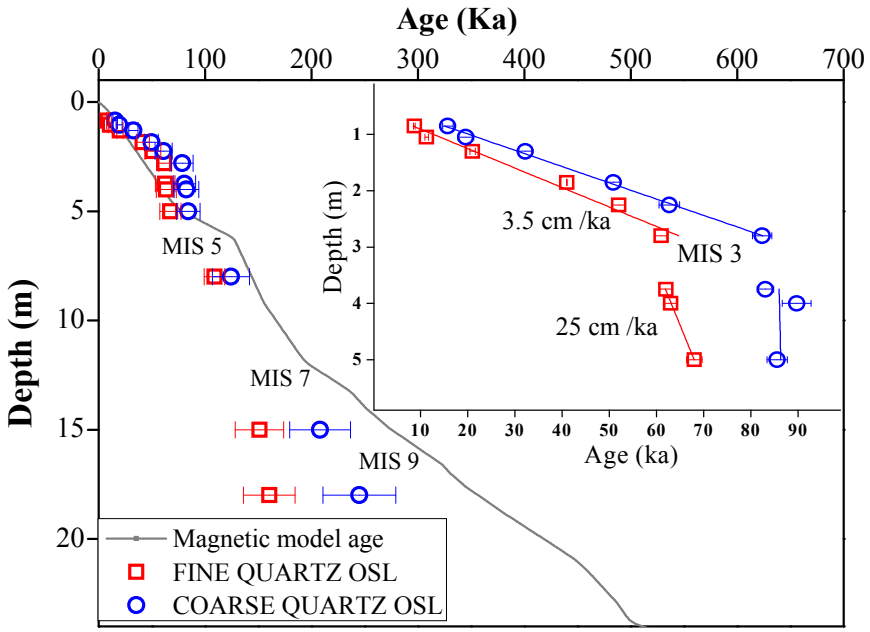

Figure V.23: *Plot of optical ages (open squares, 1 sigma total uncertainties) as a function of depth; the results from the palaeomagnetic time-depth modeling are shown by the gray line. The inset shows the optical ages (open squares, 1 sigma random uncertainties) and sedimentation rates obtained for the L1 unit.*

Although the sedimentation rates obtained using the fine and coarse-grained quartz are reasonable consistent, they cover different absolute time-ranges and, by consequence, conflict on the precise timing of the change in sedimentation rate. Indeed, the ages

obtained using fine-grained quartz suggests that the rate of loess accumulation varied during the last glacial period. The change in sedimentation rate occurred at ~60 ka, which coincides with the transition of MIS 4 to MIS 3. The fine-grained optical age chronology also allocates a weakly-developed palaeosol in the middle of the L1 unit to MIS 3; this is consistent with the prediction from the magnetic time-depth model. The fine grains do seem to underestimate the true burial age from the penultimate glacial periods onwards, but confirm that the S1 unit must have formed during MIS5.

The optical ages obtained using sand-sized quartz, on the other hand, suggest that loess accumulated at a constant rate during the Last Glacial Stage (MIS 4-2). Furthermore, the dataset indicates that the weak palaeosol, the uppermost well-developed palaeosol (S1) and the intercalated loess unit (the lower part of L1) belong to one complex that formed during MIS5. It is only for significantly older loess units (L3 onwards) that optical dating of coarse quartz grains appears to underestimate the true burial age. As both grain size fractions behave in a similar manner in the SAR protocol (recuperation, recycling ratio, and dose recovery), their apparently different age is unexpected.

Quartz from both grain-size fractions behaves in the SAR protocol in a similar manner, and procedural tests (recuperation, recycling ratio, and dose recovery) suggest that their OSL signals should be suitable for equivalent dose determination. All signals are dominated by a thermally stable fast component. The cause for the difference in age is, therefore, not understood. One could argue that incomplete resetting may account for age overestimation in the optical dating of coarse grains. This is considered unlikely to be the only cause for the observed age discrepancy. Indeed, it would require residual doses of the order of at least tens of Gy to explain the age offset for all samples. Even in fluvial environments, where exposure to sunlight is usually more restricted, dose offsets in samples older than a few ka are rarely significant (Jain, 2004). Another source of inaccuracy may be the a-value. The alfa efficiency in inducing luminescence in fine grains could not be measured directly in our study and a value of 0.04 ± 0.02 was adopted from other studies (Rees Jones et al., 1995). Adopting a lower value would slightly increase the fine grain OSL ages. However, the values obtained on sand -sized quartz are always higher than the De's in the silt-sized quartz and in the case of the younger samples not even using a nil value for the alpha efficiency would not overcome the age discrepancy. Furthermore, in the case of older samples the alpha efficiency values could be even higher than 0.04 (Mauz et al., 2006), thus leading to a more pronounced age difference.

For now, it is concluded that optical dating of quartz is a powerful tool for recognizing variations in loess sedimentation rate that occurred during the last Glacial/Interglacial cycle. At least for the loess record near Mircea Vodă it also allows establishing the chronostratigraphic position (MIS 5) of the uppermost well-developed palaeosol (S1).

V.1.8. Optical dating using silt (35-50μm) quartz

Silt size quartz is not very commonly used for luminescence dating applications due to the dosimetry problems (beta source calibration, etching and beta attenuation factors etc) arising from the use of this fraction. However, as this is quite an abundant mineral fraction in loess, several dating studies that made use of this fraction exist (see e.g. Stevens, 2007; Roberts, 2006). Three samples from Mircea Vodă loess sections were also dated using this fraction. The results are presented in comparison to data obtained on the silt-sandy and fine fractions in the following table.

Table V.7: *Equivalent doses obtained on silt quartz. The same measurement parameters as in the case of fine respectively silt-sandy quartz have been used (preheat to 220 ^{o} C, cutheat 180 ^{o} C, test dose = 17 Gy, ETOSL 40 s @ 280 ^{o} C). The number of analysed aliquots is given in brackets. For beta source dose rate a value of 0.162 Gy/s was assumed (94% of the dose rate determined for the coarse grains), for age calculation a beta attenuation factor of 0.96 being used.*

Sample code		Fine grains (4-11 μm)	Silt (medium) Grains (35-50 μm)	Silt-sandy (coarse) Grains (63-90 μm)
MV 1	De (Gy)	24.9 ± 0.4 (n=11)	28.1 ± 0.9 (n=84)	36.1 ± 2.3 (n=11)
	Age (ka)	8.7 ± 1.3	11.5± 1.5	15.1 ± 2.1
MV 4	De (Gy)	114 ± 2 (n=11)	121± 6 (n=10)	118 ± 3 (n=11)
	Age (ka)	41 ± 6	51 ± 7	51 ± 7
MV 9	De (Gy)	221 ± 5 (n=11)	236 ± 10 (n=10)	237 ± 6 (n=30)
	Age (ka)	68 ± 10	85 ± 12	86 ± 11

It can be noticed that silt san silt-sandy grains give the same age results for the older samples. In the case of the youngest sample, the age obtained on coarse grains is slightly higher than the age obtained on silt grains.

V.1.9. Further investigation into the luminescence properties of silt sandy (63-90 μm) silt (35-50 μm) and fine (4-11 μm) quartz grains

A discrepancy between the fine and coarse quartz optical ages was observed. As it was previously mentioned value for the alfa efficiency in inducing luminescence in fine grains could not been measured directly in our study and a value of 0.4 ± 0.2 was adopted from other studies (Rees Jones et al., 1995). Values of 0.3 have been also reported (Mauz et al., 2006) and adopting a lower value would slightly increase the fine grain OSL ages. However, equivalent doses obtained for sand -sized quartz are always higher than the De's in the silt-sized quartz, with the relative difference being more pronounced in the case of the younger samples and not even considering a nil value for the alpha efficiency would overcome the age discrepancy.

It had been shown that both fine and coarse grains fulfill the basic assumption of the SAR protocol (i.e. there is a linear dependence between the regenerated and the test dose signal as function of measurement cycle when the regenerative dose is kept constant (**Fig II.1**). **Figure V.24** further shows that sensitivity changes can be accurately corrected for. This, together with the good behavior of both coarse and fine grains in the basic SAR intrinsic rigor routine tests (dose recovery, recycling, IR depletion ratio) shown that both coarse and fine grains behave well in our measurement protocol. Thus the difference in the De values in unexpected if it is assumed that both fine and silt sandy material was deposited at the same time. The following sections will present the investigations performed in order to find the cause of this discrepancy.

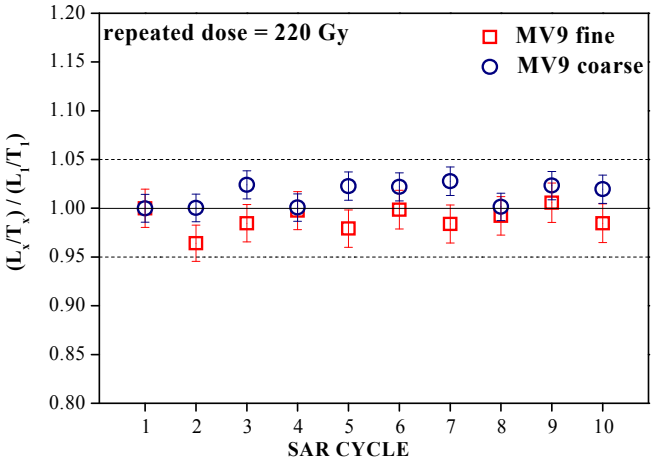

Figure V.24: *Variation of sensitivity corrected signals obtained using a constant regenerative dose of 220 Gy over 10 SAR measurement cycles. All values are normalized to data obtained in the first measurement cycle.*

V.1.9.1. Testing the possibility of the existence of an unstable medium component in OSL signals of fine grains.

Although the majority of studies concerning OSL signal components (Singarayer, 2002; Singarayer and Bailey 2003; Jain, 2003) report long term stability of the medium OSL component (with a thermal lifetime at ambient temperature of an order of magnitude of 10^5 MA), several studies have highlighted that a contamination of the OSL dosimetric signal (fast component) with a medium components can cause significant underestimation of optical ages (Choi et al., 2003, Li and Li; 2006, Steffen et al., 2009). These studies argue that the long thermal lifetime quoted above does not ubiquitously apply and the characteristics of this signal component may be related to the geological origin and history of quartz.

As mentioned in Chapter I, the OSL signal can be deconvoluted into its components. However, we have not performed this on our samples as signal deconvolution in CW-OSL measurements, as after several fitting attempts we have concluded that in many cases the

procedure may be unreliable, the results depending strongly on the choice of initial parameters, number of components and background. Deconvolution of signals composed of a sum of exponential factors is not a straightforward matter, the problem being termed ill posed (see e.g. Istratov and Vyvenko, 1999; Bos, 2009a).

Nevertheless, we are confident that the OSL dosimetric signal of our fine grains is not contaminated with an unstable medium component and in the following we will present the experimental evidence that led us to conclude this.

i) Contamination with a thermally less stable slow component is unlikely to be significant considering the background subtraction (signal: 0-0.32s; background: 1.6-2.24s) and the shape of the decay curves. For all samples, the regenerated signals are identical in shape to that of the natural and to the CW- OSL signal of calibration quartz. **(Figure V.10)** All samples have similar decay curves. In case of a thermally unstable component, it is reasonable to expect that the shapes of the decay curves are not similar.

ii) The preheat plateau is specifically intended to isolate a thermally stable signal; we observed a lack of dependence of D_e on preheat temperature (**Figure V.12 a, Figure V.14 a**)

iii) In order to compare the behavior of our signals to the finds of Choi et al., 2003; Li and Li, 2006, Steffen et al., 2009; we constructed D_e (t) plots for samples of different ages (**Figure V.25**) However we would like to note that De (t) plots should de interpreted with caution as they present data obtained by applying the SAR protocol to other components besides the fast component, and as it was previously mentioned, the SAR protocol was developed only for the fast component and thus may not be suitable for other OSL components.

We observe no dependence of D_e with stimulation time. In our case, contrary to the finds of Li and Li (2006), there is no falling trend in De (t) plots of natural signals, just the same degree of scatter in both the natural and laboratory induced signals.
The following figure (**Figure V.26)** resents the variation of equivalent dose with integration time for sample MV10. All OSL decay curves were reanalyzed using varying initial integration intervals. Then all De values from all the aliquots were normalized to the results obtained using the shortest integration interval (0-0.32s). Data points presented represent the average for the 10 aliquots analyzed for this sample in our work. It can be seen that there is no dependency of the equivalent dose obtained on the integration time.

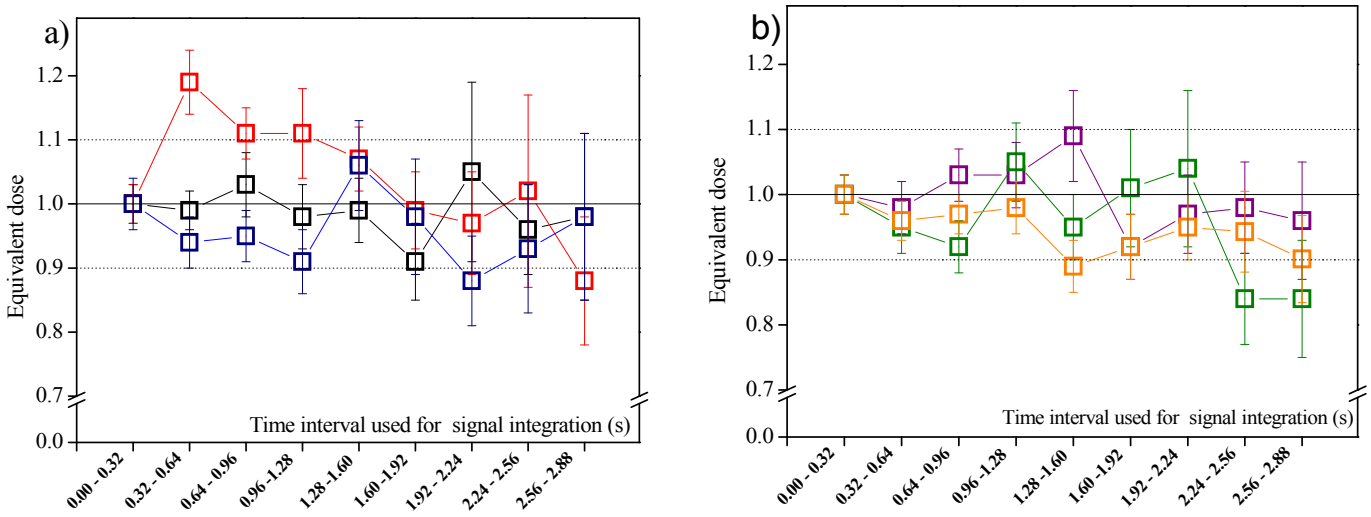

Figure V.25 *De (t) plots constructed for the natural (a) and regenerated signal (b) for three aliquots of sample MV8 fine quartz grains.*

In the case of the contamination of the signal with an unstable medium component we would expect to obtain lower equivalent doses with increasing the integration time.
As an alternative we can show that there is no dependency of equivalent doses obtained for samples of different ages when changing the interval used for background substraction. In the case of an unstable medium component, we would expect that using background intervals closer to useful signal would lead to obtaining higher values as the influence of the malign signal would be reduced.

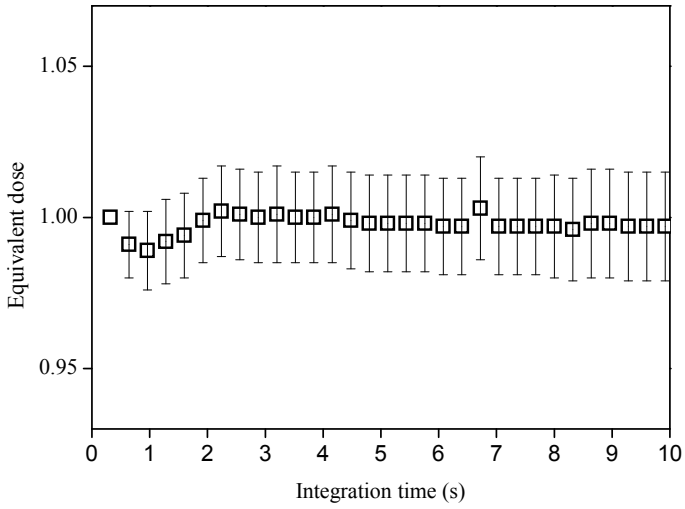

Figure V.26: *Variation on the average (obtained on 10 aliquots) equivalent dose obtained for sample MV10 fine grains by increasing the integration interval of the OSL signal with 0.32 s at a time. The background was taken from the last 3.2 seconds of stimulation. Obtained values are normalized to the data obtained using the first two channels (0-0.32s).*

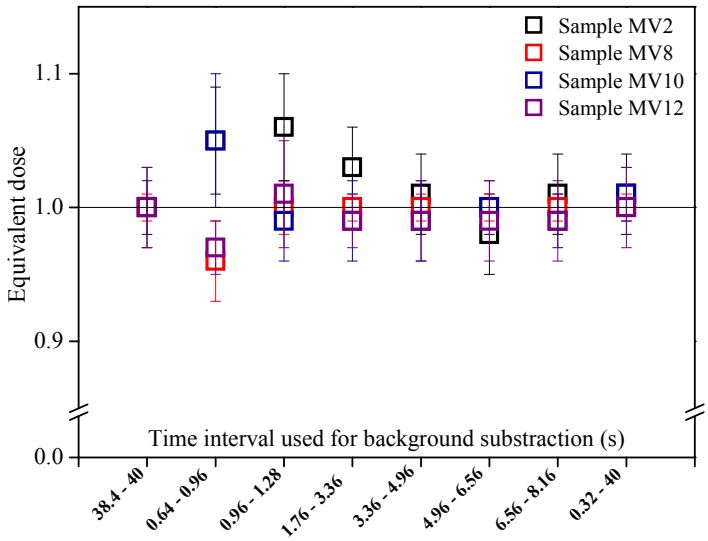

Figure V.27: *Equivalent doses obtained for samples of different ages for different background integration times.*

It is clear that, for both young and old samples, we observe no dependence of D_e on both stimulation time and integration interval. This, in combination with the other luminescence characteristics (preheat plateau, shape of decay curves, SAR-behavior) and our choice of integration limits (signal: 0-0.32s; background: 1.6-2.24s) gives confidence that significant contamination with a thermally unstable component is not likely. Nevertheless, we conducted LM-OSL measurements both on our fine and coarse grains. It has been shown that in case of first order kinetics the overlap of the OSL components at a given wavelength of stimulation is identical regardless of the stimulation mode chosen (Wallinga et al., 2008, Bos et al., 2009b). However, for purpose of visualization a peak shape representation may be desired and this may be achieved by ramped stimulation, as it was shown in Chapter I that that the position of the maximum of the OSL signal sampled by LM-OSL is dependent on the modulation ramp rate γ but also on σ, thus LM measurement can serve as an empirical tool by visual comparison of signal derived from different samples.

In **figure V.25** we present a comparison between the LM- OSL signals of different samples of fine grains as well as coarse grains compared to fine and coarse calibration quartz. It is clear that the peak maximum appear at the exact same position for all samples. As it is widely accepted that signal of calibration quartz is dominated by a fast OSL component we have reasons to be confident that all our samples have OSL signals dominated by a fast OSL components.

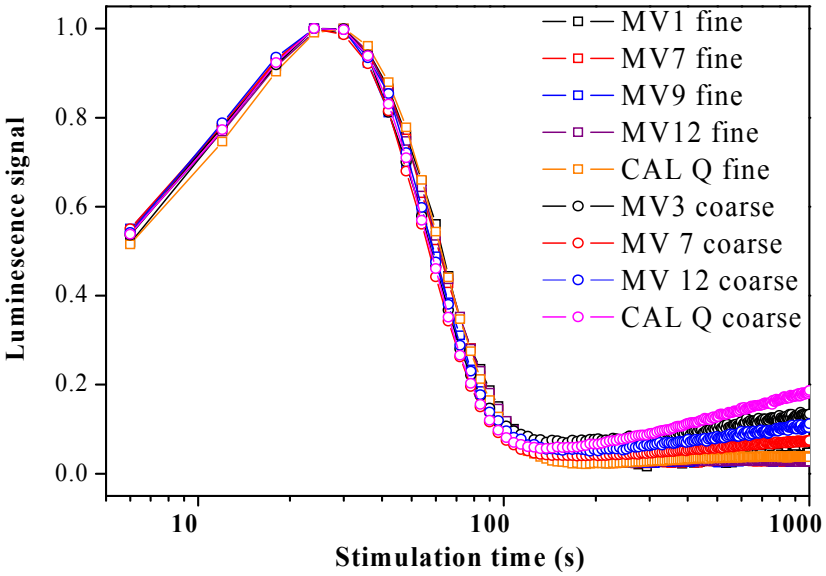

Figure V.28: *LM-OSL natural signals of fine and coarse sedimentary quartz extracted from Mircea Vodă section compared to calibration quartz. Stimulation was performed at 125 °C ramping the stimulation power from 0-100% in 3000s. One data channel represents 6 seconds of stimulation. For a better visual comparison values collected in all data channels have been normalized to the maximum value obtained in a data channel.*

A pulse anneal experiment has been conducted as well for fine and coarse grains of samples of different ages (**Figure 2.29**). The experiment consisted in measuring the natural signal of the aliquots investigated followed by repeating the same dose (of the same magnitude as the equivalent dose) in a SAR protocol, using increasing temperature preheat treatments of a duration of 10 seconds. Pulse anneal curves of our sampled signal are similar to pulse anneal curves published in literature for the fast component (Jain, 2003). A plateau up to approximately 270 °C can be noticed in all cases. The signal is eroded up to about 50% for preheats at about 300°C, while less than 10% of the signal is remaining after preheats of ten seconds at temperatures over 320 °C. The derivative of data (presented in the inset) shows a minimum at 300-350 °C. This might be evidence that the OSL sampled is deriving from the 325 °C TL trap.

The pulse anneal procedure previously presented gives information on the thermal stability of regenerated signals. LM-OSL measurements have been performed following increasing preheat (2s) (**Figure 2.30**) temperatures for both natural and regenerated signals. It can be noticed that the shape of the signals do not change with increased thermal treatment, as one would expect in the case of an unstable medium component. This further confirms that both the natural and regenerated fine and sandy fine quartz OSL signals used for luminescence dating of our samples are dominated by a thermally stable fast component.

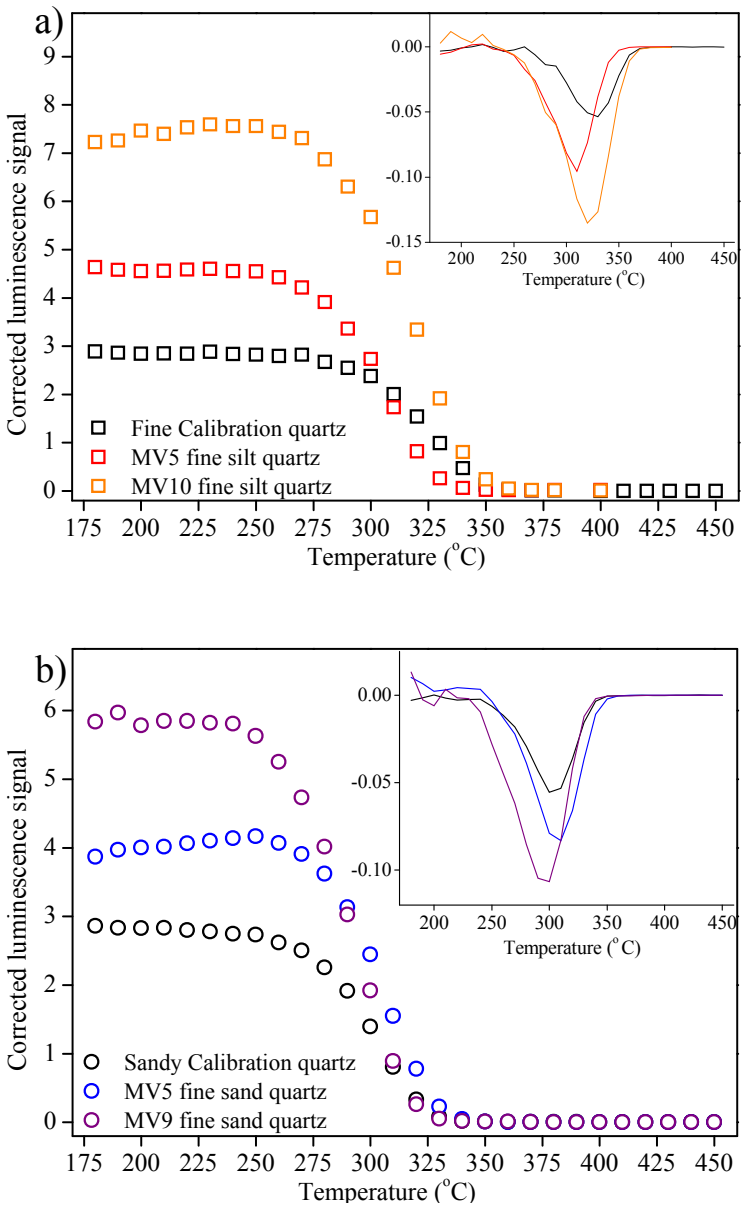

Figure V.29: *Pulse anneal curves of OSL dosimetric signal used for dating of fine and silt sandy grains analyzed. The inset shows the first order derivative of the curves. Recycling points for preheats of 200, 220, 240, 280, 300 have been inserted at the end of the sequence (data not shown).*

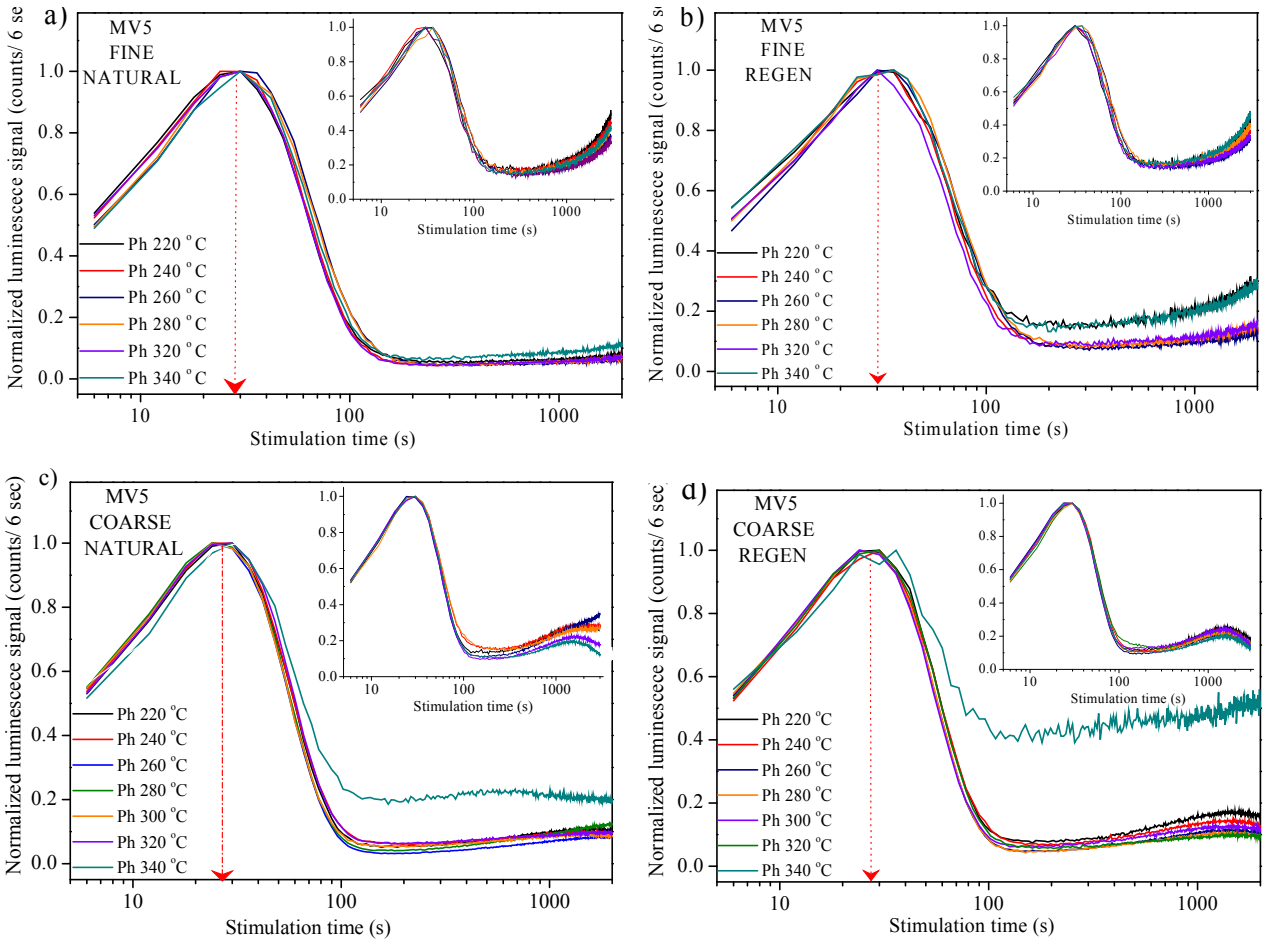

Figure V.30: *LM-OSL natural signals of fine and coarse sedimentary quartz extracted from Mircea Vodă section following preheats of 2 seconds at temperature ranging from 220 ° C to 360 °. The inserts present the corresponding test dose signals (recorded after a cutheat to 180 °C) For a better visual comparison values collected in all data channels have been normalized to the maximum value obtained in a data channel.*

V.1.9.2. Investigating the possibility of the existence of an ultrafast component in OSL signals of coarse grains

Jain et al., (2003) have shown that for some samples an ultrafast component may exist in the OSL signal. This component is thermally unstable and consequently exists only in regenerated signals and thus would lead to age overestimation. We exclude the possibility of an ultrafast component in our silt-sandy samples as the existence of such a component should have been observed in LM-OSL measurements. This conclusion is also supported by the lack of dependence of the equivalent doses on cutheat temperature (see figure V.21).

V.1.9.3. An examination of the equivalent dose distributions of fine and silt-sandy quartz grains.

The SAR protocol allows for a number of equivalent doses to be determined for each sample. It should be mentioned however, that even though the statistical uncertainties on individual equivalent doses as low as a very few percent is commonly observed, the variance of De distributions is typically larger than that expected from the uncertainties on individual dose estimates (Bailey et al., 2006).
Analyzing the random variability of equivalent doses can give information on partial bleaching, microdosimetric variations or post depositional mixing (Murray and Roberts, 1997; Olley, 1998; Roberts, 2000; Duller et al., 2003; Vandenberghe et al., 2003; Lomax, 2007; Bateman, 2007; Vafiadou, 2007).

If an analysed sample was well bleached at deposition, has gone no significant post-depositional alteration or translocation and has been subjected to a uniform radiation field the De values obtained should form a narrow Gaussian distribution.
In most cases partially bleached sediments consist of a mixture of grains exposed to light at deposition for different periods of time. Thus, some of the grains may have been exposed to sufficient daylight to zero the latent OSL signals whereas others still carry an OSL signal at burial. As equivalent doses are determined using aliquots containing at least a few thousand grains, materials that are partially bleached are likely to cause age overestimates.

In the following we will investigate whether this situation may apply to coarse grains extracted from Mircea Vodă loess section.

A way of representing De distributions is through histograms. An alternative way to visualize the distributions is by using the so called radial plots (Galbraith, 1988; Galbraith, 1990; Vermesch, 2009). A radial plot allows visualizing and comparing several

estimates with different precisions. The plot was originally developed by Galbraith for fission track dating and was subsequently also introduced in luminescence dating. In a radial plot, equivalent doses De_i are plotted in an (x, y) system where the x-axis represents the precision or the relative standard error (%) ($x_i = 1/\sigma(De_i)$) of the individual measurements. The y-axis plots $y_i = (De_i-De_0)/ \sigma (De_i)$. The central point of the plot (De_0) is the average value. Thus, measurements on any straight line radiating from the origin have the same equivalent dose but may have been measured with different precisions. Equivalent doses that are statistically consistent within 2 expected standard error of the mean will fall between a band extending ± 2s units around a common radial line.

Radial plots representing the equivalent doses obtained for the youngest loess sample analysed in this work (MV1) using the three quartz grain fractions (9-11μm, 35-50 μm, respectively 63-90 μm) are presented in **Figure V.31**. No overdispersion was noticed for the fine silt grains; for most of the samples analyzed (9) all equivalent doses obtained falling in the average ± 2 standard error of the mean interval, for the rest of the samples the overdisperision being as well very low (10-20%). This was not the case of the silt sandy grains as well (typical overdispersion in the case of large aliquots being more than 50 %).

However, the number of aliquots analyzed and present is far too low (see Rodnight, 2008) et al in order to draw consistent conclusion. **Figure V.32a** presents a histogram and the radial plot based on 81 equivalent doses obtained for sample MV7 silt sandy grains is presented in **figure V.32b**. A symmetric but broad distribution is observed but with a standard deviation of 11%, while individual measurements errors are better than 4%. The distribution however it is difficult to interpret for two reasons:

i) The analyzed sample is an old one (De~200Gy); natural luminescent signals being interpolated way above the linear part of the growth curve (see **figure V.18**).

ii) The distribution presented is obtained using large (diameter of 8 mm aliquots). From single grains studies (see e.g. Thomsen 2004) it is known that only a very few grains give rise to the bulk of the OSL signal. In such a study Duller (2000) showed that the fraction of grains that deliver 95% of the total light sum can be as less as 5%. Thus inter-aliquot scatter may be reduced if large aliquots are being used.

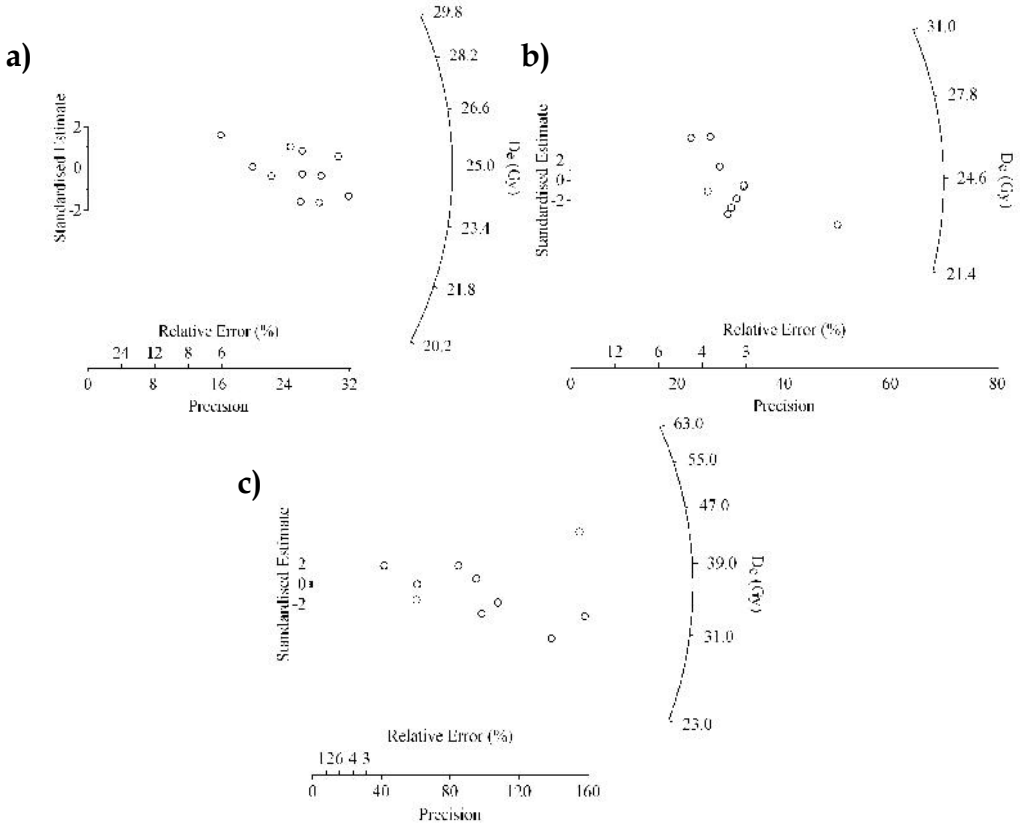

Figure V.31: *Equivalent dose distributions represented as Radial plots for fine grain aliquots (a), silt quartz aliquots (b) and coarse grain aliquots (c) of sample MV1.*

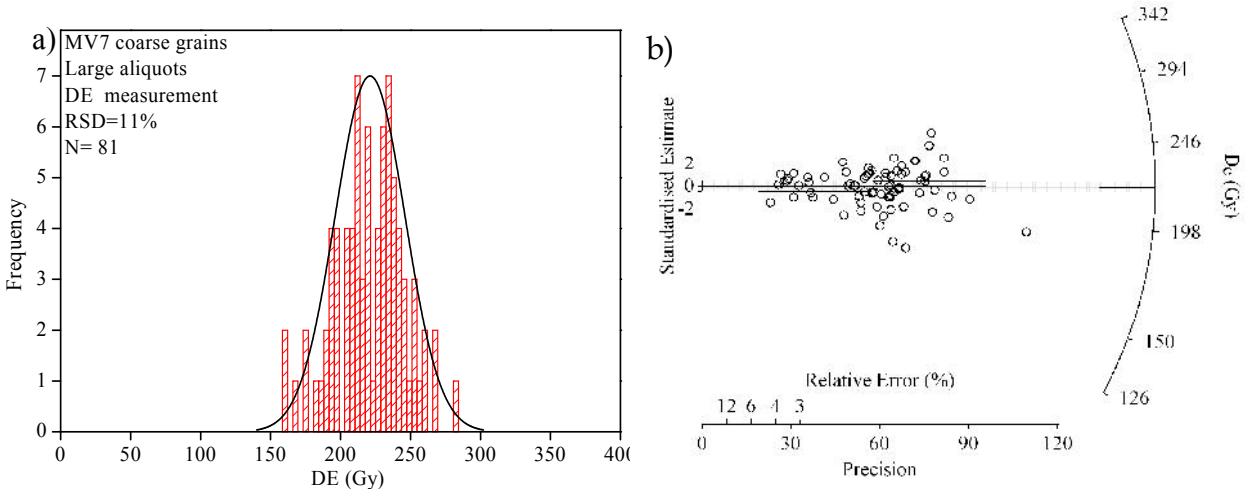

Figure V.32: ***a)*** *Histogram of equivalent doses obtained for sample MV7.The bin size was chosen to be equal to the median error of the individual estimates;* ***b)*** *same data are represented as a radial plot.*

Figure V.33 a) presents the equivalent dose distribution (represented as a histogram and as a radial plot) obtained for sample MV2 using small (2 mm diameter) aliquots. It can be observed that despite the fact that the uncertainty in each individual equivalent dose due to counting statistics is typically 3-6 % the distribution obtained on 49 disks though, is very broad, having a relative standard deviation of almost 50 %. The distribution obtained in the case of the dose recovery test (recovered dose approximating the natural dose) is symmetric and has a relative standard deviation of 10 % (**figure V.33 b)**).

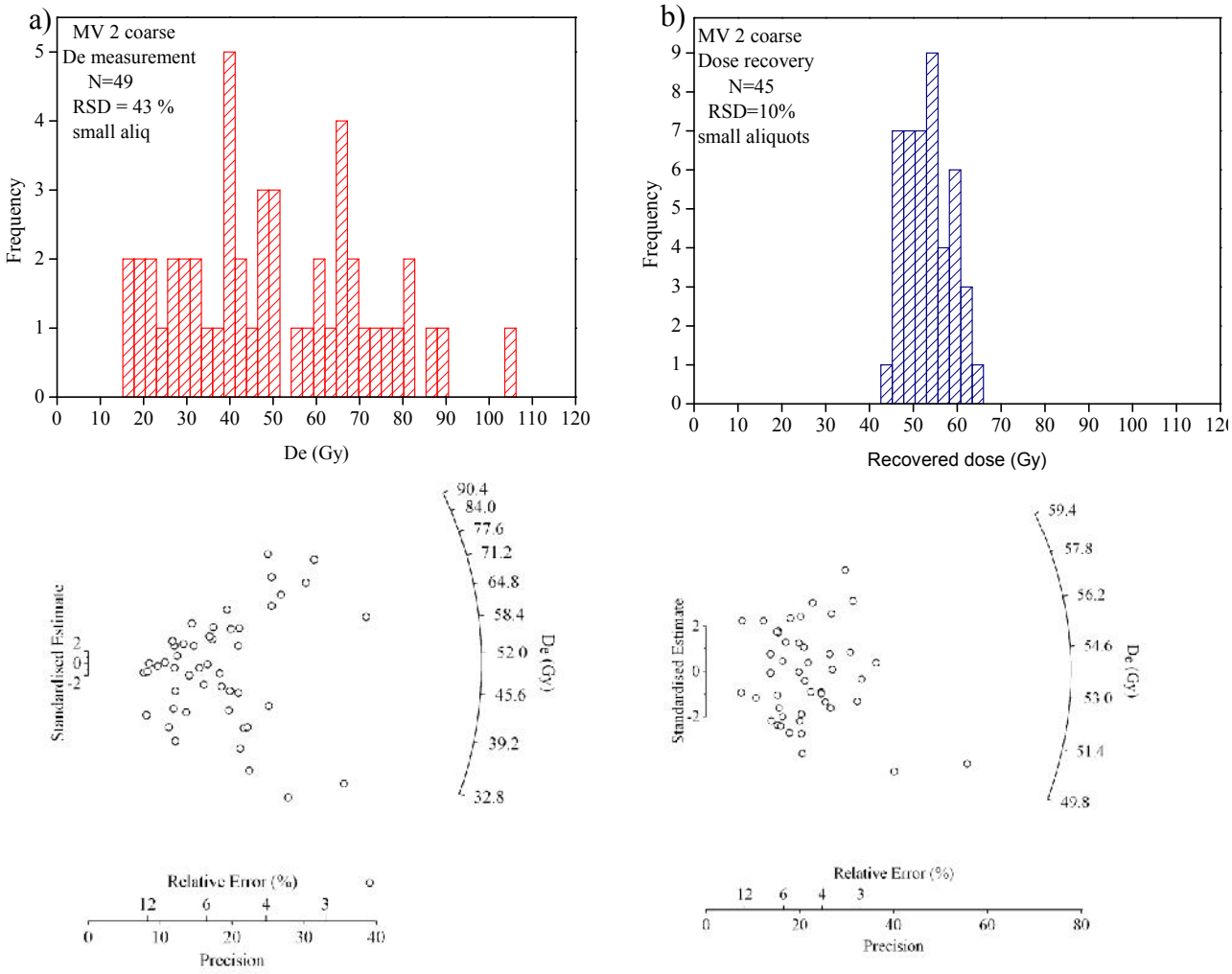

Figure V.33: ***a)*** *Distribution of equivalent doses for natural signals obtained on 49 small aliquots (2 mm diameter) of sample MV 2 coarse grains represented as a histogram and as a radial plot.* ***b):*** *Distribution of equivalent doses obtained in a dose recovery test on 45 small aliquots (2 mm diameter) of sample MV2 represented as a histogram and as a radial plot. The given dose was chosen to be approximately equal to the equivalent dose. The average recovered to given dose ratio obtained was 1.04 ± 0.02.*

This clearly indicates that an additional source of scatter is present in the natural data which is not related to analytical or instrumental uncertainties. Overdispersion was also observed in the case of coarse-silt grains (**Figure V.34**).

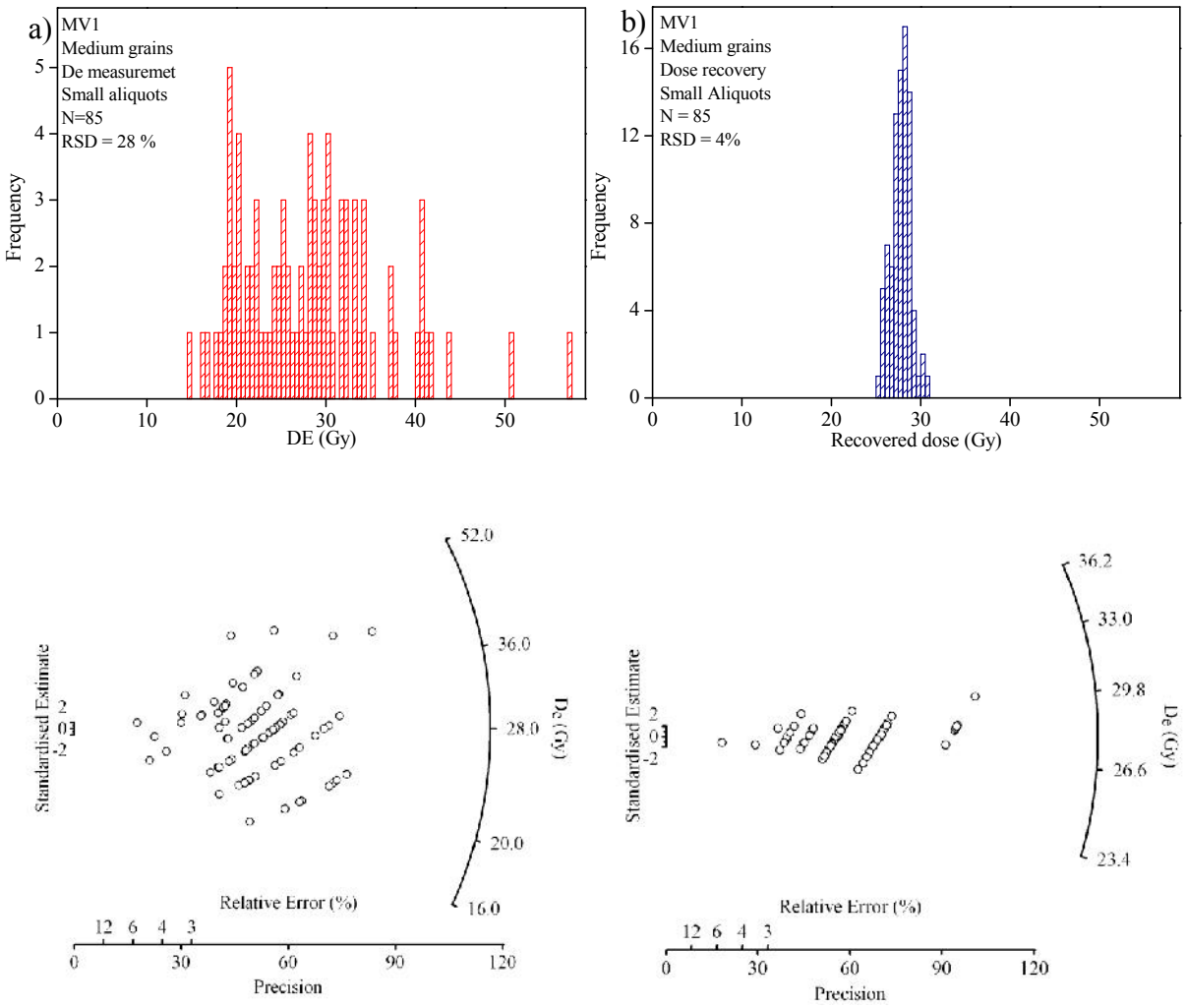

Figure V.34: ***a)*** *Histogram and radial plot of equivalent doses obtained using small aliquots of coarse silt sized quartz (35-50 μm) for sample MV1.* ***b)*** *Histogram and radial plot of equivalent doses obtained using small (2mm) aliquots of coarse silt sized quartz from the same sample obtained in a dose recovery test. The bin size in all histogram representations was chosen to be equal to the median error of individual measurements.*

Partial bleaching is the most frequent cause of overdispersion in equivalent ages. A method for identifying partial bleaching based on the analysis of the OSL signal has been suggested by Larsen et al., (2000) and Bailey, (2003). It has been argued that rising De (t) plots are an indication of partial bleaching. The limitations of using De (t) plots have been

described in the section V. 1.9.1. Their use for detecting partial bleaching is even more problematic as mentioned by Wintle and Murray, (2006), as the degree of bleaching of the slower components gives no information on the degree of bleaching of the fast component. It is worth being mentioned however that there was no observed rising trend in De (t) plots.

Many models have been proposed in literature in order for the estimated equivalent dose from a distribution of partially bleach grains to reflect the average equivalent dose of the well bleached grains. Some are quite rudimentary (e.g. Olley et al., 1998) but many are being quite sophisticated (e.g. Galbraith, 1999). The approach of Fuchs and Lang, (2001) is based on ranking the obtained equivalent doses in order starting from the lowest values to the highest. Starting from the lower value and including one additional value at the time the average and the standard deviation are calculated. This is repeated until the standard deviation is equal to the standard deviation obtained in dose recovery tests.

Selecting only the low values of the equivalent doses obtained, for a relative standard deviation approximately equal to the standard deviation obtained in the dose recovery test an equivalent dose of about 20 Gy is obtained for MV1 silt grains. This corresponds to an age of 8.1 ± 1 ka, in very good agreement with the age obtained using fine grains.
Possible variations in microdosimetry are difficult to detect and have not been explicitly investigated. The works of Vandenberghe et al., (2003, 2008) clearly demonstrate that internal radioactivity of quartz is a factor that definitely has to be considered while Mayya et al., (2006) showed that non-uniformity in the ^{40}K content on microscopic scale can lead to positively skewed distributions with relative standard deviations up to 46 % in the case of single grains**.** However, none of these can account for a dose rate difference of approximately 1 Gy/ka needed to justify the age discrepancy between the ages obtained on the two grain fractions.

To conclude with, we do not exclude that partial bleaching might be a cause for the age oversitmation of the coarser quartz fraction compared to the fine grains; this is unlikely though to be the case due to the windblown nature of the of the deposits analyzed; it is also unlikely to account alone for the difference observed for the older samples in which the De's differences amount from tens to hundreds of Gy.

V.1.9.4: Testing the possibility of the existence of thermally unstable recombination centers in coarse (silt-sandy) quartz

A question that has to be addressed is whether it is possible for different quartz types to yield different equivalent doses following common palaeodoses. As mention in Chapter II, a fundamental requirement of luminescence dating procedures is that natural and artificial irradiation are equivalent in terms of the luminescence produced. This assumption basically means that the growth curve constructed in the laboratory matches signal growth in nature. This assumption is impossible though to be tested directly as natural dose rates of our samples are ≈ $8*10^{-11}$ Gy /s while the dose rates used in laboratory are ≈ 0.1 Gy /s.

Based on the model developed in 2001 (presented in section I.4.2) Bailey (Bailey, 2004) suggested that dose rate effects in quartz may cause systematic overestimation of absorbed doses (and therefore age estimates). Based on numerical simulations he argued that this effect can be caused by competition from the relatively thermally unstable R1 recombination centre. Later on Bailey et al., (2005) investigated pulsed-irradiation regeneration of quartz OSL and showed that in the case of certain samples this technique can correct for equivalent dose overestimation.

In the following we will explain the above presented model and test whether it can be applied for the coarse quartz grains investigated in this work. Assuming that in some natural samples there would be a significant concentration of R1 centres, during natural irradiation at ambient temperatures the relatively slow flux of holes into this centres is matched by a slow rate of thermal de-trapping, leading to a relatively low equilibrium concentration of holes trapped into this centre. Consequently, competition for free (conduction band) electrons from the R1 centre is low. During laboratory irradiation, the flux of holes into the valence band is approximately 10 orders of magnitude higher, a considerably higher concentration of holes will occur in the R1 centre. These holes (trapped in R1) compete with the holes in luminescence (L) centre for electrons from the conduction band. Thus, fewer electrons will recombine in the luminescence centre. This means that for the same dose there will be less luminescence produced in the case of high dose rate irradiation then in the case of irradiating at a low dose rate, or in other words, the dose response curve generated by laboratory irradiation is lower than it should be. Based on the low energy gap between the R1 centre and the valence band (1.43eV) Bailey, (2004) suggested that performing the irradiations at high temperature (200 ^{o}C) would remove this unwanted effect, as the holes would be detrapped from R1 centre due to the thermal treatment. However, it was argued by Wallinga et al., (2002) that implying such a thermal treatment during irradiation may also induce changes in the trapping cross section of OSL centres (L centres). Due to this factor, elevated temperature would not be

desirable as it would only further complicate the dose response characteristics and Bailey, (2004) suggested separating the irradiation period into a series of short pulses and heating the sample following each pulse, and thus reducing competition from the R1 centre prior to the next irradiation pulse.

Pulsed irradiation has been investigated for two samples and the results are shown in **table V.8**

Table V.8: *Equivalent doses obtained for the samples of silt-sandy quartz investigated using pulsed irradiation compared to the equivalent doses obtained under irradiation at room temperature. n represents the number of measured aliquots. The size of the pulse use was 10.5 Gy (60s of irradiation) after each pulse a cutheat to 240 °C being implied.*

Sample code	De (Gy) Irradiation at 20 °C	De (Gy) Pulsed irradiation
MV5	158 ± 5 **(n=11)**	149 ± 5 **(n=8)**
MV6	210 ± 4 **(n=40)**	212 ± 6 **(n=11)**
MV8	247 ± 8 **(n=20)**	232 ± 4 **(n=6)**

A small (~ 6%) decrease in the average measured equivalent doses is obtained in the case of pulsed irradiation for samples MV5 and MV8, while the average equivalent doses obtained for sample MV6 are consistent. At a first look, the decrease observed both in the case of pulsed irradiation and elevated temperature irradiation might suggest the possibility of competition effects of R1 centres. However, this was not substantiated by a change in growth curve shape.

Unfortunately, older samples could not have been investigated due to the lack of material.

V.1.9.5. An examination of growth and saturation characteristics of fine and silt sandy grains

The signal versus administrated dose growth pattern up to 700 Gy of the fine, respectively silt sandy grains has been previously presented in sections. V.5.1, respectively V.6.1 (see Figure V.11, Table V.2, respectively Figure V.18, Table V.5). A very similar pattern of growth was observed for samples of different ages in the case of both fractions. It was also observed that the both in the case of fine grains as in the case of coarse grains at high doses the pattern of growth deviates from the expected monomolecular behavior ($I=I_{max}(1-exp(-(D+D_i)/D_0))$, and can be best represented by a function of the form of a single saturating exponential plus a linear term $I=I_{max}^{*}(1-exp(-(D+D_i^{*})/D_0^{*})+D \bullet a$.

It should be noted that the existence of a linear component in dose response curves constructed at high doses has been identified in other studies as well (Rhodes et al., 2006, Pawley et al 2008). The intrinsic mechanism of this behavior is far from being understood and the reliability of using this part of the growth curve has yet to be investigated (Wintle and Murray, 2006; Preusser et al 2009).

The parameters characterizing the average behavior of fine and coarse grains are given in **table V.9.** The characteristic doses (Do) obtained are comparable to the published values for the fast component of quartz (e.g. 190 Gy (Sigarayer and Bailey 2003), 97 Gy (Jain et al., 2005)).

Table V.9: *Dose response parameters obtained for irradiations up to 700 Gy.*

Grain	Monomolecular fit			Exponential + linear fit			
size	I_{max}	D_i (Gy)	D_0(Gy)	I_{max}*	D_i*(Gy)	D_0*(Gy)	a (Gy^{-1})
Fine	11 ± 0.1	-3.5 ± 6.1	**250 ± 10**	6.0 ± 0.1	-0.8 ± 1.7	**120 ± 4**	0.007±0.0002
Coarse	6.4 ± 0.1	-2.5 ± 6.4	**155 ± 7**	4.3 ± 0.1	-1.4 ± 2.1	**81 ± 3**	0.003±0.0002
Medium	6.7 ± 0.4	-4.8 ± 5.2	**140 ± 9**	5.4 ± 0.2	-2.1 ± 1.7	**92 ± 8**	0.003±0.0004

It can be observed that the fine grains have higher saturation characteristics than the coarse grains. This might be explained by assuming that the coarse and the fine grains come from different sources. The coarse material can have more local origin (a hypothesis that is also substantiated by the shape of the angular shape of the grains- figure V.7), while the fine grains could have been transported over very large distances. If deriving from different parent material, it is to be expected that the two fractions have different characteristics as it was shown that variation in the parameters concerning the defects may cause significantly different luminescence responses.

We have taken out investigation one step further and constructed much extended growth curves up to 10000 Gy. Dose response curves (L/T) are shown for two samples from Mircea Voda using different grain sizes **figure V.35**. A test dose of 17 Gy was used for both fine and coarse grains. Fitting was carried out using either a single saturating

exponential function or a double saturating exponential function (see **table V.10**). In both cases, the fits were best with a DSE function as indicated by the reduced chi square values as well as the residual sums of squares. However, it can be seen that the saturation characteristics of the two grain sizes are very different, the coarse grains saturating much earlier.

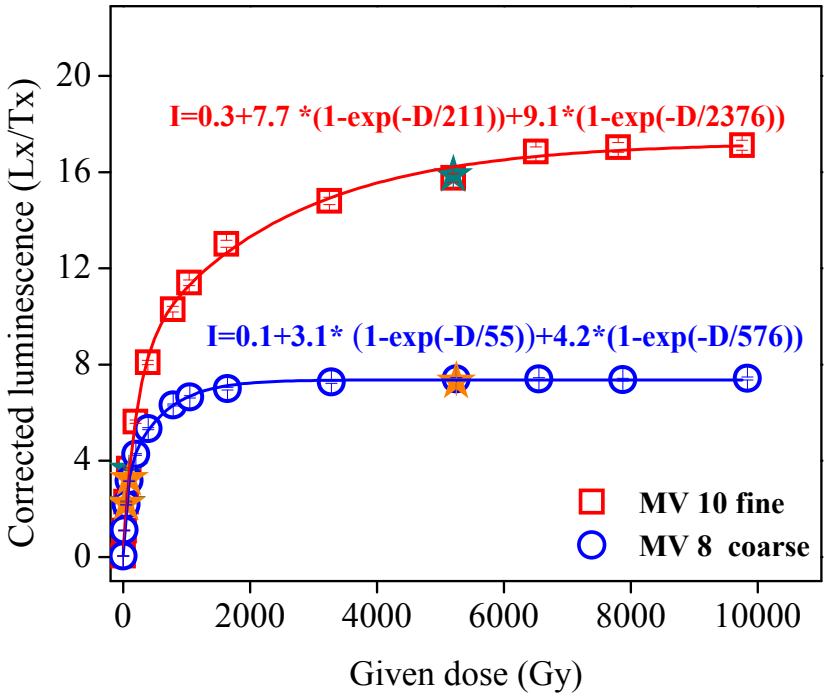

Figure V.35: *Comparison between sensitivity corrected growth curves constructed using fine and coarse quartz extracted from samples MV 10 and MV 8 collected from Mircea Vodă. The L_x/T_x data are fitted with a double saturating exponential (DSE) function. Repeated points for 46, 91 and 5000 Gy are shown as stars.*

It is important to note that this behavior is a characteristic of the fast OSL component. Dose response curves for the linearly modulated OSL (LM-OSL) signals up more than 1 kGy have been constructed. It was observed that the peak position of the LM-OSL does not change with irradiation dose. The fact that the integrated signal used to construct the dose response is indeed the fast OSL component was confirmed as well by the fact that this signal is reduced to a negligible level after an IR bleach for 8000 s at 160 ^{o}C (Singarayer and Bailey 2004, Jain et al., 2005) (**figure V.36**)

Table V.10: *Comparison between the goodness of fit using a SSE and a DSE regression model for dose response constructed up to 10 kGy for MV samples.*

Regression model	Data points used	Degrees of freedom	Reduced χ^2	Residuals sums of squares
		MV 10 4-11 µm		
SSE	14	11	0.92	10
DSE	14	9	0.085	0.76
		MV 8 63-90 µm		
SSE	14	11	0.162	1.8
DSE	14	9	0.05	0.5

In order to test whether the difference in dose response curves have an effect when a very old sample is measured, the dose response curves for a sample collected below S6 at Costinesti section were constructed. This sample was expected to have an age of at least 800 ka and thus it would be assumed that both quartz OSL signals would be in saturation; this was not the case (**figure V.37**).

The values of D_e obtained for the fine grains and the coarse grains were identical within error limits, both being much lower than expected for the known geological age of the sample. The dose response curve for the coarse grains showed negligible growth above 1 kGy, whilst negligible growth was observed for fine quartz only above 4 kGy. The natural value of L/T was below the saturation level for both grain sizes. A dose recovery experiment was carried out on four aliquots of fine grains using a dose of approximately 1.2 kGy and this could be recovered within 1%.

An issue that remains to be addressed is the observation that the natural signal of an infinitely old sample was found not to be in saturation. This was previously reported by other studies where a higher than exponential growth was observed (see e.g. Lai et al., 2010). This might imply that the laboratory constructed dose response does not reflect the growth of the signal in nature. The cause of the different pattern of growth in the dose response at very high doses for the two grain sizes might reside in the possible different origin of the grains (Buggle at al., 2008). However, this should not justify the difference in equivalent doses that leads to a systematic age overestimation of the coarse grains when compared to the fine grains.

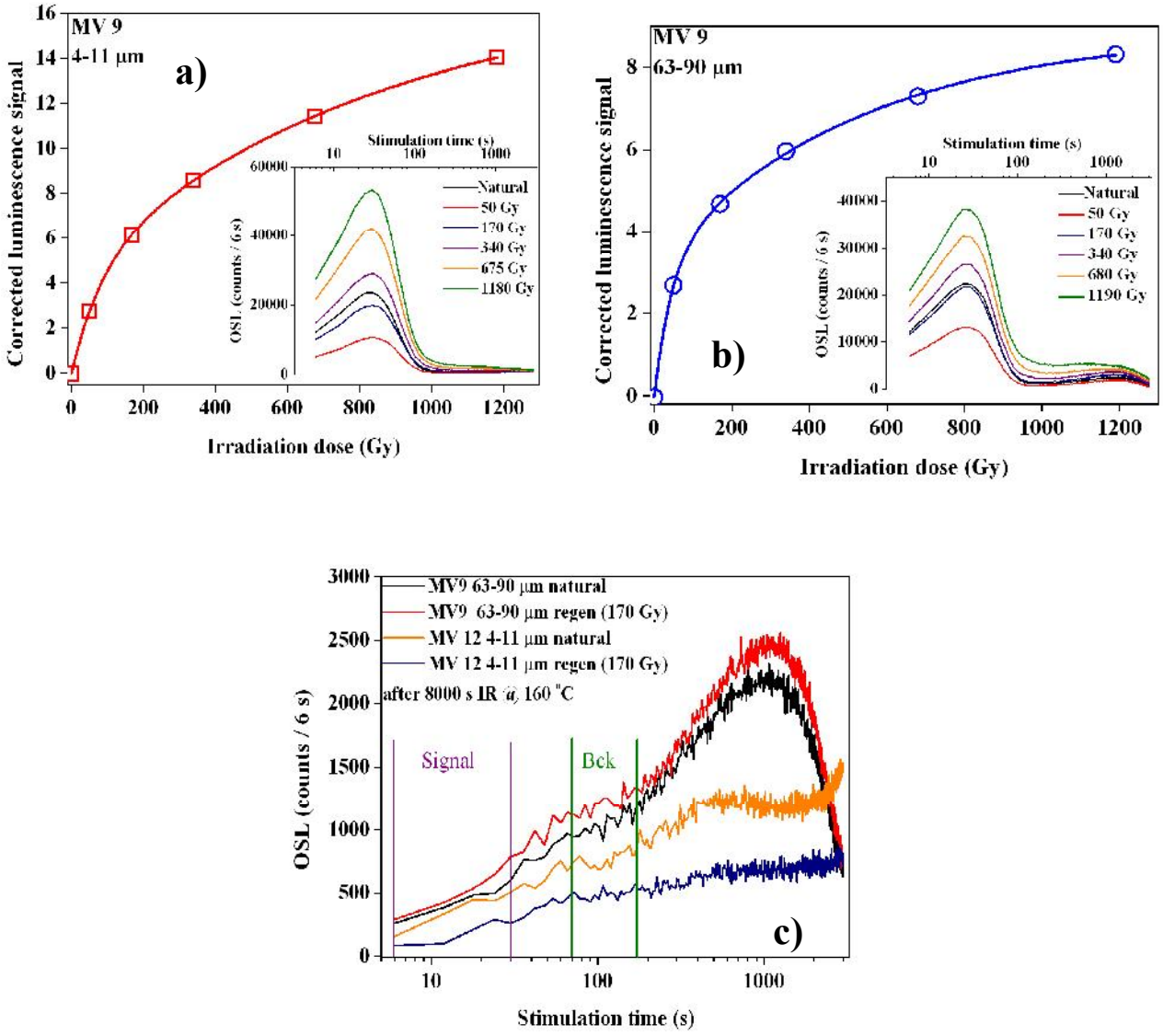

Figure V.36: ***(a)*** *Dose response curves constructed using LM-OSL signals for fine quartz extracted from sample MV9.* ***(b)*** *As in (a) but using coarse quartz. The insets in (a) and (b) show the LM-OSL for the natural regenerated signals.* ***(c)*** *Natural and regenerated LM-OSL signals obtained using fine and coarse quartz from samples MV12 and MV9 respectively. The signals were measured following an IR stimulation at 160 °C for 8000 s. The vertical lines indicate the integration region of the OSL signal (the first 30 s of stimulation) and the region used for background evaluation (between 60 and 180 s of stimulation).*

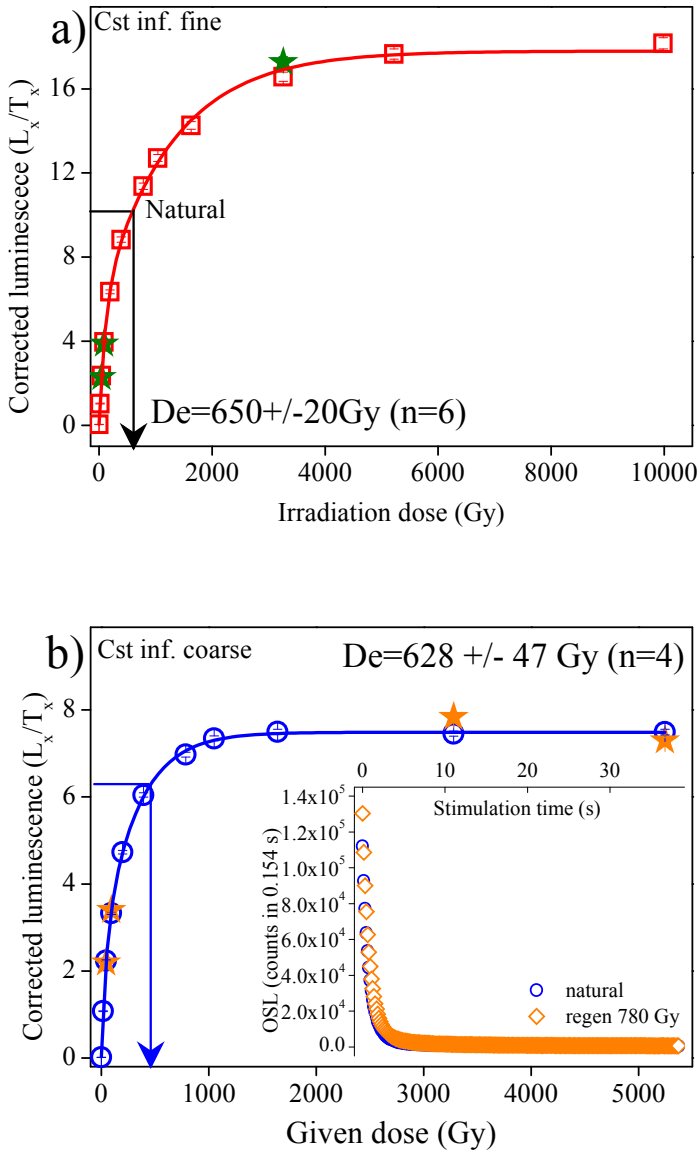

Figure V.37: ***(a)*** *Extended dose-reponse curve obtained for sample CSTinf using fine quartz.* ***(b)*** *As in (a) but using coarse quartz. Recycling points are shown as stars. The average equivalent dose obtained for each fraction is indicated as well. Typical natural and regenerated OSL decay curves are presented in insets.*

A comparison of the saturation characteristic doses obtained for the two fractions investigated in this study to similar studies worldwide is not straightforward, as these values are meaningful only in the case when the growth curve is constructed to doses high enough for the second component to be fully saturated. Such studies are quite few in the literature, possibly due to the long irradiation time needed. Nonetheless, it is intriguing to note that the values that we obtained for the fine quartz are very similar to the values reported by Lowick et al. (2010) in their study on fine material (D_{01} = 128 Gy, D_{02} = 1680 Gy), while the saturation characteristic doses obtained in this study for coarse grained quartz (D_{01} = 55 ± 3 Gy, D_{02} = 586 ± 5 Gy (n=5)) are close to the values previously reported on coarse material by Murray et al. (2007) (D_{01} = 44 Gy and D_{02} = 450 Gy for 180-250 µm quartz) and by Pawley et al. (2010) (D_{01} = 51 Gy, D_{02} = 320 Gy for 125-180 µm quartz). Further research is needed to sustain and explain this observation.

As mentioned in Chapter I, the defects giving rise to luminescence in quartz have not yet been unambiguously identified. Al is always present in quartz however, and is giving rise to $[AlO_4/M^+]^o$, $[AlO_4/H^+]^o$ and $[AlO_4]^o$ respetively (Malik et al., 1981). Recent studies correlate $[AlO_4]^o$ to the luminescence centres involved in the production of OSL (Martini et al., 2009). Studies on radiation induced ionic conductivity of quartz (Martini et al., 1986; Weil 1984) have shown that irradiation at room temperature leads to the dissociation of $[AlO_4/M^+]^o$ resulting in the formation of $[AlO_4/H^+]^o$ and $[AlO_4]^o$ centres. More recent studies point out as well that aluminium-hole centres $[AlO_4]^o$ can be produced by natural irradiation (Bahadur et al., 2008). It was pointed out as well by Mondragon et al 1988 that the relative proportion of $[AlO_4/H^+]^o$ and $[AlO_4]^o$ might be dose-rate dependent.

The growth curve saturation characteristics are a result of the growth of electron concentration at trapping sites as well as hole concentration at luminescence centres. If in the case of our samples luminescence centres are saturating faster than electron traps, and the above described mechanisms are valid this would explain the differences observed in the growth pattern of coarse grains and fine grains. If in the saturation region of the signal, the production of luminescence centres is also dose rate dependent, this might also explain the underestimation obtain when measuring natural signals, and the ability to precisely recover doses given in the laboratory. This hypothesis is substantiated by the observation that OSL signals for an indefinitely old coarse quartz sample are not in saturation (**Figure V.37**). On the other hand, other studies infer (Bailey, 2001) that the growth of OSL signals is dominated by the growth of electron concentration at trapping sites, based on various lines of evidence that suggest that in the case of quartz electrons are the minority carriers. Competition effects should not be forgotten as well, as for example Poolton et al., (2000) and Schilles (2001) demonstrated that annealing at high temperatures causes sensitivity enhancement of the fast component and suggested that this may be caused by a reduction of the non luminescent centres. Thus, at the moment the explanation of the mechanism causing the behaviour presented above is purely speculative. We believe that more work

is needed for conceptualising the process, independent processes or set of competing processes that generate the double exponential saturating behaviour of quartz OSL in order for these equivalent doses to be considered reliable.

V.1.10. Discussion

Luminescence dating is, at present, the only method that allows establishing an absolute chronology for loess deposits. The method uses grains of quartz and/or feldspar, which are both typically abundant in loess, and the windblown nature of loess ensures that the luminescence clock was completely reset prior to deposition. The first luminescence methods that have been applied to loess used thermoluminescence (TL) signals from polymineral fine (4-11 μm) grains (see e.g. Wintle, 1981; Van den haute et al., 1998, 2003). This was followed by stimulation of the polymineral fine grains with infrared light (infrared stimulated luminescence; IRSL), which became increasingly used for dating loess (Forman, 1991; Frechen and Dodonov, 1998; Frechen, 1999; Tsukamoto et al., 2001). More recent developments in dating technology allowed exploring the potential of quartz. Optically stimulated luminescence (OSL) dating has been applied to silt-sized (4-11 μm) quartz (Watanuki et al. 2003; Wang et al. 2006), middle-sized (35-63 μm) quartz (Roberts, 2006; Stevens et al. 2007; Lai et al., 2007) and sand-sized (63-90 μm) quartz (Buylaert et al., 2007; 2008). While it seems logic to assume that for a windblown material (such as loess) grains from several fractions are suitable for optical dating, this has not been explicitly demonstrated. At least to our knowledge, no studies are available that compare the luminescence characteristics and age of quartz grains of different granulometric fractions extracted from loess.

This study demonstrates that luminescence dating of loess may be more complicated. For samples collected from the loess sequence near Mircea Vodă (SE Romania), it is observed that OSL signals from silt-sized and sand-sized quartz yield ages that differ significantly. The OSL characteristics of both fractions, however, appear just as suitable for dating the deposits.

Despite an excellent behavior in the SAR measurement protocol standard procedural tests (dose recovery, recycling and recuperation) of both fine (4-11 μm) and silt-sandy (63-90 μm) quartz grains optical ages obtained on coarse grains are in between ~20 to ~70 % higher than those obtained on the silt-sized fraction, with the difference being more pronounced in the case of the younger samples. The possibility of contamination of the OSL dosimetric signal from fine grains with an unstable medium component is not substantiated by our investigations: the De in the fine grains is independent of both preheat temperature and the OSL signal integration region and LM-OSL and pulse anneal experiments provide further evidence for the samples to be dominated by a stable fast

component. Age overestimation due to an ultrafast component in coarse grained signals is also not considered as there is no dependence of the equivalent doses on the cutheat temperature and such a component should have been observed in LM measurements.

In the case of coarse grains the analysis of De distributions clearly indicates that an additional source of scatter is present in the natural data which is not related to analytical or instrumental uncertainties. The scatter in the case of young samples might be attributed to partial bleaching.

The possibility of existence dose and/or dose rate effects, at least in the case of high dose region on the dose response curve cannot be rejected. Very little is known empirically on possible dose rate dependence of OSL while different simulation studies infer that this kind of effects are prone to occur (see e.g. Chen et al., 2001a; Chen et al., 2001b; Lawless et al., 2009).

In the case of older samples, the shape of the growth curve might be a factor that leads to age overestimation. This is might be evidence that the use of the higher than exponential region of the growth curve might be problematic. We infer that the fundamental requirement of luminescence dating that the natural (low dose rate) and artificial irradiation (very high dose rate) are equivalent in terms of luminescence produced might not be fulfilled for high doses, at least in the case of certain samples.

Our results illustrate that an apparently reliable OSL laboratory measurement procedures do not necessarily guarantees an accurate determination of the true burial dose and new luminescence approaches have to be investigated in ordered for overcoming this apparent age controversy.

V.2. TESTING THE POTENTIAL OF OPTICALLY STIMULATED LUMINESCENCE DATING METHODS FOR SATING SOIL COVERS FROM THE FOREST STEPPE ZONE IN TRANSYLVANIAN BASIN

V.2.1. Introduction

The drier colder climatic period of the Holocene known as the Subboreal favored the expansion of the Boreal forests and steppes / forest-steppes in Western Eurasia. In the late Holocene a climatic transition from this climate to milder wetter conditions (Subatlantic) has taken place. Wetter conditions favored the expansion of the nemoral and subtropical forests in the same geographical area. Subsequently the steppes and forest-steppe contracted under the pressure of the nemoral forest in the western part of the Holarctis and the former vast grasslands were progressively replaced.

There are three fundamental types of forest-steppe areas derived from the extant literature which deals directly with this type of landscape (Sakalo 1961; Karamysheva and Khramtsov 1995). The typical forest-steppe is a mosaic of forests and mesic/mesoxeric grasslands (called "meadow-steppes" - very different from the ones in the steppe zone) which has a pattern dictated by the intimate relationships between the two fundamental types of ecosystems. This type is now encountered only in central-western Transylvania in the southern part of the region called 'the Transylvanian Plain' and in the Secaselor Tableland. Here the meadow-steppe grasslands and their associated Haplic and Luvic Chernozems and Phaeozems are placed on the floodplains, plateaus and shaded slopes and the nemoral forests of oak and the associated Luvisols exist only as tiny islets. The precipitations are below the level of 550 mm/ year. The second type is the expositional forest-steppe that exists in a large part of the periphery of Transylvania. In this case, the level of precipitations increases from 550 mm up to 700 mm/ year. The plateaus and the shaded slopes are entirely covered by nemoral oak forests and the meadow-steppe grasslands exist as tiny islets, usually on humid areas on the slopes which could not be inhabited by forests. As soon as the precipitation level passes over 700m/year as it happens at the borders of the Transylvanian Basin the nemoral forests of oak, hornbeam and beech and Luvisols inhabit the whole original landscape, including the sunny steep slopes. In these conditions only the geognosic forest-steppe can develop, conditioned by the presence of massive limestone rocks and gypsum formations as is the case in the north-western part of the region (Paşcovschi and Doniță 1967).

In the area of the expositional forest-steppe in the Transylvanian Basin there are many larger or smaller islands of Clinostagnic Phaeozems and Chernozems (named formerly "Black Clinohydromorph Soils" by the Romanian Pedologists) covered by Luvisols. These are gradually diminishing with increasing of the precipitations until they completely disappear as actual soils (Cernescu, 1970).

The typical forest-steppe landscape was certainly much widespread in Transylvania during the relatively dry and cold period of the Subboreal along with the meadow-steppe grasslands and their associated Chernozems and Phaeozems. The shaded slopes like the ones in **Figure V.38** – top, were almost totally covered by Chernozems and Phaeozems in almost all the Transylvanian Basin. With the increasing of the precipitation level and the onset of the Subatlantic period the nemoral forests and the Luvisols expanded on the shaded slopes and plateaus replacing the former bio-pedological structures at the periphery of Tranylvania.

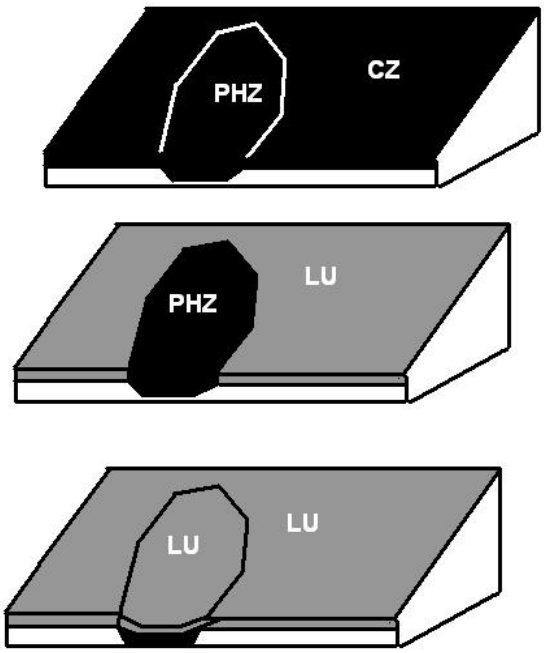

Figure V.38: *Scheme of soil cover on a long shaded (north exposed) slightly inclined slope from the typical forest-steppe (up), expositional forest-steppe (middle) and full nemoral zone (below) in the Transylvanian Basin. In the typical forest-steppe the slope surface is occupied by Chernozems (CZ) and the large derasional or landslide much humid 'slope valleys' by Phaeozems (PHZ). In the peripherical nemoral zone (expositional forest-steppe) the forest invaded the well drained parts of the slope where Luvisols appear (LU) while the mesic/mesohygrophile meadow-steppes on Clinostagnic Phaeozems survived as isolated patches on the much humid derasional or landslide slope valleys. When the annual precipitation level increases over 700 mm the nemoral forest occupies even the steep sunny slopes and also these humid slope valleys from the shaded slopes where the Luvisols replace the Phaeozems. However the very deep and very dark humus rich mollic horizon survives here below the albic horizons of the actual Luvisols due to the accumulative nature of the micro-environment in such 'slope valleys'. Such a situation can be seen on the left slope of Sărății Valley between Luna de Sus and Stolna in the western part of the Feleac Hills where the site analyzed here is located.*

The last areas to be inhabited by forests were on the slopes the much humid landslide 'valleys'. Their local conditions impeded the trees to populate them - due to their high level of humidity. Consequently the dark Phaeozems and their associated meadow-steppe grasslands survived there a longer time in the conditions of the expositional forest-steppe (**Figure V.38**- centre). However as the level of precipitations increases further above 700 mm/ year the pressure of the nemoral forests around increased a lot and the trees invaded also the landslide slope 'valleys'. Being accumulative micro-environments, the succession of soils adjacent to this major Holocene climatic, landscape and vegetational change was preserved: the Luvisols correspondent to the actual Subatlantic conditions can be found at the top of the former Phaeozems in the areas of the landslide slope valleys (**Figure V.38**- below). In the drier nowadays parts of central Transylvania, where the multi-annual precipitation level is under 550mm/year the Chernozems and Phaeozems are yet the actual soils and the remained natural components of the landscape are characteristic for the forest-steppe. The location of the site chosen for the present study is in Sărății Valley to the western border of the Transylvanian Basin, near the limit with Apuseni Mountains of the Inner Carpathians, in a densely forested area from the western part of the Feleac Hills - 15, 7 kilometers west-southwest of Cluj-Napoca city. Geographical coordinates are 46043'41.64 - 46043'18.79 N and 23023'52.30`` - 23024'31.19`` E.

The C-14 dating of the dark forest-steppe soils from such areas revealed ages in between 14.000-20.000 ka BP proving that in such drier regions the forest-steppe type of landscape and its associated soils (not necessarily also the strict vegetational types) are stable structures since the upper Pleistocene (Pendea et al., 2002; Pendea, 2005).
Unfortunately, though intuitively posed in connection with the climate change associated with the Subboreal-Subatlantic climatic transition (Badarau, 2005) no such a pedological structure was dated until now in Transylvania.

Optically stimulated luminescence (OSL) is now widely used in the dating of geological sediments such as aeolian, marine and fluvial sand or loess. One of the underlying principles of optically stimulated luminescence (OSL) dating is that sediments collected for dating have remained undisturbed since their burial. Bioturbation is a common phenomenon in soils, thus hampering the use of luminescence methods for direct dating of these formations. De replicates from undisturbed and fully bleached sediments are unskewed, show low overdispersion. Bioturbated sediments, however, may show highly skewed multi-model De distributions with higher overdispersion values (Bateman et al., 2007). True burial ages may be derived only through the application of statistical analysis and usually using single grain OSL measurements which are not straightforward (Roberts, 2000), thus OSL ages obtained on soil horizons are not very often encountered in literature.
This work tests the potential of state of the art optically stimulated luminescence dating techniques for revealing the age of fossil Clinostagnic Phaeozems and Chernozems

covered by Luvisols in Transylvanian Basin. As it was described in the former paragraphs, having an accurate chronology of these soil formations is of major importance in order to confirm that these formations are paleo-pedological relicts and prove that they truly can be used as a reflection of a late Holocene climatic transition from a drier climate – the Subboreal to a wetter milder climate – the Subatlantic.

V.2.2. Luminescence methodology

For luminescence dating, the soil samples were taken from an outcrop located in the mentioned site by using 30 cm steel tubes of 7 cm diameter which were hammered into the mid parts of the albic and mollic horizons described above. Tubes were sealed with black plastic bags and only the inner part of the material had been used.
63-90 µm quartz grains were extracted from two samples using conventional procedures under subdued red-light conditions (HCl (10%) and H_2O_2 (30%) treatment, wet sieving, heavy liquid (sodium metatungstate) density (2.63-2.75 g/cm ^{3}) separation, HF (40%) attack.

All measurements have been performed on an automated TL OSL Risø reader model DA-20 using blue light stimulation 470 ± 20 nm (36 mW/cm^2) and detecting the quartz OSL emission at 380 nm through a 7.5 mm tick Hoya U-340 filter. The purity of the quartz extracts was confirmed by the absence of a significant infrared stimulated luminescence IRSL) response at 60°C. Additionally throughout all measurements the 110 ^{o}C TL peak was monitored and the sensitivity to infrared stimulation was defined as significant if the IR depletion ratio deviated more than 10% from unity as recommended by Duller (2003). This was not the case in any of our samples analysed.

Luminescence analysis were performed on a sample of Albic Luvisol – LABORATORY CODE: 3A (LU), and a sample of Clinostagnic Phaeozem –LABORATORY CODE: 4B (PHZ). Linearly modulated-OSL measurements (Bulur et al 2001) indicated that the luminescence signal of interest is dominated by a fast component (**Figure V.39**), and thus amendable to be analysed through the single aliquot regeneration protocol (Murray and Wintle 2003, Wintle and Murray 2006).

Continuous wave blue-light stimulated luminescence signals (40 s at 125 ^{o} C) have been used for dating, integrated from the first 0.32 s of stimulation. The background correction has been performed subtracting the signal collected between 2.5 and 3.8 s of stimulation. A typical growth curve is shown in **Figure V.40.**

The main assumption underlying the SAR protocol is that sensitivity changes occurring throughout a measurement cycle can be corrected for using the luminescence responses to a constant test dose. The regenerated OSL signals can then be corrected for sensitivity changes by normalizing them to the corresponding test dose responses. Intrinsic rigor tests (as recommended by Murray and Wintle 2003; Wintle and Murray 2006) performed indicated that the quartz samples analysed behaved well in the

measurement protocol. The recycling ratios close to unity show that we can successfully correct for sensitivity change throughout the measurement cycles. The low recuperation values (< 1%) indicated that there is no significant unwanted charge transfer into the dosimetric trap

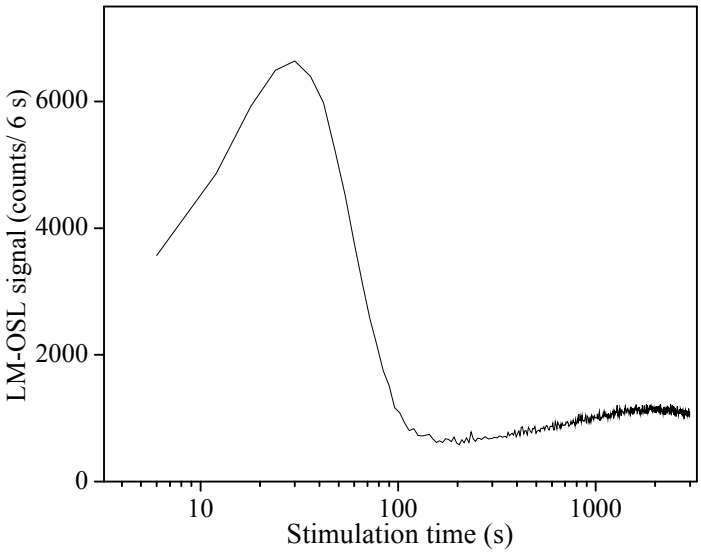

Figure V.39: *LM-OSL signal of quartz extracted from sample 4B (PHZ)*

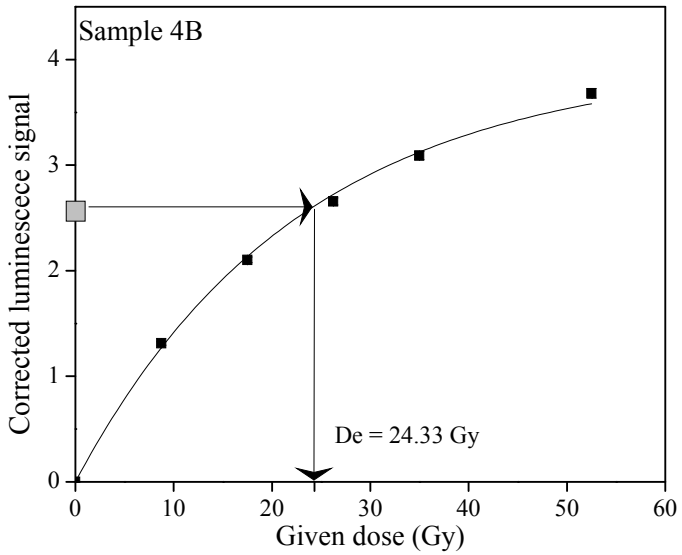

Figure V.40: *Typical dose response growth curve of quartz extracted from sample 4B (PHZ). The equivalent dose is obtained by interpolating the natural luminescence response on this growth pattern. For the represented aliquot an average equivalent dose of 24.3 Gy was obtained.*

Dose recovery tests demonstrate that we can also successfully correct for sensitivity changes occurring during the first preheat. Furthermore, the measured to given dose ratio is independent of preheat temperature as well as the equivalent dose. This is further evidence that our measurement protocol is robust (sensitivity changes are taken into account, the sampled signal is thermally stable, and any unwanted thermal transfer is irrelevant.

Equivalent doses were determined for both samples performing 30 replicate measurements. An average value of 28.3 Gy was obtained for sample 4B clinostagnic phaeozem while for sample 3A albic luvisol we have obtained an average value of 12.6 Gy.

In order for ages to be calculated the annual dose rate was computed based on natural radionuclide concentrations. The specific activities of radionuclides of interest have been determined through high resolution gamma spectrometry using an ORTEC hiperpure germanium detector having the following characteristics: active volume of 181 cm^3, 0.878 keV FWHM at 5.9KeV, 1.92 keV FWHM and 34.2 % relative efficiency at 1332.5 keV, calibrated in efficiency using IAEA standards. Radionuclides in the uranium series were assumed to be in secular equilibrium. The cosmic dose rate was estimated based on Prescott and Hutton (1994). Relevant dosimetric information is presented in **Table V.11.**

Table V.11: *Relevant dosimetric information for luminescence age determination of the analysed samples. Quoted errors are only of statistical nature.*

SAMPLE	U-238 (Bq/kg)	Th-232 (Bq/kg)	K-40 (Bq/kg)	Total dose Rate (Gy/ka)
4B (PHZ)	33 ± 1	47 ± 2	604± 18	2.9 ± 0.1
3A (LUV)	29 ± 1	36 ± 1	564± 16	2.6 ± 0.1

The equivalent dose distributions are presented as histograms and radial plots respectively in **figure V.2.4**. Overdispersion can be observed in the data. This is not an experimental artifact or a result of quartz OSL signal intrinsic characteristics, as it was demonstrated that our measurement protocol is robust. From radial plots, it can be seen that the precision in individual equivalent doses obtained is always better than 3%. The observed scatter is probably an effect quartz grain mixing in the soil layer due to pedo or bioturbation. The scatter might be also caused by the low resolution that is achieved when sampling soils for luminescence dating (7 cm in our case).

In order to find the best estimate for the true value of the burial dose measurements have to be repeated using smaller amount of grains and by applying statistical analysis of the dataset. However minimum and maximum ages based on a selected limited number of analysed aliquots are presented in **Table V.12.**

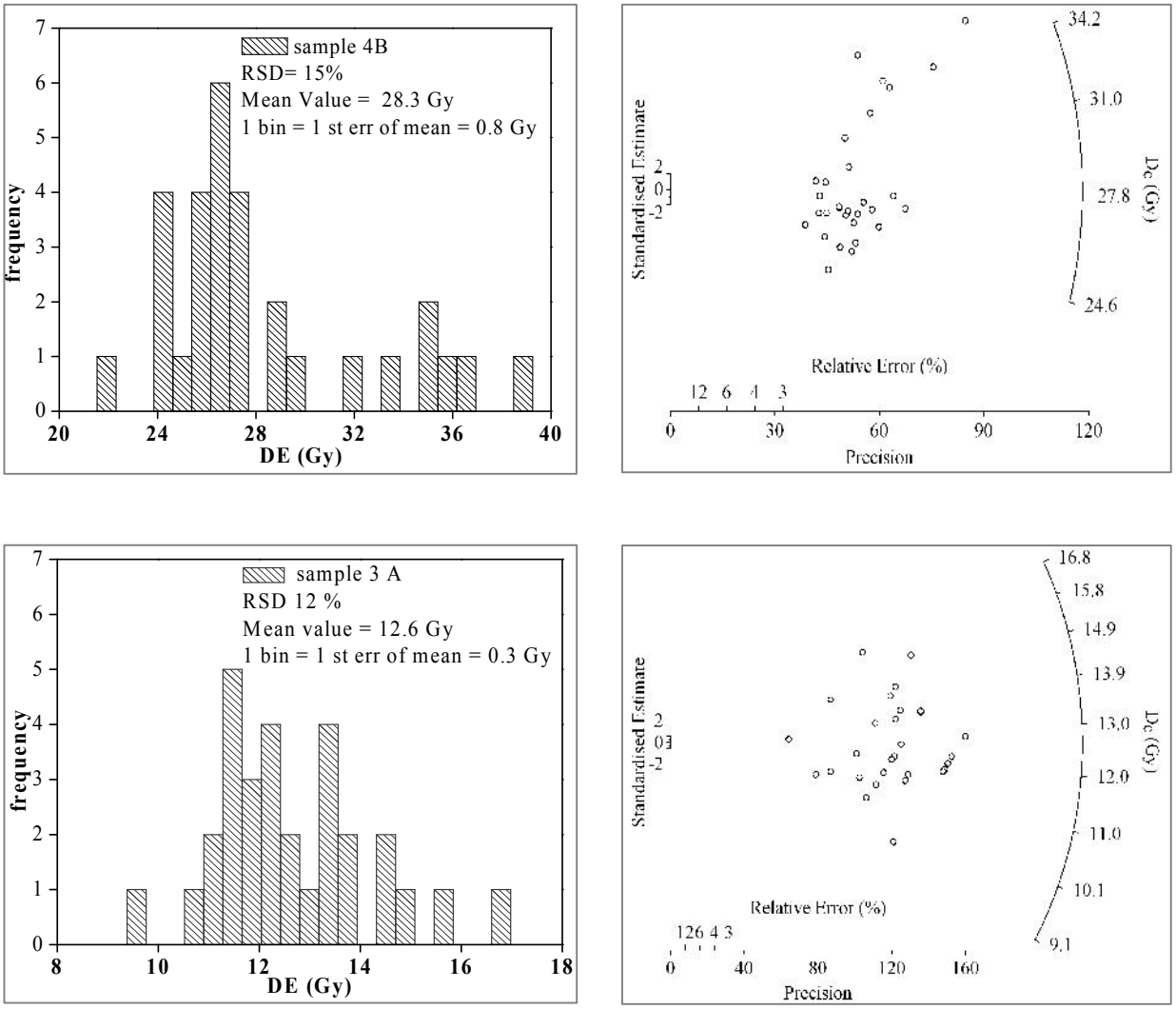

Figure V.41: *Equivalent dose distributions obtained on 30 aliquots of quartz extracted from sample 4B (chernozem) and sample 3A luvisol.*
Overdispersion can be noticed.

Table V.12: *Average, respectively maximum and minimum assumed equivalent doses derived from a selected number of aliquots denoted by n. Uncertainties quoted represent only random errors. For the age calculation a total moisture content of 20 ± 5 % was assumed and a beta attenuation factor of 0.94 ± 0.45. Systematic uncertainties of 5% concerning the calibration of the gamma spectrometer and 3% for the calibration of the radioactive source. The last columns presents the ages and the corresponding overall uncertainties calculated using the system of Aitken (1976).*

SAMPLE	De average (Gy)	De minimum (Gy)	De maximum (Gy)	AVERAGE AGE (ka)	MINIMUM Age (ka)	MAXIMUM Age (ka)
4B (PHZ)	28.8 ± 0.8 (n=30)	24.0 ± 0.8 (n=6)	35.1 ± 0.8 (n=7)	10.9 ± 1.4	9.2 ± 1.2	13.4 ± 1.8
3A (LUV)	12.6 ± 0.3 (n=30)	11.8 ± 0.2 (n=20)	14.4 ± 0.3 (n=10)	4.3 ± 0.6	4.0 ± 0.5	4.9 ± 0.5

V.2.3. Conclusion

The ages obtained can be regarded as evidence that the dark soil cover was a stable feature in the Subboreal in most of the area of Transylvania and their replacement with Luvisols reflects a climatic transition from a drier climate (Subboreal) that have favored the extension of the Boreal forests and steppic grasslands to a wetter milder one (the Subatlantic) that favored the expansion of the nemoral and subtropical forests in the Holocene. Thus the paleo-pedological structures from Transylvania and presumably from other areas of Romania which consists of a fossil mollic horizon of a Phaeozem covered by an albic horizon of an actual Luvisol can be considered as a climatic marker which resumes the climatic changes which are associated with the Subboreal-Subatlantic transition which began around 4ka BP.

SUMMARY AND CONCLUSIONS

Luminescence phenomena encompass a very wide range of processes. For the purpose of retrospective dosimetry only optically stimulated luminescence (OSL) and thermoluminescence (TL) processes are of interest. OSL and TL is the luminescence emitted from an irradiated insulator or semiconductor during exposure to light or respectively heat; thus OSL and TL are stimulated processes. The luminescence signal emitted is dependent on the irradiation history of the sample.

Although the processes giving rise to luminescence phenomena in natural wide-gap crystals such as quartz and feldspars are complicated and not fully understood this phenomenon can be exploited for dating.

In the past ten years luminescence dating has undergone extreme technological and methodological advances and at the moment is characterized by a degree of quality control seldom seen with other dating techniques. Despite this however, modern luminescence dating techniques have not been applied in a Romanian laboratory up to now. In this thesis quality control of procedures concerning sample preparation, paleodose and annual dose estimation in Luminescence Dating Laboratory, Environmental Radioactivity and Nuclear Dating Centre of Babeş-Boyai University of Cluj Napoca, Romania have been presented. State-of-the-art luminescence dating techniques have applied in key applications.

For equivalent dose measurement, the extraction of quartz and polymineral fine grains from samples using conventional luminescence dating sample preparation techniques was implemented in our laboratory. The purity of OSL signals from the extracted quartz grains was tested and confirmed by the absence of IR signals following irradiation, through the measurement of IR depletion ratios, by recording TL glow curves, and by performing pulsed OSL measurements. The dose rate delivered on different substrates and for different grains sizes by the ^{90}Sr-Y beta source mounted on the Risø TL/OSL DA-20 luminescence reader was determined by making use of gamma dosed calibration quartz supplied by Risø and equivalent dose measurement procedures were validated through an intercomparison exercise with Gent Luminescence Dating Laboratory, Belgium.

Annual dose was determined based on radionuclide concentrations determined in our laboratory by means of high resolution gamma ray spectrometry using an ORTEC hiperpure germanium detector (active volume of 181 cm^3, 0.878 keV FWHM at 5.9KeV, 1.92 keV FWHM and 34.2 % relative efficiency at 1332.5 keV). The system was calibrated

in energy using an europium source while the efficiency calibration was performed using a Monte Carlo routine which was validated using IAEA standards. A method for determining ^{226}Ra concentrations directly by making use of the interfered line at 186.2keV was implemented. ^{234}Th, ^{214}Pb, ^{214}Bi, ^{214}Bi, ^{210}Pb, ^{228}Ac, ^{208}Tl, and ^{40}K can be routinely measured in environmental samples. The procedures have been validated through an intercomparison exercise with two other different methods - alpha spectrometry (The Radiochemistry Laboratory from Veszprem), respectively instrumental neutron activation (Institute for Nuclear Research, Pitesti, Romania), and with Gent Luminescence Dating Laboratory where the same techniques are being used (high resolution gamma spectrometry with relative efficiency calibration).

Luminescence dating was applied to four pottery fragments excavated at Lumea Nouă (Alba Iulia, Romania). The aim of this study was to apply new approaches in optical dating to improve the chronological framework for the site. To this purpose, the SAR protocol was applied to both blue (OSL) and infrared stimulated luminescence (IRSL) signals from coarse (90-125 μm) quartz and polymineral fine (4-11 μm) grains, respectively. For the sake of comparison, a more conventional approach, which MAAD protocol and thermoluminescence TL signals from polymineral fine grains, was applied as well. The presence of anomalous fading in the 410 nm IRSL emission as well as blue TL emission indicated that our IRSL and TL ages would underestimate the true ages. To correct the SAR-IRSL results for fading, we applied the correction procedure proposed by Huntley and Lamothe. No correction was applied to the TL results, as it is not valid to correct the bulk signal originating from an undifferentiated fine-grained mineral mixture using the fading observed from only part of this mixture. It was concluded that **c**ompared to the TL method, the IRSL and OSL approaches are based on a more robust dating methodology. As SAR-OSL dating of quartz yielded the most precise age estimates, this was considered to be the technique of choice. The average of the four quartz SAR-OSL ages presented above placed the transition from Foeni to Petreşti culture at Lumea Nouă site around 6.2 ± 0.5 ka an extremely plausible age taking into consideration the archaeological information. Further investigations are needed for establishing a complete chronological framework for the ancient cultural development at Lumea Nouă. Nevertheless our study is a clear illustration of how luminescence dating, especially by the use of state-of-the-art techniques can contribute to this purpose.

The Romanian loess-palaeosol sequences preserve a significant terrestrial record of Quaternary climate change during at least five Glacial / Interglacial cycles. We have reported the first high resolution optically stimulated luminescence (OSL) dating study for the loess sequence near Mircea Vodă (Dobrogea, SE Romania). The study focussed on loess from the last four glacial periods and used silt-sized (4-11μm) quartz as dosimeter.
An internally consistent set of optical ages was obtained and the optical ages have been compared with a magnetic time-depth model ellaborated by Conf. Dr. Cristian Panaiotu

and Conf. Dr. Cristina Panaiotu (University of Bucharest) based on magnetic susceptibility measurements. Based on luminescence ages, evidence was presented for a varying loess accumulation rate during the Last Glacial. The optical ages indicated that this unit did not accumulate at a constant rate, with loess being deposited at a significantly lower rate during the past ~50 ka. This illustrates the limitations of proxy records (such as magnetic susceptibility) to interpret and derive a chronology for these deposits.

While it could be confirmed that the uppermost palaeosol (usually denoted by S1 in stratigraphic nomenclature) formed during the last Interglacial, comparison with independent age control (pedostratigraphy and a newly developed palaeomagnetic time-depth model) also indicated that the dating procedure underestimates the true burial age from the penultimate glacial period onwards. The SAR-OSL ages obtained for the three samples taken below the S1 soil were interpreted as age underestimates, with the degree of age underestimation increasing with depth. Interestingly, the luminescence characteristics did not indicate such behavior: the signal continues to grow to high doses, the laboratory measurement procedure is accurate, and the ages increase with depth.
We concluded that optical dating of fine-grained quartz can be used to establish a reliable chronology for Romanian loess up to ~70 ka. This age values correspond to equivalent doses of ~ 200Gy. Up to this value an exponential function and an exponential plus a linear term function give the same goodness of fit to experimental data. At least for our samples, the results obtained from the high dose linear region of the growth curve do not appear to be accurate. The procedure underestimates the true burial age when applied to loess that was deposited before the last climatic cycle; further research is necessary to establish what causes the age underestimation. Our results illustrated that an apparently reliable OSL laboratory measurement procedure not necessarily guarantees an accurate determination of the true burial.

In recent years, quartz has become the dosimeter of choice and modern optical dating technology is increasingly applied to various grain-size fractions of quartz that have been extracted from loess. While it seems logic to assume that for a windblown material (such as loess) grains from several fractions are suitable for optical dating, this has not been explicitly demonstrated. At least to our knowledge, no studies are available that compare the luminescence characteristics and age of quartz grains of different granulometric fractions extracted from loess. We have conducted such a study.

Our results indicate luminescence dating of loess may be more complicated. For samples collected from the loess sequence near Mircea Vodă (SE Romania), it was observed that the optical ages obtained on silt-sandy grains (63-90 μm) are in between ~20 and 70% higher than those obtained on the fine silt fraction (4-11 μm). Optical ages obtained on several samples of different ages using the coarse silt fraction (35-50 μm) fraction are in agreement with the ages obtained on the silt sandy fraction. The apparent controversy is of relevance to both past and future studies worldwide.

It was observed that the equivalent doses obtained for sand -sized quartz are always higher than the De's in the silt-sized quartz, with the relative difference being more pronounced in the case of the younger samples. Not even considering a nil value for the alpha efficiency would overcome the age discrepancy. As such, we conducted our investigation for determining the cause for the observed age controversy focusing on luminescence emissions.

Based on LM-OSL analysis it was concluded that all samples analysed have signals dominated by the fast component and thus are suitable for equivalent dose measurement using the SAR protocol. It was also shown that the signal used for optical dating is thermally stable. The OSL signals from all fractions behaved well in the SAR protocol (in terms of recycling, recuperation and dose recovery), indicating that the SAR protocol should be suitable for determining the equivalent dose in both. As such, there would be no cause to doubt the data generated by analysis of a single grain-size fraction of quartz (at least from a pure laboratory-methodological perspective).

Coarser fractions show overdispersion in equivalent dose distributions. Partial bleaching can be considered as a possible cause as grains size distributions in the investigated loess are bi-modal or even three-modal distributions, reflecting multiple sources of the clastic material. The coarse silt and fine sand material could have proximal source, while the silt could have a distant source. However, partial bleaching could not account alone for the age discrepancy observed in the case of older samples where residual doses of the order of at least tens of Gy would be required. Thus, we concluded that at least in the case of older samples a second mechanism should interfere.

By constructing dose response curves to high dose (up to ~700 Gy) a very similar pattern of growth was observed for samples of different ages in the case of both fractions. It was also observed that the growth can be best represented by a function of the form of a single saturating exponential plus a linear term. Growth curve characteristics of the two fractions investigated were found to be very different though, with coarse grains saturating at much lower doses. By extending the dose response investigations up to 10 kGy it was concluded that the linear term is the early expression of a second saturating exponential function. It is interesting to note that the values obtained in this study for characteristic doses of fine-grained (4-11 μm) quartz (D_{01}=211 Gy; D_{02}=2376 Gy) are in good agreement with values quoted by Lowick et al. (2010) (D_{01} = 128 Gy, D_{02} = 1680 Gy), while the saturation characteristics of coarse-grained quartz D_{01}= 55 Gy, respectively D_{02} = 576 Gy resemble data previously reported on coarse material by Murray et al. (2007) (D_{01} = 44 Gy and D_{02} = 450 Gy for 180-250 μm quartz) and by Pawley et al. (2010) (D_{01} = 51 Gy, D_{02} = 320 Gy for 125-180 μm quartz), respectively.

It should be noted that the existence of second component in dose response curves constructed at high doses has been identified in other studies as well. However, the intrinsic mechanism of this behavior is far from being understood and the reliability of

using the high dose part of the growth curve has yet to be investigated. Very little is known empirically on the possible dose rate dependence of OSL while different simulation studies infer that this kind of effects is prone to occur. For our investigated samples the possibility of existence of dose and/ or dose rate effects could not be excluded, and a speculative mechanism was proposed. We infer that the fundamental requirement of luminescence dating that the natural (low dose rate) and artificial irradiation (very high dose rate) are equivalent in terms of luminescence produced might not be fulfilled for high doses, at least in the case of certain samples.

The results obtained show that luminescence dating of loess is far less straightforward than generally is accepted and thus challenge earth-scientific as well as luminescence dating communities. Further work should refine our knowledge of the origin of luminescence signals in quartz. The upper dating limit of quartz OSL signals, particularly when displaying a different than a single saturating exponential dose response is an issue that remains to be addressed.

Optical dating of old sediments remains a difficult task.

REFERENCES

1. Adamiec G. and Aitken M. (**1998**)
Dose-rate conversion factors: update.
Ancient TL ***16***, 37-50.

2. Aitken M.J., Tite M.S., Reid J. (**1964**)
Termoluminescent dating of ancient ceramics.
Nature ***202***, 1032-1033.

3. Aitken M.J., Zimmerman D. W., Fleming S.J. (**1968**)
Termoluminescent dating of ancient pottery.
Nature ***219***, 442-444.

4. Aitken M.J. and Alldred J.C. (**1972**)
The assessment of error limits in thermoluminescent dating.
Archaeometry ***14***, 257-267.

5. Aitken M.J. (**1976**)
Thermoluminescent age evaluation and assessment of error limits: revised system.
Archaeometry ***18***, 233-238.

6. Aitken M.J. (**1985**)
Thermoluminescent Dating.
Academic Press, London, 359p. ISBN: 0-12-046380-6.

7. Aitken M. J. and Xie J. (**1990**)
Moisture correction for annual gamma dose.
Ancient TL ***8***, 6-9.

8. Aitken M.J. (**1998**)
An introduction to optical dating. The dating of Quaternary Sediments by the use of Photon-Stimulated Luminescence.
Oxford University Press, Oxford, 267p, ISBN: 0-19-854092.

9. Aitken M.J. (**1999**)
Archaeological dating using physical phenomena.
Rep. Prog. Phys. ***62***, 1333-1376.

10. Ankjaergaard C., Jain M., Kalchgruber R., Lapp T., Klein D., McKeever S.W.S., Murray A.S., Morthekai P. (**2009**)
Further investigations into pulsed optically stimulated luminescence from feldspars using blue and green light.
Radiation Measurements ***44***, 576-581.

11. Armitage S.J., Bailey R.M. (**2005**)
The measured dependence of laboratory beta dose rates on sample grain size.
Radiation Measuremets ***39***, 123-127.

12. Auclair M., Lamonthe M. and Huot S. (**2003**)
Measurement of anomalous fading for feldspars IRSL using SAR.
Radiation Measurements ***37***, 487-492.

13. Bădărau Al. S. (**2005**)
Landscape Transformation in the Transylvanian Basin, with special focus upon the biogeographical aspects.
Phd. Thesis, Babeş-Bolyai University Cluj Napoca .

14. Bahadur H., Tissoux H., Usami T., Toyoda S. (**2008**)
Radiation effects in natural quartz crystals.
Journal of Materials Science: Mater Electron ***19***, 709-713.

15. Bailey R.M., Smith B.W., Rhodes E.J. (**1997**)
Partial bleaching and the decay form characteristics of quartz OSL.
Radiation Measurements ***27***, 123-126.

16. Bailey R.M. (**2001**)
Towards a general kinetic model for optically and thermally stimulated luminescence of quartz.
Radiation Measurements ***33***, 17-45.

17. Bailey R.M. (**2003**)
The use of measurement-time dependent single-aliquot equivalent dose estimates from quartz in the identification of incomplete resetting.
Radiation Measurements ***37***, 673-686.

18. Bailey R.M. (**2004**)
Paper I- simulation of dose absorption in quartz over geological timescales and its implications for the precision and accuracy of optical dating.
Radiation Measurements ***38***, 299-310.

19. Bailey R.M., Armitage S.J., Stokes S. (**2005**)
An investigation of pulsed irradiation regeneration of quartz OSL and its implications for the precision and accuracy of optical dating. (Paper II)
Radiation Measurements 39, 347-359.

20. Bailey R.M. Arnold L.J. (**2006**)
Statistical modeling of single grain quartz De distributions and an assessment of procedures for estimating burial dose.
Quaternary Science Reviews ***25***, 2475-2502.

21. Bailiff I.K., and Poolton, N.R.J. (**1991**)
Studies of charge transfer mechanisms in feldspars.
Nuclear tracks and radiation measurements 18, 111-118.

22. Bailiff I.K. (**1999**)
The Development of Retrospective Luminescence Dosimetry for Dose Reconstruction in Areas Downwind of Chernobyl.
Radiation Protection Dosimetry ***84 (1-4)***, 411-419.

23. Bailiff I.K. (**2000**)
Characteristics of time resolved luminescence in quartz.
Radiation Measurements ***32***, 401-405.

24. Bailiff I.K., Bøtter-Jensen L., Correcher V., Delgado A., Göksu H.Y., Jungner H., Petrov A.S. (**2000**)
Absorbed dose evaluations in retrospective dosimetry: methodological developments using quartz.
Radiation Measurements, ***32***, 609-613.

25. Bailiff I K., Stepanenko V F., Göksu H Y., Jungner H., Balmukhanov S B., Balmukhanov T. S., Khamidova L. G., Kisilev V. I., Kolyado I. B., Kolizshenkov T.V., Shoikhet Y. N., Tsyb A F. (**2004**)
The Application of Retrospective Luminescence Dosimetry in Areas Affected By Fallout from the Semipalatinsk Nuclear Test Site: An Evaluation of Potential.
Health Physics, ***87 (6)***, 625-641

26. Balescu S., Lamonthe M., Mercier N., Huot S., Balteanu D., Billard A., Hus J. (**2003**)
Luminescence chronology of Pleistocene loess deposits from Romania: testing methods of age correction for anomalous fading in alkali feldspars.
Quaternary Science Reviews ***22***, 967-973.

27. Banerjee D., Bøtter-Jensen L., Murray A.S. (**1999**)
Retrospective Dosimetry: Preliminary Use of the Single Aliquot Regeneration (SAR) Protocol for the Measurement of Quartz Dose in Young House Bricks.
Radiation Protection Dosimetry ***84 (1-4),*** 421-426.

28. Banerjee D., Murray A.S., Bøtter-Jensen L. and Lang A. (**2001**)
Equivalent dose estimations using a single aliquot of polymineral fine grains.
Radiation Measurements ***33***, 73-94.

29. Bateman, M. et al. (**2007**)
Detecting post depositional sediment disturbance in sandy deposits using optical luminescence. *Quaternary Geochronology* **2**, 57-64.

30. Bărbos D. Paunoiu C. (**2004**)
Internal Report 6396/2004.
Institute for Nuclear Research, Pitesti.

31. Begy R., Cosma C., **Timar A.**, Fulea D. (**2007**)
A study on Cs-137 contamination of soils from certain regions of Transylvania
Environment and Progress ***9***, 73-76.

32. Begy R.C., Cosma C., **Timar A.,** Fulea D. (**2009a**)
The Determination of Absolute Intensity of ^{234m}Pa's 1001 keV Gamma Emission Using Monte Carlo Simulation.
Journal of Radiation Research ***50***, 277-279.

33. Begy R., Cosma C., **Timar A**., (**2009b**)
Recent changes in Red Lake (Romania) sedimentation rate determined from depth profiles of ^{210}Pb and ^{137}Cs radioisotopes"
Journal of Environmental Radioactivity ***100***, 644-648.

34. Benea V., Vandenberge D., **Timar A**., Van den Haute P., Cosma C., Gligor M., Florescu C. (**2007**)
Luminescent dating of Neolithic ceramics from Lumea Nouă, Romania.
Geochronometria ***28***, 9-16.

35. Blair, M.V., Yukihara, E.G., McKeever, S.W.S. (**2005**)
Experiences with single aliquot OSL procedures using coarse-grain feldspars.
Radiation Measurements ***39***, 361-374.

36. Bos A.J.J., Wallinga J. (**2009a**)
Analysis of quartz OSL decay curve by differentiation .
Radiation Measurements ***44***, 588-593.

37. Bos A.J.J., Wallinga J. (**2009b**)
Optically stimulated luminescence signals under various stimulation modes assuming first-order kinetics.
Physical Review B ***79***, 195118-1-11.

38. Boyle R. (**1664**)
Experiments and Considerations upon Colours and Observations on a Diamondthat Shines in the Dark.
Henry Heringham, London.

39. Bøtter-Jensen L., Duller G.A.T. Poolton N.R.J. (**1994**)
Excitation and emission spectrometry of stimulated luminescence from quartz and feldspars.
Radiation Measurements ***23***, 613-616.

40. Bøtter-Jensen L. (**1997**)
Luminescent techniques: instrumentation and methods.
Radiation Measurements ***27***, 749-768.

41. Bøtter-Jensen, L., Murray A.S., (**1999**)
Developments in optically stimulated luminescence techniques for dating and retrospective dosimetry.
Radiation Protection Dosimetry ***84***, 307-316.

42. Bøtter-Jensen, L., Bulur E., Duller G.A.T., Murray A.S., (**2000**)
Advances in luminescence instrument systems.
Radiation Measurements ***32***, 523-528.

43. Bøtter-Jensen, L., Bulur E., Murray A.S., Poolton N.R.J. (**2002**)
Enhancements in luminescence instrument techniques.
Radiation Protection Dosimetry ***101***, 119-124.

44. Bøtter-Jensen L, McKeever S.W.S, Wintle A. G. (**2003a**)
Optically Stimulated Luminescence Dosimetry
Elsevier, 355 p, ISBN 0 444 50684 5

45. Bøtter-Jensen L., Andersen C.E., Duller G.A.T and Murray A.S. (**2003b**)
Developments in irradiation, stimulation and observation facilities in luminescence measurements.
Radiation Measurements ***37***, 535-541.

46. Buggle, B., Hambach, U., Glaser, B., Gerasimenko, N., Marković, S., Glaser, I., Zöller, L., (**2008a**).
Stratigraphy and spatial and temporal paleoclimatic trends in Southeastern/Eastern European loess paleosol sequences.
Quaternary International ***196***, 1-2, 86-106.

47. Buggle, B., Glaser, B., Zöller, L., Hambach, U., Marković, S., Glaser, I., Gerasimenko, N., (**2008b**).
Geochemical characterization and origin of Southeastern and Eastern European loesses (Serbia, Romania, Ukraine).
Quaternary Science Reviews ***27***, 1050-1075.

48. Bulur E., Bøtter-Jensen L. and Murray A.S. (**2001**)
Optically stimulated luminescence from quartz measured using the linear modulation technique.
Radiation Measurements ***32***, 407-411.

49. Buylaert J.P., Vandenberge D., Murray A.S., Huot S., De Corte F. and Van den Haute P. (**2007**)
Luminescence dating of old (>70ka) Chinese loess: a comparison of single aliquot OSL and IRSL techniques.
Quaternary Geochronology **2**, 9-14.

50. Buylaert, J.P., Murray, A.S., Vandenberghe, D., Vried, M., De Corte, F., Van den haute, P., (**2008**)
Optical dating of Chinese loess using sand-sized quartz: Establishing a time frame for Late Pleistocene climate changes in the western part of the Chinese Loess Plateau.
Quaternary Geochronology ***3***, 99-113.

51. Buylaert J.-P., Murray A.S., Thomsen K.J., Jain M. (**2009**)
Testing the potential of an elevated temperature IRSL signal from K-feldspar.
Radiation Measurements ***44***, 560-565.

52. Chen R., Leung P.L. (**2001a**)
Dose dependence and dose rate dependence of the optically stimulated luminescence signal .
Journal of Applied Physics ***89****, 1*, 259-263.

53. Chen R., Leung P.L. (**2001b**)
Nonlinear dose dependence and dose rate dependence of optically stimulated luminescence and thermoluminescence.
Radiation Measurements ***33***, 475-481.

54. Chen S., Liu X., Zhang C., Tang Q. (**2009**)
The Monte Carlo simulation of the absorbed dose in quartz.
Radiation Measuremets ***44***, 626-628.

55. Chithambo, M.L., Galloway R.B., (**2000a**)
A pulsed light-emmiting diode system for stimulation of luminescence.
Meas. Sci.Technol ***11***, 418-424.

56. Chithambo, M.L., Galloway R.B., (**2000b**)
Temperature dependence of luminescence time-resolved spectra from quartz.
Radiation Measurements ***32***, 621-626.

57. Chithambo, M.L., Galloway R.B., (**2001**)
On the slow component of luminescence stimulated from quartz by pulsed blue light emitting diodes.
Nucl. Instr. Methods B. ***183***, 358-368.

58. Chithambo, M.L. (**2003**)
Dependence of the thermal influence on luminescence lifetimes from quartz on the duration of optical stimulation.
Radiation Measurements ***37***, 167-175.

59. Choi J.H., Murray A.S., Cheong C.S., Hong D.G., Chang H.W. (**2003**)
The resolution of stratigrafic inconsistency in the luminescence ages of marine terraces sedimets from Korea.
Quaternary science Reviews **22**,1201-1206.

60. Choi J.H., Duller G.A.T., Wintle A.G. (**2006**)
Analysis of quartz LM-OSL curves.
Ancient TL ***24, I***, 9-20.

61. Conea, A. (**1969**)
Profils de loess en Roumanie.
La stratigraphie des loess d'Europe. In: Fink, J. (Ed.), Bulletin de l'Association française pour l'étude du Quaternaire,.
Suppl. INQUA, 127–134.

62. Cosma C., Benea V., **Timar A.,** Barbos D., Paunoiu C. (**2006**)
Preliminary dating results on ancient ceramics from Romania by means of thermoluminescence.
Radiation Measurements ***41***, 987-990.

63. Cosma C., Petrescu I, Meilescu C., **Timar A.** (**2007**)
Properties of lignite from Oltenia and their influence on the environment
Studia Universitatis Babes-Bolyai, Ambientum, ***I, 1—2***, 65-75.

64. Cosma C. **Timar A.,** Benea V., Pop I., Jurcut T., Ciorba D. (**2008a**)
Using natural luminescent materials and highly sensitive sintered dosimeters MCP-N (LiF: Mg, Cu, P) in radiation dosimetry.
Journal of optoelectronics and advanced materials ***vol. 10, nr 3,*** 573-577.

65. Cosma C., **Timar A.**, Benea V., Somlai J. (**2008b**)
Applications of nuclear dating methods in archaeology, geology and environmental science" *ECOTERRA****, nr 19****, an V*, p.: 28-30.

66. Cosma C., Benea V., **Timar A.,** Gligor M., Varvara S. (**2008c**)
Datarea prin luminescenta stimulate termic (TL) si optic (OSL). Aplicatii in arheologie.
ACTA MVSEI APVLENSIS, Apulum, ***XLV***, 579-598

67. Cosma, C., **Timar, A.,** Benea, V., Begy, R., (**2008d**)
Nuclear and Seminuclear Dating Methods: Application in Archeology, Geology and Environmental Science. *Terrestrial radionuclides in the Environment*, Environmental Conferences Veszprem, ISBN 978 963 9696 488, pp. 23-35.

68. Cosma C., **Timar A.,** (**2008e**)
Testarea potentialului metodelor luminiscente in datarea unei sectiuni de loess din Dobrogea, *MENER, Universitatea Politehnica - Bucuresti*, 643-650

69. Cosma C., Ciorba D., **Timar A.,** Szacsvai K., Dinu A. (**2009a**)
Radon exposure and lung cancer risk in Romania.
Journal of Environmental Protection and Ecology, ***nr 1-2009,*** 94-104.

70. Cosma C., Petrescu I., Meilescu C., **Timar A.** (**2009b**)
Studies on the radioactivity of lignite from the area between the Danube and Motru (South-West Romania) and the incidence on the environment.
Journal of Environmental Protection and Ecology, ***nr 1-2009***, 192-201.

71. Cosma C., **Timar A.,** Benea V., Pop I., Moldovan M. (**2009c**)
Carbon Molecular Sieve for Radon and Thoron Monitoring"
Romanian Journal of Physics, ***nr. 3-4, vol. 54***, 401-405.

72. Daniels F., Boyd C.A., Saunders D. F. (**1953**)
Thermoluminescence as a research tool.
Science ***117***, 343-349.

73. De Corte F, (**1987**)
The k_0 standardization method: A move to the optimization of neutron activation analysis.
Rijksuniversiteit Report, Gent.

74. De Corte F., Umans H., Vandenberghe D., De Wispelaere A. and Van den Haute P. (**2005**)
Direct gamma-spectrometric measurement of the Ra-226 186.2 keV line for detecting U-238/Ra-226 disequilibrium in determining the environmental dose rate for the luminescence dating of sediments.
Applied Radiation and Isotopes ***63***, 589-598.

75. Denby, P.M., Bøtter-Jensen L., Murray A.S., Thomsen K.J., Moska P. (**2006**)
Application of pulsed OSL to the separation of the luminescence components from a mixet quartz/ feldspar sample.
Radiation Measurements ***41***, 774-779.

76. Draşovean F (**2005**)
Zona thessalo-macedoneană şi Dunărea mijlocie la sfârşitul mileniului al VI-lea şi la începutul mileniului al V-lea A.CHR. (Thessalo Macedonian and Danube region at the end of sixth millenium, beginning of fifth millemium BC).
Apulum ***XLII***, 12-26 (in Romanian).

77. Duller G.A.T. (**1991**)
Equivalent dose determination using single aliquots.
Nuclear Tracks and Radiation Measurements ***18***, 371-378.

78. Duller G.A.T. (**1997**)
Behavioral studies of stimulated luminescence from feldspars.
Radiation Measurements ***27***, 663-694.

79. Duller G.A.T., Bøtter-Jensen L., Murray A.S. (**2000**)
Optical dating of single sand-sized grains of quartz: sources of variability.
Radiation Measurements ***32***, 453-457.

80. Duller, G.A.T. (**2003**)
Distinguishing quartz and feldspar in single grain luminescence measurements.
Radiation Measurements ***37***, 161-165.

81. Duller G.A.T. (**2004**)
Luminescence dating of Quaternary sediments: recent advances.
Journal of Quaternary Science ***19***, 183-192.

82. Fattahi M., Stokes S. (**2004**)
Absorbed dose evaluation in feldspar using a single-aliquot regenerative-dose (SAR) infrared stimulated red luminescence protocol.
Radiation Measurements ***38***, 127-134.

83. Frechen M., Schweitzer U. and Zander A (**1996**)
Improvements in sample preparation for fine grain technique.
Ancient TL ***14***, 15-17.

84. Frechen M., Dodonov A.E., (**1998**)
Loess chronology of the Middle and Upper Pleistocence in Tadjikistan.
Geologische Rundschau ***87***, 2-20.

85. Frechen M. (**1999**)
Luminescence dating of loessic sediments from the Loess plateau, China.
International Journal of Earth Sciences ***87, 4,*** 675-684.

86. Frechen, M., Oches, E.A., Kohfeld, K.E., (**2003**)
Loess in Europe – mass accumulation rates during the Last Glacial Period.
Quaternary Science Reviews ***22***, 1835-1857.

87. Forman S. (**1991**)
Late Pleistocene Chronology of loess Deposition near Louchuan, China.
Quaternary Research ***36***, 19-28.

88. Fuchs M. and Lang A. (**2001**)
OSL dating of coarse-grain fluvial quartz using single-aliquot protocols on sediments from NE Peloponnese, Greece.
Quaternary Science Reviews ***20***, 783-787.

89. Fulea D. Cosma C. (**2009**)
Monte Carlo sampling for gamma and beta detectors using a general purpose PC program.
Radiation Measurements ***44***, 278–282.

90. Galbraith, R.F. (**1988**)
Graphical display of estimates having differing standard errors.
Technometrics ***30***, 271–281.

91. Galbraith R.F. (**1990**)
The radial plot: graphical assessment of spread in ages.
Nuclear Tracks and Radiation Measurements ***17***, 207-214.

92. Garcia-Talavera M, Laedermann J.P., Decombas M., Daza M.J., Quintana B. (**2001**)
Coincidence summing corrections for the natural decay series in γ ray spectrometry.
Journal of Radiation and Isotopes ***54***, 769-776.

93. Gligor M. (**2006**)
Considerații privitoare la neoliticul târziu/eneoliticul timpuriu din S-V Transilvaniei. Materiale
ceramice de la Alba Iulia-Lumea Nouă. (Considerations regarding late Neolithic/ Early Aeneolithic in S-V of Transylvania. Ceramic materials discovered at Alba Iulia- Lumea Noua). *Apulum* ***XLIII (1)***, 9-34 (in Romanian).

94. Göksu, H. Y.; Degteva, M. O.; Bougrov, G.; Meckbach, R.; Haskell, E. H.; Bailiff, I. K.; Bøtter-Jensen, L.; Jungner, H.; Jacob, P. (**2002**)
First International Intercomparison of Luminescence Techniques Using Samples From the Techa River Valley.
Health Physics, ***82***, 94-101

95. Grogler N, Houtermans FG and Stauffer H. (**1960**).
Ueber die datierung von Keramik und Ziegel durch Thermolumineszenz.
Helvetica Physica Acta ***33***, 595-596.

96. Harrison S., Kohfeld K., Roelandt C., Claquin T. (**2001**)
The role of dust in climate changes today, at the last glacial maximum and in the future.
Earth Science Reviews ***54***, 43-48.

97. Hong DG, Yi SB, Galloway RB and Tsuboi T. (**2001**).
Optical dating of archaeological samples using a single aliquot of quartz stimulated by blue light.
Journal of Radioanalytical and Nuclear Chemistry ***247***, 179-184.

98. Hossain S.M., De Corte F., Vandenberge D., Van den Haute P. (**2002**)
A comparison of methods for annual radiation dose determination in the luminescence dating of loess sediments.
Nuclear Instruments and Methods in Physics Research A ***490***, 598-613.

99. Hossain S.M. (**2003**)
A critical comparison and evaluation of methods for the annual radiation dose determination in the luminescence dating of sediments.
Ph.D. thesis, Gent University.

100. Huntley D.J., Godfrey-Smith D.I. and Thewalt M.L.W. (**1985**)
Optical dating of sediments.
*Nature **313***, 105-107.

101. Huntley D.J., Godfrey-Smith, D.I. and Haskell, E.H. (**1991**)
Light –induced emission spectra from some quartz and feldspars.
*Nuclear tracks and radiation Measurements **18***, 127-131.

102. Huntley D. J. (**1997**)
A proposal for dealing with anomalous fading.
*Ancient TL **15***, 28-29.

103. Huntley D.J. and Lamothe M. (**2001**)
Ubiquity of anomalous fading in K-feldspars and the measurement and correction for it in optical dating.
*Canadian Journal of Earth Science **38***, 1093-1106.

104. Huntley D.J., Olav B. Lian (**2006**)
Some observations on tunneling of trapped electrons in feldspars and their implications for optical dating.
*Quaternary Science Reviews **25, 19-20,*** 2503-2512.

105. Huot S. and Lamonthe M. (**2003**)
Variability of infrared stimulated luminescence properties from fractured feldspar grains.
*Radiation Measurements **37***, 499-503.

106. Hütt G., Jaek I. and Tchonka J. (**1988**)
Optical dating: K-feldspars optical response stimulation spectra.
*Quaternary Science Reviews **7***, 381-385.

107. Hütt G. and Jaek I (**2001**)
Advances in the luminescence dating: the Optically Stimulated Luminescence based procedures and their physical background.
*Proc. Estonian Acad. Sci. Geol. **50***, 214-232.

108. Istratov A.A., Vyvenko O.F. (**1999**)
Exponential analysis in physical phenomena.
*Review of scientific instruments, **vol 70, no 2,*** 1233-1257.

109. Jain M. and Singhvi A. (**2001**)
Limits of depletion of blue-green light stimulated luminescence in feldspars: implications for quartz dating.
*Radiation Measurements **24***, 883-892.

110. Jain M., Murray A.S., Bøtter-Jensen L. (**2003**)
Characterization of blue-light stimulated luminescence components in different quartz samples: implications for dose measurement.
Radiation Measurements ***37***, 441-449.

111. Jain M., Murray A.S., Bøtter-Jensen L. (**2004**)
Optically stimulated luminescence dating: How significant is incomplete light exposure in fluvial environments?
Quaternaire ***15 (1-2),*** 143-157.

112. Jain M., Murray A.S., Bøtter-Jensen L, Wintle A. G. (**2005**)
A single –aliquot regenerative-dose method based on IR (1.49 eV) bleaching of the fast OSL component in quartz.
Radiation measurements ***39***, 309-318.

113. Karamysheva, Z.J., Khramtsov, V.N., (**1995**)
The steppes of Mongolia.
Braun-Blanquetia ***17***, 5-79.

114. Kennedy GC and Knopff L. (**1960**)
Dating by thermoluminescence.
Archaeology ***13***, 147-148.

115. Kiyak N.G., Polymeris G.S., Kitis G. (**2007**)
Component resolved OSL dose response and sensitization of various sedimentary quartz samples.
Radiation Measuremets ***42***,144-155.

116. Knoll G.F. (**2000**)
Radiation Detection and Measurement (800pp, third edition)
John Wiley and sons inc. ISBN: 0-471-07338-6.

117. Koster E.A. (**2005**)
Recent advances in luminescence dating of Late Pleistocene (cold-climate) aeolian sand and loess deposits in Western Europe.
Permafrost and Periglacial Processes ***16, 1,*** 131-143.

118. Kovacheva M, (**1997**)
Archaeomagnetic database from Bulgaria: the last 8000years.
Physics of the Earth and Planetary interiors ***102***, 145-151.

119. Krbetschek M.R. and Reiser U. (**1995**)
Luminescence spectra of alkali feldspars and plagioclase.
Radiation Measurements ***24***, 473-477.

120. Krbetschek M.R., Götze J., Dietrich A. and Trautman T. (**1997**)
Spectral information for minerals relevant to luminescent dating.
Radiation Measurements ***27***, 695-748.

121. Labau, V., Gaspar, E., Paunica, T. (**1996**)
Speleothems dating using the thermoluminescence method.
Theoret. Appl. Karstology ***9***, 29–34.

122. Lai ZP., Stokes S., Bailey R., Fattahi M., Arnold L. (**2003**)
Infrared stimulated red luminescence from Chinese loess: basic observations.
Quaternary Science Reviews ***22,*** 961-966.

123. Lai ZP, Wintle A.G., Thomas S. G. (**2007**)
Rates of dust deposition between 50 ka and 20 ka revealed by OSL dating at Yuanbao on the Chinese Loess Plateau.
Palaeogeography, Palaeoclimatology, Palaeoecology ***248,*** 431-439.

124. Lai ZP. (**2010**).
Chronology and the upper dating limit for loess samples from Luochuan section in the Chinese Loess Plateau using quartz OSL SAR protocol.
Journal of Asian Earth Science, 37, 176–185.

125. Lamothe M. and Auclair M. (**1999**)
A solution to anomalous fading and age shortfalls in optical dating of feldspar minerals.
Earth and Planetary Science Letters ***171***, 319-323.

126. Lamothe M. and Auclair M. (**2000**)
The *fadia* method: a new approach in luminescence dating using the analysis of single feldspars grains.
Radiation Measurements ***32***, 433-438.

127. Lamonthe M., Auclair M., Hamzaoui C. and Huot S. (**2003**)
Towards a prediction of long term anomalous fading of feldspar IRSL.
Radiation Measurements ***37***, 493-498.

128. Lamothe M. (**2004**)
Optical dating of pottery, burnt stones, and sediments from selected Quebec archaeological sites.
Canadian Journal of Earth Sciences ***41***, 659-667.

129. Lang A., Lindauer S., Kuhn R. and Wagner G.A.T (**1996**)
Procedures used for Optically and Infrared Stimulated Luminescence Dating of Sediments in Heidelberg.
Ancient TL ***14***, 7-11.

130. Larsen N.A., Bulur E., Bøtter-Jensen L, McKeever S.W.S. (**2000**)
Use of the LM-OSL technique for the detection of partial bleaching in quartz.
Radiation Measurements ***32***, 419-425.

131. Lawless J.L. Chen R., Pagonis V. (**2009**)
Sublinear dose dependence of thermoluminescence and optically stimulated luminescence prior to the approach to saturation level.
Radiation Measuremets ***44***, 606-610.

132. Lee M.H. and Lee C. W. (**2000**)
Preparation of alpha emitting nuclides by electrodeposition.
Nuclear Instruments and Methods in Physics Research A ***447***, 593-600.

133. Li S.H. (**1991**)
Removal of the thermally unstable signal in optical dating of K-feldspar.
Ancient TL ***9***, 26-29.

134. Li B, Li S-H. (**2006**)
Comparison of De estimates using the fast component and the medium component of quartz OSL.
Radiation Measurements ***41***, 125-136.

135. Lian O.B., Roberts R., G., (**2006**)
Dating the Quaternary: progress in luminescence dating of sediments.
Quaternary Science Reviews ***25***, 2449-2468.

136. Lisiecki, L. E., and Lisiecki, P.A. (**2002**)
Application of dynamic programming to the correlation of paleoclimate records, *Paleoceanography, **17 (4)**, 1049*, doi: 10.1029/2001PA000733.

137. Lisiecki, L.E., Raymo, M.E. (**2005**)
A Pliocene-Pleistocene stack of 57 globally distributed benthic δ18O records.
*Paleoceanography, **20**, PA1003*, doi: 10.1029/2004PA001071.

138. Lomax J., Hilgers A., Twidale C.R., Bourne J.A., Radtke U. (**2007**)
Treatment of broad palaeodose distributions in OSL dating of dune sands from the western Murray Basin, South Australia.
Quaternary Geochronology **2**, 51-56.

139. Lowick S.E., Preusser, F., Wintle, A.G. (**2010**).
Investigating quartz optically stimulated luminescence dose-response curves at high doses.
Radiation Measurements 45, 975-984.

140. Malik, D.M., Kohnke E.E., Sibley W.A. (**1981**)
Low temperature thermally stimulated luminescence of high quality quartz.
Journal of applied Physics **52**, 3600-3605.

141. Markey B.G., Bøtter-Jensen L. and Duller G.A.T. (**1997**)
A new flexible system for measuring thermally and optically stimulated luminescence.
Radiation Measurements ***27***, 83-89.

142. Marković, S.B., Oches, E., Sümegi, P., Jovanović, M., Gaudenyi, T. (**2006**)
An introduction to the Middle and Upper Pleistocence loess-palaeosol sequence at Ruma brickyard, Vojvodina, Serbia.
Quaternary International ***149***, 80-86.

143. Marković, S.B., Bokhorst, M.,P., Vandenberghe J., McCoy, M., D., Oches, E.A., Hambach, U., Gaudenyi, T., Javanović, M., Zöller, L., Stevens, T., Machalett, B. (**2008**)
Late Pleistocence loess-palaeosol sequences in the Vojvodina region, north Serbia.
Journal of Quaternary Science, ***23(1)***, 73-84.

144. Martini M., Spinolo G., Vedda A. (**1986**)
Radiation induced conductivity of as-grown and electrodiffused quartz.
Journal of Applied Physics ***60***, 1705-1708.

145. Martini M., Fasoli M., Galli A. (**2009**)
Quartz OSL Emission Spectra and the Role of [Al O_4] Recombination Centres
Radiation Measurements ***44***, 458-461.

146. Mauz B., Packman S., Lang A. (**2006**)
The alfa effectiveness in silt size quartz: New data obtained by single and multiple aliquot protocols.
Ancient TL, ***vol 24, No 2***, 47-52.

147. Mayya Y.S., Morthekai P., Murari M.K., Singhvi A.K. (**2006**)
Towards quantifying beta microdosimetric effects in single-grain quartz dose distributions. *Radiation Measurements* ***41***, 1032-1039.

148. McKeever S.W.S. and Chen R. (**1997**)
Luminescence models.
Radiation Measurements, ***27***, 625-661.

149. McKeever S.W.S. (**2001**)
Optically stimulated luminescence dosimetry.
Nuclear Instruments and Methods in Physics Research B, ***184,*** 29-54.

150. McIntosh G and Catanzariti G. (**2006**)
An introduction to archaeomagnetic dating.
Geochronometria ***25***, 11-18.

151. Mejdahl V. (**1969**)
Thermoluminescence dating of ancient Danish ceramics.
Archaeometry ***11***, 99-104.

152. Mejdahl V. (**1979**)
Thermoluminescence dating: beta dose attenuation in quartz grains.
Archaeometry ***21***, 61-67.

153. Mejdahl V. (**1985**)
Thermoluminescence dating based on feldspars.
Nuclear Tracks and Radiation Measurements ***10***, 133-136.

154. Meisl N.K. and Huntley D.J. (**2005**)
Anomalous fading parameters and activation energies of feldspars.
Ancient TL ***23***, 1-7.

155. Mondragon, M.A., Chen C.Y., Halliburton L.E. (**1988**)
Observation of a dose rate dependence in the production of point defects in quartz.
Journal of applied Physics ***63***, 4937-4941.

156. Murray A.S., Roberts R.G. (**1997**)
Determining the burial time of single grains of quartz using optically stimulated luminescence.
Earth Plan. Sci Lett ***152***, 163-180.

157. Murray A.S. and Wintle A.G. (**1998**)
Factors controlling the shape of the OSL decay curve in quartz.
Radiation Measurements ***29***, 503-515.

158. Murray A.S. and Wintle A.G. (**1999**)
Isothermal decay of optically stimulated luminescence in quartz.
Radiation Measurements ***30***, 119-125.

159. Murray A.S. and Wintle A.G. (**2000**)
Luminescence dating using an improved single-aliquot regenerative dose protocol.
Radiation Measurements ***32***, 57-73.

160. Murray A.S. and Olley J.M. (**2002**)
Precision and accuracy in the optically stimulated luminescent dating of sedimentary quartz: a status review.
Geochronometria ***21***, 1-16.

161. Murray A.S. and Wintle A.G. (**2003**)
The single aliquot regenerative dose protocol: potentials for improvement in reliability.
Radiation Measurements ***37***, 377-381.

162. Murray A.S., Svendsen J.I., Mangerud J., Astakhov V.I. (**2007**)
Testing the accuracy of quartz OSL dating using a known-age Eemian site on the river Sula, northern Russia.
Quaternary Geochronology ***2***, 102-109.

163. Murray, A.S., Buylaert, J.-P., Henriksen, M., Svendsen, J.-I, Mangerud, J. (**2008**)
Testing the reliability of quartz OSL ages beyond the Eemian.
Radiation Measurements ***43***, 776-780.

164. Murray A.S., Buylaert J.P. Thomsen K.J., Jain M. (**2009**)
The effect of preheating on the IRSL signal from feldspar.
Radiation Measurements, ***44***, 554-559.

165. Olley J.M., Caitcheon G.C., and Murray A.S. (**1998**)
The distribution of apparent doses as determined by optically stimulated luminescence in small aliquots of fluvial quartz: implications for dating young sediments.
Quaternary Science Reviews, ***17***, 1033-1040.

166. Panaiotu, C.G., Panaiotu, E.C., Grama, A., Necula, C. (**2001**)
Paleoclimatic Record from Loess-Paleosol Profile in Southeastern Romania.
Phys. Chem. Earth (A) ***11-12***, 893-898.

167. Paşcovschi S., Donița, N. (**1967**)
Vegetația lemnoasă din silvostepa României. Editura. Academiei R.S.R., Bucureşti.

168. Paul I. (**1992**)
Cultura Petreşti (Petresti Culture).
Bucureşti, Museion Publishing House (in Romanian), 205 pp.

169. Pawley S.M., Bailey R.M., Rose J., Moorlock B.S.P., Hamblin R.J.O., Booth S.J., Lee J.R. (**2008**)
Age limits on Middle Pleistocene glacial sediments from OSL dating, north Norfolk, UK.
Quaternary Science Reviews, **27**, 1363-1377.

170. Pawley, S.M., Toms, P., Armitage, S.J., Rose, J., (**2010**).
Quartz luminescence dating of Anglian Stage (MIS 12) fluvial sediments: Comparison of SAR age estimates to the terrace chronology of the Middle Thames valley, UK.
Quaternary Geochronology 5, 569-582.

171. Poolton N. R. J., Smith, G.M., Riedi, P.C., Bulur E., Bøtter-Jensen L., Murray A.S., Adrian M. (**2000**)
Luminescence sensitivity changes in natural quartz induced by high temperature annealing: a high frequency EPR and OSL study.
Journal of Physics D. - Applied Physics ***33***, 1007-1017.

172. Pendea, I.F., Szanto, Zs, Badarau, Al. S., Dezsi, S. (**2002**)
Age and pedogenic reconstruction of a paleo-relict chernozem soil from Central Transylvanian Basin.
Geologica Carpathica, ***53,*** 37-38.

173. Pendea, F. (**2005**)
Late Quaternary geomorphic paleoenvironments in the Transylvanian Basin, Romania. Phd Thesis, Babeş-Bolyai University Cluj Napoca.

174. Poolton N.R.J., Wallinga J., Murray A.S., Bulur E., Bøtter-Jensen L. (**2002a**)
Electrons in feldspar I: on the wavefunction of electrons trapped at simple lattice defects.
Phys. Chem. Min. ***29****,* 217-225.

175. Poolton N.R.J., Ozanyan K. B., Wallinga J., Murray A.S., Bøtter-Jensen L. (**2002b**)
Electrons in feldspar II: a consideration of the conduction band-tail states on luminescence processes.
Phys. Chem. Min. ***29****,* 217-225.

176. Prescott J.R., Huntley D.J. and Hutton J.T. (**1993**)
Estimation of equivalent dose in thermoluminescence dating- the Australian slide method.
Ancient TL ***11****,* 1-5.

177. Prescott J.R. and Hutton J.T. (**1994**)
Cosmic ray contributions to dose rates for luminescence and ESR dating: large depths and long –term variations.
Radiation Measurements ***23****,* 497-500.

178. Prescott J.R. and Robertson G.B. (**1997**)
Sediment dating by luminescence: a review.
Radiation Measurements ***27****,* 893-922.

179. Preusser F., Chithambo M.L., Gotte T., Martini M., Ramseyer K., Sendezera J., Susino G.J., Wintle A.G. (**2009**)
Quartz as a natural luminescence dosimeter
Earth Science Reviews ***97****,* 196-226.

180. Rees-Jones, J, Tite, M.S. (**1995**)
Optical dating results for British archaeological sediments.
Archaeometry ***36****,* 177-187.

181. Rhodes, E.J., Singarayer J. S., Raynal J. P., Westaway K. E., Sbihi-Alaoui F.Z. (**2006**)
New age estimates for the Paleolithic assemblages and Pleistocence succession of Casablanca, Morocco.
Quaternary Science Reviews ***25****,* 2569-2585.

182. Roberts R.G. (**1997**)
Luminescence dating in archaeology: from origins to optical.
Radiation Measurements ***27****,* 819-892.

183. Roberts, R.G., et al. (**2000**)
Distinguishing dose population in sediment mixtures: a test of single-grain optical dating procedures using mixtures of laboratory-dosed quartz.
Radiation Measurements ***32***, 459-465.

184. Roberts H.M. and Wintle A.G. (**2001**)
Equivalent dose determinations for polymineralic fine-grains using the SAR protocol: application to a Holocene sequence of the Chinese Loess Plateau.
Quaternary Science Reviews ***20***, 859-892.

185. Roberts H.M. and Wintle A.G. (**2003**)
Luminescence sensitivity changes of polymineral fine grains during IRSL and (post-IR) OSL measurements.
Radiation Measurements ***37***, 661-671.

186. Roberts H.M. (**2006**)
Optical dating of coarse-silt quartz from loess: Evaluation of equivalent dose determination and SAR procedural checks.
Radiation Measuremets ***41***, 923-929.

187. Roberts H.M. (**2008**)
The development and application of luminescence dating to loess deposits: a perspective on the past, present and future.
Boreas, ***37***, 483–507.

188. Rodnight H. (**2008**)
How many equivalent dose values are needed to obtain a reproducible distribution?
Ancient TL, ***26, 1,*** 3-9.

189. Ropp R.C. (**2004**)
Luminescence and the solid state.
Elsevier 2004, 711p. ISBN: 0-444-51661-1.

190. Sakalo, D.J. **(1961)**
The forest-steppe landscape of the European part of the USSR and its vegetation.
Botaniceskii Jurnal ***46(7)***, 969-978.

191. Schilles T., Poolton N.R.J., Bulur E., Bøtter-Jensen, L., Murray A.S., Smith G., Riedi , P.C., Wagner G.A. (**2001**)
A multi-spectroscopic study of luminescence sensitivity changes in natural quartz induced by high temperature annealing.
Journal of Physiscs D- Applied physics ***34***, 722-731.

192. Singarayer J.S. (**2002**)
Linearly modulated optically stimulated luminescence of sedimentary quartz: physical mechanisms and implications for dating.
PhD Thesis, University of Oxford, 237 p.

193. Singarayer J.S. and Bailey R.M. (**2003**)
Further investigations of the quartz optically stimulated luminescent components using linear modulation.
Radiation Measurements ***37***, 451-458.

194. Singhvi, A.K., Bluszcz, A., Bateman, M.D., Someshwar Rao, M. (**2001**)
Luminescence dating of loess- palaeosol sequences and coversands: methodological aspects and palaeoclimatic implications.
Earth-Science Reviews ***54***, 193-211.

195. Smith B.W. and Rhodes E.J. (1994)
Charge movements in quartz and their relevance to optical dating.
Radiation Measurements ***23***, 329-333.

196. Spooner N.A. (**1992**)
Optical dating: preliminary results on the anomalous fading of luminescence from feldspars.
Quaternary Science Reviews ***11***, 139-145.

197. Spooner N.A. (**1994a**)
On the optical dating signal from quartz.
Radiation measurements ***23***, 593-600.

198. Spooner N.A. (**1994b**)
The anomalous fading of infra-red stimulated luminescence from feldspars.
Radiation Measurements 23, 625-632.

199. Stevens, T., Armitage, S.J., Huayu, L., Thomas, D.S.G. (**2007**)
Examining the potential of high resolution OSL dating of Chinese loess.
Quaternary Geochronology ***2***, 15-22.

200. Steffen D., Preusser F., Schlunegger F. (**2009**)
OSL quartz age underestimation due to unstable signal components.
Quaternary Geochronology ***4***, 353-362.

201. Stoneham D., Stokes S. (**1991**)
An investigation of the relationship between the 110 ^{o}C peak and the OSL in the sedimentary quartz.
Nuclear Tracks and Radiation Measurements ***18***, 119-123,

202. Stokes S. (**1999**)
Luminescence dating applications in geomorphological research.
Geomorphology ***29***, 153-171.

203. Stokes S, Colls A.E.L. Fattahi M., Rich J. (**2000**)
Investigations of the performance of quartz single aliquot DE determination procedures.
Radiation Measurements ***32***, 585-594.

204. Stokes S., Fattahi M. (**2003**)
Red emission luminescence from quartz and feldspar for dating applications: an overview.
Radiation Measurements ***37***, 383-395.

205. Sun J.M., Kohfeld K.E. and Harrison S.P. (**2000**)
Records of Aeolian dust deposition on the Chinese Loess Plateau during the Late Quaternary.
MPI-BGC Tech. Rep 1.

206. Takano M, Yawata T and Hahimoto T. (**2003**)
Luminescence dosimetry of archaeological and ceramic samples using a single- aliquot regenerative dose method.
Journal of Radioanalytical and Nuclear Chemistry ***255***, 365-368.

207. Tegen, I., Lacis A.A., Fung I. (**1996**)
The influence of climate forcing of mineral aerosols from disturbed soils.
Nature ***280***, 419-422.

208. Templer R. H. (**1986**)
The localized transition model of anomalous fading.
Radiation Protection Dosimetry ***17***, 493-497.

209. **Timar A**. (**2006**)
Comparing quartz OSL and polymineral IRSL ages for Chinese loess: a case study.
MsD Thesis, Universitatea Babes Bolyai -Gent University.

210. **Timar A.,** Cosma C., Benea V., Begy R., Jobagy V., Szeiler G., Barbos D., Fulea D. (**2007**)
Estimation of environmental radionuclide concentration in soils, a comparison of methods for the annual radiation dose determination in luminescence dating.
Studia Universitatis, Babes-Bolyai, Geologia, ***52 (1)***, 80-81.

211. **Timar A.,** Cosma C., Benea V., Begy R.C., Jobaggy V., Szeiler G., Fulea D. (**2008a**)
A comparison of methods for external dose rate determinatin in luminescence dating of archaeological materials
Foldkergi Radioizotopok a Kornyezetunnkben, Pannon Egyetemi Kiado, Egyhazy Tiborne-Editor, p. 35-44.

212. **Timar A.** (**2008b**)
Fenomenul de termoluminescenta si luminescenta stimulata optic si aplicatiile sale in datare, Varste absolute prin metode nucleare cu aplicatii in arheologie, geologie si mediu.
Masa Rotunda. Alba-Iulia, Quantum, Editor: Cosma C., Varvara S., Gligor, M., p.: 33-43.

213. **Timar A.,** Cosma C, van den Haute P., Vandenberghe D. (**2008c**)
Datarea secventelor de loess-palaeosol prin luminescenta stimulata optic.
Varste absolute prin metode nucleare cu aplicatii in arheologie, geologie si mediu. *Masa Rotunda. Alba-Iulia, Quantum*, Editor: Cosma C, Varvara S., Gligor, M., p.: 66-78

214. **Timar A.,** Vandenberghe D., Vasiliniuc S., Cosma C. (**2009a**)
Optical dating of Romanian loess: A comparison between sand-sized and silt-sized quartz.
Book of Abstracts Loessfest '09 – International conference on loess research, 31 st August – 1 st September 2009, Novi Sad, Serbia, p. 77-78

215. **Timar A.,** Vandenberghe D., Vasiliniuc S., Cosma C. (**2009b**)
On the optical age of sand-sized and silt-sized quartz grains extracted from Romanian loess.
Book of Abstracts - UK Luminescence and ESR Meeting, Royal Holloway, University of London, 26th-28th August 2009.

216. **Timar A.,** Vasiliniuc S., Vandenberge D., Cosma C. (**2009c**)
Absolute dating of Romanian loess using luminescence techniques: palaeoclimatic implications.
Ecoterra **22-23,** *45-47.*

217. **Timar A.,** Vandenberghe D., Panaiotu E.C., Panaiotu C.G., Necula C., Cosma C. and Van den haute P. (**2010a**)
Optical dating of Romanian loess using fine-grained quartz.
Quaternary Geochronology, ***5***, 143-148.

218. **Timar Gabor A.,** Vandenberghe D.A.G., Vasiliniuc, S., Panaoitu, C. E., Panaiotu, C. G., Dimofte, D., Cosma, C. (**2010b**)
Optical dating of Romanian Loess a comparison between silt-sized and sand-sized quartz.
Quaternary International (QUATINT - S-10- 00155).

219. **Timar Gabor A.,** Vandenberghe D.A.G., Vasiliniuc, S., Panaoitu, C. E., Panaiotu, C. G., Cosma, C. (**2010c**)
Further investigations on the optical age of fine silt (4-11 μm), coarse silt (35-50 μm) and fine sand (63-90μm) quartz grains extracted from Romanian loess.
Xth international conferecence *"Methods of Absolute Chronology"-Book of abstracts*, page 29.

220. **Timar Gabor, A.,** Vasiliniuc, Ş., Bădărau, A.S., Begy, R., Cosma C. (**2010d**)
Testing the potential of optically stimulated luminescence dating methods for dating soil covers from the forest steppe zone in Transylvanian basin.
Carpathian Journal of Earth and Environmental Sciences- in press.

221. Thomsen K. (**2004**)
Optically Stimulated Luminescence Techniques in Retrospective Dosimetry using Single Grains of Quartz extracted from Unheated Materials
PhD thesis Risø National Laboratory, Roskilde, Denmark, 176p.

222. Thomsen K.J., Bøtter-Jensen, L., Denby P.M., Moska P., Murray A.S. (**2006**)
Developments in luminescence measurement techniques.
Radiation Measurements ***41***, 768-773.

223. Thomsen K.J., Murray A.S., Jain M., Bøtter-Jensen L. (**2008**)
Laboratory fading rates of various luminescence signals from feldspar-rich sediment extracts.
Radiation Measurements ***43***, 1474-1486.

224. Tsukamoto S., Fukuasawa H., Ono Y.and Fang X. (**2001**)
Infrared Stimulated Luminescence and Thermoluminescence Dating of loess from Lanzhou, China.
Quaternary Research ***40***, 385-392.

225. Vandenberghe D., Hossain S.M., De Corte F. and Van den haute P (**2003**)
Investigations of the origin of the equivalent dose distribution in a Dutch coversand.
Radiation Measurements ***37***, 433-439.

226. Vandenberghe D. (**2004**)
Investigation of the optically stimulated luminescence dating method for applications to young geological sediments.
PhD thesis, Gent University, Gent, Belgium, 289p.

227. Vandenberge D., De Corte F., Buylaert J-P., Kučera J., Van den haute P. (**2008**)
On the internal radioactivity in quartz.
Radiation Measurements ***43***, 771-775.

228. Vandenberghe D.A.G., De Meester E., Velghe G., Zöller L., Van den haute P. (**2009**)
A chronological study of the loess deposits over- and underlying the Eltville tephra using the newest luminescence techniques applied to sand-sized quartz: results from two Late-Weichselian type localities. *Abstract book Loessfest '09 – International Conference on Loess Research,* 31 August – 1 September, 2009, Novi Sad, Serbia, 31.

229. Van den haute P., Vancraeynest L. and de Corte F. (**1998**)
The Late Pleistocene loess deposits of eastern Belgium New TL age determinations.
Journal of Quaternary Science ***13***, 487-497.

230. Van den haute P., Frechen M., Buylaert J.-P., Vandenberghe D. and De Corte F. (**2003**)
The last Interglacial palaeosol in the Belgian loess belt: TL age record.
Quaternary Science Reviews ***22***, 985-990.

231. Vafiadou et al. (**2007**)
Optically stimulated luminescence dating investigations of rock and underlying soil from three case studies.
Journal of Archaeological Science ***34***, 1659-1669.

232. Văsaru G, Cosma C (**1998**)
Geocronologie Nucleară.
Editura Dacia, Cluj Napoca, 346p, ISBN:973-35-0650-8.

233. Vermeesch P (**2009**)
Radial Plotter: A Java application for fission track, luminescence and other radial plots.
Radiation Measurements ***44***, 409–410.

234. Visocekas R. (**1985**)
Tunneling radiative recombination in labradorite: its association with anomalous fading of thermoluminescence.
Nuclear Tracks ***10***, 521-529.

235. Visocekas R. (**2000**)
Monitoring anomalous fading on TL of feldspars by using far-red emission as a gauge.
Radiation Measurements ***32***, 499-504.

236. Visocekas R., Spooner N.A., Zink A. and Blanc P. (**1994**)
Tunnel afterglow, fading and infrared emission in thermolominescence of feldspars.
Radiation Measurements ***23***, 377-385.

237. Wallinga J., Murray A.S. and Wintle A.G. (**2000a**)
The single-aliquot regenerative –dose (SAR) protocol applied to coarse-grain feldspar.
Radiation Measurements ***32***, 691-695.

238. Wallinga J., Duller G.A.T. (**2000b**)
The effect of optical absorption on the infrared stimulated luminescence age obtained on coarse –grain feldspars.
Quaternary Science Reviews ***19***, 1035-1042.

239. Wallinga J., Murray A.S., Wintle A.G., Bøtter-Jensen L (**2002**)
Electron trapping probability in natural dosemeters as function of irradiation temperature.
Radiation Protection Dosimetry ***101***, 339-344.

240. Wallinga J., Bos A.J.J., Duller G.A.T (**2008**)
On separation of quartz OSL signal components using different stimulation modes.
Radiation Measurements ***43***, 742-747.

241. Wang X, Lu Y and Zhao H. (**2006**)
On the performance of single-aliquot regenerative –dose (SAR) protocol for Chinese loess: fine quartz and polymineral grains.
Radiation Measurements ***41***, 1-8.

242. Watanuki T., Murray A.S., Tsukamoto S. (**2003**)
A comparison of OSL ages derived from silt- sized quartz and polymineral grains from Chinese loess.
Quaternary Science Reviews **22**, 991-997

243. Weil, J.A. (**1984**)
A review of electron-spin spectroscopy and its application to the study of paramagnetic defects in crystalline quartz.
Physics and Chemistry of Minerals ***10***, 149-165.

244. Wintle A.G. (**1973**)
Anomalous fading of thermoluminescence in mineral samples.
Nature ***245***, 143-144.

245. Wintle A.G. (**1977**)
Detailed study of a thermoluminescent mineral exhibiting anomalous fading
Journal of Luminescence ***15***, 385-393.

246. Wintle A.G. and Huntley D.J. (**1979**)
Thermoluminescence dating of deep sea ocean core.
Nature ***279***, 710-712.

247. Wintle A.G. and Huntley D.J. (**1980**)
Thermoluminescence dating of ocean sediments.
Canadian Journal of Earth Sciences ***17***, 348-360.

248. Wintle, A. G. (**1981**)
Thermoluminescence dating of Late Devensian loesses in southern England.
Nature ***289***, 479–480.

249. Wintle A.G. (**1990**)
A review of current research on TL dating of Loess.
Quaternary Science Reviews ***9***, 385-397.

250. Wintle A.G. (**1997**)
Luminescent dating: laboratory procedures and protocols.
Radiation Measurements ***27***, 769-817.

251. Wintle A.G. and Murray A.S.(**1997**)
The relationship between quartz termoluminescence, photo-transferred thermoluminescence and optically stimulated luminescence.
Radiation Measurements ***27***, 611-624.

252. Wintle A.G. and Murray A.S. (**1999**)
Luminescence sensitivity changes in quartz.
Radiation Measurements ***30***, 107-118.

253. Wintle A.G. and Murray A.S. (**2000**)
Quartz OSL: Effects on the thermal treatment and their relevance to laboratory procedures.
Radiation Measurements ***32***, 387-400.

254. Wintle A.G. and Murray A.S. (**2006**)
A review of quartz optically stimulated luminescence characteristics and their relevance in single-aliquot regeneration dating protocols.
Radiation Measurements ***41***, 369-391.

255. Wintle A.G. (**2008a**)
Luminescence dating: where it has been and where it is going
Boreas, ***37***, 471–482.

256. Wintle A.G. (**2008b**)
Fifty years of luminescence dating.
Archaeometry ***50, 2***, 276–312

257. Zimmerman D.W. (**1967**)
Thermoluminescence from fine grains from ancient pottery.
Archaeometry ***10***, 26-28.

258. Zimmerman D.W. (**1971**)
Thermoluminescence dating using fine grains from pottery.
Archaeometry ***13***, 29-52.

ACKNOWLEDGEMENTS

I believe that only those who have actually been involved in the process of writing a PhD know how hard this job can be sometimes and how much support is needed. The work I have carried out in the last three years (and a little bit more) in the frame of this PhD project matured me, provided me great satisfactions, offered me the chance to visit beautiful places and meet wonderful people. However, none of these would have been possible without the help of some key persons.

First of all I want to express all my gratitude to my supervisor Professor Constantin Cosma for his scientific guidance and advice he gave me throughout the last five years. I thank him for all the efforts he made in order for the Luminescence Laboratory in Cluj to exist. Last but not least, I want to thank him for being so kind, for always making time for me and most of all for giving me precious freedom of choice.

And of course, all my colleagues here in Faculty of Environmental Science. Dr. Robert Begy whom with I collaborated on annual dose measurement techniques but also easily managed to share a very small office space years ago, Dr. Alexandra Dinu for always offering her help, Dr. Mircea Moldovan for sometimes taking over some of my chores, and last but not least the best colleague one can have, Ştefan Vasiliniuc. Ştefan helped me very much in the laboratory during the toughest year, which was of course the last one. I wish him great success with his ongoing thesis on luminescence.

I have to thank the Paleomagnetic Team in Bucharest (Conf. Dr. Cristina Panaiotu and Conf. Dr. Cristian Panaiotu) for advice, for guiding me in the sampling campaigns and for giving me access to their unpublished data (both paleomagnetism and grain size).

I have a great deal of appreciation for my informal supervisor Dr. Dimitri Vandenberghe. He taught me the basics of luminescence dating during my MsD and offered me constant support and guidance throughout my PhD work. He was a model for me in luminescence at the beginnings and he remains a model for my work. I want to thank him for providing me with the chance to visit Risø and meet "Guru" Andrew Murray in person and for recommending me to be invited to give a talk in Xinning, thus offering me the chance to step on the Tibetan Plateau.

From the group in Gent I also have to thank Professor Van den haute for always welcoming me so kind into the laboratory and Gilles Velghe for his assistance and for making the long hours spent in the dark room almost pleasant by being so friendly.

I am in debt to the international luminescence dating community in general for being so opened to newcomers. The kind words I was offered during meetings by" luminescence VIPs" like Professor Wintle, Professor Singhvi, Dr. Duller, Dr. Bailey and many others gave me a lot of confidence in myself and in my work.

Finally I have to thank the most precious people in my life: my family. My best friend-my mother, who knows everything a non-specialist can about luminescence, my father who I know that would make any sacrifice in order for me to be happy and successful and last but not least my ex-faculty-colleague, friend and now husband Mihai for supporting and understanding me. My greatest achievement of the last years is undoubtedly my relationship with my physicist husband.

ROMÂNIA

MINISTERUL EDUCAȚIEI, CERCETĂRII,TINERETULUI SI SPORTULUI

CONSILIUL NAȚIONAL AL CERCETĂRII ŞTIINȚIFICE DIN ÎNVĂȚAMÂNTUL SUPERIOR

UNITATEA EXECUTIVĂ PENTRU FINANȚAREA ÎNVĂȚĂMÂNTULUI SUPERIOR ŞI A CERCETĂRII ŞTIINȚIFICE UNIVERSITARE

„Povestea doctoratului meu”

„The story of my PhD”

Dozimetrie retrospectivă luminescentă cu aplicații în arheologie, geologie și mediu

ALIDA IULIA TIMAR (GABOR)

Universitatea Babeș-Bolyai Cluj-Napoca
Tel: +40 264405300
Fax: +40 2640591906
e-mail: alida.timar@ubbcluj.ro
alida_timar@yahoo.com

Profesor coordonator
Prof. Dr. Cosma Constantin

Retrospective luminescence dosimetry: applications in archaeology, geology and environmental studies

Scurtă prezentare a lucrării de doctorat

Fenomenele luminescente sunt generate de o serie vastă de procese fizice. În scopul aplicaţiilor de dozimetrie retrospectivă insă, doar procesul de termoluminescenţă şi cel de luminescenţă stimulată optic sunt de interes. Aceste fenomene constă in emisia fotonică care apare in cazul stimularii termice, respectiv optice a unui izolator sau a unui semiconductor care a fost în prealabil expus la un flux de radiaţii ionizante, această emisie fiind dependentă de doza absorbită. Mecanismul intrisec de producere a acestor fenomene în cazul cristalelor naturale, cu bandă interzisă largă, cum ar fi cuarţul sau feldspaţii este complicat şi în momentul de faţă nu este înteles în totalitate. În ciuda acestui fapt însă, el poate fi aplicat cu succes pentru datare.

În ultima decadă, metodele experimetale luminescente au cunoscut însemnate progrese tehnologice cât şi metodologice, în momentul de faţă fiind caracterizate printr-un grad de rigoare intrinsecă rar egalat de alte metode de datare. Cu toate acestea însă, tehnicile moderne de datare prin luminescenţă nu au fost aplicate până acum in nici un laborator din ţara noastră.

Metoda datării luminiscente implică aplicarea simultană a doua tipuri de masuratori: cuantificarea semnalului optic indus de radioactivitatea ambientala in locul in care s-a păstrat proba şi măsurarea exactă a dozei anuale care la randul sau este o problemă complicată, realizându-se prin măsuratori care includ spectrometria gama de înaltă rezoluţie, spectrometria alfa sau activarea cu neutroni. O a treia problemă ce trebuie rezolvata este legata de prelucrarea probelor în vederea măsurarii semnalului luminescent.

Scopul tezei mele a fost dezvolatara şi implementarea unor tehinicilor recente pentru determinarea cu acurateţe atât a paleodozei cât şi a dozei anuale şi aplicarea acestora în câteva aplicaţii cheie.

Pentru determinarea paleodozei sau a dozei echivalente, procedurile convenţionale de separare a cuarţului din sedimente şi ceramici au fost

Short abstract of the PhD thesis

Luminescence phenomena encompass a very wide range of processes. For the purpose of retrospective dosimetry only optically stimulated luminescence (OSL) and thermoluminescence (TL) processes are of interest. OSL and TL is the luminescence emitted from an irradiated insulator or semiconductor during exposure to light or respectively heat; thus OSL and TL are stimulated processes. The luminescence signal emitted is dependent on the irradiation history of the sample. Although the processes giving rise to luminescence phenomena in natural wide-gap crystals such as quartz and feldspars are complicated and not fully understood this phenomenon can be exploited for dating. In the past ten years luminescence dating has undergone extreme technological and methodological advances and at the moment is characterized by a degree of quality control seldom seen with other dating techniques. Despite this however, state of the art luminescence dating techniques have not been applied in a Romanian laboratory up to now.

The scope of my thesis was to assure quality control of procedures concerning paleodose and annual dose estimation in our laboratory and implement state of the art measurement techniques in key applications.

For equivalent dose measurement, the extraction of quartz and polymineral fine grains from samples using conventional luminescence dating sample preparation techniques was implemented in our laboratory. The purity of the extracted quartz grains was tested and confirmed by the absence of IR signals following irradiation. The dose rate delivered on different substrates and for different grains sizes by the ^{90}Sr-Y beta source mounted on the Risø TL/OSL DA-20 luminescence reader was determined by making use of gamma dosed calibration quartz supplied by Risø and equivalent dose measurement procedures were validated through an intercomparison exercise with Gent Luminescence Dating Laboratory, Belgium.

The annual dose was derived based on radionuclide concentrations determined in our laboratory by

implemetate. Imbogaţirea extractelor în cuarţ a fost verificată prin analize microscopice, iar lipsa contaminării semnalului utilizat pentru datare a fost testată prin analizarea raspunsului obţinut în urma stimulării in infraroşu. Debitul dozei absorbite în urma iradierii cu sursa de ^{90}Sr-Y montată pe iradiatorul automat al cititorului de luminescenţă Risø TL OSL DA-20 de către granule de diverse mărimi fixate pe diverse substrate a fost determinat folosind cuarţ de calibrare iradiat gamma. Procedurile experimetale folosite în determinare paleodozei au fost validate prin efectuarea unui exercitiu de intercomparare cu Gent Luminescence Dating Laboratory, Belgia.

Doza anuala a fost calculata pe baza concentratiilor de radionuclizi existente in probe, determinate prin spectometrie gamma de înaltă rezoluţie, folosind un detector cu semiconductor Ge de puritate înaltă ORTEC. Sistemul a fost calibrat în energie fosind o sursă de Eu iar în eficacitate folosind un algoritm Monte Carlo, validat prin măsurarea de surse standard ale Agentiei Internationale Atomice Viena. A fost implementată o metodă pentru determinarea concentraţiei de ^{226}Ra în mod direct, prin utilizarea liniei gamma interferate cu energia de 186.2 KeV, iar concentraţiile de ^{234}Th, ^{214}Pb, ^{214}Bi, ^{214}Bi, ^{210}Pb, ^{228}Ac, ^{208}Tl, şi ^{40}K au fost determinate in toate probele analizate.Validarea metodelor a fost facuta prin efectuarea unui exerciţiu de intercomparare cu alte doua laboratoare care folosesc metode independente: spectrometrie alfa (Departamentul de Radiochimie al Universităţii din Veszprém, Ungaria), respectiv activare cu neutroni (Institutul pentru Cercetări Nucleare, Mioveni, Piteşti, România). De asemenea, concentratiile de radionuclizi din probele de loess analizate au fost determinate prin spectrometrie gamma şi în laboratorul de datare din Universitatea Gent.

Metodele de datare prin luminescenţă au fost aplicate pentru patru fragmente de ceramică neolitică provenite din cultura Lumea Nouă, Alba Iulia, scopul acestui studiu fiind îmbunătăţirea cronologiei acestui sit. Protocolul unialicotă SAR (single aliquot regeneration) a fost aplicat atât pentru emisia UV a cuarţului grosier (90-125 µm) prin stimulare în albastru (OSL) cât şi pentru emisia în domeniul albastru al granulelor fine (4-11µm) polimînerale extrase din probe în urma stimulării în infraroşu (IRSL). Pentru comparare, tehnica convenţională a dozelor aditive folosind mai multe alicote (MAAD) a fost de asemena aplicată pentru semnalul luminescent obţinut în urma stimulării termice (TL). Vârstele obţinute prin aceste tehnici diferite au fost in bună concordanţă, dar s-a concluzionat că tehnica SAR OSL este mai robustă, şi are o precizie mai bună. Vârsta OSL medie obţinută plasează tranziţia de la Cultura Foeni la Cultura Petreşti în situl Lumea Nouă la 6.2±0.5ka, interval ce este în bună concordanţă cu aşteptările arheologilor. Pentru stabilirea unei cronologii complete a evoluţiei culturale a sitului Lumea Nouă continuarea investigaţiilor se impune, dar cu toate acestea studiul nostru reprezintă o primă confirmare a faptului că metodele luminescente pot contribui semnificativ la realizarea acestui deziderat.

A doua aplicaţie cheie a metodelor luminescente este datarea sedimentelor, în principal a celor de natură eoliană. Aceste depuneri reprezintă o

means of high resolution gamma ray spectrometry using an ORTEC hiperpure germanium detector. The system was calibrated in energy using an europium source while the efficiency calibration was performed using a Monte Carlo routine which was validated using IAEA standards. A method for determining ^{226}Ra concentrations directly by making use of the interfered line at 186.2keV was implemented. ^{234}Th, ^{214}Pb, ^{214}Bi, ^{214}Bi, ^{210}Pb, ^{228}Ac, ^{208}Tl, and ^{40}K can be routinely measured in environmental samples. The procedures have been validated through an intercomparison exercise with two other different methods - alpha spectrometry (The Radiochemistry Laboratory from Veszprém), respectively instrumental neutron activation (Institute for Nuclear Research, Piteşti, Romania), and with Gent Luminescence Dating Laboratory where the same techniques are being used (high resolution gamma spectrometry with relative efficiency calibration).

Luminescence dating was applied to four pottery fragments excavated at Lumea Nouă (Alba Iulia, Romania). The aim of this study was to apply new approaches in optical dating to improve the chronological framework for the site. To this purpose, the SAR protocol was applied to both blue (OSL) and infrared stimulated luminescence (IRSL) signals from coarse (90-125 µm) quartz and polymineral fine (4-11 µm) grains, respectively. For the sake of comparison, a more conventional approach, which uses MAAD protocol and thermoluminescence TL signals from polymineral fine grains, was applied as well. It was concluded that compared to the TL method, the IRSL and OSL approaches are based on a more robust dating methodology. As SAR-OSL dating of quartz yielded the most precise age estimates, this was considered to be the technique of choice. The average of the four quartz SAR-OSL ages presented above placed the transition from Foeni to Petreşti culture at Lumea Nouă site around 6.2 ± 0.5 ka, an extremely plausible age taking into consideration the archaeological information. Further investigations are needed for establishing a complete chronological framework for the ancient cultural development at Lumea Nouă. Nevertheless our study is a clear illustration of how luminescence dating, especially by the use of state-of –the-art techniques can contribute to this purpose.

The Romanian loess-palaeosol sequences preserve a significant terrestrial record of Quaternary climate change during at least five Glacial / Interglacial cycles. In comparison to similar sequences elsewhere in Central and Eastern Europe, the deposits in Romania have been less extensively studied. We have carried out a first optically stimulated luminescence (OSL or optical) study for the loess-sequence near Mircea Vodă (Dobrogea, SE Romania) using silt-sized (4-11µm) and silt –sandy (63-90 µm) quartz as dosimeter. Obtained OSL ages confirmed that the uppermost palaeosol (usually denoted by S1 in stratigraphic nomenclature) formed during the last Interglacial. Both sets of optical ages indicate that the L1 unit did not accumulate at a constant rate, with loess being deposited at a significantly lower rate during the past ~50 ka. This illustrates the limitations of proxy records to interpret and derive a chronology for these deposits. The age results for the L1 unit con-

arhivă a schimbărilor climatice din timpul Pleistocenului, ratele crescute de depunere ale acestor sedimente fiind indicatori ai perioadelor reci, vântoase si aride. Implementrea unor metode fizice pentru obţinerea unor vârste ce reflectă in mod absolut momentul depunerii acestor materiale este vitală pentru a avea o buna intelegere a schimbărilor climatice reflectate de aceste secvenţe. Secvenţele de loess si paleosolurile intercalate din Dobrogea reprezintă in detaliu schimbările climatice din ultimii 650 ka fiind unele dintre cele mai complete secvenţe de acest tip din Europa. Metodele de datare prin luminescenta stimulată optic au fost aplicate atât pe probe de cuarţ fin (4-11 µm) cât şi grosier (63-90 µm) extrase din probe colectate din statele L1, L2, L3 şi L4 ale secţiunii Mircea Vodă obţinându-se astfel o primă cronologie de mare rezoluţie a depunerilor eoliene din Sud Estul României. Vârstele obţinute confirmă faptul că primul paleosol bine dezvoltat s-a format în timpul ultimului stadiu interglaciar şi indică faptul că depunerile eoliene din cursul ultimului stadiu glaciar-interglaciar au avut loc în mod continuu dar nu cu o rată constantă, viteza de depunere fiind mai mică în ultimii 50 ka faţa de perioada 60-70ka. Vârstele obţinute pentru L1 demonstrează limitările aplicarii metodelor de datare relative pentru obţinerea cronologiei depunerilor de natură eoliană, infirmând presupunerea convenţională a sedimetării cu viteză constantă. Rezultatul studiului nostru este însă în acord cu informaţiile recente obţinute prin aplicarea metodelor de datere luminescente în datarea secvenţelor de loess paleosol din diferite zone ale platoului de loess din China, unde de asemenea s-a constatat existenţa ratelor de sedimentare diferite. Prin urmare, studiul nostru accentuează necesitatea aplicării unor metode de datare absolute pentru obtinerea cronologiei depunerilor de loess din România şi demonstrează potenţialul utilizării datărilor prin metode luminescente în interpretarea acestor arhive ale paleoclimatului.

Importanța temei abordate în cadrul tezei de doctorat pe plan național și internațional

Cu toate că metodele de datare prin luminescenţă sunt considerate un instrument deosebit de valoros în studii de arheologie şi geologie la nivel mondial (a se vedea spre exemplu monografiile şi lucrarile extinse Aitken 1985, 1998, Roberts 1997, Stokes 1999, Duller 2004, Wintle 2008 a,b- doar pentru a da câteva exemple), aceste tehnici nu au fost aplicate în mod constant şi riguros în ţara noastră până în momentul de faţă. Menionăm că au existat câteva încercări de utilizare a termoluminescenţei pentru datarea de material arheologic în Cluj Napoca în anii 80 (profesor V.Morariu) şi pentru datarea speleothemelor in Bucureşti (Labău et al 1996), dar cercetarile au fost stopate din motive pe care nu le cunoştem. Interesul grupului nostru condus de profesorul C.Cosma în acest domeniu există de mai mult de un deceniu (Văsaru, Cosma, 1999), prima aplicaţie fiind facută cu ajutorul unui dispozitiv Harshaw modest, cu caracteristici tehnice specitrast with the commonly held assumption that loess sedimentation in this region occurred at a constant rate. They are, however, in line with the recent insights gained from optical dating of Chinese loess, as at several localities in the Chinese loess plateau, loess accumulation rates have been found to vary during the last glacial period. As such, our study further demonstrates the importance of absolute dates for interpreting these detailed archives of regional climate and environmental change.

Describe the importance of your PhD topic, both on national and international levels

Despite the obvious importance and success of luminescence techniques worldwide (review works of Aitken 1985, 1998, Roberts 1997, Stokes 1999, Duller 2004, Wintle 2008 a, b- just to name a few) the method was not thoroughly applied in Romania up to now. It should be mentioned that some attempts in using thermoluminescence for dating were made in the past by Professor V.V. Moraiu in Cluj in the 1980s and by a group in Bucharest in 1990s (Labău et al 1996) but the research was abruptly ceased for reasons we are not aware of. The interest of the group of Professor Cosma in luminescence dating dates for more than a decade ago (Văsaru, Cosma 1999), and our first applications have been carried out using a Harashaw 2000 dosimetric system (Cosma et al 2006, 2008). In 2006, the material means necessary in order to develop a modern luminescence laboratory affiliated to the Faculty of Environmental Sciences of Babeş-Bolyai University Cluj were finally obtained through a research grant (CEEX 749/2006). The work presented in this thesis started in the same year and is undoubtedly linked to the development of the first state of the art luminescence dating laboratory in Romania.

At the moment the laboratory in Cluj is fully operational and is providing transfer of knowledge to other two luminescece dating laboratories under developement in Iasi and Bucharest.

The first aim of our work was to ensure that the methodology applied in Luminescence Dating Laboratory in Cluj both in the case of gamma spectrometric measurements (for radionuclide specific activity determination in environmental samples) as well as for sample preparation and luminescence measurements are robust in order to be able to obtain accurate values for both anual dose and equivalent doses of samples investigated. In order to do that, both internal checks and intercomparison exercises with other laboratories have been performed. The second but more important aim of this thesis was to apply state of the art luminescence methodology in dating archaeological and geological materials of interest.

For archaeological applications, the Lumea Nouă site was chosen, as this location is considered to be of major importance for reconstructing the Neolithic and Aeneolithic periods in Romania and well known for its Neolithic painted pottery. (Benea et al., 2007)

Most efforts were conducted into appling luminescence methods for dating geological materials, in particular the famous loess palaeosol sequence of Mircea Vodă. We have chosen this application

fice dozimetriei de personal prin termoluminescenţă, care nu sunt satisfacătoare în cazul aplicaţiilor de datare (Cosma et al, 2006, 2008).

În anul 2006, graţie unui contract de finaţare (CEEX 749-2006-C.Cosma) necesităţiile materiale vitale pentru dezvolatrea unui laborator modern de datare prin luminescenţă in cadrul Facultaţii de Ştiinţa Mediului, Universitatea Babeş-Bolyai Cluj Napoca au fost asigurate. Întreaga mea activitate desfaşurată în cursul perioadei studiilor doctorale este indisolubil legată de dezvoltarea acestui laborator. În momentul de faţă laboartorul este complet funcţional şi oferă consiliere şi sprijin altor doua laboratoare de datare prin luminescenţă aflate in curs de dezvoltare in Iaşi şi Bucureşti.

Pricipalul scop al tezei mele a fost implementarea şi dezvoltarea metodelor de preparare a probelor şi analiză luminescentă pentru determinarea palodozei, a metodelor gamma spectrometrice pentru determinarea concentraţiei de radionuclizi din probe de mediu pentru determinarea dozei anuale şi verificarea acurateţii acestor proceduri. Pentru aceasta, am aplicat teste de rigoare internă şi am participat in exerciţii de intercomparare cu alte laboratoare.

Al doilea deziderat a constat în aplicarea metodelor in studii de caz cheie. Ca aplicaţie în arheologie s-au datat ceramici provenite din situl Lumea Nouă. Acest sit are o importanţă e majoră pentru reconstrucţia perioadelor Neolitic şi Eneolitic pe teritoriul Romaniei, fiind bine cunoscut in special pentru ceramica tipică pictată (Cosma et al 2006, Benea et al 2007).

Marea parte a eforturilor au fost însă direcţionate pentru aplicarea metodei în geologie şi paleoclimatologie prin realizarea unei cronologii de mare rezoluţie a depunerilor de natură eoliană pentru secţiunea de loess din apropierea localităţii Mircea Vodă, Dobrogea. Am ales această aplicaţie deoarece în comunitatea ştiinţifică internaţională este unanim acceptat faptul că secţiunile de loess reprezintă o arhivă detaliată a schimbărilor climatice din cursul Pleistocenului, depozitele din România fiind mult mai puţin studiate decât formaţiunile similare din Europa de Vest (Frechen, 2003). Mai mult decât atât, aceste depozite sunt considerate a fi printre cele mai complete din Europa, presupunâdu-se că reprezintă legatura dintre depozitele tipice periglaciare din vest şi depunerile tipic eoliene din China.

O schemă cronostratigrafică a depunerilor de loess din România bazată pe studii geomorfologice, litologice şi pedostratigrafice a fost realizată anterior (Conea, 1969), iar studii recente asupra proprietăţilor magnetice ale acestor roci sedimentare şi ale paleosolurilor intercalate au evidenţiat potenţialul utilizării variaţiei susceptibilităţii magnetice în corelaţie cu curbele de variaţie izotopică δO18 ca indicator paleoclimatic (Panaiotu et al. 2001, Buggle et al 2008). Cu toate acestea, metodele mentionate mai sus se bazează pe presupunerea că depunerile au avut loc in mod continuu, cu o rată de sedimetare constantă şi că stratele nu contin hiaturi de eroziune. Prin urmare, utilizând aceste metode, se poate obtine doar o informaţie indirectă asupra vârstelor stratelor în ansamblu.
Metodele de datare prin luminescenţă sunt in moment de faţă singurele tehnici care permit determ

because it is widely recognized that Romanian loess sequences preserve a significant terrestrial record of Quaternary climate change, but in comparison to similar sequences elsewhere in Central and Eastern Europe, the deposits in Romania have been less extensively studied (Frechen et al., 2003). Having an absolute chronology on Romanian loess sequences is of uttermost importance as these sequences are thought to be amongst the thickest and most complete in Europe, and they form the link between the glacial loess deposits of Western and Central Europe and the non-glacial loess deposits that extend all the way to China.

A chronostratigraphical framework for the Romanian loess deposits has previously been established through geomorphological, lithological and pedostratigraphical analysis (Conea, 1969). Luminescence dating has seen very little application to Romanian loess. We are only aware of the exploratory study by Balescu et al. (2003). In this study, four IRLS ages were obtained for a section near Tuzla (Dobrogea, SE Romania). Recent studies of the magnetic properties of the loess / palaeosol sequences have demonstrated the potential of magnetic susceptibility as a climatic proxy (see e.g. Panaiotu et al., 2001; Buggle et al., 2008); the variations in magnetic susceptibility are then matched to orbitally tuned δ18O records to derive a depositional chronology for the sequences. However, this approach assumes that the deposits are complete (i.e. no erosive hiatuses are present), and it can only provide indirect age information for entire units.

An important interference that emerges from detailed studies is the fact that loess record is seldom continuous and even during the last interglacial-glacial cycle large amplitude changes in sedimentation rates occurred.

Luminescence dating is, at present, the only method that allows establishing an absolute chronology for loess deposits. Moreover, the characteristics of loess make it an ideal material for developing, testing and applying luminescence techniques. Indeed, luminescence dating uses grains of quartz and/or feldspar, which are both typically abundant in loess, and the windblown nature of loess ensures that the luminescence clock was completely reset prior to deposition. Thus, obtaining an absolute chronostratigraphical framework for the Romanian loess deposits is essential to determine (i) the timing of climatic events that are registered in the loess, (ii) the rate of processes such as sedimentation and pedogenesis and (iii) the correlation between the loess sequences that are spread all over Europe.

We point out as well that by reconstructing past climates and the climatic variation throughout time data obtained can be used to test the accuracy of computer models that simulate climatic change. Simulations of the radiative impacts of dust under present climate conditions have been performed and already incorporate the effects of anthropogenically derived dust (Tegen et al 1996). However, the impact of the changes in the productivity of natural dust sources over geological time and the incorporation of dust deflation, transport and deposition processes is just beginning as spatially extensive data sets documenting the observed changes in

minarea de vârste absolute pentru depunerile de loess. Mai mult decât atât, datorită naturii eoliene a depunerilor de loess, aceste reprezintă un material ideal pentru metodele OSL, transportul granulelor asigurând resetarea semnalului luminescent.

O concluzie de importantă majoră rezultată in urma aplicării acestor metode este faptul că depunerile eoliene sunt în cazuri rare caracterizate prin rate de sedimetare constante, variaţii semificative ale acestui parametru având loc în cursul ultimului ciclu interglaciar-glaciar.

Prin urmare, obţinerea unei cronostatigrafii absolute a depunerilor eolinene din România este de importanţă majoră pentru a avea informaţii despre: cronologia evenimetelor climatice înregistrate în loess (formarea paleosolurilor), rata proceselor de sedimetare şi pedogeneză, posibile corelari între evenimentele climatice înregistrate în sectiuni din diferite zone geografice.

Precizăm de asemenea, că reconstrucţia paleoclimatelor şi a variaţiilor climatice din trecut poate sevi la verificarea modelelor climatice actuale. Influenţa depunerilor de praf de origine antropogenă au fost deja incluse în simulări (Tegen et al, 2006), dar impactul acestui poluant trebuie luată în considerare în strânsă corelaţie cu variaţiile de origine naturală ale cantităţii de praf din atmosfetă (Harrison et al, 2001). Analiza ratelor de sedimetare terestre (în speţă în depunerile de loess) în relaţie cu evoluţia paleoclimatului poate furniza date importante in acest sens. Prin urmare, realizarea unor cronologii absolute de mare rezoluţie pentru secvenţele de loess conduce la obţinerea de parametrii de input pentru verificare modelelor climatice actuale, servind nu numai în caracterizarea variaţiilor din trecut cât şi pentru predicţiile viitoare.

Contribuțiile potențiale raportate la cele mai recente realizări existente în fluxul principal de publicații

Loessul este considerat un material ideal pentru aplicarea metodelor de datare prin luminescenţă. În cursul acestei teze de doctorat a fost realizată o primă cronologie absolută de mare rezoluţie a depunerilor din secvenţa Mircea Vodă (Dobrogea, SE România), aplicând metode de datare prin luminescenţă stimulată optic. Studiul a fost facut pe probe colectate din ultimele patru perioade glaciare, folosind ca dozimetru granulele fine (4-11µm) de cuarţ (Timar et al. 2010). Vârstele obţinute corespund informaţiilor pedostratigrafice şi au fost comparate cu informaţii adâncime-vârstă obţinute in urma modelării matematice a variaţiei susceptibilităţii magnetice (prin curtoazia doamnei conferenţiar Cristina Panaiotu şi domnului conferenţiar Cristian Panaiotu- Universitatea Bucureşti). Vârstele OSL obţinute indică însă faptul că depunerile eoliene din cursul ultimului stadiu glaciar-interglaciar au avut loc în mod continuu dar nu cu o rată constantă, viteza de depunere fiind mai mică în ultimii 50 ka faţa de perioada 60-70ka. Vârstele obţinute pentru L1 demonstrează limitările aplicarii metodelor de datare relative pentru obţinerea cronologiei depunerilor de natură eoliană, infirmând presupunerea convenţională a sedimetării cu viteză constantă. Această constatare este insă în acord cu

dust accumulation rates during the last interglacial-glacial cycle are required in order to test model simulation of dust cycles (Harrison et al 2001). Thus investigation of sediment deposition in relation to palaeoclimatic changes is a major focus in modern earth modeling because having an accurate knowledge of the aeolian sedimentation rates during the Quaternary may help in creating extended models of dust cycles and thus of climate change, with eventually making predictions on future trends possible. Thus, dating sedimentary deposits is important for environmental sciences not only as a matter of reconstructing the past trends but also for predicting future ones.

Potential contributions compared to the most recent achievements in the main publications

Loess is generally considered as an ideal material for luminescence dating. We have reported the first optically stimulated luminescence (OSL) ages for the loess sequence near Mircea Vodă (Dobrogea, SE Romania). The study focussed on loess from the last four glacial periods and used silt-sized (4-11µm) quartz as dosimeter (Timar et al., 2010a). An internally consistent set of optical ages was obtained and the optical ages have been compared with a magnetic time-depth model ellaborated by Dr. Cristian Panaiotu and Dr. Cristina Panaiotu (University of Bucharest) based on magnetic susceptibility measurements. Based on luminescence ages, evidence was presented for a varying loess accumulation rate during the Last Glacial. the optical ages indicate that this unit did not accumulate at a constant rate, with loess being deposited at a significantly lower rate during the past ~50 ka. This illustrates the limitations of proxy records (such as magnetic susceptibility) to interpret and derive a chronology for these deposits. The age results for the L1 unit contrast with the commonly held assumption that loess sedimentation in this region occurred at a constant rate. They are, however, in line with the ideas emerging from the study of Singhvi et al. (2001), and the recent insights gained from optical dating of Chinese loess; at several localities in the Chinese loess plateau, loess accumulation rates have been found to vary during the last glacial period (see e.g. Stevens et al. 2007; Buylaert et al., 2008).

While it could be confirmed that the uppermost palaeosol (usually denoted by S1 in stratigraphic nomenclature) formed during the last Interglacial, comparison with independent age control (pedostratigraphy and a newly developed palaeomagnetic time-depth model) also indicated that the dating procedure underestimates the true burial age from the penultimate glacial period onwards. The SAR-OSL ages obtained for the three samples taken below the S1 soil are interpreted as age underestimates, with the degree of age underestimation increasing with depth. Interestingly, the luminescence characteristics do not indicate such behavior. These results are consistent with those reported for old (>70 ka) Chinese loess (Buylaert et al., 2007; 2008), and with the more general suggestion that SAR may underestimate the true age (to some degree) in the older age range (see e.g. Murray et al., 2007). Our results are in contrast to the findings by Murray et al. (2008) for quartz extracted from a

concluziile studiului efectuat de Singhvi in 2001, şi cu rezulate recente obţinute in urma datării unor secvenţe diferite din platoul de loess din China (Stevens et al. 2007, Buylaert et al 2008).

Vârstele luminescente obţinute confirmă corelarea primului paleosol bine dezvoltat (notat cu S1 în nomenclatura stratigrafică) cu ultimul Interglaciar. În cazul probelor colectate însă din statele L2, L3 si L4 s-a constatat că vârstele SAR-OSL obţinute prin metode luminescente subestimează timpul trecut din momentul depunerii. În mod interesant însă, caracteristicile semnalului luminescent reprodus în laborator nu indică faptul că acest fenomen ar trebui sa aibă loc. Aceste rezultate sunt în concordanţă cu observaţiile raportate pentru cuarţul extras din loess din China cu vârste de peste 70ka (Buylaert et al. 2007, 2008) şi cu sugestia mai generală că protocolul SAR ar conduce la obţinerea de doze echivalente care subestimează într-o oarecare masură paleodozele pentru vârste mari (Murray et al., 2007). Rezultatele sunt însă în dezacord cu concluziile unui studiu efectuat pe cristale de cuarţ extrase din un depozit din zona râului Seyda din nordul Rusiei. În acest studiu (Murray et al., 2008), doze naturale de aproximativ 350 Gy au fost obţinute folosind regiunea liniară supra-exponenţială a curbei de creştere a semnalului luminescent în funcţie de doză, rezultând vârste OSL în bună concordanţă cu informaţia geologică.

Studiul nostru a concluzionat că metodele SAR OSL pot fi aplicate pe cuarţ fin extras din loessul de origine dobrogeană pentru a obtine o cronologie de mare acurateţe pâna la vârste de 70ka, vârstă ce sorespunde unei doze echivalente de 200Gy. Cel putin în acest caz, se pare că folosirea regiunii liniare supra-exponenţiale a curbei de creştere a semnalului luminescent nu conduce la obţinera de vârste de mare acurateţe, iar în cazul dozelor mari posibilele influenţă a debitului folosit in laborator trebuie luată in vedere.

Rezultatele menţionate anterior au fost prezentate în cadrul "12th International Conference on Luminescence and Electron Spin Resonance Dating (LED 2008)", 18–22 September 2008, Peking University, Beijing, China, unde am obţinut premiul "Vagn Mejdahl"pentru contribuţii remaracabile ca student.

În ultimii ani, cuarţul a ocupat poziţia de dozimetru preferat pentru datarea prin luminescenţă a depozitelor de loess. Diverse aplicaţii au fost facute folosind diferite mărimi ale granulelor minerale: cuarţ fin (4-11 µm) (Watanuki et al. 2003; Wang et al. 2006; Lu et al. 2007; Timar et al., 2010), mediu (35-63 µm) (Roberts, 2006; Stevens et al. 2007; Lai et al., 2007) sau nisipos (63-90 µm) (Buylaert et al., 2007; 2008), presupunându-se ca pentru un depozit de natură eoliana oricare dintre aceste fracţiuni este potrivită pentru a obţine momentul depunerii. Nu există insă nici un studiu care să demonstreze explict acest lucru, prezentând o comparaţie între vârste obţinute folosind diferite fracţiuni. În anul 2009 am realizat un asemenea studiu pentru secţiunea Mircea Vodă, concluzionând ca vârstele obţinute pe granule fine diferă semnificativ de cele obţinute folosind cuarţ nisipos (63-90 µm) (Timar Gabor et al., 2010).

deposit on the Seyda River in northern Russia. In the latter study, natural doses of ~350 Gy were obtained using the high dose linear region of the growth curve, which resulted in optical ages that were in excellent agreement with the independent age controls.

We concluded that optical dating of fine-grained quartz can be used to establish a reliable chronology for Romanian loess up to ~70 ka. This age values correspond to equivalent doses of ~ 200Gy. Up to this value an exponential function and an exponential plus a linear term function give the same goodness of fit to experimental data. At least for our samples, the results obtained from the high dose linear region of the growth curve do not appear to be accurate. The procedure underestimates the true burial age when applied to loess that was deposited before the last climatic cycle; further research is necessary to establish what causes the age underestimation. Our results illustrated that an apparently reliable OSL laboratory measurement procedure not necessarily guarantees an accurate determination of the true burial.

These finds have been presented at "12th International Conference on Luminescence and Electron Spin Resonance Dating (LED 2008)", 18–22 September 2008, Peking University, Beijing, China, where I was awarded with "Vagn Mejdahl Prize" for Outstanding Poster Presentation.

In recent years, quartz has become the dosimeter of choice and modern optical dating technology is increasingly applied to various grain-size fractions of quartz that have been extracted from loess. Optically stimulated luminescence (OSL) dating has been applied to silt-sized (4-11 µm) quartz (Watanuki et al. 2003; Wang et al. 2006; Lu et al. 2007; Timar et al., 2010), middle-sized (35-63 µm) quartz (Roberts, 2006; Stevens et al. 2007; Lai et al., 2007) and sand-sized (63-90 µm) quartz (Buylaert et al., 2007; 2008). While it seems logic to assume that for a windblown material (such as loess) grains from several fractions are suitable for optical dating, this has not been explicitly demonstrated. At least to our knowledge, no studies are available that compare the luminescence characteristics and age of quartz grains of different granulometric fractions extracted from loess. We have conducted such a study on samples collected from Mircea Vodă loess section (Timar et al 2010 b). This study demonstrated that luminescence dating of loess may be more complicated. For samples collected from the loess sequence near Mircea Vodă (SE Romania), it is observed that OSL signals from silt-sized and sand-sized quartz yield ages that differ significantly. The OSL characteristics of both fractions, however, appear just as suitable for dating the deposits. The signals are dominated by a fast component and they are thermally stable. The OSL signals from the two fractions behave well in the SAR protocol (in terms of recycling, recuperation and dose recovery), indicating that the SAR protocol should be suitable for determining the equivalent dose in both. As such, there would be no cause to doubt the data generated by analysis of a single grain-size fraction of quartz (at least from a pure laboratory-methodological perspective). For now, it

Caracteristicile semnalului OSL pentru ambele categorii de granule au fost analizate in detaliu, trecând toate testele de rigoare intrinsecă specifice metodei şi indicând astfel faptul că datarea secţiunii utilizând oricare dintre cele doua fracţiuni şi protocolul SAR conduce la rezultate de bună acurateţe. Rezultatele obţinute conduc însă la o controversă logică cu relevanţă pentru studiile viitoare. Deşi studiul nostru reprezintă un caz individual se pare că observaţii similare au mai fost facute foarte recent (Vandenbergheet al., 2009). Studiul nostru arată faptul ca datarea loessului, cel puţin în cazul vârstelor mari, ramâne o temă de cercetare dificilă.

Aceste rezultate au fost diseminate prin conmunicări orale la "International conference on loess research - LOESSFEST '09 ", 31 August -3 September 2009, Novi Sad, Serbia şi "10th international conference "Methods of Absolute Chronology", 21-25 April 2010, Gliwice, Poland.

Bibliografie / References:

1. Aitken M.J., 1985. Thermoluminescent Dating. Academic Press, London, 359p. ISBN: 0-12-046380-6.
2. Aitken M.J., 1998. An introduction to optical dating. The dating of Quaternary Sediments by the use of Photon-Stimulated Luminescence. Oxford University Press, Oxford, 267p, ISBN: 0-19-854092.
3. Balescu, S., Lamothe, M., Mercier, N., Huot, S., Balteanu, D., Billard, A. and Hus, J., 2003. Luminescence chronology of Pleistocene loess deposits from Romania: testing methods of age correction for anomalous fading in alkali feldspars. Quaternary Science Reviews. 22/10-13, 967-973.
4. Benea V., Vandenberge D., Timar A., Van den Haute P., Cosma C., Gligor M., Florescu C., 2007. Luminescent dating of Neolithic ceramics from Lumea Nouă, Romania. Geochronometria 28, 9-16.
5. Buggle, B., Hambach, U., Glaser, B., Gerasimenko, N., Marković, S., Glaser, I., Zöller, L., 2008. Stratigraphy and spatial and temporal paleoclimatic trends in Southeastern/Eastern European loess paleosol sequences. Quaternary International, (in press) doi:10.1016/j.quaint.2008.07.013.
6. Buylaert J.P., Vandenberge D., Murray A.S., Huot S., De Corte F. and Van den Haute P., 2007. Luminescence dating of old (>70ka) Chinese loess: a comparison of single aliquot OSL and IRSL techniques. Quaternary Geochronology 2, 9-14.
7. Buylaert, J.P., Murray, A.S., Vandenberghe, D., Vried, M., De Corte, F., Van den haute, P., 2008. Optical dating of Chinese loess using sand-sized quartz: Establishing a time frame for Late Pleistocene climate changes in the western part of the Chinese Loess Plateau. Quaternary Geochronology 3, 99-113.
8. Conea, A. 1969. Profils de loess en Roumanie. La stratigraphie des loess d'Europe. In: Fink, J. (Ed.), Bulletin de l'Association française pour l'étude du Quaternaire,.Suppl. INQUA, 127–134.
9. Cosma C., Benea V., Timar A., Barbos D., Paunoiu C., 2006. Preliminary dating results on ancient ceramics from Romania by means of thermoluminescence. Radiation Measurements 41, 987-990.
10. Cosma C. Timar A., Benea V., Pop I., Jurcut T., Ciorba D., 2008. Using natural luminescent materials and highly sensitive sintered dosimeters MCP-N (LiF:Mg,Cu,P) in radiation dosimetry. Journal of optoelectronics and advanced materials vol. 10, nr 3, 573-577.
11. Duller G.A.T., 2004. Luminescence dating of Quaternary sediments: recent advances. Journal of Quaternary science 19, 183-192.
12. Frechen, M., Oches, E.A., Kohfeld, K.E., 2003. Loess in Europe – mass accumulation rates during the Last Glacial Period. Quaternary Science Reviews 22, 1835-1857.
13. Harrison S., Kohfeld K., Roelandt C., Claquin T., 2001. The role of dust in climate changes today, at the last glacial maximum and in the future. Earth Science Reviews 54, 43-48.
14. Labau, V., Gaspar, E., Paunica, T., 1996. Speleothems dating using the thermoluminescence method. Theoret. Appl. Karstology 9, 29–34.
15. Lai ZP, Wintle A.G., Thomas S. G., 2007. Rates of dust deposition between 50 ka and 20 ka revealed by OSL dating at Yuanbao on the Chinese Loess Plateau. Palaeogeography, Palaeoclimatology, Palaeoecology 248, 431-439.
16. Lu Y.C., Wang X. L., Wintle A.G., 2007. A new OSL chronology for dust accumulation in the last 130 000 yr for the Chinese Loess Plateau, Quaternary Research, 67, 152-160.
17. Murray A.S., Svendsen J.I., Mangerud J., Astakhov V.I., 2007. Testing the accuracy of quartz OSL dating using a known-age Eemian site on the river Sula, northern Russia. Quaternary Geochronology 2, 102-109.
18. Murray, A.S., Buylaert, J.-P., Henriksen, M., Svendsen, J.-I, Mangerud, J., 2008. Testing the reliability of quartz OSL ages beyond the Eemian. Radiation Measurements 43, 776-780.
19. Panaiotu, C.G., Panaiotu, E.C., Grama, A., Necula, C., 2001. Paleoclimatic Record from Loess-Paleosol Profile in Southeastern Romania. Phys. Chem. Earth (A) 11-12, 893-898.

These finds have been presented at International conference on loess research - LOESSFEST '09", 31 August - 3 September 2009, Novi Sad, Serbia and "10th international conference "Methods of Absolute Chronology", 21-25 April 2010, Gliwice, Poland.

20. Roberts R.G., 1997. Luminescence dating in archaeology: from origins to optical. Radiation Measurements 27: 819-892.
21. Roberts H.M., 2006. Optical dating of coarse-silt quartz from loess: Evaluation of equivalent dose determination and SAR procedural checks. Radiation Measuremets 41, 923-929.
22. Singhvi, A.K., Bluszcz, A., Bateman, M.D., Someshwar Rao, M., 2001. Luminescence dating of loess- palaeosol sequences and coversands: methodological aspects and palaeoclimatic implications. Earth-Science Reviews 54, 193-211.
23. Stevens, T., Armitage, S.J., Huayu, L., Thomas, D.S.G., 2007. Examining the potential of high resolution OSL dating of Chinese loess. Quaternary Geochronology 2, 15-22.
24. Stokes S., 1999. Luminescence dating applications in geomorphological research. Geomorphology 29, 153-171.
25. Tegen, I., Lacis A.A., Fung I., 1996. The influence of climate forcing of mineral aerosols from disturbed soils. Nature 280, 419-422.
26. Timar A., Vandenberghe D., Panaiotu E.C., Panaiotu C.G., Necula C., Cosma C. and Van den haute P., 2010a. Optical dating of Romanian loess using fine-grained quartz. Quaternary Geochronology, 5, 143-148.
27. Timar Gabor A., Vandenberghe D.A.G., Vasiliniuc , S., Panaoitu , C. E., Panaiotu, C. G., Dimofte, D., Cosma, C., 2010. Optical dating of Romanian Loess a comparison between silt-sized and sand-sized quartz. Quaternary International. (QUATINT - S-10- 00155).
28. Vandenberghe D.A.G., De Meester E., Velghe G., Zöller L., Van den haute P., 2009. A chronological study of the loess deposits over- and underlying the Eltville tephra using the newest luminescence techniques applied to sand-sized quartz: results from two Late-Weichselian type localities. Abstract book Loessfest '09 – International Conference on Loess Research, 31 August – 1 September, 2009, Novi Sad, Serbia, 31.
29. Văsaru G, Cosma C., 1998. Geocronologie Nucleară. Editura Dacia, Cluj Napoca, 346p, ISBN:973-35-0650-8.
30. Wang X., Lu Y., Zhao H., 2006. On the performance of single aliquot regenerative-dose (SAR) protocol for Chinese loess: fine quartz and polymineral grains. Radiation Measurements 41, 1-8.
31. Watanuki T., Murray A.S., Tsukamoto S., 2003. A comparison of OSL ages derived from silt-sized quartz and polymineral grains from Chinese loess, Quaternary Science reviews 22, 991-997.
32. Wintle A.G., 2008a. Luminescence dating: where it has been and where it is going.Boreas, Vol. 37, p. 471–482.
33. Wintle A.G., 2008b. Fifty years of luminescence dating. Archaeometry 50, 2, 276– 312.

Modul de valorificare/diseminare a rezultatelor cercetării (publicare articole, participare la conferințe, potențiale aplicații ale temei)

PUBLICAŢII ISI

1. Cosma C., Benea V., **Timar A.**, Barbos D., Paunoiu C. **(2006)** "Preliminary dating results on ancient ceramics from Romania by means of thermoluminescence." Radiation Measurements nr. 41, 987-990.
2. Benea V., Vandenberge D., **Timar A.**, Van den Haute P., Cosma C., Gligor M., Florescu C. **(2007)** "Luminescent dating of Neolithic ceramics from Lumea Nouă, Romania." Geochronometria nr. 28, 9-16.
3. Cosma C., **Timar A.**, Benea V., Pop I., Jurcut T., Ciorba D. **(2008)** "Using natural luminescent materials and highly sensitive sintered dosimeters MCP-N (LiF:Mg,Cu,P) in radiation dosimetry." Journal of optoelectronics and advanced materials vol. 10, nr 3, 573-577.
4. Cosma C., Ciorba D., **Timar A.**, Szacsvai K., Dinu A. **(2009)** "Radon exposure and lung cancer risk in Romania." Journal of Environmental Protection and Ecology, nr 1., 94-104.
5. Cosma C., Petrescu I., Meilescu C., **Timar A. (2009)** "Studies on the radioactivity of lignite from the area between the Danube and Motru (South-West Romania) and the incidence on the environment." Journal of Environmental Protection and Ecology, nr 1., 192-201.

Further use and dissemination of the reserach results (articles, conference participations, potential applications of the topic

ISI PUBLICATIONS

1. Cosma C., Benea V., **Timar A.**, Barbos D., Paunoiu C. **(2006)** "Preliminary dating results on ancient ceramics from Romania by means of thermoluminescence." Radiation Measurements nr. 41, 987-990.
2. Benea V., Vandenberge D., **Timar A.**, Van den Haute P., Cosma C., Gligor M., Florescu C. **(2007)** "Luminescent dating of Neolithic ceramics from Lumea Nouă, Romania." Geochronometria nr. 28, 9-16.
3. Cosma C., **Timar A.**, Benea V., Pop I., Jurcut T., Ciorba D. **(2008)** "Using natural luminescent materials and highly sensitive sintered dosimeters MCP-N (LiF:Mg,Cu,P) in radiation dosimetry." Journal of optoelectronics and advanced materials vol. 10, nr 3, 573-577.
4. Cosma C., Ciorba D., **Timar A.**, Szacsvai K., Dinu A. **(2009)** "Radon exposure and lung cancer risk in Romania." Journal of Environmental Protection and Ecology, nr 1., 94-104.
5. Cosma C., Petrescu I., Meilescu C., **Timar A. (2009)** "Studies on the radioactivity of lignite from the area between the Danube and Motru (South-West Romania) and the incidence on the environment." Journal of Environmental Protection and Ecology, nr 1., 192-201.

6. Begy R.C., Cosma C., **Timar A.**, Fulea D. **(2009)** "The Determination of Absolute Intensity of ^{234m}Pa's 1001 keV Gamma Emission Using Monte Carlo Simulation." Journal of Radiation Research, nr. 50, 277-279.
7. Cosma C., **Timar A.**, Benea V., Pop I., Moldovan M. **(2009)** "Carbon Molecular Sieve for Radon and Thoron Monitoring" Romanian Journal of Physics, nr. 3-4, vol. 54, 401-405.
8. Begy R., Cosma C., **Timar A., (2009)** "Recent changes in Red Lake (Romania) sedimentation rate determined from depth profiles of ^{210}Pb and ^{137}Cs radioisotopes" Journal of Environmental Radioactivity, nr. 100, 644-648.
9. **Timar A.**, Vandenberghe D., Panaiotu E.C., Panaiotu C.G., Necula C., Cosma C. and Van den haute P. **(2010)** Optical dating of Romanian loess using fine-grained quartz. Quaternary Geochronology, 5, 143-148.
10. **Timar Gabor A.**, Vasiliniuc, Ş., Bădărau, A.S., Begy, R., Cosma C., **(2010)**. Testing the potential of optically stimulated luminescence dating methods for dating soil covers from the forest steppe zone in Transylvanian basin.- Carpathian Journal of Earth and Environmental Sciences - Acceptat.

Trimise- in recenzie:

11. **Timar Gabor A.**, Vandenberghe D.A.G., Vasiliniuc , S., Panaoitu , C. E., Panaiotu, C. G., Dimofte, D., Cosma, C. **(2010)**. Optical dating of Romanian Loess a comparison between silt-sized and sand-sized quartz. Quaternary International. (QUATINT - S-10- 00155).
12. Timar Gabor A., Ivașcu C., Vasiliniuc Ș., Dărăban L., Ardelean I., Cosma C., Cozar O. **(2010)** Thermoluminescence and optically stimultaed luminescence properties of $O.5P_2O_5xBaO(0,5-x)Li_2O$ glass systems for medical dosimetry. Applied Radiation and Isotopes (ARI-D-10-00199).

PUBLICAŢII BDI

13. Timar A., Cosma C., Benea V., Begy R., Jobagy V., Szeiler G., Barbos D., Fulea D. **(2007)**, Estimation of environmental radionuclide concentration in soils, a comparison of methods for the annual radiation dose determination in luminescence dating, Studia Universitatis, Babes-Bolyai, Geologia, 52 (1), 80-81.

ALTE PUBLICAŢII ÎN VOLUME CU RECENZORI

14. Cosma C., Petrescu I, Meilescu C., **Timar A. (2007)**, Properties of lignite from Oltenia and their influence on the environment, Studia Universitatis Babes-Bolyai, Ambientum, I, 1—2 p.: 65-75.
15. Begy R., Cosma C., **Timar A.**, Fulea D. **(2007)**, A study on Cs-137 contamination of soils from certain regions of Transylvania, Environment and Progress (Environment-Research, Protection and Management) Editori: Munteanu L., Mihaiescu R. nr 9., p.: 73-76.
16. Cosma, C., **Timar, A.**, Benea, V., Begy, R., **(2008)**, Nuclear and Seminuclear Dating Methods: Application in Archeology, Geology and Environmental Science, Terrestrial radionuclides in the Environment, Environmental Conferences Veszprem, ISBN 978 963 9696 488, pp. 23-35.

6. Begy R.C., Cosma C., **Timar A.**, Fulea D. **(2009)** "The Determination of Absolute Intensity of 234mPa's 1001 keV Gamma Emission Using Monte Carlo Simulation." Journal of Radiation Research, nr. 50, 277-279.
7. Cosma C., **Timar A.**, Benea V., Pop I., Moldovan M. **(2009)** "Carbon Molecular Sieve for Radon and Thoron Monitoring" Romanian Journal of Physics, nr. 3-4, vol. 54, 401-405.
8. Begy R., Cosma C., **Timar A., (2009)** "Recent changes in Red Lake (Romania) sedimentation rate determined from depth profiles of 210Pb and 137Cs radioisotopes" Journal of Environmental Radioactivity, nr. 100, 644-648.
9. **Timar A.**, Vandenberghe D., Panaiotu E.C., Panaiotu C.G., Necula C., Cosma C. and Van den haute P. **(2010)** Optical dating of Romanian loess using fine-grained quartz. Quaternary Geochronology, 5, 143-148.
10. **Timar Gabor A.**, Vasiliniuc, Ş., Bădărau, A.S., Begy, R., Cosma C., **(2010)**. Testing the potential of optically stimulated luminescence dating methods for dating soil covers from the forest steppe zone in Transylvanian basin.- Carpathian Journal of Earth and Environmental Sciences - Accepted.

Submitted:

11. **Timar Gabor A.**, Vandenberghe D.A.G., Vasiliniuc , S., Panaoitu , C. E., Panaiotu, C. G., Dimofte, D., Cosma, C. **(2010)**. Optical dating of Romanian Loess a comparison between silt-sized and sand-sized quartz. Quaternary International. (QUATINT - S-10- 00155).
12. Timar Gabor A., Ivașcu C., Vasiliniuc Ș., Dărăban L., Ardelean I., Cosma C., Cozar O. **(2010)** Thermoluminescence and optically stimultaed luminescence properties of $O.5P_2O_5xBaO(0,5-x)Li_2O$ glass systems for medical dosimetry. Applied Radiation and Isotopes (ARI-D-10-00199).

IDB PUBLICATIONS

13. **Timar A.**, Cosma C., Benea V., Begy R., Jobagy V., Szeiler G., Barbos D., Fulea D. **(2007)**, Estimation of environmental radionuclide concentration in soils, a comparison of methods for the annual radiation dose determination in luminescence dating, Studia Universitatis, Babes-Bolyai, Geologia, 52 (1), 80-81.

OTHER PEER-REVIEWED PUBLICATIONS

14. Cosma C., Petrescu I, Meilescu C., **Timar A. (2007)**, Properties of lignite from Oltenia and their influence on the environment, Studia Universitatis Babes-Bolyai, Ambientum, I, 1—2 p.: 65-75.
15. Begy R., Cosma C., **Timar A.**, Fulea D. **(2007)**, A study on Cs-137 contamination of soils from certain regions of Transylvania, Environment and Progress (Environment-Research, Protection and Management) Editori: Munteanu L., Mihaiescu R. nr 9., p.: 73-76.
16. Cosma, C., **Timar, A.**, Benea, V., Begy, R., **(2008)**, Nuclear and Seminuclear Dating Methods: Application in Archeology, Geology and Environmental Science, Terrestrial radionuclides in the Environment, Environmental Conferences Veszprem, ISBN 978 963 9696 488, pp. 23-35.

17. Cosma C., Benea V., **Timar A.**, Gligor M., Varvara S. **(2008)**, Datarea prin luminescenta stimulate termic (TL) si optic (OSL). Aplicatii in arheologie, ACTA MVSEI APVLENSIS, Apulum, XLV, 579-598.
18. **Timar A.**, Cosma C., Benea V., Begy R.C., Jabaggy V., Szeiler G., Fulea D. **(2008)**, A comparison of methods for external dose rate determinatin in luminescence dating of archaeological materials, Foldkergi Radioizotopok a Kornyezetunnkben, Pannon Egyetemi Kiado, Egyhazy Tiborne- Editor, p. 35-44.

ARTICOLE ŞI ABSTRACTE EXTINSE APARUTE ÎN VOLUMELE UNOR CONFERINŢE

19. Cosma C., **Timar A., (2008)**, Testarea potentialului metodelor luminiscente in datarea unei sectiuni de loess din Dobrogea, MENER, Universitatea Politehnica - Bucuresti, p.: 643-650.
20. **Timar A. (2008)**, Fenomenul de termoluminescenta si luminescenta stimulata optic si aplicatiile sale in datare, Varste absolute prin metode nucleare cu aplicatii in arheologie, geologie si mediu., Masa Rotunda. Alba-Iulia, Quantum, Editor: Cosma C., Varvara S., Gligor, M., p.: 33-43.
21. **Timar A.**, Cosma C, van den Haute P., Vandenberghe D. **(2008)**, Datarea secventelor de loess-palaeosol prin luminescenta stimulata optic, Varste absolute prin metode nucleare cu aplicatii in arheologie, geologie si mediu. Masa Rotunda. Alba-Iulia, Quantum, Editor: Cosma C, Varvara S., Gligor, M., p.: 66-78
22. **Timar A**., Vandenberghe D., Vasiliniuc S., Cosma C., **(2009)**, Optical dating of Romanian loess: A comparison between sand-sized and silt-sized quartz, Loessfest '09 – Internation conference on loess research, Novi Sad, Serbia, p. 77-78.

PARTICIPARI LA CONFERINTE

1. **Conferinţa naţională "16th National Seminar of Etnoarchaeology and 19th National Symposium of Archaeometry, 11-12 December 2007, Cluj-Napoca, Romania.** "Luminescent methods in dating neolithic ceramics"- **prezentare orala**
2. **Conferinţa internaţională "9th international conference "Methods of Absolute Chronology", 25-27 April 2007, Gliwice, Poland.** "Luminescence dating of Neolithic ceramics from Romania"- **prezentare poster**
3. **Conferinţa internaţională "IXth European Society for Isotope Research Workshop", 23-28 June 2007, Cluj-Napoca, Romania.** "Estimation of environmental radionuclide concentration in soils, a comparison of methods for the annual radiation dose determination in luminescence dating" – **prezentare orala**
4. **Conferinţa internaţională "Sustainable Development in the Balkan Area: Vision and Reality (B.EN.A-ICAI Conference)", 18- 20 July 2007**, Alba-Iulia, Romania. "Studies on the radioactivity of lignite from the area between the Danube and Motru and the incidence on the environment"- prezentare orala "Radon exposure and lung cancer risk in Romania"- **prezentare poster**
5. **Conferinţa internaţională "Isotopic and Molecular Processes (PIM 2007)", 20-22 September 2007, Cluj-Napoca, Romania.** "Charcoal -

17. Cosma C., Benea V., **Timar A.**, Gligor M., Varvara S. **(2008)**, Datarea prin luminescenta stimulate termic (TL) si optic (OSL). Aplicatii in arheologie, ACTA MVSEI APVLENSIS, Apulum, XLV, 579-598.
18. **Timar A.**, Cosma C., Benea V., Begy R.C., Jabaggy V., Szeiler G., Fulea D. **(2008)**, A comparison of methods for external dose rate determinatin in luminescence dating of archaeological materials, Foldkergi Radioizotopok a Kornyezetunnkben, Pannon Egyetemi Kiado, Egyhazy Tiborne- Editor, p. 35-44.

ARTICLES AND EXTENDED ABSTRACTS IN CONFERENCE VOLUMES

19. Cosma C., **Timar A., (2008)**, Testarea potentialului metodelor luminiscente in datarea unei sectiuni de loess din Dobrogea, MENER, Universitatea Politehnica - Bucuresti, p.: 643-650.
20. **Timar A. (2008)**, Fenomenul de termoluminescenta si luminescenta stimulata optic si aplicatiile sale in datare, Varste absolute prin metode nucleare cu aplicatii in arheologie, geologie si mediu., Masa Rotunda. Alba-Iulia, Quantum, Editor: Cosma C., Varvara S., Gligor, M., p.: 33-43.
21. **Timar A.**, Cosma C, van den Haute P., Vandenberghe D. **(2008)**, Datarea secventelor de loess-palaeosol prin luminescenta stimulata optic, Varste absolute prin metode nucleare cu aplicatii in arheologie, geologie si mediu. Masa Rotunda. Alba-Iulia, Quantum, Editor: Cosma C, Varvara S., Gligor, M., p.: 66-78
22. **Timar A**., Vandenberghe D., Vasiliniuc S., Cosma C., **(2009)**, Optical dating of Romanian loess: A comparison between sand-sized and silt-sized quartz, Loessfest '09 – Internation conference on loess research, Novi Sad, Serbia, p. 77-78.

CONFERENCE ATTENDANCE

1. **National conference "16th National Seminar of Etnoarchaeology and 19th National Symposium of Archaeometry, 11-12 December 2007, Cluj –Napoca, Romania.** "Luminescent methods in dating neolithic ceramics"- **oral presentation**
2. **International conference "9th international conference "Methods of Absolute Chronology", 25-27 April 2007, Gliwice, Poland.** "Luminescence dating of Neolithic ceramics from Romania"- **poster presentation**
3. **"International conference IXth European Society for Isotope Research Workshop", 23-28 June 2007, Cluj-Napoca, Romania.** "Estimation of environmental radionuclide concentration in soils, a comparison of methods for the annual radiation dose determination in luminescence dating" – **oral presentation**
4. **International conference "Sustainable Development in the Balkan Area: Vision and Reality (B.EN.A-ICAI Conference)", 18-20 July 2007, Alba-Iulia, Romania.** "Studies on the radioactivity of lignite from the area between the Danube and Motru and the incidence on the environment"- prezentare orala "Radon exposure and lung cancer risk in Romania."- **poster presentation**
5. **International conference "Isotopic and Molecular Processes (PIM 2007)", 20-22 September 2007, Cluj-Napoca, Romania.** "Charcoal-TLD combined method used for radon

TLD combined method used for radon monitoring"- prezentare orala "Using natural luminescent materials and MCP-N (LiF:Mg, Cu, P) chips in environmental monitring"- **prezentare poster**

6. **Masa rotundă" Varste absolute prin metode nucleare cu aplicatii in arheologie, geologie si mediu", 29-30 August 2008, Alba-Iulia, Romania.** "Datarea sedimentelor prin luminescenţă stimulată optic" – **prezentare orală**
7. **Conferinţa internaţională "12th International Conference on Luminescence and Electron Spin Resonance Dating (LED 2008)", 18–22 September 2008, Peking University, Beijing, China.** "Optical dating of Romanian loess using fine-grained quartz" – **prezentare poster**
8. **Conferinţa internaţională"International conference on loess research -LOESSFEST '09", 31 August -3 September 2009, Novi Sad, Serbia.** "Optical dating of Romanian loess: a comparison between sand-sized and silt-sized quartz" **– prezentare orala**
9. **Conferinţa naţională cu participare internaţionala "Environment – Research, Protection and Management", 05 - 08 November 2009, Cluj-Napoca, Romania.** "Absolute dating of Romanian loess- luminescence methodology and palaeoclimatical implications"- **prezentare poster**
10. **Conferinţa internaţională "10th international conference "Methods of Absolute Chronology", 21-25 April 2010, Gliwice, Poland.** "Further investigations on the optical age of fine silt (4-11 μm), coarse silt (35-50 μm) and fine sand (63-90μm) quartz grains extracted from Romanian loess"- **prezentare orala.**

Relatarea succintă a sprijinului acordat şi a obstacole întâmpinate pe parcursul realizării tezei d edoctorat

Sunt recunoscătoare coordonatorului meu ştiinţific, Profesor Dr. Constantin Cosma pentru îndrumare, pentru faptul că m-a susţinut întotdeauna şi pentru eforturile facute pentru ca laboratorul de datare prin luminescenţă din cadrul Universităţii Babeş-Bolyai să existe.

Ramân îndatorată doamnei Conf. Dr. Cristina Panaoiotu şi domnului Conf. Dr. Cristian Panaiotu (Universitatea Bucureşti) pentru ajutor în campaniile de colectare a probelor şi pentru ca mi-au oferit acces la rezultate nepublicate ale cercetărilor lor (atât paleomagnetism cât şi analize granulometrice).

Multumesc colegilor de la Departamentul de Radiochimie al Universităţii din Veszprém şi de la Sucursala pentru Cercetări Nucleare Mioveni, Piteşti pentru participare la execitiul de inercomparare.

În perioada 2007-2008 am efectuat o serie de stagii de cercetare în Gent Luminescence Dating Laboratory, fiind înmatriculată pentru 8 luni ca cercetător vizitator în cadrul Universitaţii Gent, sub coordonarea a Dr. Dimitri Vandenberghe şi Prof. Dr. P. Van den haute. O parte din cercetarea prezentată în teza mea de doctorat se bazează pe activitătile desfăsurate în cadrul acestor vizite. Suportul logistic şi transferul constant de know-how oferit de Gent Luminescence Dating Laboratory au adus o contribuţie esenţială in dezvolatrea mea profesională.

Multumesc de asemenea pentru susţinerea financiară de care am beneficiat prin granturile CEEX 749-2006 (C.Cosma) şi TD-395 (A. Timar).

monitoring"- oral presentation "Using natural luminescent materials and MCP-N (LiF:Mg, Cu, P) chips in environmental monitring"- **poster presentation**

6. **Round table " Varste absolute prin metode nucleare cu aplicatii in arheologie, geologie si mediu", 29-30 August 2008, Alba-Iulia, Romania.** "Datarea sedimentelor prin luminescenţă stimulată optic" – **oral presentation**
7. **International conference "12th International Conference on Luminescence and Electron Spin Resonance Dating (LED 2008)", 18–22 September 2008, Peking University, Beijing, China.** "Optical dating of Romanian loess using fine-grained quartz" – **poster presentation**
8. **International conference"International conference on loess research -LOESSFEST '09", 31 August -3 September 2009, Novi Sad, Serbia.** "Optical dating of Romanian loess: a comparison between sand-sized and silt-sized quartz" – **oral presentation**
9. **International conference "Environment – Research, Protection and Management", 05 - 08 November 2009, Cluj-Napoca, Romania.** "Absolute dating of Romanian loess- luminescence methodology and palaeoclimatical implications"- **poster presentation**
10. **International conference "10th international conference "Methods of Absolute Chronology", 21-25 April 2010, Gliwice, Poland.** "Further investigations on the optical age of fine silt (4-11 μm), coarse silt (35-50 μm) and fine sand (63-90μm) quartz grains extracted from Romanian loess"- **oral presentation**

Brief overview of the support received, and main obstacles during the PhD thesis

I am grateful for the support of my supervisor Professor Constantin Cosma, for his guidance for all the efforts he made in order for the Luminescence Laboratory in Cluj to exist.

I have to acknowledge the excelent collaboration with the Paleomagnetic Team from Bucharest. Conf. Dr. Cristina Panaiotu (Faculty of Geology and Geophysics, University of Bucharest) and Conf. Dr. Cristian Panaiotu (Faculty of Physics, University of Bucharest), "entrusted" me with a great research topic, guided me in the sampling campaigns and gave me access to their unpublished data (both paleomagnetism and grain size analysis).

I thank the colleagues in Radioachemistry Department from University of Veszprém, Hungary and in Institute for Nuclear Research Mioveni, Piteşti Romania, for their collaboration in intercomparison exercises.

I have performed several research stages in Gent Luminescence Dating Laboratory being enrolled (2007-2008 in total for about eight months) as a visitor junior researcher in Gent University, Belgium under the scientific supervision of Dr. Dimitri Vandenberghe and Professor P. Van den haute. Part of the work presented in my PhD thesis was carried out during the frame of these visits. The constant transfer of knowledge and the logistic support provided by Gent Luminescence Dating Laboratory is highly acknowledged.

I am thankful for financial support of CEEX-749/2006 (Constantin Cosma) and CNCSIS TD-395 (Alida Timar) research grants.

Sugestii pentru CNCSIS privind finanțarea tinerilor doctoranzi în vederea finalizării tezei de doctorat

Consider că orice tip de finaţare destinată tinerilor doctoranzi este binevenită, atât pentru finalizarea tezei, dar, în ceea se priveşte logistica cel puţin, poate la fel de importantă şi pentru demararea unor activităti în primii doi ani. În mod special, consider importante granturile de mobilitate internaţională, pentru participări la conferinţe şi efectuarea de vizite în alte laboratoare.În cazul meu particular, consider că o mare parte din reusitele profesionale se datorează faptului că am reușit să fiu in mod constant în contact cu comunitatea ştiinţifică internaţională activă în acelaşi domeniu de cercetare.

O scurtă prezentare cronologică a evenimentelor cheie din povestea doctoratului meu

• Octombrie 2006 – înmatricularea.
• Octombrie 2006 – August 2007 – investigaţii gamma spectrometrice pentru determinarea concentraţiei de radionuclizi din probe de mediu.
• Decembrie 2006 – vizită de cercetare in Departamentul de Radioachimie al universitaţii din Veszprém.
• Iunie 2007 – prima mea comunicare orală la o conferinţă internaţională de prestigiu ("IXth European Society for Isotope Research Workshop") Fotografia 1 – alături de domnul profesor Cosma Constantin.

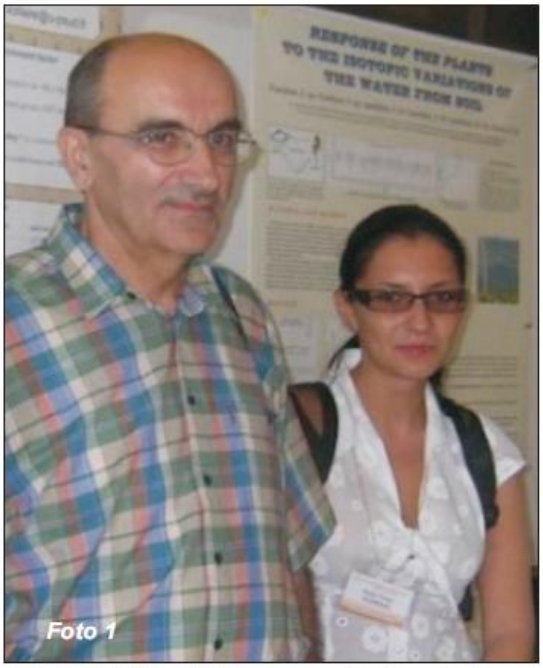

Foto 1

• August 2007 – Prima campanie de colectare a probelor de loess sub supravegherea doamnei Conf. Dr. Cristina Panaiotu – Fotografia 2
• Octombrie 2007 – Iunie 2008 - serie de stagii de cercetare în Gent Luminescence Dating Laboratory, Gent, Belgia – Fotografia 3

Suggestions to CNCSIS on funding young doctoral students to finalize their PhD thesis

I encourage any funding opportunities for doctoral students, not only in the final stage of their thesis but also for those who are just at the beginning. In particular, I would suggest more funds to be alocated for international mobility programmes for conference attendance and visits to other laboratories and universities. At least in my case, I believe that my achievements have been very much influenced by that fact that I managed to stay in contact to the international scientific community.

A short illustrated chronology of „milestone events" in „the story of my PhD"

• October 2006 – Enrolment.
• Octomber 2006 – August 2007 – Gamma spectrometric investigations for radionuclide concentration determination in environmental samples.
• June 2007 – My first oral presentation at an international conference (Picture 1 – togheter with my supervisor Profesor Constantin Cosma)
• August 2007 – Loess sampling campaign under the supervision of Conf. Dr. Cristina Panaiotu (Picture 2)

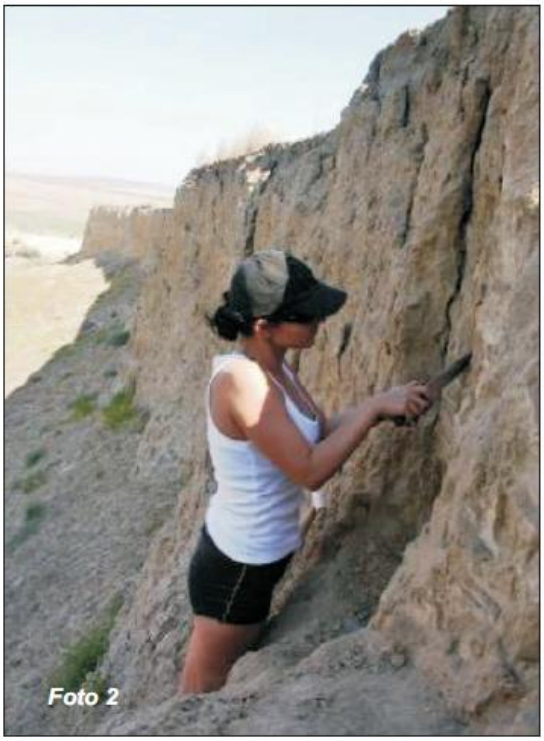
Foto 2

• October 2007 – June 2008 – Study stay in Gent University, Belgium (Picture 3)
• February 2008 – Visit to Risø National Laboratory at the invitation of Dr. Dimitri Vandenberghe.
• June 2008 – The decision of a lifetime- a choice between a PhD position in The Nordic Laboratory for Luminescence Dating and Aarhus University (world leader in luminescence dating research) under the supervision of Professor Andrew Murray (one of the greatest researchers in luminescence and probably


Foto 3

• Februarie 2008 – vizită de cercetare la Risø National Laboratory, Danemarca.
• Iunie 2008 – o decizie enormă pentru viitor – alegerea intre o bursă de cercetare la Nordic Laboratory for Luminescence Dating şi Aarhus University (incontestabil liderul mondial în cercetare în domeniul datării prin luminescenţă) sub coordonarea profesorului Andrew Murray (probabil cel mai apreciat cercetător activ în acest domeniu pe plan internaţional) şi o poziţie de asistent universitar în cadrul Universităţii Babeş-Bolyai. Am ales a doua variantă, concentrându-mi eforturile din următoarele luni pentru dezvoltarea laboratorului de luminescenţă din Cluj. – Fotografiile 4 şi 5.
• Septembrie 2008 -12th International Conference on Luminescence and Electron Spin Resonance Dating Peking University, Beijing, China – conform tradiţiei la această conferinţă de prestigiu se acordă premii pentru cele mai bune prezentări ale studenţilor. Am obţinut premiul Vagn Mejdahl pentru prezentarea "Optical dating of Romanian loess using fine-grained quartz". In Fotografia 6 apar alături de ceilalţi premianţi: Anine Larsen (The Nordic Laboratory for Luminescence Dating and Aarhus University), Renaud Joannes-Boyau (The Australian National University) şi Rome´e Kars (Delft University of Technology) si de profesor Ann Wintle.

Foto 6

• Septembrie 2008 - la recomandarea a Dr. Dimitri Vandenberghe am fost invitată oficial de către profesorul Zhong Ping Lai să tin o prelegere la Quinghai Institute of Salt Lakes (Chinese Academy of Sciences), Xinning. Fotografia 7- pe platoul Tibetan.
• August 2009 – vizită de cercetare la Gent University
• Septembrie 2009 – reîntoarcerea la Mircea Vodă pentru a colecta o probă suplimentară – Foto 8.

the mostly valued active professor in this field) and a teaching assistant professor in Babeş-Bolyai University of Cluj Napoca. I have chosen the latter, and in the following months I have contributed to the developement of the luminescence dating laboratory in Cluj. (Pictures 4 and Picture 5)


Foto 4


Foto 5

• September 2008 -12th International Conference on Luminescence and Electron Spin Resonance Dating Peking University, Beijing, China. Four prizes were awarded to students who presented papers at the conference: to Anine Larsen (The Nordic Laboratory for Luminescence Dating and Aarhus University), who received the Martin Aitken Prize for Best Oral Presentation; to Renaud Joannes-Boyau (The Australian National University), Rome´e Kars (Delft University of Technology) and myself, Alida Timar (Babes Bolyai University), who each received the Vagn Mejdahl Prize for an Outstanding Poster Presentation. (Picture 6)


Foto 7


Foto 8

• Septembrie 2009 – LOESSFEST '09 – Fotografia 9 prezintă participanţii la excursia organizată la finalul conferinţei.
• Decembrie 2009 – sustinerea tezei, dar...
• Fotografia 10 – împreună cu colegul Ştefan Vasiliniuc, colectând probe din secţiunea Costineşti, pentru ca o noua poveste frumoasă de doctorat să poată începe.


Foto 10

• September 2008- at the recommendation of Dr. Dimitri Vandenberghe I was invited by Professor Zhong Ping Lai to lecture at Quinghai Institute of Salt Lakes (Chinese Academy of Sciences), Xinning. (Picture 7- on Tibethan Plateau).
• August 2009- One week visit to Gent University.
• September 2009- back at Mircea Vodă for one extra sample (Picture 8)
• September 2009- LOESSFEST '09, Picture 9- presents the participants to the field trip organised after the conference.


Foto 9

• December 2009 – Defense of my thesis, but...
• Picture 10 - Sampling Costinesti Section for the thesis work of my colleague Ştefan Vasiliniuc, and thus another beautiful story of a Phd just started.

TABLE OF CONTENTS

CHAPTER III
The annual dose

CHAPTER IV
Applications of luminescence dating in archaeology
Luminescence dating of Neolithic ceramics from Romania

CHAPTER V
Applications of luminescence dating in geology and environmental studies